UNIVERSITY OF SUSSEX

MARIELLA MANNINO

DOCTOR OF PHILOSOPHY BIOCHEMISTRY

IMPROVING TREATMENT OF GLIOBLASTOMA: NEW INSIGHTS IN TARGETING CANCER STEM CELLS EFFECTIVELY

Declaration

I hereby declare that this thesis has not been and will not be, submitted in whole or in part to another University for the award of any other degree.

Signed ……

Mariella Mannino

Acknowledgements

My acknowledgements consist of a series of “Thank You” and will follow a chronological order.

Thank you to my parents, my brother and my grandparents, for making me feel I can do anything I wish in life (very heart-warming… but a bit disappointing when one realizes the truth…!).

Thank you to the University of Palermo, for making me want to move to the UK.

Thank you to Claudio, my husband, for loving me from Palermo.

Thank you to John Yarnold, for being so inspiring, kind, caring and generous; in my mind, a modern version of Socrates (I’m not implying I’m Plato!).

Thank you to everybody at John’s office, especially Grace Sharp, for making me feel at home.

Thank you to Anthony Chalmers and Tony Carr, for supporting me and giving me the opportunity to undertake a PhD.

Thank you to Nadia Lovegrove, for making tissue culture so irresistible.

Thank you to the Gnomes that with their kindness and friendship made the GDSC a truly happy place for me (after two years, I still miss the GDSC very much and treasure many relationships that started there).

Thank you to the GDSC football players, for lots of fun games and some animated moments too…

Thank you to Helfrid Hochegger, for accepting me in his group and leaving me free.

Thank you to Nadia Hegarat for helping me in many ways at all times.

Thank you to British weather for not tempting me very often with sunny days.

Thank you to Brighton, for being such a vibrant and welcoming city.

Thank you to Owen Wells, for his encouragement during writing up.

Thanks again to my parents and Claudio, for helping me while writing my thesis with a severe form of baby brain.

University of Sussex

Mariella Mannino

Doctor of Philosophy Biochemistry

Improving treatment of glioblastoma: new insights in targeting cancer stem cells effectively.

Summary

Glioblastoma is the most common primary malignant brain tumour in the adult population. Despite multimodality treatment with surgery, radiotherapy and chemotherapy, outcomes are very poor, with less than 15% of patients alive after two years. Increasing evidence suggests that glioblastoma stem cells (GSCs) are likely to play an important role in the biology of this disease and are involved in treatment resistance and tumour recurrence following standard therapy.

My thesis aims to address two main aspects of this research area: 1) optimization of methods to evaluate treatment responses of GSCs and their differentiated counterparts (non-GSCs), with a particular focus on a tissue culture model that resembles more closely the tumoral niche; 2) characterization of cell division and centrosome cycle of GSCs, investigating possible differences between these cells and non-GSCs, that would allow the identification of targets for new therapeutic strategies against glioblastomas.

In the first part of my project, I optimized a clonogenic survival assay, to compare sensitivity of GSCs and non-GSCs to various treatments, and I developed the use of a 3-dimentional tissue culture system, that allows analysis of features and radiation responses of these two subpopulations in the presence of specific microenvironmental factors from the tumoral niche.

In the second part, I show that GSCs display mitotic spindle abnormalities more frequently than non-GSCs and that they have distinctive features with regards to the centrosome cycle. I also demonstrate that GSCs are more sensitive than non-GSCs to subtle changes in Aurora kinase A activity, which result in a rapid increase in polyploidy and subsequently in senescence, with a consistent reduction in clonogenic survival. Based on these findings, I propose that kinases involved in the centrosome cycle need to be explored as a novel strategy to target GSCs effectively and improve outcomes of glioblastoma patients.

Contents

Abbreviations

2DG	2-deoxyglucose
53BP1	p53-binding protein 1
ADC	antibody-drug conjugate
ALDH	aldehyde dehydrogenase
Arl13B	ADP-ribosylation factor-like protein 13B
ATM	ataxia telangiectasia mutated
AurA	aurora kinase A
BER	base excision repair
BMPs	bone morphogenetic proteins
BSA	bovine serum albumin
CAR	chimeric antigen receptors
CENP-F	centromere protein F
Cdk	cyclin dependent kinase
Chk	checkpoint kinase
CNS	central nervous system
CSCs	cancer stem cells
DAPI	4',6-diamidino-2-phenylindole
EBRT	fractionated external beam radiotherapy
ECM	extracellular matrix
EdU	5-ethynyl-2'-deoxyuridine
EGF	epidermal growth factor
EGFR	epidermal growth factor receptor
EGFRvIII	EGFR variant III
EMEA	European Medicines Agency
eNOS	endothelial nitric oxide synthase
EZH2	Enhancer of Zeste 2
FACS	Fluorescence Activated Cell Sorting
FDA	Food and Drug Administration
FGF	fibroblast growth factor
γH2AX	phosphorylated histone 2A
GSCs	glioblastoma stem cells
HATs	histone acetyltransferases

hBMEC	human brain microvascular endothelial cells
HBO	hyperbaric oxygen
HDAC	histone deacetylase
HGF	hepatocyte growth factor
HIF	hypoxia inducible factor
HRP	horseradish peroxidase
IR	ionizing radiation
KPS	Karnofsky PS
MAP	mitogen-activated protein
MDR	multidrug resistance
MGMT	O6-methylguanine–DNA methyltransferase
MMR	mismatch repair
MRN	MRE11–RAD50–NBS1
NO	nitric oxide
PARP	poly ADP-ribose polymerases
PBS	phosphate-buffered saline
PCM	pericentriolar material
PDGF	platelet-derived growth factor
PDT	potential doubling time
PFA	paraformaldehyde
PI	propidium iodide
PI3K	phosphatidylinositol 3-kinase
PKCβ	protein kinase C β
Plk	polo-like kinase
PS	performance status
PSMA	prostate-specific membrane antigen
PTEN	phosphatase and tensin homolog
QoL	quality of life
REMBRANDT	Repository of Molecular Brain Neoplasia Data
ROS	reactive oxygen species
RTOG	Radiation Therapy Oncology Group
SCF	stem cell factor
SCFR	stem cell factor receptor
SCS	spinal cord stimulation
SD	standard deviation

SOs	significant others
SSBs	single strand DNA breaks
TEMS	Tie2-expressing monocytes
TGF-β	transforming growth factor beta
TMZ	temozolomide
TTF	Tumour Treating Fields
VEGF	vascular endothelial growth factor
VEGFRs	VEGF receptors

Figures

Page

Tables

Page

Chapter 1

Introduction

1.1 Glioblastoma: what impact does this disease have and how are we treating it?

Glioblastoma is the most common primary malignant brain tumour in adults[1]. According to cancer registries in the UK and the US, the incidence of central nervous system tumours has increased in the last decades[2, 3]. Glioblastoma has reached an annual incidence rate of approximately 3 cases per 100.000 people[1]. Despite improvement in treatment outcome, the survival rates are still very poor, with only one third of patients alive after one year, less than 15% and 5% after two and five years, respectively[1]. Glioblastomas are very challenging from a clinical point of view too, as they can induce not only focal neurological signs (paraesthesia, hemiparesis, aphasia, visual disturbances) and symptoms of increased intracranial pressure (headache, nausea, vomiting), but also fatigue, cognitive deficits (problems with memory and concentration) and mood and personality changes[4]. These clinical manifestations constitute a serious challenge for the quality of life (QoL) of patients and their significant others (SOs), when compared to healthy individuals as well as to patients with other malignancies with similar prognosis and their SOs: high grade glioma patients reported more severe social dysfunctioning than non-small cell lung cancer patients, while their SOs in addition to decreased social functioning presented also lower mental health scores than SOs of non-small cell lung cancer patients[5, 6]. The significant social impact of glioblastoma, together with its dismal prognosis, highlights the importance of finding more effective treatments to improve both prognosis and QoL of these patients.

In recent years, investigation of molecular and genetic alterations has improved our understanding of the complex biology of these tumours, allowing identification of distinct genetic profiles associated with different subtypes of glioblastoma[7]. Glioblastomas are classified into the following classes [8-12]:

- Classical. These tumours exhibit the most common genomic alterations described in glioblastomas, i.e. chromosome 7 amplifications, chromosome 10 deletions, EGFR (epidermal growth factor receptor gene) amplification and CDKN2A (encoding for INK4A and ARF) deletion.
- Mesenchymal. This subtype shows high expression of CHI3L1 (chitinase-3-like protein 1 gene) and MET (c-Met or hepatocyte growth factor receptor gene), high frequency of NF1 (neurofibromin 1 or neurofibromatosis-related protein NF-1 gene) mutation/deletion and more pronounced necrosis and inflammation, with expression of genes involved in wound healing and NF-KB signalling.
- Proneural. These tumours are more common in younger patients and have a higher rate of PDGFRA (platelet-derived growth factor receptor alpha gene), IDH1 (isocitrate

dehydrogenase 1 gene) and TP53 (tumour protein p53 gene) abnormalities. All these characteristics have also been associated with secondary glioblastomas, i.e. glioblastomas derived from progression of lower-grade gliomas, as opposed to primary glioblastomas which arise *de* novo[13].

- Neural. This subtype is characterised by expression of GABRA1 (gamma-aminobutyric acid receptor subunit alpha-1 gene), NEFL (neurofilament light polypeptide gene), SLC12A5 (potassium-chloride transporter member 5 gene) and SYT1 (synaptotagmin-1 gene), all neuron markers.

Several studies analysed the correlation between specific genetic profiles and clinical outcome, suggesting their possible predictive role in terms of benefit from anticancer treatment[12, 14-17]. Though, their use to personalize therapy of glioblastomas, guiding selection of therapeutic options, is still premature[18, 19].

Current standard treatment primarily involves neurosurgical evaluation to assess feasibility of maximal safe resection. When appropriate, this procedure should always be performed, given that extent of surgery is associated with increased survival[20, 21] and bulk reduction results in decompression of surrounding structures with improvement of symptoms. Approximately 20-30% of patients are not eligible for surgery at all and simply undergo a diagnostic biopsy[4]. Following surgery or biopsy, patients are evaluated based on their performance status (PS) and age:

- Karnofsky PS (KPS) ≥70 and age ≤70 years, fractionated external beam radiotherapy (EBRT) with concurrent and adjuvant temozolomide (TMZ)[22];
- KPS ≥70 and age >70 years, fractionated EBRT with concurrent and adjuvant TMZ (not licensed in all countries), fractionated EBRT or TMZ (evidence for different options reviewed in Laperriere et al 2013[23]);
- KPS <70, fractionated EBRT or TMZ or best supportive care[24, 25].

Following approval of the current standard regimen with temozolomide, other new therapeutic approaches have been shown to be active in patients with relapsed glioblastoma. Amongst these, two received approval by the US Food and Drug Administration (FDA)[26], but not by the European Medicines Agency (EMEA):

- Bevacizumab, a humanized monoclonal antibody that targets vascular endothelial growth factor (VEGF). This approach has a strong theoretical rationale in glioblastomas, given that: these tumours have a very high vasculature density[27]; glioblastoma cells express VEGF[28]; targeting blood vessels is likely to disrupt the perivascular niche of cancer stem cells[29]. The FDA licensed the use of bevacizumab for recurrent glioblastoma, based on the results of two phase ll clinical trials, which showed objective responses in pre-treated patients, with

a median survival of around 9 months[30, 31]. The EMEA refused approval because "validity of objective response rates as a surrogate endpoint for clinical benefit has not been established" and "due to the lack of a randomised concurrent control"[32]. Following the initial enthusiasm towards anti-angiogenic drugs, a phase lll trial, evaluating the use of bevacizumab as first line therapy in combination with current standard treatment, was conducted by the Radiation Therapy Oncology Group (RTOG): no overall survival improvement from the addition of bevacizumab was reported[33]. Several clinical trials are on-going and will likely address some of the controversies regarding the use of bevacizumab in glioblastomas, such as the optimal treatment schedule and dose, the most appropriate therapeutic agent for combination, the most reliable way to evaluate radiographic response[34].

- Tumour Treating Fields (TTF), consisting in low intensity, intermediate frequency, alternating electric fields, emitted by a portable device and administered via transducer arrays applied onto the scalp[35]. The anticancer effect is due to cell death of the proliferating tumour population, which some investigators interpret as a consequence of mitotic spindle disruption during the metaphase to anaphase transition and aggregation of macromolecules and organelles during telophase[36, 37]. The FDA approved the use of TTF for recurrent glioblastoma based on the results of a phase lll clinical trial comparing TTF alone to physician's choice chemotherapy: overall survival did not differ in the two arms; responses were more frequent in the experimental arm, though not significantly; toxicity and quality of life were more favourable in patients treated with TTF[38]. Currently, a randomised phase III clinical trial is enrolling newly diagnosed patients who have undergone standard radiochemotherapy: TTF in combination with adjuvant temozolomide will be compared to temozolomide alone[39]. This trial will give an indication of whether this new treatment modality can be beneficial as first line therapy in glioblastoma patients.

1.2 Current clinical research on glioblastomas: what are the targets and are these linked to cancer stem cells?

Currently, there are numerous clinical trials exploring different approaches to improve outcome of patients with glioblastoma. In order to review these, I referred to the online database on the National Cancer Institute website (http://www.cancer.gov/clinicaltrials/search) and searched for relevant references, focusing on possible links with cancer stem cells (CSCs), which form the subject of my thesis. The main approaches grouped according to their target or therapy mode are summarized below, with a "CSC link" paragraph where relevant:

- **inhibitors of VEGF receptors (VEGFRs) and other protein kinases.** These drugs are anti-angiogenic agents but, differently to bevacizumab, which binds extracellular VEGF, they target intracellular pathways of VEGFRs and other receptors for angiogenic cytokines, such as platelet-derived growth factor (PDGF) and fibroblast growth factor (FGF). Given that these are amongst the mechanisms involved in resistance to bevacizumab treatment[40], multi-kinase inhibitors might have a stronger anti-tumoral effect, especially as some of these agents also inhibit other pathways that are dysregulated in cancer cells, such as mitogen-activated protein (MAP) kinase, c-kit and RET tyrosine kinase pathways.

  CSC link with VEGFRs. A recent study showed that glioblastoma stem cells (GSCs) preferentially express VEGFR2 and that they exhibit a persistent autocrine VEGF–VEGFR2–Neuropilin-1 loop which increases their viability, self-renewal and tumorigenicity[41]. The authors suggest that this signalling pathway contributes to bevacizumab resistance, which would in part be due to the formation of new blood vessels, following bevacizumab-induced disruption of the tumour vasculature, by cancer cells expressing high levels of VEGFR2.

  CSC link with PDGFRs. A recent study reported that GSCs have higher levels of PDGFRβ, compared to other cells, and that targeting PDGFRβ in GSCs reduces their CSC marker expression, self-renewal, migration and invasion ability and *in vivo* tumour growth[42]. The authors also report the results of a survival analysis of the Repository of Molecular Brain Neoplasia Data (REMBRANDT), which suggest that higher levels of PDGFRβ are associated with poorer prognosis in glioblastoma patients.

  CSC link with MAP kinases (also known as extracellular-signal-regulated kinases, ERKs). GSCs have been shown to undergo differentiation and become less tumorigenic following blockage of MEK/ERK activity by inhibitors or siRNA[43].

- **other anti-angiogenic drugs, inhibiting**:
  - **endoglin**, a transforming growth factor beta (TGF-β) co-receptor expressed on proliferating tumour endothelial cells, which is involved in several mechanisms of vascularization: angiogenesis (formation of new blood vessels from pre-existing vessels), vasculogenesis (de novo generation of blood vessels through differentiation of circulating bone marrow-derived endothelial progenitor cells) and vascular mimicry (formation of new blood vessels through trans-differentiation of cancer cells into endothelial cells)[44]. The use of its inhibitor alone or in combination with bevacizumab is supported by the observation that its expression is up-regulated on tumour endothelial cells following inhibition of the VEGF pathway and generally in hypoxic areas[45, 46].

    CSC link with endoglin. GSCs have been shown to be responsible for vascular mimicry in glioblastomas[47-49]. A study analysing the prognostic value and staining pattern of different vessel markers in paediatric high grade gliomas, found an association between endoglin and poor prognosis, and, most importantly in this context, showed that a proportion of endoglin positive blood vessels were also positive for the putative GSC marker CD133[50]. The authors suggest that this observation is an indication of vascular mimicry and that targeting endoglin might have a therapeutic advantage by disrupting the microenvironment where GSCs preferentially reside.
  - **angiopoietins 1 and 2**, two cytokines that are involved in angiogenesis and play a role in anti-angiogenic treatment resistance through various mechanisms, such as vessel co-option (use of pre-existent blood vessels which are hijacked by tumour cells that migrate along them) and recruitment of Tie2-expressing monocytes (TEMs), myeloid cells that have been shown to stimulate tumour angiogenesis[40].

    CSC link with angiopoietin 1. GSCs have been shown to express the endothelial vascular receptor Tie2. Activation of Tie2 by angiopoietin 1 increases resistance of these cells to various chemotherapy agents, their adhesion to endothelial cells and invasion ability[51, 52]. Inhibition of the angiopoietin 1/Tie2 axis could potentially improve outcome by increasing chemosensitivity, disrupting the perivascular niche and reducing tumour invasiveness.
  - **protein kinase C β (PKCβ)**, a protein kinase which has been implicated in various processes involved in cancer progression, such as VEGF-induced angiogenesis, proliferation, apoptosis and invasiveness of tumour cells[53].
  - **integrins $\alpha_v\beta_3$, $\alpha_v\beta_5$ and $\alpha_5\beta_1$**, heterodimeric receptors that mediate cell-cell and cell-extracellular matrix (ECM) interactions and are involved in angiogenesis and invasion

of solid cancers[54]. These integrins are potentially promising targets in glioblastomas, given that: $\alpha_v\beta_3$ and $\alpha_v\beta_5$ are up-regulated not only in tumour blood vessels but also in glioma cells[55]; integrin $\alpha_5\beta_1$, in addition to its pro-angiogenic role, is involved in TMZ resistance and expression levels of the α_5 subunit are correlated with poorer prognosis in high grade gliomas[56].

- **antibody-drug conjugate (ADC) against prostate-specific membrane antigen (PSMA)**, a transmembrane glycoprotein expressed in endothelial cells of glioblastoma blood vessels and absent in normal brain[57]. The potential advantage of this approach is that it targets directly the endothelium of the tumour vasculature, therefore avoiding two possible causes of treatment resistance, the blood-brain barrier protection and activation of alternative pro-angiogenic pathways.
- **molecules inhibiting the epidermal growth factor receptor (EGFR) only** (Cetuximab and Erlotinib)**, EGFR and ErbB2** (Lapatinib) **or EGFR, ErbB2 and ErbB4** (Dacomitinib). The rationale for targeting EGFR is based on the observation that it is amplified or mutated in over 40% of glioblastomas[58], with up to 40% of the EGFR-amplified tumours harbouring the constitutively active EGFR variant III (EGFRvIII) mutation[59], and that these genetic abnormalities are associated with increased proliferation and invasion of glioma cells[60]. Despite these promising findings, analysis of the impact of EGFR amplification and mutation on survival of glioblastoma patients has shown conflicting results, as have various clinical trials[61]. Approaches aimed at improving the efficacy of EGFR-targeting treatments include:
    - **immunotherapy approaches** with the aim of inducing specific immune responses against EGFRvIII-expressing cells. One involves the use of a cancer vaccine, consisting of the EGFRvIII peptide sequence conjugated to a carrier protein, given with GM-CSF[62]; the other consists of the administration of anti-EGFRvIII white blood cells, obtained by transducing peripheral lymphocytes from glioblastoma patients with vectors for anti-EGFRvIII chimeric antigen receptors (CAR)[63].

      CSC link with EGFRvIII. During the development of the second approach, EGFRvIII expression was shown in all the tested GSC lines and these were efficiently targeted by the anti-EGFRvIII CAR-engineered T cells[63].
    - **inhibitors of multiple ErbB family members**. The potential advantage of this approach is based on the observation that ErbB2 and ErbB3 harbour activating mutations in a subpopulation of glioblastoma patients[58] and that they undergo in vitro compensatory activation following EGF deprivation[64].

CSC link with ErbB family members. The latter study tested the effect of EGF withdrawal on GSCs and compared colony formation ability of these cells following inhibition of EGFR alone (cetuximab) to blockage of EGFR and ErbB2 (lapatinib)[64]. Dual inhibition gave a greater reduction in clonogenicity and decreased activation of downstream targets of the ErbB family, such as Erk 1 and 2 and Akt. Given these findings and that these pathways have been linked to CSC biology (see above for Erk[43] and below for Akt), the authors suggest that inhibiting multiple ErbB family members is likely to target more effectively the subpopulation of cells responsible for treatment resistance.

- **multi-tyrosine kinase inhibitors**. These drugs mainly target the Src family, c-Kit and/or Eph/ephrin signalling.
    - Src and Src-family kinases are downstream effectors of several growth factor receptors and, therefore, regulate various processes involved in tumour progression. Their relevance as targets in glioblastomas is suggested by their frequent activation in glioblastoma cell lines and patient specimens[65, 66], and their role in mediating the oncogenic effect of EGFR and EGFRvIII in an *in vivo* model[67].
    - c-Kit (also known as stem cell factor receptor, SCFR) is a tyrosine kinase receptor that following binding with its ligand, the stem cell factor (SCF), activates several signalling cascades, including Src, MAPK and phosphatidylinositol 3-kinase (PI3K) signalling, and therefore induces proliferation, survival, migration and angiogenesis[68]. Several studies have reported amplification of its gene in glioblastomas, although the percentage of tumours harbouring this varies considerably amongst different patient series (between 4% and 47%), as does its prognostic significance[69-72].
    - the Eph receptors are the largest family of tyrosine kinases, and together with their ligands, the ephrins, they are involved in regulation of glioma cell growth, migration and invasion, and angiogenesis. Given that these proteins have both tumour growth promoter and suppressor potentials, their role in glioma progression is complex and probably results from an imbalance in their function[73]. Also, Ephs and ephrins frequently show altered expression in glioblastomas, with a significant correlation to patient outcome. All these findings suggest that targeting Eph/ephrin signalling could be a potentially effective anti-cancer strategy.

      CSC link with Eph/ephrin signalling. Two recent studies showed that GSC express EphA2 and that knockdown or downregulation of EphA2 causes reduction of GSC

stemness, with decreased self-renewal, stem marker expression and tumorigenicity[74, 75].

- **molecules inhibiting the PI3K-AKT-mTOR pathway**. This signalling pathway is often deregulated in glioblastomas. The Cancer Genome Atlas project showed that 15% of patients had amplification or activating mutations of PIK3CA, the gene encoding the p110a subunit of PI3K, or PIK3R1, the gene encoding the p85 regulatory subunit of PI3K[58]. The same study reported that in 36% of cases there was an inactivating genetic alteration of phosphatase and tensin homolog (PTEN), a tumour suppressor that antagonizes PI3K activity. Furthermore, given that PI3K is activated by EGFR, the amplifications and activating mutations of this receptor's gene mentioned above also have a positive effect on PI3K signalling. These data suggest that the PI3K-AKT-mTOR pathway could be a promising target for glioblastomas.

  CSC link with the PI3K-AKT-mTOR pathway. Several studies have shown a role of PI3K signalling in GSC biology. Treatment with PI3K inhibitors was shown to give a reduction of GSCs identified with two different approaches, the side population method and CD133 expression[76, 77]. The study using CD133 expression to enrich for GSC also showed a reduction in sphere formation ability and tumour growth *in vivo*, following treatment with NVP-BEZ235, a dual PI3K/mTOR inhibitor. This effect was potentiated by combining this drug with MEK/ERK inhibition[43]. Another study investigating the positive impact of hypoxia on expansion of CD133+ cells, showed that this effect could be reversed by inhibiting PI3K or mTOR[78]. More recently, the interaction between CD133 and PI3K was analysed, showing that CD133 directly regulates PI3K/Akt signalling: CD133+ cells had higher levels of PI3K activity than CD133- cells; also, following CD133 knockdown the PI3K/Akt pathway was inhibited, with a concomitant reduction in sphere formation and tumorigenicity of GSCs[79]. The effect of PI3K/Akt/mTOR pathway inhibition on radiosensitivity of GSCs was investigated in two studies, with partially conflicting results: despite the common observation of autophagy induction, one paper reported no effect on radiosensitivity or even a tendency to reduce it, the other showed an increase[80, 81]. These data highlight the importance of the PI3K-AKT-mTOR pathway in GSC biology and the need for a better understanding of its interactions in order to design more effective combination approaches[82].

- **molecules inhibiting hepatocyte growth factor (HGF)/MET signalling**. A vast body of evidence supports the rationale for targeting HGF (also known as scatter factor) and its receptor, MET, in glioblastoma patients. MET amplification and overexpression have been reported in 4% and 29% of patients, respectively[58, 83]. Higher levels of MET expression are

associated with poorer prognosis[83-85]. One study also demonstrated a significant correlation between MET overexpression in glioblastoma patient specimens and increased tumour invasiveness both radiologically and on the molecular level[83]. This finding is consistent with the well-known role of HGF/MET signalling in promoting 'invasive growth' of cancer cells[86]. MET has also been implicated in treatment resistance to EGFR and VEGF inhibitors: both types of anticancer agents caused an increase of MET activity in glioma cells, *in vitro* and *in vivo*, with the induction of a pro-survival and invasive response[87-89]. Based on these data, one of the proposed uses of HGF/MET signalling inhibitors is in combination with EGFR or VEGF inhibitors. Another promising approach is combining MET pathway inhibition with radiotherapy, given that blocking MET signalling radiosensitizes glioma cells, both *in vitro* and *in vivo,* through impairment of DNA damage repair[90-92].

CSC link with HGF/MET signalling. Several studies demonstrated the role of MET in regulating the GSC phenotype. The first, which used glioblastoma-derived neurosphere cultures, showed that HGF treatment increased their self-renewal ability and impaired their capacity to differentiate in response to differentiating stimuli, via the induction of transcription factors known to regulate the expression of stem-like features, such as Nanog, Sox2, c-Myc, Oct4 and Klf4. MET inhibition gave the opposite effect[93]. Another study analysing glioblastoma patient specimens showed that MET-positive cells were closer to blood vessels compared to MET-negative cells, a feature known to be characteristic of GSCs[29]. These authors also reported that tumour-derived MET^{high} cells formed neurospheres and generated tumours *in vivo* more efficiently than their matched $MET^{low/negative}$ cells[94]. Two recent studies using in vivo models further confirmed the role of MET in regulating stemness of GSCs through a process of cellular reprogramming[95, 96].

- **histone deacetylase (HDAC) inhibitors**. An imbalance in acetylation of histones and other proteins, due to increased activity of HDACs or inactivity of histone acetyltransferases (HATs), results in epigenetic changes that are now recognized to play an important role in tumourigenesis and treatment resistance[97]. Both pre-clinical and clinical data indicate that HDAC inhibitors could potentially be an effective treatment against glioblastomas. Pre-clinical studies have shown that these drugs have several anticancer mechanisms, including: induction of cell death via apoptosis, mitotic failure, accumulation of reactive oxygen species and autophagy; inhibition of angiogenesis; increase in natural killer cell-mediated anticancer immune response[97, 98]. Promising clinical data come not only from early phase clinical trials with vorinostat, a small-molecule inhibitor of most HDACs, but also from retrospective analyses of the effects of valproic acid on outcomes of glioblastoma patients[99-102]. Valproic acid, which was used for its antiepileptic properties,

gave a benefit in terms of overall survival in newly diagnosed patients treated with radiation with or without temozolomide. This positive effect supports the development of HDAC inhibitors in the clinic, given that it is mainly explained by the HDAC inhibitory properties of valproic acid, which confer to this drug not only antitumoral activity, but also radiosensitizing action[103, 104].

CSC link with HDAC. HDAC inhibitors have been shown to inhibit neurosphere formation, induce differentiation and reduce tumorigenicity of GSCs. This effect was linked to up-regulation of the noncanonical Notch ligand Delta/Notch-like epidermal growth factor (EGF)-related receptor (DNER) in one study[105], to decreased expression of the histone methyltransferase Enhancer of Zeste 2 (EZH2) in another[106]. These findings confirm the complexity of the mechanism of action of HDAC inhibitors and highlight the need for a better understanding of its antitumoral effect in order to maximize its benefits in the clinic.

- **poly ADP-ribose polymerases (PARP) inhibitors**. The rationale for the use of these drugs in glioblastoma patients is mainly based on enhancing the cytotoxic effect of DNA lesions caused by standard therapy[107]. TMZ and ionizing radiation cause various types of damage to DNA, some of which are recognized and processed by the base excision repair (BER) pathway. Given that PARP is implicated in BER, several studies have tested the effect of combining PARP inhibitors with TMZ and/or radiotherapy. Early studies showed that PARP inhibition increased sensitivity of glioblastoma cells to TMZ both *in vitro* and *in vivo*[108, 109]. Subsequent research demonstrated that PARP inhibitors also induce radiosensitization of glioma cells and that this effect is replication dependent[110, 111]. This feature is potentially very promising for increasing the therapeutic index of radiotherapy in glioblastomas given that these tumours are highly proliferative while their surrounding normal tissue is virtually non-dividing.

  CSC link with PARP. A recent study suggested that GSCs rely on PARP to tolerate the effects of the increase in reactive oxygen species observed in these cells, i.e. single strand DNA breaks and oxidative base damage. PARP inhibition reduced self-renewal of GSCs *in vitro* and, in combination with radiotherapy *in vivo*, it decreased the radiation-induced enrichment of GSCs[112].

- **microtubule inhibitors**. These drugs stabilize microtubules during cell division and therefore induce blockage of cells in G2/M phase and apoptosis. Hence, they target dividing cells and have a radiosensitizing effect, as G2 and M are phases during which cells are more sensitive to radiation. This mechanism of action supports their use in glioblastomas given that these tumours have a high percentage of proliferating cells and that they are treated with radiotherapy. Amongst microtubule inhibitors, a first generation

taxane, paclitaxel, was tested with or without radiotherapy and yielded modest results in terms of response and survival in phase II clinical trials[113-115]. This disappointing outcome has been attributed to the low concentration of drug in the central nervous system (CNS), despite its highly lipophilic nature. It has been suggested that this feature is partly due to the fact that Paclitaxel is a substrate of the transporter P-glycoprotein 1 (p-gp), a multidrug resistance (MDR) protein[116]. Consequently, microtubule inhibitors with an increased CNS penetration and not affected by MDR mechanisms were developed and are being tested in the clinic[117-120].

- **hypoxia modifying techniques**. Two modalities are currently being tested to increase oxygen concentration in glioblastoma patients:
    - **hyperbaric oxygen (HBO) therapy**. HBO modifies the partial pressure of oxygen (pO_2) in the tumour by increasing plasma pO_2 and this effect is maintained for minutes following the end of each treatment session[121]. A phase II clinical trial showed the safety of HBO when combined to chemo-radiation and suggested its efficacy in terms of survival[122].
    - **cervical spinal cord stimulation (SCS)**. SCS increases tumour pO_2 by augmenting the regional blood flow. The mechanism underlying this vascular effect remains uncertain and the biological consequences of this microenvironment modification need to be evaluated[123].

  Both techniques are likely to increase radiosensitivity of tumour cells in hypoxic areas, while SCS also has the potential of improving regional drug delivery based on its positive effect on blood flow.

  CSC link with hypoxia. The role of hypoxia in GSC biology is well established and is reviewed in section 1.4. Treatments that increase tumour pO_2 could potentially reduce growth and stemness of glioblastoma cells, though it is not known whether the transient modifications in pO_2 caused by HBO and SCS are capable of reversing the hypoxia-induced changes in GSCs.

- **proteasome inhibitors**. The 26S proteasome is involved in regulating several processes, such as cell cycle progression, apoptosis, cell adhesion and migration, angiogenesis. Altered proteasomal activity that results in deregulation of these functions is associated with carcinogenesis[124]. *In vitro* experiments showed that proteasome inhibitors induce apoptosis and reduce proliferation of glioblastoma cell lines and explants[125, 126]. These drugs also exhibited an inhibitory effect on O6-methylguanine–DNA methyltransferase (MGMT), a DNA repair protein involved in TMZ resistance, supporting the rationale for a

therapeutic approach combining proteasome inhibitors to current standard treatment[127, 128]. A phase I clinical trial showed the feasibility and safety of this strategy[129].

CSC link with proteasome. The role of proteasomes in GSC biology is difficult to interpret based on the current literature, as various studies have used different approaches and have given partially conflicting results. One of the main groups researching this area published several papers showing that:

- lower proteasomal activity is associated with GSC phenotype, i.e. neurosphere formation, CSC markers expression, tumorigenicity[130].
- patients with glioblastomas with lower proteasomal activity have a significantly shorter overall survival[131].
- GSCs have a different metabolic state compared to more differentiated tumour cells, as they rely less on glycolysis, they consume less glucose, produce less lactate and have higher ATP levels; these features were associated with lower proteasomal activity[131]. These findings are consistent with recent data suggesting a metabolic regulation of proteasomes[132].
- proteasomal activity in GSCs is downregulated by Musashi-1, an mRNA-binding protein overexpressed in CSCs; this contributes to maintenance of the stem cell phenotype[133].

Based on these data, the authors suggest that proteasome inhibition might not be an effective approach to target GSCs[133]. Though, a study comparing toxicity of various chemotherapy agents in GSCs and neural stem cells found that proteasome inhibition with bortezomib induced apoptosis in GSCs while sparing normal cells and that this effect was inversely correlated with baseline proteasome expression and activity[134]. Also in favour of the possible efficacy of proteasome inhibitors in targeting GSCs is a comparative expression microarray analysis of GSCs that survived radiochemotherapy, showing that these cells have: reduction in glucose uptake, increase in lipid catabolism, activation of oxidative stress responses, blockage of proliferation and differentiation, and intensification of cellular maintenance and repair activities. Amongst various genes upregulated to mediate these effects are those involved in ubiquitin-proteasomal pathways[135]. These findings are consistent with those above concerning the metabolic state of GSCs, but appear to be in contrast with regards to proteasomal activity. This inconsistency could be due to the use of different populations in the two studies, as the latter focused on selected GSCs obtained from the expansion of few cells surviving ionizing radiation and TMZ *in vitro*.

Finally, several studies testing the efficacy in glioblastomas of another proteasome inhibitor, disulfiram, showed that this drug reduced proliferation and self-renewal of GSCs

both *in vitro* and *in vivo*[136, 137]. Disulfiram also targets aldehyde dehydrogenase (ALDH), a putative GSC marker, but *in vitro* data suggest that the cytotoxic effect on GSCs is due to inhibition of proteasomal activity[138].

Given these findings, the use of proteasome inhibitors in glioblastoma patients appears promising, especially in combination with chemoradiation.

This brief review of the main approaches that are currently being tested in clinical trials demonstrates the complexity of glioblastomas and highlights how relevant and topical the cancer stem cell theory is in this disease. I will now introduce, in the next section, this theory and review the main findings regarding the role of GSCs in treatment resistance.

1.3 Cancer stem cell theory: what is the evidence for the existence and the clinical significance of these cells in glioblastomas?

The cancer stem cell theory postulates that tumours are composed by a heterogeneous population of cells with a specific hierarchy; only those cells that are at the top of that hierarchy, i.e. CSCs, are able to self-renew and propagate tumours, and therefore are responsible for clinical recurrence[139]. The traditional model also recognizes the heterogeneity of cell populations within a cancer, but holds any of the cells composing the tumour bulk responsible for recurrence. According to the cancer stem cell model only treatments that target CSCs can effectively eradicate cancers and result in a positive long term outcome for patients.

GSCs are characterised by the following features:

- capacity to generate a continuously growing tumour. This characteristic is tested evaluating induction of invasive tumoral masses following intracranial injection of 10^6, 10^5, 10^4, 10^3 or even 10^2 selected cells in mice.
- self-renewal ability. Self-renewal is a process by which cells divide to generate one or two daughter cells that retain self-renewal capacity[140]. A self-renewing cell division can be:
    - symmetrical, which results in two identical daughter stem cells with the same developmental potential as the mother cell;
    - asymmetrical, which gives one stem cell and one more differentiated progenitor cell.

  This feature is of paramount importance as its regulation under various stimuli allows GSCs to regenerate differentiating daughter cells, which form the tumour bulk, while maintaining a pool of self-renewing stem cells[141].

  Self-renewal is evaluated *in vitro* testing the ability of single cells to form neurospheres when cultured in the appropriate conditions.

  CSC division and the rationale for targeting this process to eradicate GSCs will be reviewed in detail in the last section of this introduction.
- potential to differentiate into the heterogeneous lineages of cancer cells that make up glioblastomas, i.e. astroglial, neuronal and oligodendroglial cells. This feature is tested evaluating expression levels of stem cell and differentiation markers in cells exposed to differentiating stimuli, such as serum-containing medium.

  Enhancement of this attribute has been investigated as an anticancer approach in differentiation therapies, at first with retinoids and more recently with bone morphogenetic proteins (BMPs). Despite the preliminary encouraging findings on the use

of retinoic acid in glioblastomas, a phase II clinical trial in newly diagnosed patients did not suggest an advantage in adding this drug to radiation and/or chemotherapy, and therefore did not justify phase III testing[142]. Research on the use of BMPs in glioblastomas is mostly preclinical, but it has already highlighted many complexities. On the one hand, BMP4 and BMP7 have been proposed as potential therapeutic agents following *in vitro* and *in vivo* studies showing that they are capable of inducing CSC differentiation and prolonging survival of mice injected with GSCs[143, 144]. On the other hand, a study testing the effect of BMP2 on several GSC lines demonstrated that treatment with this protein induced differentiation or proliferation depending on the status of BMP receptor 1B in these cells[145]. Also, a recent study showed that GSCs overexpress Gremlin 1, a BMP antagonist, and that this allows them to maintain their stemness despite high levels of BMPs in the tumour[146]. Given these findings, a better understanding of the BMP signalling pathway and its regulation is needed to design treatments that can effectively induce terminal differentiation of CSCs in glioblastoma patients and therefore yield the desired therapeutic outcome.

The first *in vitro* evidence for the existence of CSCs in brain tumours was published in 2002, when Ignatova *et al*. reported the isolation from high grade gliomas of cells that could form clones under culture conditions used in neural stem cell research, i.e. these cells could grow as neurospheres in serum free medium supplemented with epidermal growth factor (EGF), fibroblast growth factor (FGF) and insulin[147]. These "neural stem-like cells" were also shown to differentiate and express astroglial and neuronal markers following serum stimulation. Soon after, Singh *et al*. confirmed these findings *in vitro* and developed an intracranial xenograft assay, showing that a subpopulation of cells isolated from glioblastoma specimens was capable of inducing tumours phenotypically resembling the patient's original specimen[148, 149]. These cells, selected for CD133 expression, gave tumours at a very high frequency (100 cells were sufficient) and could be serially transplanted, while the rest of the population, i.e. CD133-negative cells, was not tumorigenic, following the injection of up to 10^5 cells.

Thereafter, a vast number of studies reported the isolation of CSCs from glioblastoma patient specimens, using various techniques and yielding a wide range of results in terms of tumorigenicity of selected cells. Anthony Chalmers and I summarised these findings in a review at the beginning of my doctoral studies (see Appendix)[150]. At the time, two main methods were used to enrich populations for stem cells:

1) expression of putative stem cell markers, such as CD133, A2B5, SEEA-1 and integrin α6[149, 151-159].

2) growth in serum free medium supplemented with growth factors, as spheres (in uncoated flasks) or adherent cultures (in extracellular matrix or laminin coated flasks)[154, 160-165].

Since then, the variety of methods has not diminished, but it is now widely accepted that a single marker is unlikely to define GSCs derived from all patient specimens[166]. Identification of GSCs based on analysis of CD133 staining, for example, can be misleading given that: expression levels of this marker fluctuate throughout the cell cycle[167-169]; recognition of the cell-surface epitope by specific antibodies is influenced by posttranslational modifications[170].

Also unchanged is the lack of standardization of the culture conditions, despite their well-known strong impact on CSC biology[171]. Even the nomenclature to define these cells is still not clear, as different names (cancer stem cells, stem-like cancer cells, tumour-initiating cells) are used in various studies and often not in the same way[172, 173]. This impossibility to identify a universal technique for the isolation of GSCs *in vitro* and the lack of standardization in the CSC methodology probably constitute the main arguments against the cancer stem cell theory. However, these controversies are outweighed by the consistency of clinical data regarding the prognostic value of GSC features, summarized in table 1. The vast majority of studies showed a statistically significant correlation between various GSC features in glioblastoma patient specimens and poorer outcome. A few reported no difference and a couple a positive effects on overall survival. Limitations of these data are that: 1) most studies were retrospective; 2) multivariate analysis was not always performed and in most cases did not include all the established prognostic factors; 3) a wide range of cut-offs in GSC marker expression were used to define subgroups, for example for CD133 the cut-off ranged from 1% to 50% in different studies; 4) studies on putative GSC markers focused only on one or two proteins. The weakness of the latter approach in this setting was highlighted by a very interesting study analysing CD133 expression in paired glioblastoma patient specimens, comprising a sample from the primary tumour and one from the recurrence after adjuvant chemoradiation[174]. Following the observation that a more pronounced increase in CD133 expression in recurrent tumours was associated with a significantly longer survival after recurrence, CD133 positive cells were characterized more in detail to verify their nature. Co-labelling with CD34 and CD45 was used to quantify the fraction of CD133-positive cells of endothelial and hematopoietic origin, respectively. Analysis of tumour-specific chromosomal aberrations and *in vivo* tumorigenicity assays allowed the identification of normal neural stem cells amongst the CD133-positive population. Surprisingly, these experiments showed that a minority of the CD133-positive population was of tumoral origin and that the percentage of normal neural stem cells was associated with a significantly longer patient survival after recurrence. These findings demonstrate the need for more extensive approaches when identifying GSCs and

analysing their clinical significance. Amongst those used in the studies summarized in table 1, analysis of multiple gene expression profiles and ability to grow as neurospheres in specific culture conditions probably constitute the most reliable methods.

Table 1. Clinical studies analysing the correlation between GSC features and patient outcome.

Study	**Type of analysis**	**Number of patient specimens**	**Analysed factors**	**Multivariate analysis factors**	**Statistics for endpoint**
Strojnik et al 2007[175]	Retrospective	87 gliomas (54 glioblastomas)	A) Nestin expression B) Musashi expression	Patient age and gender, cathepsins B and L.	A) Shorter OS: $p < 0.001$. B) OS: no significant difference.
Mangiola et al 2007[176]	Retrospective	20 glioblastomas	Nestin and JNK expression		OS: no significant difference.
Zhang et al. 2008[177]	Retrospective	125 gliomas	Co-expression of Nestin and CD133	Tumour grade	Shorter OS: $p < 0.01$
Pallini et al. 2008[178]	Prospective	44 glioblastomas	A) CD133 expression (≥2% vs <2%) B) in vitro neurosphere formation ability (present vs absent)	Symptom duration, extent of resection, patient age, MGMT status and p53 status.	Higher risk of death A) HR 2.22 ($p = 0.03$) B) HR 2.92 ($p = 0.005$)
Zeppernick et al 2008[179]	Retrospective	95 gliomas (47 glioblastomas)	A) CD133 expression (>1% vs ≤1%) B) organization of these cells (cluster vs single cells)	Histological grade, patient age and extent of resection	Shorter OS: A) HR 17.46 ($p < 0.001$) B) HR 5.62 ($p < 0.001$).
Murat et al 2008[180]	Retrospective	80 glioblastomas from two prospective clinical trials comparing RT+TMZ (A) to RT alone (B)	Hox genes, comprising CD133 gene	Patient age, MGMT status and EGFR expression.	(A) Shorter OS: HR 3.32 ($p = 0.001$). (B) OS: no significant difference.

Chinnaiyan et al 2008[181]	Retrospective	153 glioblastomas from RTOG prospective clinical trials	Nestin expression (high, intermediate and low, based on intensity and positive area)		OS and PFS: no significant difference.
Laks et al 2009[182]	Retrospective	15 glioblastomas	"Renewable neurosphere formation"	Ki67 staining.	Shorter OS: HR 17 (p =0.49) Shorter PFS: HR 4.7 (p =0.034)
Sihto et al 2009[183]	Retrospective	43 glioblastomas	SCF (high vs low)		Shorter OS: p =0.034
Colman et al 2010[184]	Retrospective	4 glioblastoma microarray data sets (MDA, MGH, UCLA, UCSF) for identification + 2 FFPE sample sets (68 and 101 glioblastomas) for validation	9-gene set including CD133 and nestin	Age and KPS.	Shorter OS: HR 2.7 (p =0.0003)
Rossi et al 2011[185]	Prospective	106 glioblastomas	β-catenin and Gli1 expression		OS: $r \leq -0.65$
Metellus et al 2011[186]	Prospective	48 glioblastomas	CD133 expression (high vs low, with mean level as cutoff)	Age, extent of surgery and MGMT gene promoter methylation.	Shorter OS: HR, 1.91 (p =0.007).
Kim et al 2011[187]	Retrospective	88 glioblastomas	Nestin expression [high (<50% positive cells) vs low] CD133 expression (positive vs negative) CD15 (positive vs negative)		OS: no significant difference.

He et al 2011[188]	Prospective	59 HGGs (33 glioblastomas)	CD133 expression (positive vs negative)		Shorter PFS: HR 2.838 (p =0.001)
Adam et al 2012[189]	Retrospective	1. 93 glioblastomas (own institution) 2. 177 glioblastomas (REMBRANDT dataset)	ALDH1A1 expression [high (>7% positive cells) vs low (≤7%)]	1. Age and MGMT gene promoter methylation.	Shorter OS: 1. HR 0.483 (p <0.01)* 2. trend towards longer OS (p = 0.071)*.
Nakata et al 2013[190]	Prospective	179 glioblastomas	LGR5 expression [high (>10% positive cells) vs low (≤10%)]	Age and gender	Shorter OS: p =0.002
Sandberg et al 2013[191]	Retrospective bioinformatics analysis	1) 77 HGGs (Phillips dataset) 2) 85 HGGs (Freije dataset)	30-gene signature expression (high vs low)		Shorter OS: 1) p =0.00859 2) p =0.00325
Shibahara et al 2013[192]	Retrospective	112 glioblastomas	CD133 expression (high vs low)	TTD: Ki67, 9p deletion and 10q loss. TTL: extent of surgical resection, Ki67 and MGMT gene promoter methylation.	Shorter TTD: HR 2.9 (p =0.038). Shorter TTL: HR 0.44 (p =0.0056)*. OS: no significant difference.
Kase et al 2013[193]	Retrospective	42 glioblastomas	CD133 expression [< median (28%) vs ≥ median)	Radiotherapy dose, chemotherapy and KPS.	Shorter OS: HR 1.99 (p =0.04)*
Binder et al 2013[194]	Retrospective bioinformatics analysis	181 glioblastomas (REMBRANDT dataset)	PODXL expression (high vs intermediate)		Shorter OS: HR 1.67 (p =0.001)

Shin et al 2013[195]	Retrospective	67 glioblastomas	CD133 expression (positive cells <50 % vs ≥50 %)	Age, gender, extent of surgery, treatment (TMZ, chemoradiation), expression levels of CD34, VEGF and IDH1.	Longer OS: HR 2.49 (p=0.037)
Dahlrot et al 2013[196]	Retrospective	187 glioblastomas	Musashi-1 expression		OS: no significant difference.
Lathia et al 2014[197]	Retrospective bioinformatics analysis	1) 76 HGGs (Phillips dataset) 2) 180 glioblastomas (REMBRANDT dataset) 3) 185 glioblastomas (Odense dataset)	JAM-A expression		OS: 1) JAM-A low longer OS than JAM-A medium and high ($p < 0.05$) 2) JAM-A low longer OS than JAM-A high ($p < 0.05$) 3) JAM-A low longer OS than JAM-A high ($p < 0.05$)
Hale et al 2014[198]			CD36 expression (high vs low)		Poorer prognosis

OS, overall survival. JNK, c-Jun NH2-terminal kinase. MGMT, O6-methylguanine–DNA methyltransferase. HR, hazard ratio. RT, radiotherapy. TMZ, temozolomide. EGFR, epidermal growth factor receptor. RTOG, Radiation Therapy Oncology Group. PFS, progression free survival. SCF, stem cell factor. MDA, MD Anderson. MGH, Massachusetts General Hospital. UCLA, University of California-Los Angeles. UCSF, University of California-San Francisco. FFPE, formalin-fixed paraffin embedded. KPS, Karnofsky performance status. HGG, high grade glioma. ALDH1A1, aldehyde dehydrogenase 1 family member A1. LGR5, leucine-rich repeat containing G protein-coupled receptor 5. TTD, time to distant recurrence. TTL, time to local recurrence. PODXL, podocalyxin-like protein. VEGF, vascular endothelial growth factor. IDH1, isocitrate dehydrogenase 1. JAM-A, junctional adhesion molecule A.

*positive prognostic effect.

Further evidence for the existence of GSCs comes from two studies using *in vivo* lineage tracing. The first consisted in the observation of matched cell populations, stem and non-stem (GSC-enrichment based on CD133 expression), derived from a glioblastoma patient specimen, labelled with two fluorescent proteins and injected into a xenograft model with a ratio of 1:9[199]. Cells were then monitored with serial *in vivo* intravital microscopy to measure the respective growth and test their relative tumorigenic potential. Analysis of sequential time points showed that GSCs were responsible for tumour formation and that their volume increased by 52 fold, while non-stem cells remained relatively unchanged (0.92 fold increase). Based on expression patterns of another putative CSC marker, SOX2, the authors also suggest that the cell population derived from GSCs is heterogeneous in terms of differentiation, i.e. it displays a hierarchy. This study is definitely more informative than standard xenotransplantation models with regards to the contribution of CSCs to cancer formation, though it does not explore their role in treatment resistance and tumour recurrence, which are the most relevant questions in the clinical setting. These were addressed by another study using *in vivo* lineage tracing in a genetically engineered mouse model of glioma[200]. The authors introduced a Nestin-ΔTK-IRES-GFP transgene into glioma prone mice, obtaining tumours with a relatively quiescent GFP+ subpopulation and a proliferating GFP- one. To test the role of these cells in treatment resistance, they treated mice with TMZ and observed that most of the GFP- cells were killed, while the quiescent GFP+ population survived. Pulse chase labelling with bromodeoxyuridine analogues demonstrated that, following TMZ treatment, GFP+ cells started to proliferate and at 7 days post-chemotherapy the proliferating population was mostly GFP-. To confirm that the originally GFP+ cells were responsible of recreating a heterogeneous population of cells and therefore giving rise to tumour recurrence, the mice were also treated with ganciclovir, which would selectively kill GFP+ cells thanks to the inclusion of a herpes simplex thymidine kinase 'suicide gene' in the GFP construct. Sequential treatment with TMZ and ganciclovir resulted in a significant reduction in maximal tumour cell density and a prolonged survival compared to TMZ only, suggesting that the relatively quiescent GFP+ subpopulation was indeed responsible for post-chemotherapy tumour growth. These findings constitute a very important chapter in the story of the CSC theory and are viewed by many experts in the field as a clear demonstration of the importance of targeting these cells to eradicate tumours and improve patient outcome[201, 202].

1.4 Glioblastoma stem cell features: what is the role of the microenvironment in maintaining these?

A large body of evidence is also accumulating on the pivotal role of the microenvironment in regulating stemness and treatment resistance of glioblastoma cells. The first indication of the importance of microenvironmental factors in GSC biology came from studies analysing the distribution of tumour cells expressing CSC markers. A comparative analysis of the distance from tumour capillaries of Nestin+ and Nestin- cells in glioblastoma patient specimens showed that cells expressing the putative stem cell marker were significantly closer to the vascular structures and were in direct contact with endothelial cells[29]. The perivascular location of GSCs was confirmed by another study investigating the distribution of CD133+ cells in glioblastoma specimens: these cells were observed in perivascular niches, in pseudopalisade formations surrounding necrotic areas and as dispersed single cells[203]. In these tumour sections, there were also many CD133+ blood vessels. This observation found an explanation in the findings of two studies, which demonstrated that CD133+ glioblastoma cells are able to differentiate into endothelial cells, both *in vitro* and *in vivo*[47, 48]. A study analysing the role of hypoxia inducible factor (HIF) 2α in GSC showed that up to 10% of tumour cells adjacent to blood vessels and necrotic areas expressed HIF2α and most of these co-expressed CD133[204]. Taken together, these data suggest an association between GSCs and perivascular and necrotic niches. Several *in vitro* and *in vivo* studies confirmed and elucidated the mechanisms underlying these interactions. The main findings of these studies are summarised below.

Perivascular niche. A study using a 3-dimentional organotypic 'explant' system derived from glioblastoma specimens, showed that selective elimination of endothelial cells via a toxin conjugate results in a reduction in neurosphere formation ability, hence a decrease in self-renewal of GSCs[205]. Another study, which used a genetically engineered mouse model of PDGF-induced glioma, observed a spatial relationship between endothelial cells expressing endothelial nitric oxide synthase (eNOS) and Nestin+ tumour cells expressing soluble guanylyl cyclase (the main receptor for nitric oxide, NO)[206]. Based on this observation and on *in vitro* experiments, the authors suggested that the effect of endothelial cells on stemness of glioma cells is mediated by NO through the Notch pathway. The link between endothelial cells, Notch signalling and GSCs, was confirmed by a study analysing the distribution of Notch ligands in glioblastoma patient specimens: Notch ligands were found in cells adjacent to Nestin+ cells, often in endothelial cells[207]. Also, *in vitro* experiments co-culturing GSCs with human brain microvascular endothelial cells (hBMEC) demonstrated an increase in self-renewal ability and in CSC marker expression, which was reversed following knockdown of Notch ligands in

hBMECs. Hence, the authors suggested that endothelial cells create a 'Notch signalling activating environment' that promotes stemness. Another study testing the effect of endothelial cell-conditioned medium on neurosphere formation, showed that self-renewal ability of GSCs was partially retained and that this culture condition was able to maintain activation of mTOR downstream targets, suggesting that endothelial cells sustain GSC self-renewal by secreting mTOR activating factors[208]. A study using a porous, polymeric scaffold as a system to evaluate the impact of paracrine endothelial cell signalling on GSCs, demonstrated that co-transplantation of human brain endothelial cells (hCMECs) with GSCs grown in the 3D model increased tumour growth relative to GSCs alone[209]. Also *in vitro* exposure of GSCs to conditioned medium from hCMEC 3D cultures induced a higher expression level of putative stem cell markers, Nestin and SOX2.

Data from other studies suggest that GSC maintenance induced by endothelial cells is also mediated by laminins and by their receptors, integrins. One showed that, in glioblastoma patient specimens, laminin α2 is expressed by tumour associated endothelial cells in integrin α6+ areas and that tumour formation *in vivo* is delayed when GSCs are injected with endothelial cells with laminin α2 knockdown[210]. A previous study from the same group demonstrated that integrin α6 is co-expressed with CD133 in glioblastoma patient specimens and that targeting this protein in GSCs reduces neurospheres formation and tumour growth *in vivo*[159]. Another integrin that might be involved in the link between the perivascular niche and GSCs is integrin α3, given that it has been shown to be preferentially expressed in tumour cells localized around blood vessels and in the invading front and that its levels are significantly higher in CD133+ cells[211].

On the one hand, these findings reveal how important the perivascular niche is for GSC biology, providing a strong rationale for targeting its elements as a therapeutic approach. On the other, they highlight how multifaceted the interaction between endothelial cells and GSCs is, suggesting that treatments aimed at perturbing this relationship need to take into account these complexities to avoid the failure experienced with previous drugs targeting blood vessels.

Perinecrotic niche. Necrotic areas in glioblastomas are the result of lack of oxygen and nutrients. Several studies have demonstrated that hypoxia increases CSC features in glioblastoma cell lines. This effect was attributed to activation of HIF1α in an *in vitro* study which showed that culturing GSC populations at 1% oxygen increased their self-renewal ability and positivity for CD133, while it reduced expression of differentiation markers[78]. The above mentioned analysis on the role of HIFs in GSCs demonstrated that targeting HIF1α or HIF2α in GSCs inhibited their self-renewal ability *in vitro* and tumorigenicity *in vivo*[204]. Though, the

authors suggested that HIF2α, not HIF1α, is the specific mediator of the effects of low oxygen levels on GSCs, based on co-expression of HIF2α and CD133 in glioblastoma patient specimens and on different mRNA levels of HIF1α and HIF2α in GSCs grown in hypoxia. Similar results were reported by another group, that demonstrated: increase in self-renewal and CD133 expression in cells incubated at 1% oxygen; up-regulation of both HIF1α and HIF2α in GSCs grown in hypoxic conditions; abrogation of the effect of hypoxia on self-renewal following knockdown of HIF1α or HIF2α; reduction of the hypoxia-induced up-regulation of CD133 in HIF2α knockdown cells but not in those with HIF1α knockdown[212]. These three studies consistently suggest a role of hypoxia in GSC biology, even though they show partially conflicting results with regards to the impact of low oxygen levels on HIF1α and HIF2α expression in GSCs and the effect of HIF knockdowns on CSC features. This inconsistency is probably due to differences in experimental procedures and, most importantly, to the use of different cell lines in the three studies, as suggested indirectly by the results included in another publication from the group proposing a specific role of HIF2α[213]. In this study they used a different cell line and showed a response of non-stem cells to hypoxia with regards to HIF2α mRNA levels, which was not seen in the other cell lines included in their previous publication.

Other investigators tested the effect of hypoxia on GSCs focusing on two aspects of cancer biology: cellular metabolism and immunosuppression.

Metabolism. Cancer cell metabolism differs from that of normal cells as it relies mainly on glycolysis for ATP production, even in the presence of sufficient oxygen levels[214]. This phenomenon, known as 'Warburg effect', translates in increased glucose uptake and lactate production. Adaptive responses to the hypoxic tumour microenvironment, together with altered signalling due to oncogene activation, are proposed as the main causes of this metabolic difference[215]. Several compounds that target glycolysis have been developed to exploit this phenomenon therapeutically. A study testing the effects of 2-deoxyglucose (2DG), a glucose analogue, on primary glioblastoma cell lines, showed that it forced them into mitochondrial metabolism and reduced CD133 and nestin expression inducing neuronal differentiation; 2DG also induced apoptosis, although this effect was reduced in hypoxic conditions[216]. While these findings suggest a possible role of glycolysis inhibitors in targeting GSCs, data from other two studies do not support this approach. One study evaluated in GSCs the effect on ATP production, i.e. energy production, of 2DG, used to target glycolysis specifically, and oligomycin, an inhibitor of mitochondrial ATP synthase, used to disrupt oxidative phosphorylation[131]. Both drugs given as a single agent reduced ATP levels marginally, while the combination had a substantial effect (40-50% decrease), suggesting that GSCs are

able to satisfy their energetic needs by using oxidative phosphorylation as well as glycolysis. Furthermore, analysis of glucose uptake and lactate production showed that GSCs consume less glucose and generate less lactate compared to more differentiated tumour cells, suggesting they rely less on glycolysis. Based on these findings, the authors concluded that therapeutic approaches aimed at disrupting glycolysis, or more generally a single metabolic pathway, are unlikely to be effective in killing GSCs[131]. Another study characterized metabolism of GSCs after dividing them into treatment sensitive and resistant clones, based on their clonogenic survival following ionizing radiation alone or in combination with TMZ. The two CSC subpopulations differed with regards to glucose uptake and response to inhibition of glycolysis (with 2DG) or fatty acid oxidation (with Etomoxir): treatment resistant GSC clones had lower glucose uptake; treatment sensitive clones showed a reduction in ATP production following exposure to either 2DG or Etomoxir, while treatment resistant clones had a decrease in ATP levels only after inhibition of fatty acid oxidation. Based on these findings and on results of a microarray analysis performed on the two subpopulations, the authors suggested that glioblastoma recurrence is driven by GSCs with a glucose restriction-like phenotype, that use fatty acid oxidation, rather than glycolysis, as their preferential energy source for ATP production[135].

Immunosuppression. Hypoxia was also shown to increase another feature attributed to GSCs, immunosuppression, given that *in vitro* experiments demonstrated the following: GSC populations produced more immunosuppressive cytokines when cultured in hypoxic conditions; exposure to GSC-conditioned medium resulted in reduction of T cell proliferation, interferon γ production by CD3+ T cells and phagocytosis in monocytes; these effects were augmented if GSCs were grown at low oxygen levels[217].

The interaction between GSCs and cells of the immune system is another important component of the CSC-microenvironment cross-talk, which is receiving increasing attention due to the development and clinical testing of several glioblastoma vaccines. This research field still has significant limitations with regards to experimental systems, given that generally used *in vivo* xenografts are unlikely to be truly representative models for tumour-immune system interactions. Indirect proof is provided by the inconsistency in the results of flow cytometry analyses characterizing inflammatory cell infiltrates in rat gliomas and in glioblastoma human specimens. In animal models, there was marked microglia infiltration in the tumours, their periphery and in the tumour-free brain; macrophages were less present within the tumours and their periphery, and rare in the tumour-free tissue; lymphocytes were more common than macrophages, but their number and distribution differed considerably amongst tumour models[218]. In glioblastoma patient specimens, macrophages were the most

common cell type in the tumoral mass; in the samples from the 'overlying normal cortex' the inflammatory cell infiltrates were quite scarce[219]. As suggested by the authors of the latter study, the observed differences might be partly due to the inherent immunogenicity of rat models, as suggested by the higher amount of lymphocytes found in the experimental tumours and the more pronounced inflammatory infiltrate present in the normal brain of the animals. Despite these limitations, these studies have highlighted the presence of monocyte lineage cells in gliomas. Increasing evidence suggests that these cells induce immunosuppression and promote glioblastoma growth and invasion[220]. Some findings also indicate a crosstalk between microglia/macrophages and GSCs. A study evaluating this interaction showed that: in glioblastoma patient specimens, there was a positive correlation between localization of microglia/macrophages and CD133+ cells; in an *in vitro* migration assay, GSC-conditioned medium attracted microglia/macrophages more efficiently than medium from more differentiated tumour cells[221]. Consistently with these results, another group reported a positive correlation in the localization of microglia/macrophages and CD133+ cells in the invasive front of glioma patient specimens, suggesting a pro-invasive effect of the immune system cells on GSCs[222].

These findings on the role of the tumoral niche in GSC biology have contributed to a more complex view of the cancer stem cell theory, which does not simplistically hold GSCs *per se* responsible for tumour recurrence, but rather identifies the origin of treatment resistance in the plasticity of GSCs modulated by microenvironmental factors.

1.5 Glioblastoma stem cells and treatment responses: what is the role of the microenvironment in regulating these?

The majority of studies analysing the effects of the microenvironment on treatment resistance of GSCs focused on ionizing radiation. Before analysing the findings regarding intrinsic and microenvironment-regulated radiosensitivity of CSCs in glioblastomas, I will review the existing data on resistance of GSCs to standard chemotherapy, i.e. TMZ, starting with a brief introduction on its mechanism of action.

1.5.1 Temozolomide resistance.

TMZ is an alkylating agent, which causes three main lesions: O6-Methyl-Guanine (O6-Me-G, 6%), N7-Methyl-Guanine (N7-Me-G, 70%) and N3-Methyl-Alanine (N3-Me-A, 9%)[223]. N7-Me-G and N3-Me-A are promptly repaired by the DNA base excision repair (BER) pathway, and therefore generally do not result in a cytotoxic effect. O6-Me-G is repaired by MGMT, which restores guanine by removing the methyl group. If levels of MGMT are insufficient, O6-MeG persists and during S phase it mispairs with thymine, instead of cytosine. This error is detected by the DNA mismatch repair (MMR) system, which is only able to recognise and excise the mispaired thymine on the daughter strand, leaving O6-MeG in the template strand. This results in cycles of thymine reinsertion and excision, with persistent DNA strand breaks and consequent replication fork collapse, which triggers G2/M cell cycle arrest via ATR/CHK1-dependent signalling. Given this mechanism of action, intrinsic cellular sensitivity to TMZ is dependent on the functionality of repair proteins involved in processing DNA damage, i.e. TMZ resistance is associated with high levels of MGMT and functional MMR. The clinical relevance of MGMT levels is fairly well established, based on several clinical studies showing that MGMT gene silencing, mostly due to methylation of its promoter, is associated with longer survival following TMZ treatment[224]. The data on MGMT and TMZ resistance in GSCs is rather complex. The association between MGMT methylation and protein expression is not clear in *in vitro* studies. The largest published analysis, including twenty GSC enriched cell lines, did not find a correlation between methylation status and protein expression; sensitivity to TMZ was correlated to MGMT levels, but not to its methylation[225]. Similarly, another study comparing TMZ response in CD133+ and CD133- cells, showed that cellular sensitivity to TMZ was inversely correlated to MGMT protein levels, but not to methylation status; surprisingly, the most sensitive population of cells was expressing the CSC marker[226] . In contrast with these findings are those from a study showing that CD133+ cells had higher levels of MGMT mRNA expression and were more resistant to TMZ, compared to CD133- cells[227]. Another group reported yet contrasting findings from analysing patient-matched GSC and non-GSC early

passage cultures: no difference in MGMT methylation status or expression levels in the two populations; TMZ sensitivity was not influenced by *in vitro* enrichment for CSCs, as it was patient specific and similar in matched populations[228]. In conflict with these results are those from two studies analysing the association between differentiation status, MGMT and GSC sensitivity to TMZ. *In vitro* differentiation of GSC populations, induced by BMP2 treatment or by changing the culture conditions, sensitized cells to TMZ and this effect was correlated to MGMT expression and methylation status, respectively[229, 230]. The variability of these findings is probably due to several factors: lack of standardization of the tested dose levels of TMZ, which can strongly impact the output of sensitivity assays; small number of cell lines used in most studies; characterization of cell lines rarely done for other factors associated with TMZ resistance, such as MMR functionality and p53 status.

Besides intrinsic cellular mechanisms, determinants of TMZ resistance in glioblastoma patients are represented by microenvironmental factors responsible for intratumoral drug concentration. TMZ concentration is influenced locally by structure and functionality of tumour vasculature and by blood flow. The importance of these factors was demonstrated with two different approaches. One used an MRI technique to analyse changes in tumour blood flow in newly diagnosed glioblastomas treated with a pan-VEGF receptor tyrosine kinase inhibitor, in combination with chemoradiation: the antiangiogenic drug increased tumour perfusion in a subset of patients, probably due to induction of a transient period of vessel normalization, and this was associated with improved overall survival[231]. Another showed that it was possible to predict the fraction of glioblastoma cells killed with chemotherapy in individual patients, by using a mathematical model based on three parameters: fraction of blood volume within the tumour, distribution of vessel diameters and drug diffusion distance through cancer tissue[232].

To my knowledge, the effect of increasing tumour blood flow on GSC response to TMZ has not been analysed specifically. Though, given that the perivascular niche is one of the preferential locations of GSCs, it is likely that these cells would be amongst the first to be exposed to higher TMZ concentrations, following treatments which increase perfusion and normalize the structure of blood vessels.

With regards to other microenvironmental factors, some evidence suggests the possible role of hypoxia in influencing TMZ sensitivity of GSCs. A study analysing distribution of cells expressing hypoxia-induced factors, CD133, differentiation markers and MGMT, in glioblastoma patient specimens, showed a link between hypoxic conditions, GSCs and TMZ resistance: there was a gradient from the core to the periphery, consisting in higher levels of CD133 and MGMT in the hypoxic core, which gradually decreased towards the outer layers; also, cell lines derived from

the core and intermediate areas were more resistant to TMZ *in vitro*, compared to those derived from the periphery[233].

This brief review summarizing the literature on sensitivity of GSCs to TMZ again highlights many complexities in the mechanisms underlying response of CSCs to standard treatment in glioblastomas, suggesting the need for a more standardized and comprehensive approach when analysing the impact of intrinsic and extrinsic factors on treatment resistance.

1.5.2 Radioresistance.

I will now discuss the data regarding radiosensitivity of GSCs, starting with a critical analysis of the landmark paper which was the first to claim that GSCs are the radioresistant entity in glioblastomas, based on the following findings[152]:

- CD133+ cells are more clonogenic than CD133- cells after irradiation. Although clonogenic survival is the 'gold standard' method to test clinically relevant radiosensitivity, there were two important limitations in the way this assay was performed: only one dose level was tested (5 Gy); no quantification of colony formation was shown (only images with photos of representative plates).
- tumorigenicity of CD133+ cells is not affected by *in vitro* irradiation with 2 Gy and decreased slightly with 5 Gy. Even though these results show that single doses of ionizing radiation have limited effect on the tumorigenic potential of CD133+ cells, they cannot be interpreted as an indication of the relative radioresistance of these cells, given that a comparison with CD133- cells was not possible due to the inability of these cells to form tumours in this study.
- CD133+ cells have a higher repopulation potential than CD133- cells, both *in vitro* and *in vivo*, following irradiation. This was demonstrated performing an experiment in which the two subpopulations were differentially labelled, mixed, treated (or not) with ionizing radiation, implanted in the brains of athymic nude mice (only for the *in vivo* setting) and quantified after a set period of time. Enrichment in the CD133+ fraction was observed in untreated as well as treated samples, but was more pronounced in the latter, suggesting that CD133+ cells not only proliferate more in the experimental conditions, but also have higher survival ability following radiation. Consistent with these findings are those from two subsequent studies, mentioned above, using *in vivo* lineage tracing, which demonstrated that a subpopulation of glioblastoma cells expressing putative stem cell markers have an advantage in terms of growth in xenograft models and post-treatment repopulation of the tumour[199, 200]. Indirect confirmation also came from a small clinical study analysing the percentage of CD133+ cells in matched pre- and post-treatment high

grade glioma specimens from ten patients undergoing high-dose irradiation: CD133 expression was significantly higher in the post-radiotherapy specimens[234].

- CD133+ cells exhibit more pronounced activation of the DNA damage checkpoint than CD133- cells. This was suggested by the results of western blots showing higher levels of phosphorylated ATM, Rad17, Chk1 and Chk2 following irradiation in the CD133+ subpopulation. A subsequent publication from the same group proposed that this response is regulated by the surface protein L1CAM through up-regulation of NBS1, a component of the MRE11–RAD50–NBS1 (MRN) complex that activates ATM and early checkpoint responses[235]. Though, the absence of experiments with non-GSCs in the latter study precludes the possibility of interpreting this mechanism as a GSC-specific one.
- CD133+ cells are more efficient at repairing ionizing radiation induced DNA damage than CD133- cells. Kinetics and efficiency of single and double strand break repair were evaluated with alkaline comet assays and immunofluorescence quantification of cells positive for phosphorylated histone 2AX, respectively.

Following this paper, several other studies analysed radiosensitivity of GSCs, mostly focusing on DNA damage responses of these cells. Despite the abundance of publications, only the following three studies performed a comparative analysis of radiosensitivity of GSCs and non-GSCs using clonogenic survival assays:

- one compared clonogenicity of CD133+ and CD133- subpopulations from two cell lines, following 0, 1, 2, 3 and 4 Gy. While CD133+ cells from one cell line were more radioresistant than the CD133- counterpart, there was no difference in radiosensitivity of the two subpopulations from the other cell line[236].
- one compared clonogenicity of CD133+ and CD133- cells from seven cell lines, following 2 Gy. CD133+ cells from all cell lines were more clonogenic than their CD133- counterpart after irradiation[237].
- one compared clonogenicity of subpopulations enriched or depleted for stemness, using different culture conditions, from three cell lines, following 0, 1, 2, 3, 4 and 5 Gy. GSCs from all cell lines were more radioresistant[238].

Apart from the dishomogeneity in CSC-enrichment methods and tested dose levels amongst the four studies, there were also important differences in the conditions used for the clonogenic assays:

- Bao *et al.* plated both subpopulations in serum-free medium without growth factors for 24 hours post-treatment followed by transfer to medium with serum[152];

- Mc Cord *et al.* plated both subpopulations on poly-L-lysine coated wells in serum-free medium[236];
- Yang *et al.* plated both subpopulations in soft agar[237];
- Carruthers *et al.* seeded both subpopulations in Matrigel-coated wells, maintaining GSCs in serum-free medium and non-GSCs in serum-containing medium[238].

The importance of the experimental conditions chosen for clonogenic assays is highlighted by the latter study, which also performed neurosphere formation assays on GSCs from two of the three cell lines: in both cell lines 2 Gy caused a more pronounced reduction in neurosphere formation than in colonies grown in Matrigel-coated wells[238]. Despite the limitations related to the lack of standardization of clonogenic assays for CSCs, on the whole these findings suggest that cells with GSC features are more resistant to ionizing radiation. The variety of experimental conditions used to measure clonogenicity of GSCs and non-GSCs reflects one of the main issues in the cancer stem cell field, i.e. designing methods for comparative analyses of sensitivity to ionizing radiation and chemotherapy between the two subpopulations of cells. Given the pivotal role of clonogenic survival assays in *in vitro* cancer research, I decided to dedicate part of my doctoral studies to optimizing this method.

Two of the four studies also evaluated DNA damage responses[236, 238]. Though only the more recent one made a comparative analysis between GSCs and non-GSCs, showing that: 1) GSCs have a more pronounced activation of the G2/M checkpoint after ionizing radiation (5 Gy) than their differentiated counterpart, as indicated by the lower percentage of GSCs positive for phosphorylated histone H3, a mitotic marker, 3 and 6 hours post-treatment; 2) GSCs exhibited a lower number of phosphorylated histone 2AX foci per cell 24 hours after ionizing radiation (1 Gy)[238]. The authors suggested that these responses were mediated by different levels of ATM activation following ionizing radiation, though these were not seen in all cell lines and no quantification was shown of the western blots. Also, they reported a potent, yet similar, radiosensitizing effect of ATM inhibition on both subpopulations, suggesting that other mechanisms are responsible for the observed relative radioresistance of GSCs in their study. Even if not specific to GSCs, ATM inhibition appears to be a promising strategy to kill these cells, given that other studies have shown a marked effect of ATM inhibitors in combination with ionizing radiation on GSC survival, using both *in vitro* and *in vivo* models[239, 240].

Another recent study made a comparative analysis of single strand DNA breaks (SSBs) and oxidative base damage in matched CD133+ and CD133- cells, following the observation that the former population had higher levels of reactive oxygen species (ROS): both DNA lesions were increased in CD133+ cells[112]. Consistently, PARP activity was higher in this population and treatment with a PARP inhibitor reduced colony formation in CD133+ cells, while having no

significant effect on the CD133- counterpart. Combination of ionizing radiation and PARP inhibition in both subpopulations was evaluated with viability assays, caspase 3/7 activity at three days post-treatment (as a measure of apoptosis) and quantification of phosphorylated histone 2AX foci: all experiments showed that PARP inhibition increased the effect of radiation on CD133+ cells, whereas had negligible or no impact on CD133- cells. These findings have two important limitations: lack of clonogenic survival analysis; inconsistency of data on constitutive levels of SSBs with that reported for other cell lines in previous publication from the same group[152]. Nevertheless, the authors suggested that PARP inhibitors could be a promising approach to target GSCs, based on the hypothesis that these cells rely on PARP to tolerate the observed enhanced constitutive DNA damage. Ongoing clinical trials will likely give indications of the veracity of this hypothesis (see section 1.2).

In contrast with the theory that radioresistance of GSCs is due to enhanced DNA repair responses is a paper which made a comparative analysis of double and single strand break repair in matched CD133+ and CD133- cells, showing no difference between the two subpopulations[241]. The authors proposed that resistance of GSCs to ionizing radiation was correlated with their longer cell cycle duration and increased basal activation of checkpoint proteins. Though this hypothesis was not supported by their data, given that: GSCs had a longer potential doubling time (PDT) compared to established cell lines; while, when matched CD133+ and CD133- cells were analysed, the former subpopulation had a shorter PDT, hence a shorter cell cycle. Also, the checkpoint activation data consisted only in a representative image of a western blot, with no quantification shown.

In order to determine whether radiation induced DNA damage responses of GSCs to ionizing radiation could be influenced by factors other than intrinsic to the cells, a study quantified phosphorylated histone 2AX and 53BP1 foci in CD133+ and CD133- cells grown *in vitro* and in orthotopic xenografts[242]. While there was no difference in DNA double strand break induction and repair between the two subpopulations from two cell lines cultured *in vitro*, both types of foci were reduced in CD133+ cells compared to CD133− cells in the *in vivo* setting. Quantification of CD133+ cells in untreated and irradiated mice showed that the latter group had a higher percentage of cells expressing the putative stem cell marker. Based on these findings, the authors suggested that the brain microenvironment specifically increases radioresistance of GSCs.

More evidence for the influence of microenvironmental factors on radiation responses comes from two studies mentioned above, in the “Perivascular niche” section:

- one evaluated responses of GSCs to ionizing radiation by comparing their neurosphere formation rate following treatment of cells grown in a 3-dimentional organotypic ‘explant’

system or in neurosphere cultures: a single dose of 10 Gy reduced their self-renewal ability more dramatically in the latter condition, suggesting that radiosensitivity of GSCs is influenced by microenvironmental factors present in the explants[205]. Surprisingly, the effect of radiation on the percentage of CD133+ cells in the two conditions was the opposite, i.e. neurosphere cultures maintained a higher proportion of cells expressing the putative stem cell marker following treatment with 10 Gy. Apart from this partial contradiction, another limitation of the study is the use of a high single dose, whose effect should be correlated with caution to that of clinically relevant doses.

- the other analysed the impact of laminin α2 on radiation responses of CD133+ cells, showing that in the presence of this integrin, compared to the control condition (BSA), these cells had: 1) increased survival, measured in terms of viability 48 and 72 hours after 1, 3 and 6 Gy; 2) reduced phosphorylated histone 2AX, quantified as the number of cells with > 10 foci 24 hours after ionizing radiation (3 Gy)[210]. Although these findings suggest that radioresistance of GSCs might be influenced by the presence of specific integrins in the tumoral niche, they need to be confirmed with clonogenic survival assays and a more rigorous analysis of DNA damage responses, given that short-term viability and the use of a cut-off of 10 foci per cell are not recognised methods to test radiosensitivity in a clinically relevant manner.

Despite their limitations, on the whole, these findings suggest that microenvironmental factors, together with intrinsic cellular features, are determinants of radioresistance, highlighting the need for studies that analyse responses of GSCs to ionizing radiation in experimental models that allow inclusion of elements from the tumoral niche.

Based on the data above regarding the tumoral niche, I decided to dedicate part of my doctoral studies to developing the use of a tissue culture system that allows analysis of features and radiation responses of GSCs and non-GSCs in the presence of specific microenvironmental factors.

1.6 Aims of my research on glioblastoma cancer stem cells.

The aims of my project are:

- optimization of the following methods for cancer stem cells:
    - a clonogenic survival assay, to compare sensitivity of GSCs and non-GSCs to cytotoxic therapies;
    - a 3 dimentional culture system, to grow GSCs and non-GSCs in the presence of microenvironmental factors and evaluate their features and treatment responses in a model that resembles *in vivo* conditions more closely than the traditional tissue culture plastics.
- characterization of mitosis in GSCs and non-GSCs, with the intention to elucidate possible differences between the two subpopulations, that would allow us to identify targets for an effective therapeutic strategy to improve outcomes of patients with glioblastoma.

I decided to optimize methods for GSCs and non-GSCs to address the need for the development of laboratory techniques that allow comparative analyses of the two subpopulations, as mentioned in the previous section (1.5.2), but also as a preparatory step for the part of my project investigating cell division of CSCs.

My interest in mitosis originated from the following:

- cell division is one the identifying properties of CSCs, as its regulation enables them to divide both symmetrically and asymmetrically, giving rise to differentiating daughter cells, which form the tumour bulk, as well as maintaining a pool of self-renewing stem cells.
- one of the studies, mentioned above, using *in vivo* lineage tracing in a genetically engineered mouse model of glioma, showed that post-treatment cancer growth is due to a relatively quiescent subpopulation of cells, which, following chemotherapy, produces transient subsets of highly proliferating cells repopulating the tumour[200].

Confirmation of the strength of this approach comes from findings on the role of mitotic kinases in GSCs. A study, which combined the results of a functional genetic approach with a bionetwork created from glioblastoma patient molecular signatures as a strategy to identify targets differentially required for expansion of GSCs, generated a mitotic checkpoint kinase, BUB1B, as a top-scoring hit[243]. This output was validated by knockdown experiments, demonstrating that targeting BUB1B reduced neurosphere formation and differentially blocked growth, both *in vitro* and *in vivo*, of GSCs from several primary cell lines, while having no significant effect on neural stem cells. Based on these findings and on results of mechanistic studies, the authors suggest that GSCs have an added requirement for BUB1B and propose targeting this protein as a therapeutic strategy against glioblastomas. Another target linked to

mitosis was proposed by a study analysing the interaction of the transcription factor FOXM1 and the mitotic kinase MELK (maternal embryonic leucine-zipper kinase) in GSCs, based on the following data: FOXM1 and MELK had higher expression levels in CD133+ cells compared to CD133- cells; immunofluorescence analysis showed that FOXM1 co-stained with the putative CSC markers SOX2 and nestin; disruption of MELK-mediated FOXM1 signalling, using the antibiotic Siomycin A, reduced neurosphere formation ability of GSCs and delayed growth of GSC-induces xenograft models[244]. Based on these findings, the authors suggest targeting the FOXM1-MELK interaction as a therapeutic strategy against glioblastomas. A previous publication suggested polo-like kinase 1 (Plk1), a mitotic kinase, as a target to kill GSCs and improve treatment outcome of glioblastoma patients, based on the following findings: analysis of microarray data from 467 patients showed that Plk1 was highly expressed in these tumours and was correlated to poor survival; treatment with BI2536, a Plk1 inhibitor, reduced self-renewal of GSCs; targeting Plk1, with siRNA or BI2536, induced differentiation of GSCs, demonstrated by down-regulation of the putative CSC marker SOX2 and up-regulation of a glial differentiation marker[245].

The main hypothesis of my project originates from these data as I propose that GSCs have distinctive mitotic features, compared to non-GSCs, and that these represent effective targets to kill this subpopulation of cells.

Chapter 2

Materials and Methods

2.1 Materials

2.1.1 Cell lines

G7, E2, S2 and G1 primary glioblastoma cell lines were a generous gift of Colin Watts (Cambridge).

Human glioblastoma established cell line U87-MG was obtained from the European Collection of Animal Cell Cultures (ECACC).

2.1.2 Ionizing radiation

Cells were irradiated with 250 kVp X-rays (dose rate 0.5 Gray/min).

2.1.3 Drugs

- Aurora kinase A inhibitor: MLN8237, Millenium.
- Nocodazole, Sigma.
- PARP inhibitor: AZD2281, a gift of Kudos Pharmaceuticals/AstraZeneca.
- Polo-like kinase I: BI2536, Axon Medchem.
- Paclitaxel, Sigma.

2.1.4 Antibodies

Primary antibodies are listed in table 2.1.

Secondary antibodies were Alexa Fluor, Invitrogen (dilution 1:1500).

Table 2.1 Primary antibodies

Antigen	Source (catalogue number)	Species	Dilution (assay)
53BP1	Bethyl Laboratories (A300-272A)	Rabbit	1:1000 (IF)
Acetylated α-tubulin	Sigma (clone 6-11B-1)	Mouse	1:1000 (IF)
ARL13B	Abcam (ab83879)	Rabbit	1:200 (IF)
Aurora A	Epitomics (1800-1)	Rabbit	1:1000 (WB)
Caspase 3	Abcam (ab4051)	Rabbit	1:200 (IF)
	Cell Signaling (9668)	Mouse	1:1000 (WB)
CENP-F	Abcam (ab5)	Rabbit	1:800 (IF)
Centrin-2	Gift from Elmar Schiebel	Rabbit	1:500 (IF)
Fibronectin	Abcam (ab26245)	Mouse	1:800 (IF)
γH2AX	Millipore (05-636)	Mouse	1:1600 (IF)
Histone H3	Millipore (05-499)	Mouse	1:1000 (WB)
			1:100 (FACS)
Nestin	Abcam (ab6320)	Mouse	1:200 (IF)
Total p53	Cell Signaling (9282)	Rabbit	1:1000 (WB)
Phosphorylated p53	Cell Signaling (9286)	Mouse	1:1000 (WB)
Phosphorylated Aurora A	Cell Signaling (3079)	Rabbit	1:100 (IF)
Phosphorylated histone H3	Cell Signaling (3465)	Rabbit	1:200 (IF)
			1:50 (WB)
Polo-like kinase 1	Abcam (ab14210)	Mouse	1:400 (WB)
SOX2	Abcam (ab75485)	Mouse	1:50 (IF)
α-tubulin	Abcam (ab7291)	Mouse	1:1000 (IF)
	Abcam (ab18251)	Rabbit	1:1000 (IF)
γ-tubulin	Abcam (ab11316)	Mouse	1:250 (IF)

IF, immunofluorescence; WB, western blot; FACS, Fluorescence Activated Cell Sorting.

2.1.5 Other reagents

- Accutase™.
- B-27, Invitrogen.
- CellTracker Green CMFDA (5-Chloromethylfluorescein Diacetate), Molecular Probes.
- CellTracker Blue CMAC (7-Amino-4-Chloromethylcoumarin), Molecular Probes.
- Click-iT® EdU Alexa Fluor® 647 Imaging Kit, Life Technologies C10340.
- Collagen type IV, Sigma C5533.
- Concanavalin A, Sigma.
- Epidermal growth factor, Invitrogen PHG0313.
- Fibronectin, Sigma F0556.
- Fibroblast growth factor, Invitrogen PHG0263.
- Fluoromount, Sigma.
- HyClone, Thermo Scientific HyClone, 12822966.
- Immobilon Western Chemiluminescent HRP Substrate, Merck Millipore WBKLS0500.
- Laminin, Sigma L4544.
- MaxGel™ ECM Matrix, Sigma E0282.
- Neurobasal-A medium, Invitrogen.
- Phalloidin, Invitrogen.
- ProLong Gold mounting solution containing DAPI, Molecular Probes.
- Senescence detection kit, Abcam ab65351.
- Vitronectin, Sigma V8379.
- Western blot lysis buffer: 20mM Tris pH 7.5, 137mM NaCl, 10% glycerol, 1% triton, 2mM EDTA, 0.05% b-mercaptoethanol, protease and phosphatase inhibitors.
- Western blot sample buffer: 0.01% bromophenol blue, 62.5mM Tris-HCl pH 6.8, 7% SDS, 20% sucrose and β-mercaptoethanol.

2.2 Methods

2.2.1 Generation of GSC and non-GSC populations and cell culture

G7, E2, S2 and G1 primary glioblastoma cell lines were derived from freshly resected glioblastoma patient specimens as described in Fael Al-Mayhani *et al*. Protocols for tissue collection were compliant with the UK Human Tissue Act 2004 (HTA Licence ref 12315) and approved by the local regional Ethics Committee (LREC ref 04/Q0108/60). Each patient gave their informed consent prior to undergoing surgery. In summary, anonymised patient specimens were minced, digested, filtrated and washed. Cells were then seeded in serum-free media and allowed to form primary aggregates, which were then plated onto extracellular matrix (ECM)-coated flasks (ECM 1:10 dilution, Sigma, UK) and allowed to form a monolayer.

To obtain cancer stem cell enriched populations (referred to as 'GSCs' in the text), cell lines were cultured in Neurobasal-A medium supplemented with B-27, epidermal growth factor (20 ng/ml), fibroblast growth factor (20ng/ml), glutamine and penicillin/streptomycin (referred to as 'GSC medium' in the text). All cell lines grew as neurospheres in these culture conditions.

To induce differentiation, hence obtain matched differentiated populations (referred to as 'non-GSCs'), cell lines were cultured in MEM supplemented with HyClone, NEAA, L-glutamine, sodium pyruvate and penicillin/streptomycin (referred to as 'non-GSC medium'). All cell lines formed adherent colonies in these conditions.

In order to test whether the primary glioblastoma cells grown as neurospheres were enriched for GSCs, in comparison to those cultured as adherent colonies, the two subpopulations were characterized for key features that distinguish GSCs from their differentatiated counterparts (see section 1.3). These experiments were performed by other members of the Anthony Chalmers Laboratory. G7 and E2 cell lines were analysed for expression of stem cell and differentiation markers, using western blotting and fluorescence activated cell sorting: neurosphere cultures exhibited higher levels of CD133, nestin and Sox2, while they had lower levels of the astrocytic differentiation marker GFAP, compared to adherent cultures (view data in Mannino *et al.* 2014 in the appendix). The two cell lines were also tested for their ability to form tumours in CD1 nude mice. Intracranial injection of 10^5 G7 neurospehere cells generated highly invasive tumours in 100% of cases; injection of 10^5 G7 cells from adherent cultures also formed tumours but these had well defined edges and did not exhibit an invasive pattern. Following intracranial transplantation of 10^5 E2 neurosphere cells, pathology analysis showed the presence of a highly invasive mass in the injection site and of infiltrative cells in both hemispheres in 100% of mice; in contrast, injection of 10^5 E2 cells from adherent cultures did not generate tumour masses (view data in Mannino *et al.* 2014 in the appendix). These

findings confirm that the use of different culture conditions is a legitimate method to obtain subpopulations of cells enriched for GSCs or non-GSCs, i.e. they validate the approach I chose for my project.The majority of experiments in my doctoral studies are carried out with the G7 cell line. This choice was based on the availability of a relatively large stock of G7 cells with low passage number and the higher growth rate of these cells, compared to E2 and S2 cells. These aspects made this cell line the most suitable one for optimizing various methodologies and performing experiments in triplicates.

Detailed characterization, with gene sequencing and methylation analysis, of GSCs and non-GSCs of the primary cell lines is not part of my project and is being performed by other members of the Anthony Chalmers laboratory. Available data is cited were relevant in the results chapters.

When cell lines are split or prepared for experiments, they are incubated with Accutase™ to induce detachment between cells in GSCs and from flasks in non-GSCs, obtaining a single cell suspension.

To culture cells on Alvetex®, GSCs and non-GSCs are seeded onto the polystyrene disks as single cell suspensions in their respective medium, which is changed every four days at first and then more frequently, depending on changes in the colour of the medium indicating a reduction in pH due to increase in cell number and waste products.

2.2.2 Neurosphere formation assay

Cells are retrieved from flasks to obtain a single cell suspension, counted and diluted serially to achieve a final concentration of 1 cell/200 µl. The cell suspension is seeded in 96 well plates with a multichannel pipette, plating 200 µl/well. Plates are incubated for at least two weeks. EGF and FGF are added every 5 days. Spheres are counted with the Gel Count (Oxford Optronix).

2.2.3 Clonogenic survival assays

The following is the protocol that I used for all clonogenic survival assays. I optimized it as an adapted version of the neurosphere formation assay (see above). For the protocol development see chapter three.

Cells are retrieved from flasks to obtain a single cell suspension, counted and diluted serially to achieve a final concentration of 1 cell/100 µl for drug sensitivity tests, 1 cell/200 µl for radiosensitivity assays. The cell suspension is seeded in 96 well plates with a multichannel pipette, plating 100 µl/well for drug sensitivity tests, 200 µl for radiosensitivity assays. Plates

are then treated: drugs are added to the plates six to twelve hours after seeding and left for the whole duration of the experiment; ionizing radiation (IR) is delivered six hours after seeding; in the combined treatment with MLN8237 and IR, the drug was added as usual and plates were irradiated 24 hours later. Plates are incubated for at least two weeks. EGF and FGF are added every 5 days to the plates with GSCs. Colonies are counted after at least 15 or 21 days (depending on the cell line), using the Gel Count for GSCs and methylene blue staining for non-GSCs. To prepare plates for Gel Count scanning, two simple steps are performed: 1) wells are filled up completely with PBS, making sure not to create any air bubbles; 2) the bottom of the plate is wiped with IMS (industrial methylated spirit) to remove dust. For methylene blue staining, a standard protocol adapted to the 96-well format is used, as follows: the medium is removed with a sharp downward movement holding the plate upside down; 70% ethanol is added with a multichannel pipette to fix the cells and left for ten minutes; after ethanol is removed (with the same vigorous movement as before!), methylene blue is added with a multichannel pipette and left for at least 30 minutes; plates are then rinsed with water and left to dry.

2.2.4 Cell sorting with Fluorescence Activated Cell Sorting using FACSAria™ I

Cells are retrieved from flasks to obtain a single cell suspension, counted and resuspended in PBS, containing 1mM Na_2EDTA (to reduce clumping and clogging), at a concentration of $1x10^6$ cells/ml. The cell suspension is filtered using 40µm cell strainers prior to sorting, again to reduce clumping and clogging. To minimize mechanical stress on cells, a 100µm nozzle and low pressure mode is used.

2.2.5 Coating Alvetex® with extracellular matrix (ECM) components

2.2.5.1 MaxGel™ human ECM

ECM is thawed on ice and then diluted with medium (tips are cooled in the freezer prior to pipetting ECM). The diluted ECM is applied gently and slowly on the scaffold, which is transferred onto a mesh for a few minutes. The scaffold disk is inserted in the well and incubated for 30 minutes at 37°C. The single cell suspension is added slowly moving the tip around the well.

2.2.5.2 Customized ECM mixture

The customized ECM mixture contains collagen, fibronectin, laminin and vitronectin. First of all, collagen and vitronectin are reconstituted in acetic acid and water, respectively. Then, each solution is diluted in HBSS to obtain the desired concentration, as follows: collagen 1mg/ml,

fibronectin 5µg/ml, laminin 10µg/ml, vitronectin 0.5µg/ml. The solutions are mixed and applied gently and slowly on the scaffold, which is transferred onto a mesh for a few minutes. The scaffold disk is inserted in the well and incubated for 2 hours at 37°C. The disks are then rinsed twice with medium and the single cell suspension is added slowly moving the tip around the well.

2.2.6 Preparation of frozen samples of scaffold

The scaffold disk is removed from the well, quickly rinsed three times with PBS and cut into small pieces (approximately 6 x 4 mm). A drop of optimal cutting temperature (OCT) compound is placed on a cork disk and a scaffold piece is immersed in it, taking care to orient it standing or lying. The sample is transferred into an isopentane bath first and then into a liquid nitrogen bath. The samples are retrieved from the liquid nitrogen bath and stored at -80°C in a plastic bag. Samples are cut with a cryostat and placed on polylysine coated slides.

2.2.7 Immunofluorescence

2.2.7.1 2D culture system.

For experiments evaluating centrosome maturation, mitotic spindle phenotype and cell cycle distribution, cells are retrieved from flasks to obtain a single cell suspension and pipetted on Concanavalin A coated coverslips. They are then fixed with 70% methanol for 5 minutes.

For phosphorylated Aurora kinase A analysis, cells are retrieved from flasks to obtain a single cell suspension, cytospun on Concanavalin A coated coverslips and fixed with 4% paraformaldehyde (PFA) and 70% methanol, sequentially for 5 minutes each.

For all the above experiments, cells are permeabilized in PBS 0.3% Triton for 5 minutes, blocked in 3% BSA for 30 minutes and incubated with primary antibodies for one hour at 37°C. Slides are then washed and probed with the appropriate secondary antibody for one hour at room temperature. Coverslips are mounted using ProLong Gold mounting solution containing DAPI.

Images are acquired on DeltaVision microscope equipped with a UPLS Apochromat NA 1.40, 60x oil immersion objective (Olympus), standard filter sets (excitation 360/40, 490/20, 555/28; emission 457/50, 528/38, 617/40) and a CoolSNAP HQ2 camera (Photometrics). Z series are acquired using softWoRx software (version 4.0.0; Applied Precision). When applied, deconvolution is performed using SVI Huygens Professional Deconvolution Software (Version 3.5). For 3D view and quantitative analysis of γH2AX foci, DAPI volume, γ tubulin and phosphorylated AurA centrosomal accumulation, DeltaVision files are imported into Imaris

software (version 6.3.0; Bitplane) and processed with the relevant algorithm. Measurements are exported to Excel (Microsoft) and plotted. The γ tubulin and phosphorylated AurA data was further analysed using Mann-Whitney U test.

2.2.7.2 3D culture system (Alvetex®).

Medium is removed from the well, PFA is added and left for 10 minutes. The scaffold disk or piece is immersed in PBS and stored in a well at 4°C until staining. Reagents and incubation times are as for coverslips. The difference in the protocol is that the cells are within the scaffold, rather than on a coverslip; hence, the various solutions (diluted primary antibody, PBS, diluted secondary antibody, etc.) are placed in adjacent wells in a plate and the scaffold piece is moved from one well to another using appropriate tweezers. For mounting, the scaffold piece is placed on top of a drop of mounting medium on a slide and then covered with a coverslip.

Confocal images are acquired using LSM Zeiss Axiovert 200M-LSM 510 META COMBI Confocal Microscope with Coherent Enterprise II 693 UV laser, equipped with the following objectives: 63x and 40x water immersion, 20x.

2.2.8 Chromosome spreads

Cells are treated with nocodazole for 6 hours, collected, spun down and incubated in KCl (75mM) for 10 minutes. KCl is removed and fixative (methanol:glacial acetic acid, 3:1) is added slowly and left for 10 minutes. Cells are spun down, resuspended with fixative, spun down again and resuspended in fixative. A drop of cell suspension is then pipetted onto a pre-wet (50% ethanol) slide from at least 20 cm high. Slides are left to dry and are mounted with ProLong Gold mounting solution containing DAPI.

Images are acquired as described in section 2.2.7.1.

2.2.9 Ploidy analysis

Cells are retrieved from flasks to obtain a single cell suspension, pipetted on Concanavalin A coated coverslips and fixed with 4% paraformaldehyde for 10 minutes. Cells are permeabilized, blocked and probed with phalloidin for 30 minutes. Coverslips are mounted using ProLong Gold mounting solution containing DAPI.

Random images are acquired as described in section 2.2.7.1.

2.2.10 Fluorescence Activated Cell Sorting (FACS) analysis

Cells are retrieved from flasks to obtain a single cell suspension, washed with PBS, fixed with 70% ethanol (it is important to vortex cells gently while adding ethanol to avoid clumping of GSCs) and stored in fridge. They are then centrifuged at 1500 rpm for 3 minutes, rinsed twice with 3%BSA/PBS (with addition of EDTA for all steps to avoid clumping) and re-suspended in 500µl of 3%BSA/PBS solution containing 250µg/ml of RNase A and 5µg/ml of propidium iodide (PI). After at least I hour incubation in the dark at room temperature, analysis of DNA content of cells is performed using the FACSCanto (BD). Plots of PI area versus cell counts are done with FACSDiva software (BD).

For mitotic index analysis, after the cells are rinsed twice with 3%BSA/PBS, they are incubated for 1 hour at room temperature in 50µl of anti-phosphorylated histone H3 antibody diluted in 3%BSA/PBS, washed once with 500µl of 3%BSA/PBS and incubated for 1 hour at room temperature in 50µl of secondary antibody diluted in 3%BSA/PBS. Cells are then rinsed once and re-suspended in 500µl of 3%BSA/PBS solution containing 250µg/ml of RNase A and 5µg/ml of PI.

2.2.11 Western blot

Cells are retrieved from flasks to obtain a single cell suspension, counted and washed once with PBS. To prepare cell lysates, cells are re-suspended in 40 µl IP lysis buffer and 10 µl 5x sample buffer and then incubated on ice for 20 min, before sonication. Cell lysates are boiled for 5 minutes at 95°C and loaded to electrophoresis in SDS polyacrylamide gel. Gels are then transferred with a semi-dry technique to nitrocellulose membranes, which are blocked for 30 minutes with 5% milk/PBS/0.1% NP-40. Membranes are incubated overnight at 4°C with primary antibody diluted in the blocking buffer, washed three times for 5 minutes with PBS and incubated with the appropriate horseradish peroxidase (HRP) conjugated secondary antibody for 1 hour at room temperature. Three washing steps with PBS are done before chemiluminescent detection is performed. Emission is captured with radiograph films using the Xograph compact 4 automatic X-ray film processor.

2.2.12 Cell tracking

Cells are retrieved from flasks to obtain a single cell suspension, divided into two parts and incubated separately with 1µM CellTracker Green CMFDA and 1µM CellTracker Blue CMAC for 45 minutes. Medium with dyes is removed, cells are incubated in fresh medium for 24 hours ± 50 nM MLN8237. Cells are collected from flasks, spun down, re-suspended, pipetted on

Concanavalin A coated coverslips and fixed with 4% paraformaldehyde for 10 minutes. They are then stained with phalloidin (as in ploidy analysis). Coverslips are mounted using Fluoromount.

Random images are acquired as described in section 2.2.7.1.

2.2.13 β-galactosidase staining

Cells are treated with 0 and 50 nM MLN8237. After 2 and 7 days they are stained according to an adapted version of the manufacturer's protocol. Cells are retrieved from flasks to obtain a single cell suspension and transferred to plastic tubes (polypropylene plastic tubes only for whole experiment). Cells are incubated with the fixative solution for 10-15 minutes at room temperature, washed twice with PBS and incubated with the staining solution mix. Cells are then incubated at 37°C for 1 hour and cytospun on slides. Coverslips are mounted using Fluoromount.

Random images are acquired on microscope Axio Lb A1 (Zeiss) equipped with an AxioCam ERc 5s and a 40x objective. β-galactosidase positive and negative cells are counted on a computer monitor and percentages of β-galactosidase positive cells are calculated and blotted.

2.2.14 Edu labelling

GSCs and non-GSCs are treated with 0, 2 and 4 nM of BI2536. After 24 hours of incubation, they are stained according to an adapted version of the manufacturer's protocol. Following 23 hours of treatment, they are incubated with EdU solution for 1 hour, retrieved from flasks, cytospun on coverslips and fixed with 4% PFA for 10 minutes. Cells are then rinsed twice with 3% BSA/PBS solution, permeabilized with 0.5% Triton for 20 minutes and, after other two rinsing steps, they are incubated with the Click-iT® reaction cocktail for 30 minutes at room temperature in the dark. Cells are rinsed once and incubated with the primary antibody for 1 hour, washed three times and incubated with the secondary antibody for one hour at room temperature in the dark. Coverslips are mounted using ProLong Gold mounting solution containing DAPI.

Random images are acquired as described in section 2.2.7.1.

2.3 Statistics

Experiments are performed in triplicate, unless otherwise stated. In the graphs, data are generally presented as means with standard deviations.

Statistical significance is evaluated with the two-tailed Student's *t*-test or the Mann-Whitney U test and a P value < 0.05 is considered statistically significant.

Chapter 3

Optimization of methods for cancer stem cells

3.1 Introduction

Starting with the first isolation of cells with CSC features from glioblastoma patient specimens, which applied cell culture techniques developed for neural stem cells, the methodology used in GSC research has often found inspiration in the normal stem cell field. Due to the heterogeneous nature of cancer and given the completely different aims of research investigating GSCs and neural stem cells, application and adaptation of methods from the latter field has important limitations. An example is represented by the variable results obtained with neural stem cell markers when used to identify GSCs[166]. Also, non-adherent sphere culture, a valuable technique exploiting a recognised feature of GSCs, generates some important issues, such as: increased heterogeneity of cellular populations compared to 2D cultures[164, 165]; difficulties in designing experiments for comparative analysis of sensitivity to chemotherapy and ionizing radiation between GSC enriched populations and their differentiated counterparts. Various groups have addressed these issues in different ways, introducing distinct possible biases. Although the non-adherent sphere culture technique is one of the sources of the lack of standardization that characterizes the GSC field, the following findings suggest the value of this method in glioblastoma research: 1) the ability of cancer cells to grow as neurospheres is correlated with poorer patient outcome (see general introduction for detailed data); 2) a study, comparing efficacy of various TMZ dosing schemes against GSC lines, showed good correlation between *in vitro* findings and data from clinical trials[246]; 3) serum-free medium supplemented with growth factors, i.e. medium for non-adherent sphere cultures, was demonstrated to preserve more closely glioblastoma genotype and phenotype[247-249]. While the latter data question the value of comparative analyses with cellular populations grown in serum-containing medium, a recent proteomic study characterizing primary cell lines, derived from patient specimens as adherent or as sphere cultures, demonstrated that each subpopulation type displayed distinct features of glioblastomas, suggesting that both culture conditions are potentially useful tools to improve our understanding of this disease[250]. Furthermore, most of our knowledge of cancer biology is based on studies analysing adherent cells grown in serum-containing medium and many assays were developed and validated using these culture conditions.

In conformity with this evidence, the first aim of my project was to optimize a clonogenic survival assay to compare sensitivity of GSCs and non-GSCs to various treatments, the former grown as neurospheres, the latter as adherent cultures. As described in detail in the first part of this chapter, my approach consisted in optimizing the neurosphere formation assay, in

terms of plating accuracy and time consumption, and then creating an adapted version of the standard clonogenic survival assay.

The normal stem cell field has also produced exciting advances in 3-dimensional (3D) cell culture models, which need to be implemented as fundamental tools to investigate CSC behaviour and treatment-response in conditions that resemble more closely their tumoral niche, given the data, discussed in the general introduction, regarding the emerging role of the microenvironment in GSC biology. The second part of this chapter illustrates the experiments that I carried out to optimize the use of a 3D model to analyse features of GSCs and non-GSCs in the presence of various elements of their tumoral niche and to evaluate whether these factors influence response of the two subpopulations to cytotoxic treatments, particularly to ionizing radiation.

3.2 Optimizing the clonogenic survival assay

The first aim of my project was to optimize a clonogenic survival assay to compare sensitivity of GSCs and non-GSCs to ionizing radiation and cytotoxic agents. For the initial steps in the optimization process, I used U87 MG cells that had been cultured in 'GSC-medium' (see section 2.2.1) and formed neurospheres.

I started by seeding increasing numbers (25, 50, 100, 250, 500 and 1000) of cells in a 24-well plate and observed them daily: sphere-looking aggregates were seen as soon as day 1; by day 7, wells plated with 1000 cells contained up to 40 spheres; from day 9, the number of sphere-looking aggregates started to decrease due to merging of various aggregates. I could not identify any differences in the appearance between sphere-looking aggregates formed at day 1 and those formed later on.

I then selected U87 cells cultured in 'GSC-medium' for CD133 expression using magnetic sorting and seeded increasing numbers (100, 250 and 500) of CD133+ and CD133- cells in a 24-well plate. Again sphere-looking aggregates were present very early, at day 3; by day 5, there were up to 26 sphere-looking aggregates in wells plated with 500 CD133+ cells; from day 7, the number of sphere-looking aggregates in the CD133+ plate started to decrease due to merging of various aggregates. There was no difference in the maximum number of sphere-looking aggregates per well counted in CD133+ and CD133- plates.

Given that U87 cells have a cell cycle of about 24 hours, I concluded that spheres observed at days 1 and 3 and part of those observed at later time points were due to cell clumping. The decrease in the number of spheres after day 7 was consistent with this interpretation. Hence, to completely exclude this phenomenon, I decided to perform all clonogenic survival assays in 96-well plates by seeding cells at a density of one cell per well. I also chose to abandon CD133 magnetic sorting to select for stemness, following the interpretation of the above lack of difference in the light of published data showing that CD133- cells, as well as CD133+ cells, displayed GSC features[153]. Based on increasing evidence that specific culture conditions enrich or deplete cellular populations for stemness, I decided to use this method to obtain matched GSC and non-GSC subpopulations[162, 163].

I tested two methods to seed one cell per well, using mostly G7 GSCs: serial dilution and cell-sorting with FACSAria I. I evaluated precision of serial dilution, by seeding cell populations in multiple flasks at different times and observing the cells down the microscope in the following days. The percentage of wells with cells had a variation of less than 5% within each sample and more than 95% of positive wells had single cells when observed on the same day. Given that other studies had reported the use of FACSAria to seed GSC populations as single cells in 96-

well plates, I tested the effect on neurosphere formation rate of sorting G7 GSCs through this flow-cytometer: there was a reduction of at least 25% in the number of neurospheres when cells were seeded with FACSAria, compared to manual plating based on serial dilution, even when the 100 µm nozzle and low pressure mode were used to sort cells. Based on these findings and on published data, suggesting that hydrodynamic forces generated in flow cytometers cause significant cell damage and apoptosis, I decided to use serial dilution to seed one cell per well[251].

The next step was to optimize the assay in terms of time consumption of the colony counting step, which until then was performed by scoring the presence of neurospheres under the microscope. To achieve this, I tested the feasibility of using a colony counter, GelCount™, to quantify the number of neurospheres. This system identifies colonies based on several parameters, such as shape, density and size. Once the optimal settings to identify G7 neurospheres were determined, all plates were scored with GelCount™. A representative image of the bitmap generated by the software is shown in figure 3.1. The only necessary procedure, prior to counting, was filling the wells with PBS, making sure no bubbles formed. This was to avoid artefacts that could hamper colony detection, such as those shown in figure 3.2.

Given that my aim was to optimise a method to compare sensitivity of GSCs and non-GSCs to ionizing radiation and cytotoxic agents, I then tested whether a clonogenic assay with one cell per well in 96-well plates was also feasible with non-GSCs, which formed adherent colonies. As shown in figure 3.3, colonies were visible and easily identifiable following methylene blue staining.

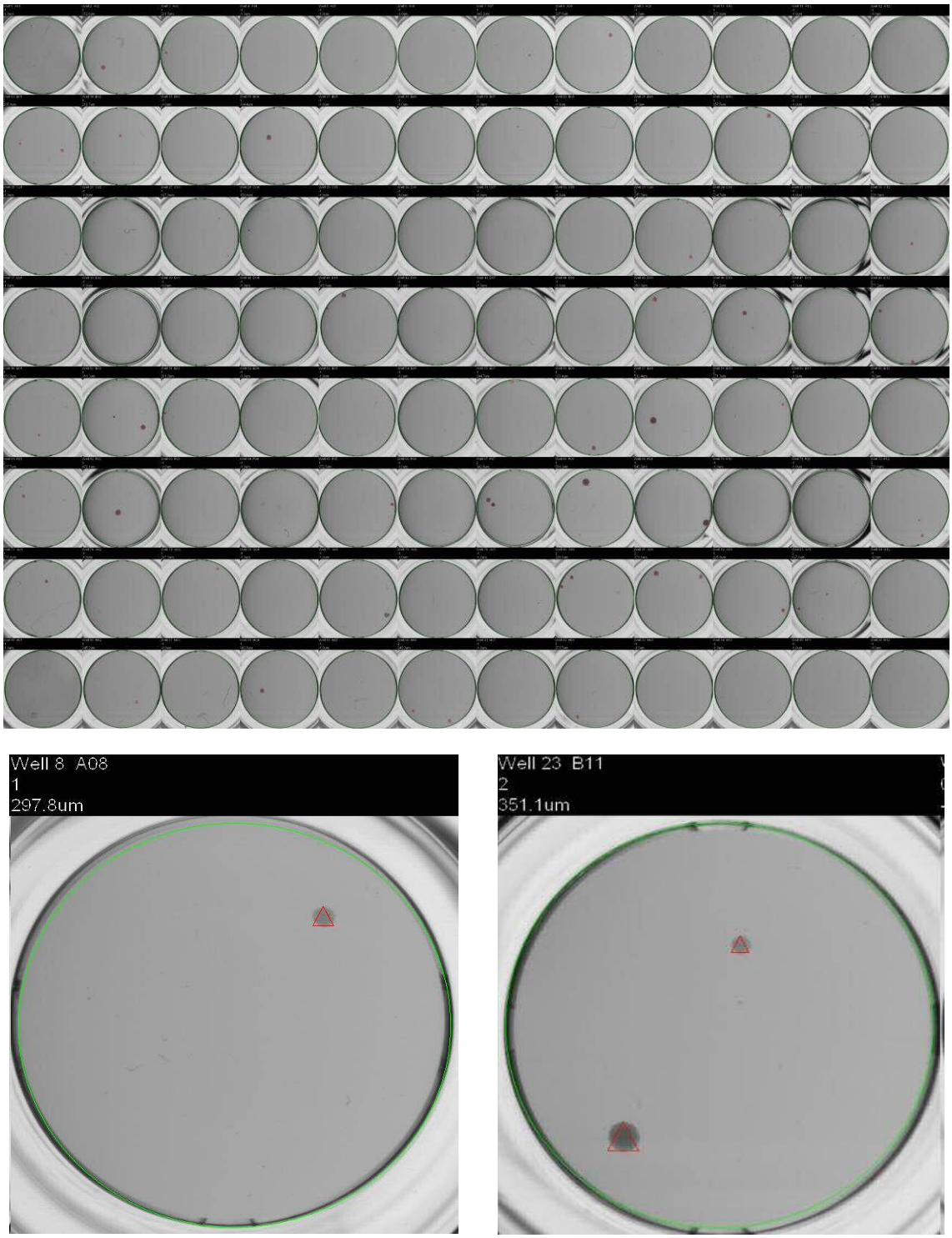

Figure 3.1 Representative image of bitmap created by Gelcount™.

Above is the image of the entire 96-well plate, while below are enlargements showing two wells, each one containing a colony identified by the counter and marked with a red triangle.

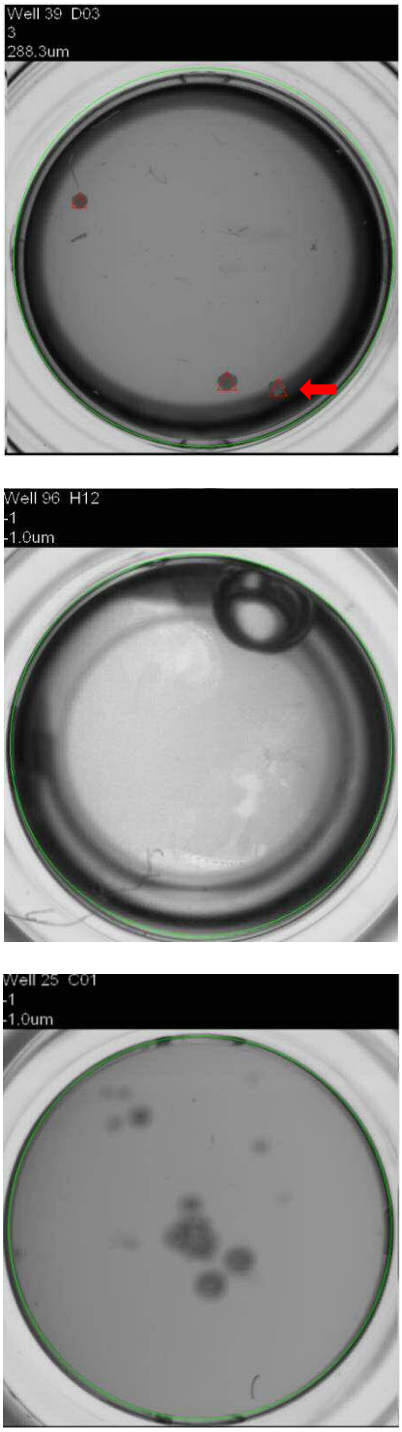

Figure 3.2 Representative images of artefacts created by suboptimal filling of the wells and the presence of large or small air bubbles.

Incomplete filling of wells results in the presence of a dark meniscus on the periphery of the well, which can hamper detection of colonies in that area (red arrow in the top image indicates a colony which had been missed by the software and was subsequently identified by me while viewing the images on the monitor). Two examples of meniscus are shown in the top and central images.

Artefacts created by large and few small air bubbles are shown in the central and bottom images, respectively.

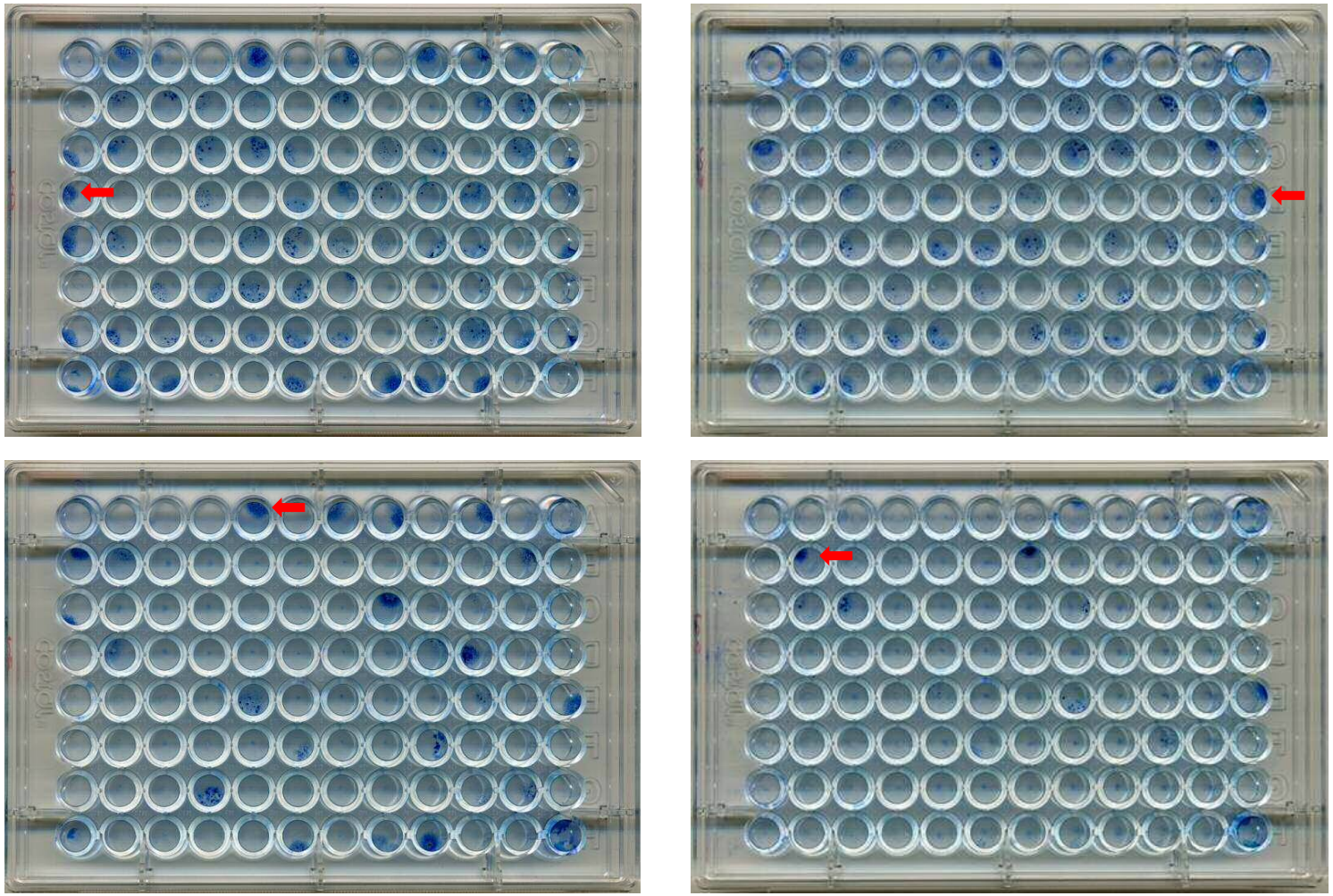

Figure 3.3 Representative images of 96-well plates with adherent colonies stained with methylene blue.

Plates were seeded with G7 non GSCs, treated with 0, 2, 3 and 5 Gy, incubated for 15 days and stained with methylene blue. Red arrows indicate colonies.

3.3 Preliminary evaluation of sensitivity to ionizing radiation and DNA repair inhibitors.

I performed clonogenic assays with G7 and E2 matched GSCs and non-GSCs to compare their intrinsic radiosensitivity. I observed no difference in survival between the two subpopulations of G7 cells, while, amongst E2 cells, non-GSCs were more radioresistant (see figure 3.4). Keeping in mind that only G7 cells' data represent results of three independent experiments, they are consistent with findings from a study which reported no difference in clonogenicity in one of the two tested cell lines, but in contrast with the other studies which showed that GSCs are more radioresistant than non-GSCs[152, 236-238]. This inconsistency is probably due to variations in experimental procedures, given that one of the above studies used the same cell lines, i.e. G7 and E2, though cultured in different medium, and performed clonogenic survival assays with another protocol[238].

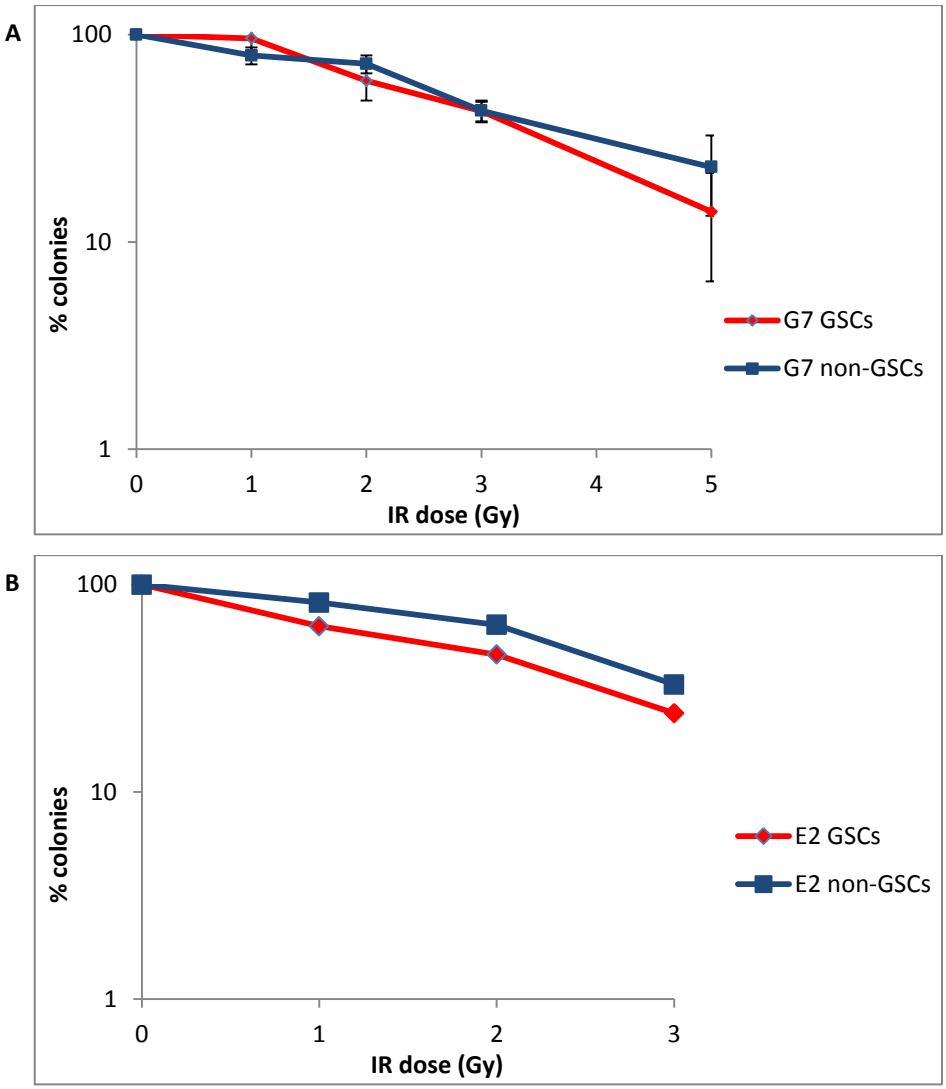

Figure 3.4 Preliminary clonogenic survival assays comparing radiosensitivity of G7 and E2 matched GSCs and non-GSCs.

G7 GSCs and non-GSCs showed no difference in survival (A), while E2 GSCs were more sensitive than matched non-GSCs (B). **A.** Results for G7 cells are representative of three independent experiments. Error bars indicate means ± SD. **B.** Each data point for E2 cells is derived from the mean of the number of colonies counted in two 96-well plates.

I also performed preliminary clonogenic assays with G7 matched GSCs and non-GSCs comparing their sensitivity to a PARP inhibitor, AZD2281. GSCs were more resistant compared to non-GSCs, which showed a dramatic decrease in survival. Again, keeping in mind that these results are preliminary and that they need to be confirmed and tested in other cell lines, they are in contrast with published data showing that GSCs are more sensitive to PARP inhibition[112]. Though, this inconsistency is likely to be cell line dependent, given that G7 non-GSCs were very sensitive to relatively low doses of the PARP inhibitor AZD2281.

Detailed analysis of intrinsic cellular radiosensitivity and radiation responses of GSCs, as well as exploring the possible role of DNA repair inhibitors as radiosensitizers, was not the scope of my project. This field was and is being investigated further by other members of the Anthony Chalmers laboratory.

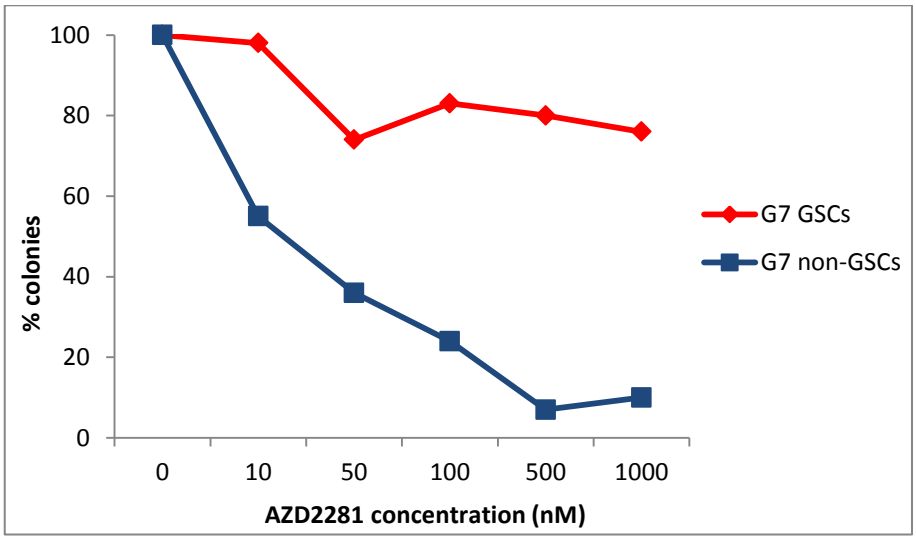

Figure 3.5 Preliminary clonogenic survival assays comparing sensitivity of G7 matched GSCs and non-GSCs to PARP inhibition.

G7 non-GSCs were more sensitive to AZD2281 than GSCs, showing a marked reduction in survival. Each data point is derived from the mean of the number of colonies counted in two 96-well plates.

3.4 Optimizing the use of a 3D culture system for GSCs and non-GSCs.

The second part of this chapter covers optimization of the use of a 3D system to culture GSCs and non-GSCs in the presence of microenvironmental factors from the tumoral niche and test the effect of these on responses of the two subpopulations to ionizing radiation and cytotoxic agents.

Amongst the various 3D culture systems, Anthony Chalmers (my supervisor at the time) and I chose to test the use of a 200 µm thick polystyrene scaffold, named Alvetex® (see figure 3.6), for numerous reasons. A) It allows several molecular and cellular techniques to be carried out on cells grown on it, such as: tissue processing, fixation, embedding and sectioning; histological staining; cryostat sectioning; immunocytochemistry; bright-field, fluorescence, confocal and electron microscopy; isolation of viable cells for passaging; isolation of cells for FACS, extraction of nucleic acid and total protein. B) Its composition, i.e. polystyrene, is inert and is the same as that of flasks used in tissue culture; hence, it is unlikely to introduce unknown effects on cells from other materials. C) It does not require specific medium or culture conditions, allowing us to continue growing GSCs and non-GSCs in their respective media. D) It is extremely user-friendly.

The choice of Alvetex® for our project, whose ultimate aim was to create a 3D model that would allow us to measure toxicity of various treatments on GSCs in a more reliable and clinically relevant system, was also supported by data (published at the time) reporting its use for hepatotoxicity studies, showing the superiority of this 3D system in terms of maintenance of cell structure, function and viability, compared to 2D cultures[252]. Since I started optimizing its use for our purpose, several other investigators employed Alvetex® to study various aspects of normal and cancer cells, suggesting that it is a very flexible system that could be used routinely to investigate cellular responses in a 3D tissue culture model, possibly replacing xenografts in some experiments[253].

The first step was to verify whether G7 GSCs were able to grow within the scaffold. I stained with Draq5 G7 GSCs that I'd previously seeded onto the scaffold and left to grow in the incubator for 7 days. As shown in figure 3.7, G7 GSCs were present deep in the scaffold. I then confirmed that the cells had grown in the whole thickness of the scaffold by analysing the distribution of G7 GSCs in frozen sections (see figure 3.8).

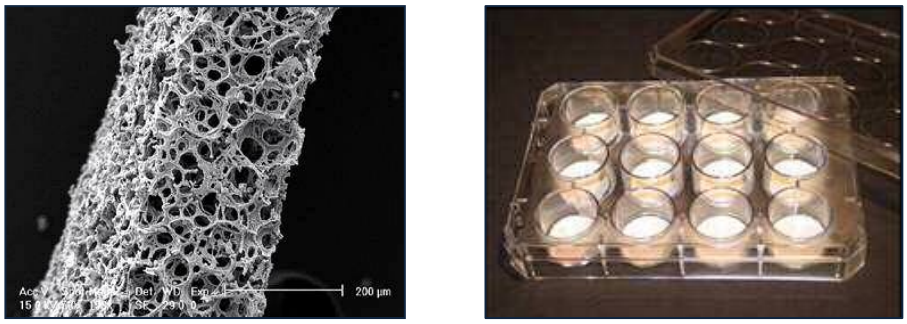

Figure 3.6 Images showing the 3D culture system Alvetex®.

On the left is a scanning electron microscope (SEM) image, showing the architecture of the scaffold. On the right is a photo of the 12-well plate format. Both images are taken from the Reinnervate brochure.

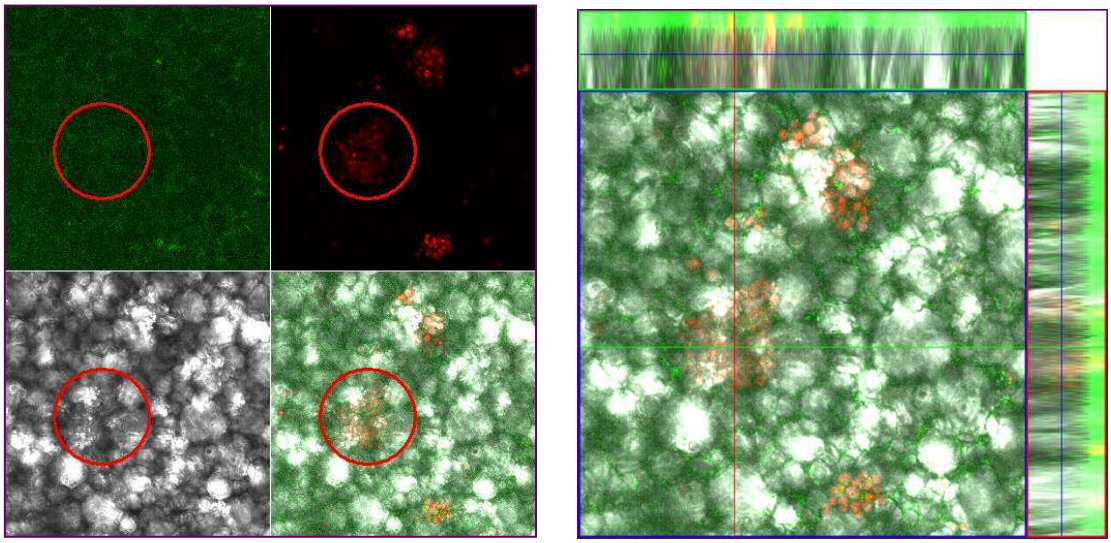

Figure 3.7 G7 GSCs are able to grow within the scaffold.

On the left, confocal microscope images taken with brightfield and fluorescence mode of G7 GSCs grown within the scaffold (fresh sample); red circle indicates cells stained with Draq 5™, shown in red. On the right, z-stack of same set of images; red and green lines indicate corresponding points in the orthogonal planes, showing localization of stained cells within the pictured scaffold (20x).

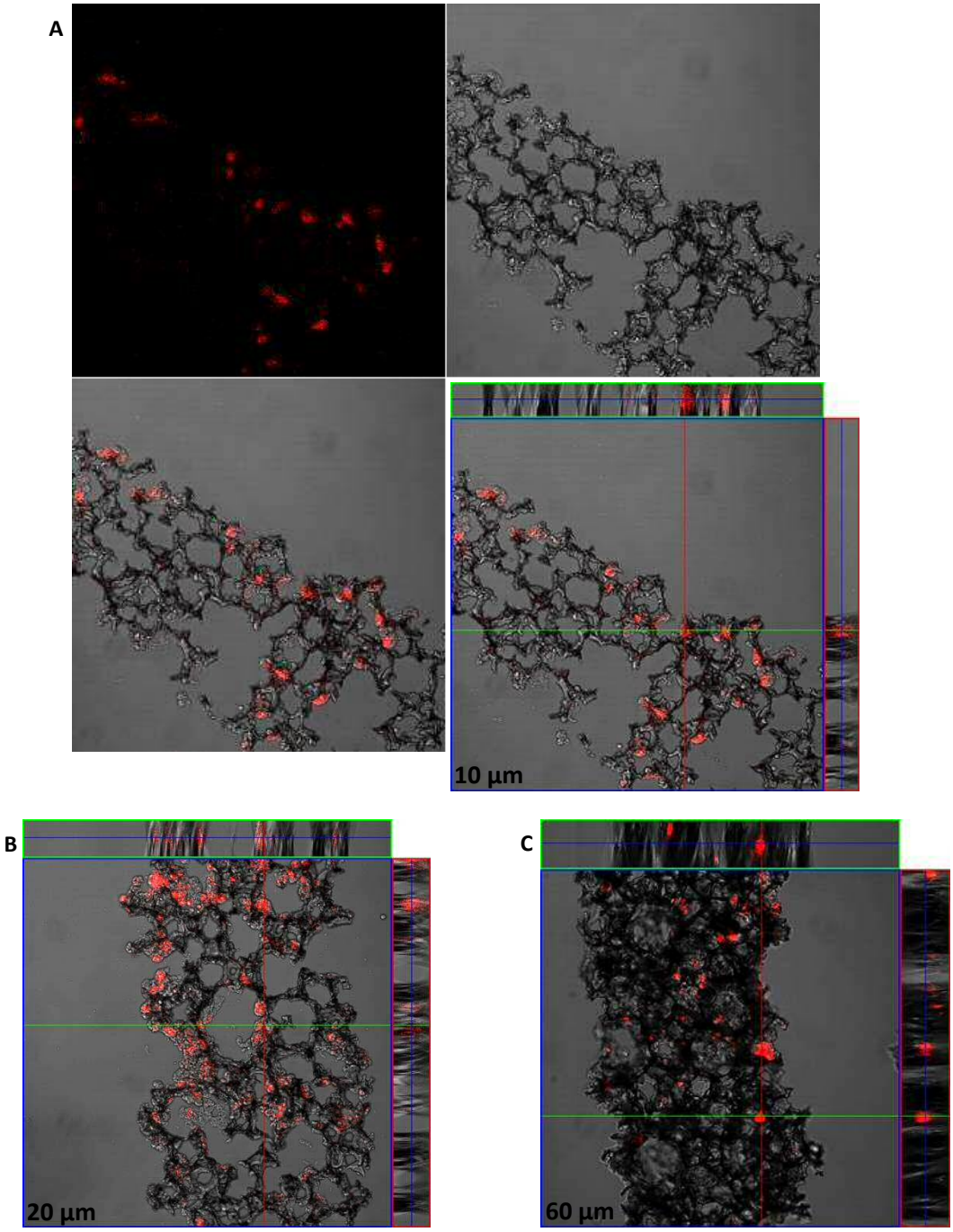

Figure 3.8 G7 GSCs are able to grow through the whole thickness of the scaffold.

Confocal microscope images of G7 GSCs grown within the scaffold (sections of frozen sample), taken with bright-field and fluorescence mode. Sections of frozen samples were cut along the width of the scaffold, with increasing thickness, as indicated in lower left corner of z-stack images (A bottom right, B and C). Nuclei of cells are stained with Hoechst (shown in red). In z-stack images, red and green lines indicate corresponding points in the orthogonal planes, showing localization of stained cells within the pictured scaffold.

The second step was to verify the feasibility of coating the scaffold with ECM components. I tested a commercially available ECM mixture first, and then a specific combination of some of the ECM components which have been shown to compose the vascular basement membrane in glioblastomas, i.e. collagen, fibronectin, laminin and vitronectin[254]. Figures 3.9 and 3.11.A demonstrate the ubiquitous distribution of fibronectin in fresh portions and in sections of frozen samples of the scaffold, while figure 3.10 shows the specificity of the anti-fibronectin antibody binding. I then seeded G7 GSCs on scaffolds coated with the specific mixture, showing that they were able to grow within the scaffold in the presence of the ECM components (see figure 3.11.B).

Coating the scaffold with customized mixtures of ECM components is valuable as it allows analysis of specific interactions of GSCs and non-GSCSs with one or more of these microenvironmental factors in a 3D culture system. This is particularly intriguing following recently published data, suggesting that these interactions need to be studied from two different perspectives. 1) How ECM components, present in the tumoral niche, influence GSC behaviour; an example of this is the role of laminin α2 expressed on tumour-associated endothelial cells in maintenance of GSCs (see perivascular niche section)[210]. 2) How GSCs modulate the microenvironment. This is suggested by a study, analysing mRNA and protein expression in GSCs as they differentiate: following exposure to serum *in vitro*, there was an increase in cell adhesion molecules, such as integrin α2 and αV, and ECM components, such as collagen IV, fibronectin and laminin; also, a treatment schedule combining TMZ with RGD peptide, which inhibits the interaction between integrins and fibronectin, resulted in prolonged survival of xenograft models obtained by injecting GSCs intracranially[255]. Based on these findings, the authors suggested that, by inducing an increase in certain ECM components, GSCs create a specific "differentiation niche", which promotes tumour recurrences; they propose targeting the interaction between GSCs and ECM as a therapeutic strategy against glioblastomas. Given that in this and in many other studies GSCs are simply seeded onto uncoated or ECM-coated dishes to mimic interactions in the tumoral niche, it follows that a 3D system, like Alvetex®, in which cancer cells are able to grow up to several weeks in the presence of exogenous or secreted ECM components, is likely to improve the methodology and produce more reliable and clinically relevant results.

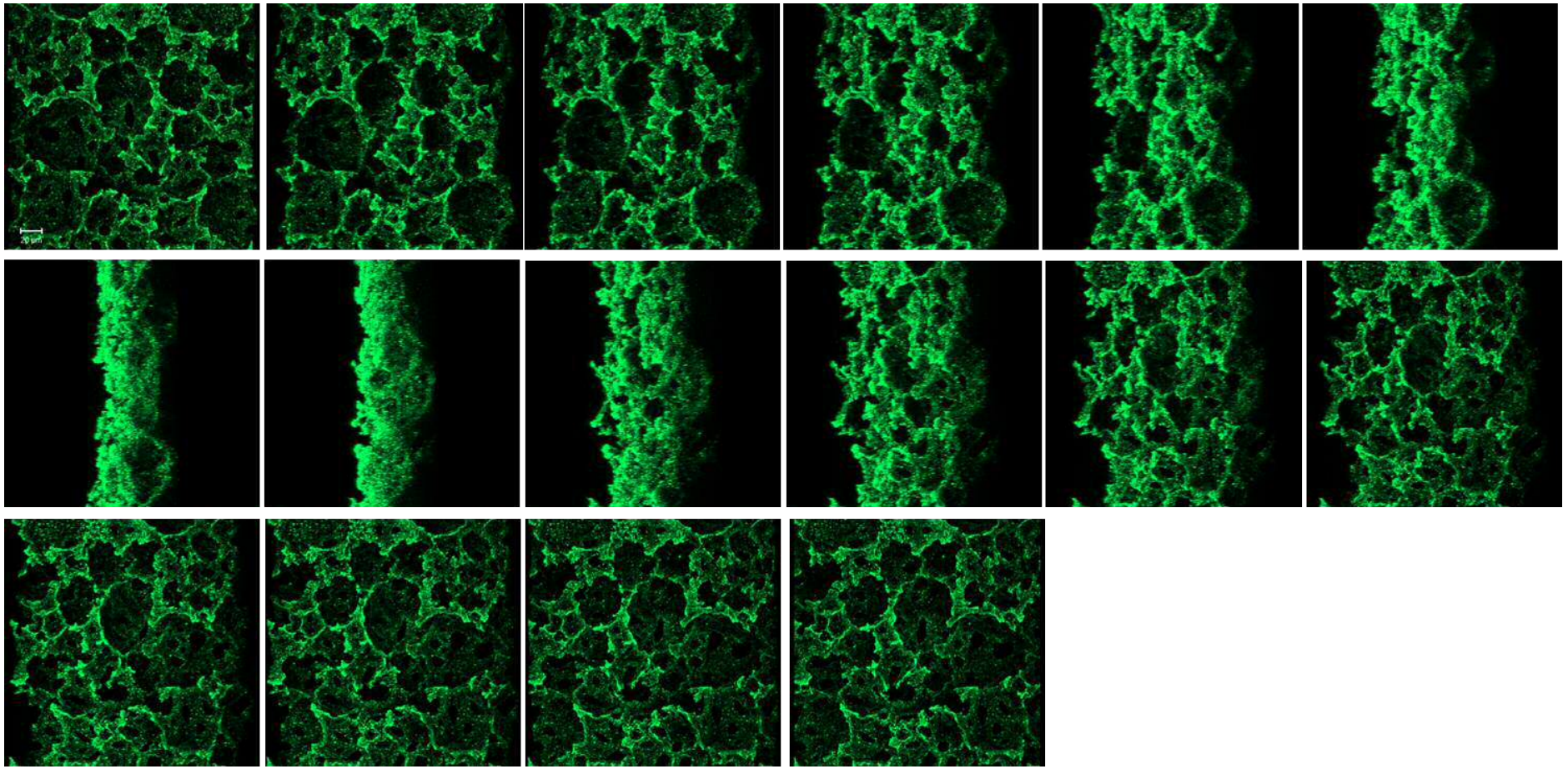

Figure 3.9 The scaffold is coated homogenously and ubiquitously with ECM mixture.

The sequence of images displays rotation of the 3D reconstruction of a z-stack of fluorescence confocal microscope images, showing distribution of anti-fibronectin antibody (green) on ECM-coated scaffold.

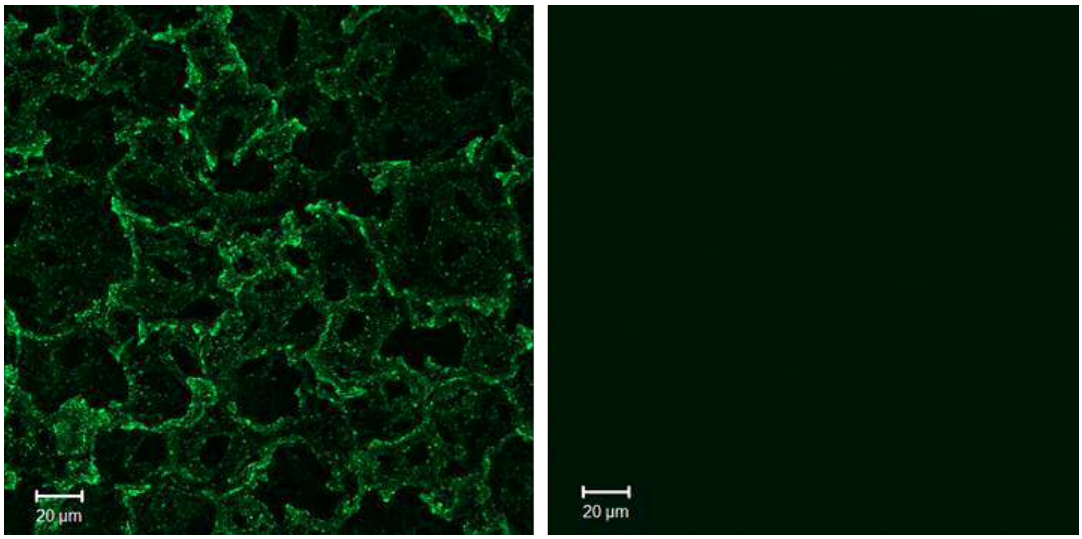

Figure 3.10 Binding of anti-fibronectin antibody is specific.

On the left, fluorescence confocal microscope image showing distribution of anti-fibronectin antibody (green) on ECM-coated scaffold. On the right, isotype control (40x).

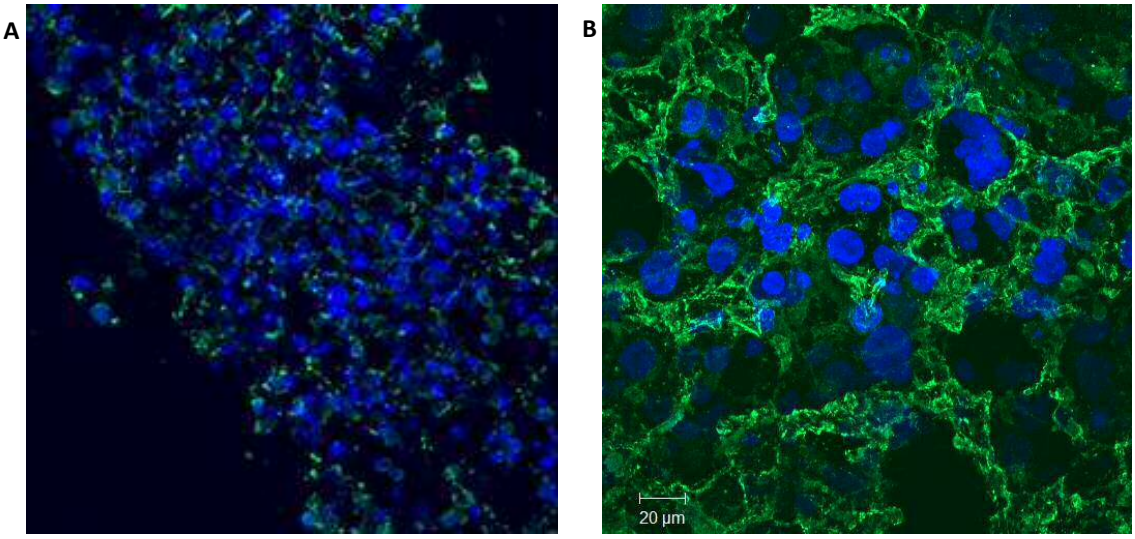

Figure 3.11 ECM-coating is present in the whole thickness of the scaffold and G7 GSCs are able to grow within the coated scaffold.

A. Fluorescence confocal microscope image of section of frozen sample, showing distribution of anti-fibronectin antibody (green) in the whole thickness of scaffold; nuclei of cells are stained with DAPI, shown in blue (20x). **B.** Fluorescence confocal microscope z-stack image of fresh sample, showing nuclei of G7 GSCs (stained with DAPI, blue) grown within a scaffold coated with an ECM mixture containing fibronectin, detected with an anti-fibronectin antibody, shown in green (40x).

The next step was to verify whether cells grown on the scaffold could be characterized for expression of stem cell markers. I stained GSCs and non-GSCs grown within the scaffold for Nestin and SOX2. As seen in figure 3.12, this experiment confirmed that characterization was possible and, most importantly, that GSCs had higher levels of stem cell markers than non-GSCs, i.e. cells grown on the scaffold exhibited patterns of stem cell marker expression consistent with their differentiation status.

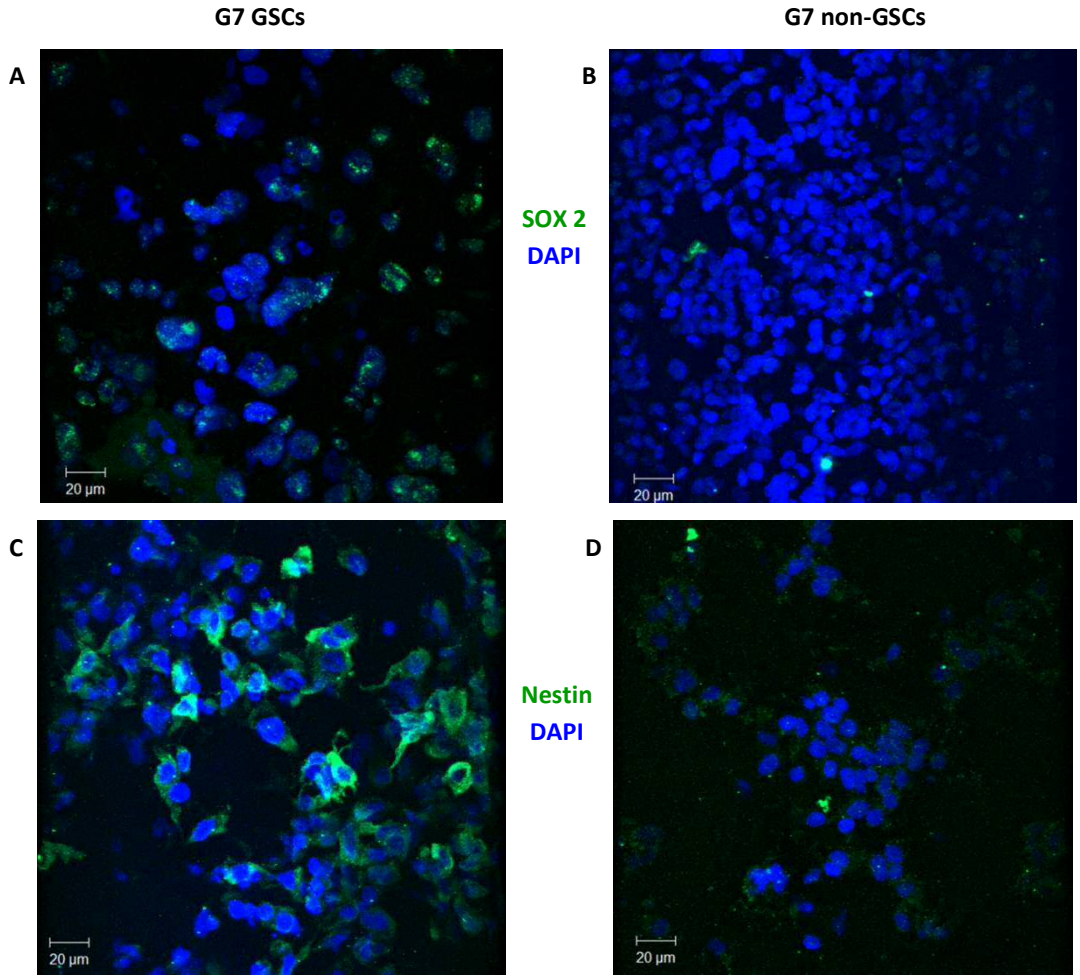

Figure 3.12 G7 GSCs grown within the scaffold express higher levels of SOX2 and Nestin compared to G7 non-GSCs.

Fluorescence confocal microscope images of G7 GSCs (A and C) and non-GSCs (B and D), showing expression of SOX2 (A and B) and Nestin (C and D). Both markers are shown in green, nuclei of cells were stained with DAPI, shown in blue (40x).

For the rest of my immunofluorescence experiments with cells grown within the scaffold, I decided to stop using sections of frozen samples and continued working only with fresh ones, given that: 1) confocal microscopy allowed me to image groups of cells within the scaffold without having to section it; 2) avoiding all the steps involved in freezing and sectioning was likely to result in more accurate images; 3) fresh samples were less time consuming. However, testing the feasibility of imaging our populations of cells within sections of frozen and paraffin embedded (data not shown) samples was an important step in the preparation of another project that is being pursued by other members of the Anthony Chalmers laboratory at the University of Glasgow, using this 3D *in vitro* culture system in conjunction with frozen or paraffin embedded glioblastoma patient specimens to further characterize GSCs and their interaction with microenvironmental factors. Figure 3.13 shows images of the preliminary experiments I contributed to, in which we used the same antibodies as for the scaffold to analyse distribution of fibronectin, nestin and SOX2, in patient samples.

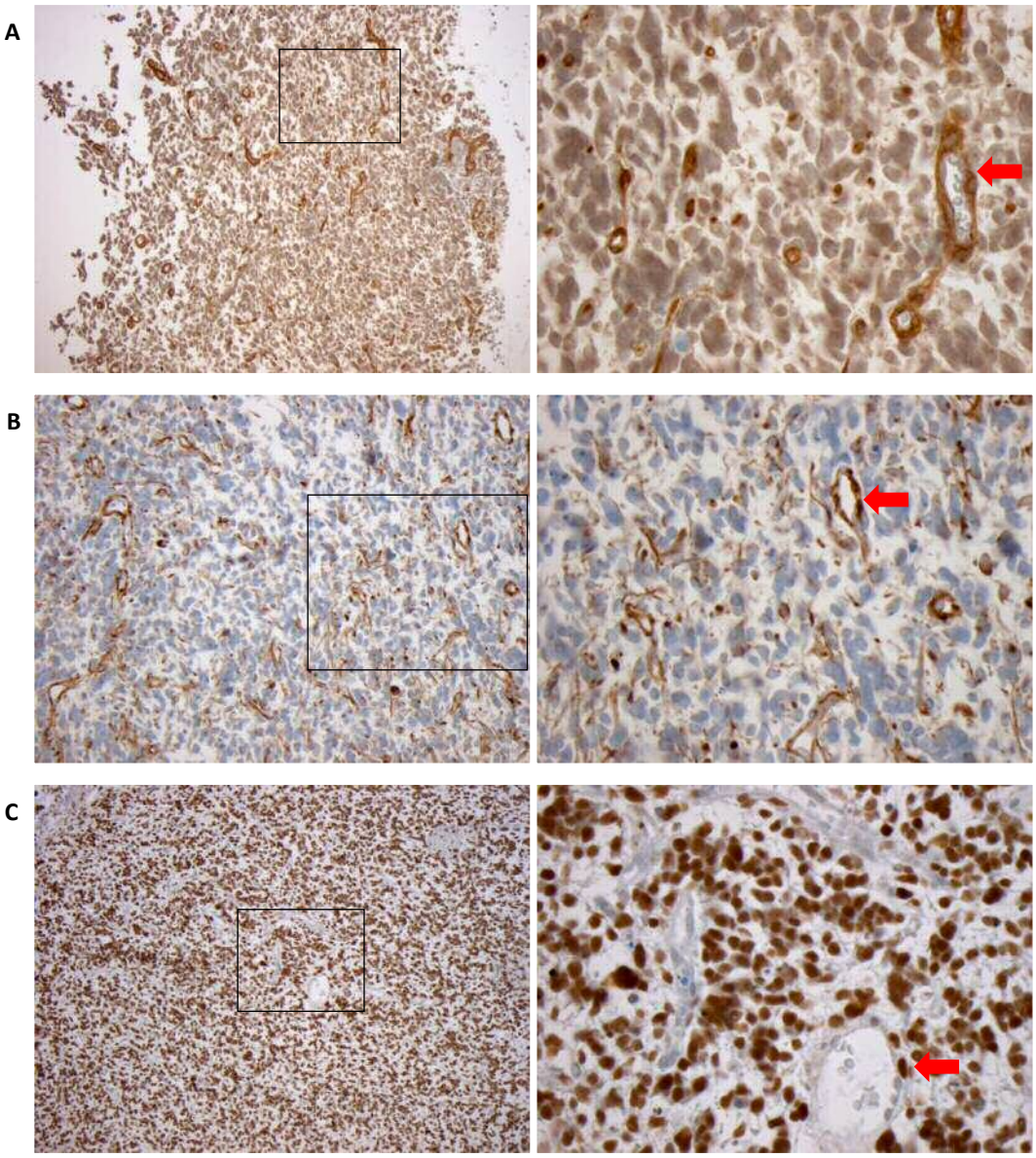

Figure 3.13 Fibronectin, nestin and SOX2 distribution in glioblastoma patient specimens.

Representative light microscope images of sections of paraffin embedded patient specimens stained with immunohistochemistry, using HRP detection (brown), for fibronectin (A), nestin (B) and SOX2 (C), followed by counterstaining with haematoxylin (light blue). The images on the right show enlarged views of selected areas (indicated by black rectangles) from each image on the left. Red arrows indicate examples of blood vessels.

3.5 Optimizing the use of Alvetex® to study radiation responses of GSCs and non-GSCs.

Once I demonstrated that GSCs and non-GSCs could be cultured on the scaffold in the presence of microenvironmental factors, I started testing whether studying radiation responses in the same model was feasible. Besides clonogenic survival assays, which represent the gold standard method, radiosensitivity of cancer cells is measured by quantifying induction and resolution of phosphorylated histone H2A (gamma H2AX), as a surrogate marker of DNA double strand break repair, and evaluating percentage of apoptotic cells following ionizing radiation. Hence, I tested whether quantifying gamma H2AX foci in cells grown and irradiated within the scaffold was possible. Figure 3.14 shows representative images of G7 GSCs cultured on Alvetex® and analysed for gamma H2AX at 1, 4 and 24 hours, following treatment with 3 Gy.

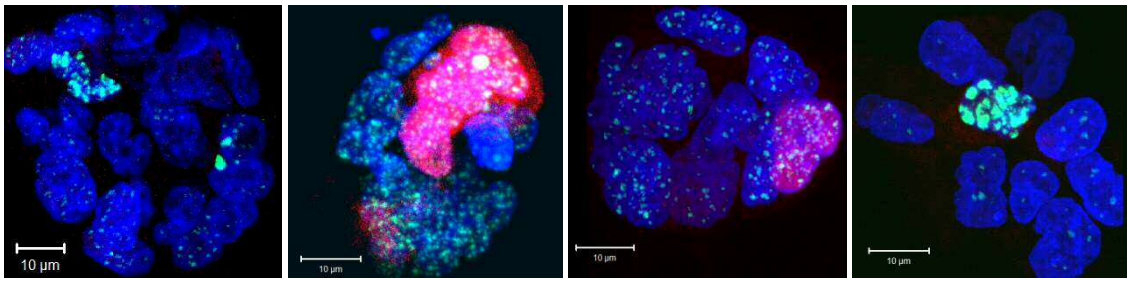

Figure 3.14 G7 GSCs grown and irradiated within the scaffold can be evaluated for formation and resolution of gamma H2AX foci.

Fluorescence confocal microscope images of G7 GSCs, showing gamma H2AX (in green) and CENP-F (in red) staining, at 0, 1, 4 and 24 hours (from left to right) after treatment with 3 Gy; nuclei of cells were stained with DAPI, shown in blue (40x).

In order to optimize this assay, first I used deconvolution to improve the contrast and resolution of gamma H2AX foci and then the 3D view on the Imaris (version 6.3.0; Bitplane) software, which allows an interactive visualization of the entire z-stack. As seen in figure 3.15, with this processing technique, foci appeared clearer and more distinct.

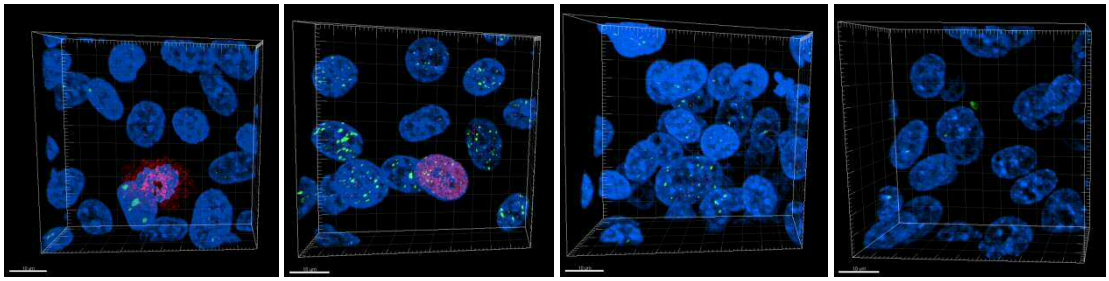

Figure 3.15 Use of deconvolution and Imaris software 3D view to optimize gamma H2AX foci counting in cells grown and irradiated within the scaffold.

3D view on Imaris software of deconvolved fluorescence confocal microscope images of G7 non-GSCs, showing gamma H2AX (in green) and CENP-F (in red) staining, at 0, 1, 4 and 24 hours (from left to right) after treatment with 2 Gy; nuclei of cells were stained with DAPI, shown in blue (63x).

Then, in order to reduce the variability in foci counting related to the state (i.e. tiredness) of the operator, I evaluated the feasibility of quantifying gamma H2AX foci by using the Imaris software, and specifically the 'spot function'. In figure 3.16, an example of a deconvolved image of G7 GSCs viewed and processed with Imaris shows how foci are identified and marked with the 'spot function', demonstrating that this is feasible and accurate, especially as the operator can easily check the results on the computer monitor.

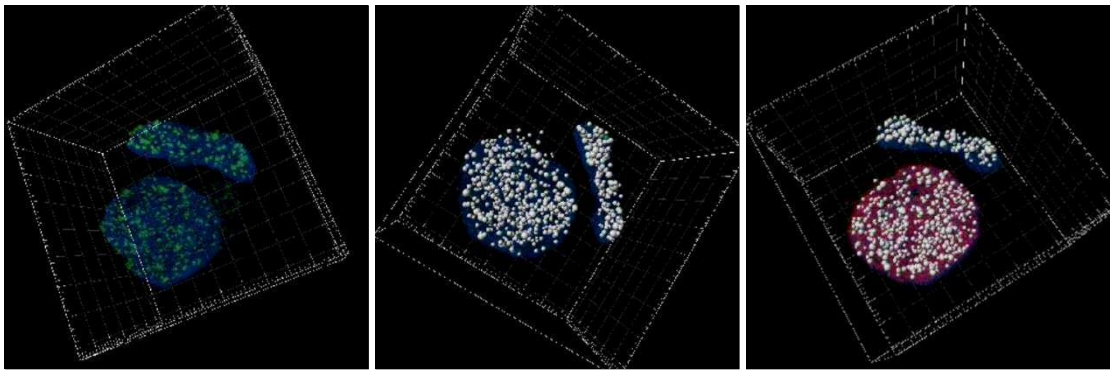

Figure 3.16 Use of the 'spot function' on the Imaris software to identify gamma H2AX foci in cells grown and irradiated within the scaffold.

3D view on Imaris software of deconvolved fluorescence confocal microscope images of G7 GSCs, showing gamma H2AX (in green) and CENP-F (in red) staining 1 hour after treatment with 3 Gy; nuclei of cells were stained with DAPI, shown in blue (63x). Each identified focus is marked with a white sphere.

Given that the output of the software in terms of number of spots (i.e. foci) is referred to the entire image, the next step was to establish the most accurate and user-friendly way to obtain a quantification of the spots per cell. I tested whether the 'area of interest function' was an appropriate tool to identify each cell in the images, but found that it was extremely time-consuming and was not suitable for my purpose, given the shape and spatial distribution of the cells in the various planes. Furthermore, data from the mitotic kinase project indicated that it was not accurate to estimate the DNA content of GSCs simply by performing DAPI probing without co-staining with markers for cell cortex, as GSCs have a slightly higher percentage of polynucleated cells and often present nuclei of irregular shapes (see section 4.3). Given these findings, I tested whether the volume rendering algorithm in the Imaris software was an appropriate tool to obtain a reproducible quantification of nuclear volume, which could be used as a denominator to normalize the number of foci. Figure 3.17 shows a representative image of the view of the volume rendering, together with the 'spot function', on the monitor of the Imaris workstation. Figure 3.18 displays the data from one of the experiments that I carried out during the optimization process, comparing induction and resolution of radiation induced gamma-H2AX foci in cells grown and irradiated within the scaffold and on coverslips. Differently to other studies that quantified radiation-induced gamma-H2AX foci per cell, showing no difference between GSCs and non-GSCs at early time points[238, 242], these preliminary results suggest that the two subpopulations differ in their DNA repair ability 1 hour post-irradiation. Though, interpretation of these findings with regards to DNA damage induction and resolution in GSCs and non-GSCs needs to be cautious as further testing and validation is warrented.

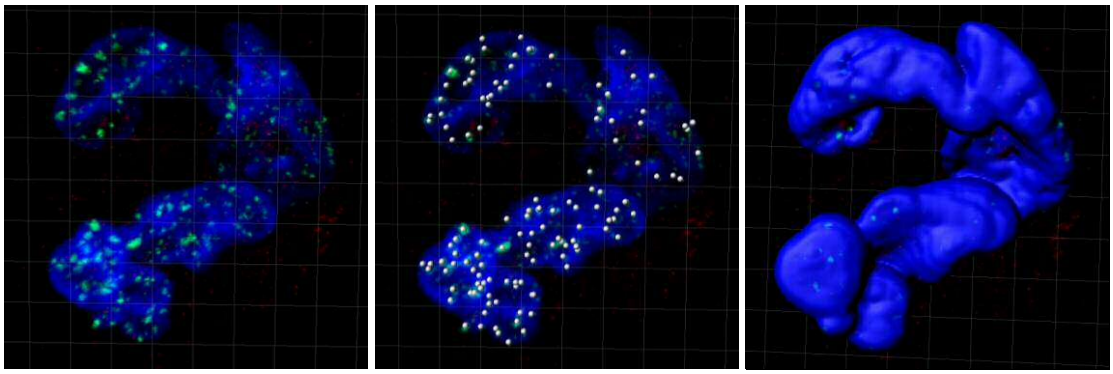

Figure 3.17 Use of the 'spot function' and the volume rendering algorithm on the Imaris software to quantify nuclear volume of cells grown within the scaffold.

3D view on Imaris software of deconvolved fluorescence confocal microscope images of G7 GSCs, showing gamma H2AX (in green) staining 1 hour after treatment with 3 Gy; nuclei of cells were stained with DAPI, shown in blue (63x). Each identified focus is marked with a white sphere (central image). On the right, example of visualization of volume rendering of DAPI staining.

Samples and treatment		DAPI Volume (μm^3)	Number of foci	Foci/volume ratio
GSCs (3D)	0 Gy	72862	410	**0.006**
	3 Gy 1h	182136	4862	**0.027**
	3 Gy 4hh	79705	880	**0.011**
	3 Gy 24hh	86144	426	**0.005**
Non-GSCs (3D)	0 Gy	51612	85	**0.002**
	3 Gy 1h	53168	767	**0.014**
	3 Gy 4hh	39064	512	**0.013**
	3 Gy 24hh	42422	103	**0.002**
2D non-GSCs	0 Gy	84062	250	**0.003**
	3 Gy 1h	103820	2219	**0.021**
	3 Gy 4hh	88474	1365	**0.015**
	3 Gy 24hh	67483	442	**0.007**

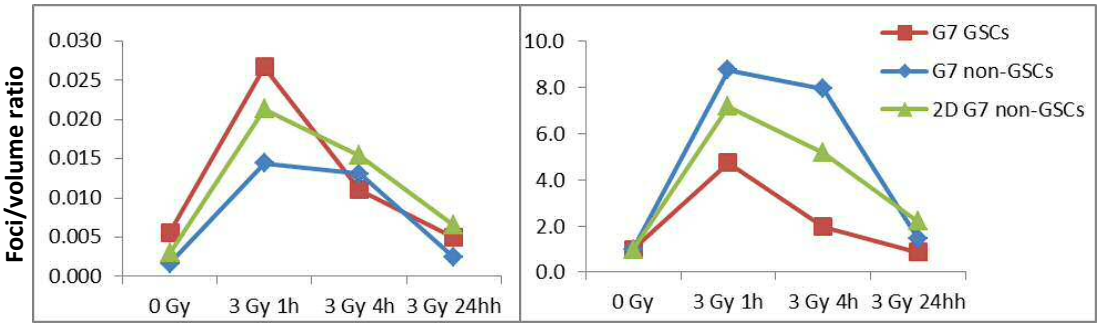

Figure 3.18 Use of the 'spot function' and the volume rendering algorithm on the Imaris software to quantify induction and resolution of radiation induced gamma-H2AX foci in cells grown and irradiated within the scaffold and on coverslips.

In the table above, output data obtained by processing deconvolved fluorescence confocal microscope images with the 'spot function' and the volume rendering algorithm on the Imaris software. Images of cells stained for gamma H2AX were taken at 0, 1, 4 and 24 hours after treatment with 3 Gy. The foci/volume ratios are plotted in the graphs at the bottom, as raw data on the left, as normalised to untreated on the right.

One of the potential benefits of normalizing the number of foci to the DAPI content with the volume rendering algorithm is that it addresses possible variations in DNA content between two populations, i.e. it reduces the known inaccuracies due to differences in cell cycle distribution[256]. Other studies, that developed the use of computer software modules to automatically interpret and/or count foci on microscopy images, validated them by comparing their output with the most commonly used method, i.e. manual counting either directly viewing the samples with a microscope or subsequently looking at previously captured images on a monitor[257]. I did not perform correlation analysis with manual foci quantification, because I routinely carefully inspected all images processed with the 'spot function' to correct any misinterpretations. In fact, the above experiments were not designed to develop a fully automated interpretation tool for counting foci, but rather a semi-automated one with the aim of improving the accuracy of simple visual interpretation, while reducing time-consumption. Other evaluations of the accuracy of this approach, such as correlation with clonogenic survival data, would be difficult to interpret, given that previous studies have not found positive results[258].

Finally, I tested whether I could evaluate apoptosis in cells grown and irradiated within the scaffold by quantifying the number of cleaved caspase 3 positive cells. As seen in figure 3.19, GSCs stained for cleaved caspase 3 are easily identified and quantified.

A

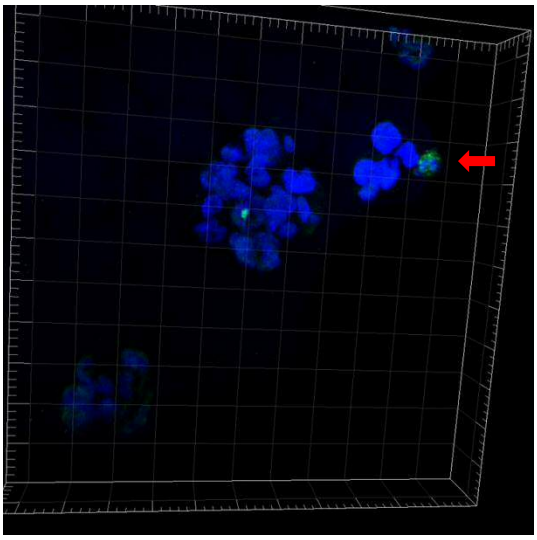

B

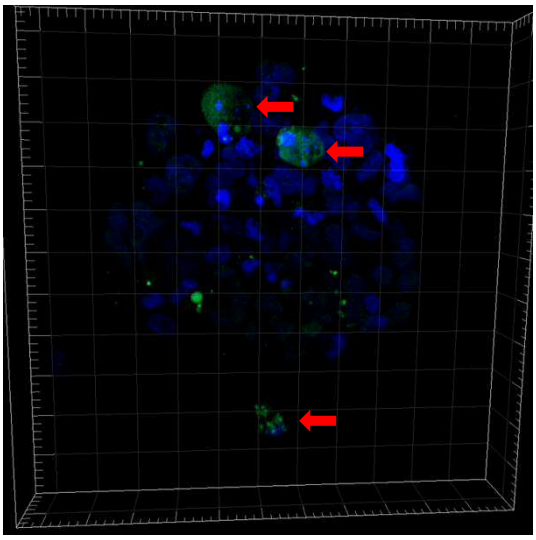

C

Treatment	Cleaved caspase 3 + cells/total number of cells	
	Normoxia	Hypoxia
0 Gy	6/353	3/196
3 Gy 12 hh	7/526	1/198
3 Gy 18 hh	36/691	8/326
3 Gy 48 hh	10/407	7/429

D

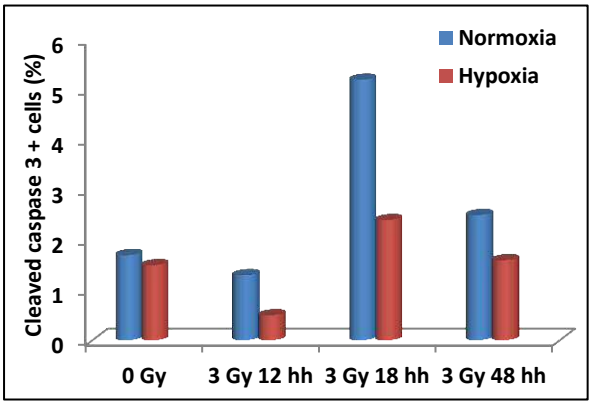

Figure 3.19 G7 GSCs grown and irradiated within the scaffold can be evaluated for apoptosis rates.

A and **B.** Fluorescence confocal microscope images of G7 GSCs, showing cleaved caspase 3 (in green) staining, at 0 and 18 hours (from left to right) after treatment with 3 Gy; nuclei of cells were stained with DAPI, shown in blue (40x). Red arrows indicate apoptotic cells. **C.** Data obtained by quantifying cleaved caspase 3 positive cells in fluorescence confocal microscope images viewed on the Imaris software. Images of G7 GSCs, grown within the scaffold in incubators with 21% (normoxia) and 3% (hypoxia) pO2, were taken at 0, 12, 18 and 48 hours after treatment with 3 Gy. **D.** The percentages of cleaved caspase 3 positive cells are plotted in the graph.

3.6 Discussion

In this chapter, I describe optimization of methods to study both GSCs and non-GSCs. These tools allow analysis of treatment responses related to intrinsic cellular characteristics as well as those induced by microenvironmental factors.

For the clonogenic survival assay, I adopted a different approach to those used in the published studies comparing radiosensitivity in GSCs and non-GSCs. Bao *et al*. chose to expose both subpopulations to serum-free medium without growth factors for 24 hours post-treatment and then changed to serum-containing medium to induce attachment and allow colony visualization with the standard methylene blue staining method[152]. Mc Cord *et al*. used poly-L-lysine coated wells with serum-free medium for both subpopulations[236]. These studies selected GSCs and non-GSCs based on CD133 expression and applied the same growth conditions to all the cells. Their approach has the advantage of evaluating radiosensitivity by quantifying the same type of colony grown in the same conditions, but it has the limitation of using pro-attachment methods (addition of serum to medium, withdrawal of growth factors, exposure to poly-L-lysine) that are likely to induce pro-differentiation signals in GSCs. Carruthers *et al*. plated GSCs in serum-free medium and non-GSCs in serum-containing medium, seeding both subpopulations in Matrigel™-coated 6 wells dishes[238]. Therefore, they used the culture condition to select for stemness and induced growth of GSCs as adherent monolayer cultures by plating them on Matrigel™, a technique routinely used in several of their experiments, including the tumorigenicity assay. This approach has the advantage of analysing radiosensitivity maintaining the two subpopulations in their culture conditions and, at the same time, evaluating similar types of colonies. As briefly mentioned in the introduction to this chapter, I chose a strategy that combined the neurosphere formation assay with an adapted version of the standard clonogenic survival assay, given that both in vitro techniques have been correlated to clinical outcome of cancer patients[259, 260]. It is not possible to predict which approach is the most clinically relevant one based on published data. This evaluation would need a comparative study of the various methods analysing radiosensitivity of several patient derived primary cell lines and calculating the correlation of each set of results with clinical outcome.

Concerning the 3D model, I have already analysed the rationale for choosing and optimizing the use of Alvetex® to culture GSCs and non-GSCs. Comparing my experience to published data regarding the use of 3D systems to culture glioblastoma cells, my work gives additional contributions to this field, given that other studies have simply grown cells within the chosen 3D model, without introducing elements of the tumoral niche[261, 262]. The only exception is a

pre-implantation co-culture with endothelial cells for a tumorigenicity assay in a study analysing regulation of GSCs by IL-8; no other evaluation of the effects of this interaction on the 3D system was reported by the authors[209]. Not only I have shown that GSCs and non-GSCs can grow on the scaffold in the presence of several microenvironmental factors, I have also demonstrated that these cells can be interrogated in these conditions with regards to their response to treatment, quantifying DNA damage surrogate markers and apoptosis. The next step will be to assess how this 3D culture system compares to *in vivo* models in terms of clinical relevance, evaluating the possibility of replacing animals for a portion of the pre-clinical investigational studies. I was not able to start this work due to the lack of facilities to create intracranial xenografts at University of Sussex. Other members of Anthony Chalmers laboratory in Glasgow generated these *in vivo* models using G7 and E2 cell lines and are currently developing this research area.

In conclusion, I propose that the techniques I have optimized are useful tools that are likely to allow a more comprehensive approach in glioblastoma research and a better selection of therapeutic agents for *in vivo* pre-clinical experiments.

Chapter 4

Glioblastoma stem cells are highly sensitive to subtle changes in Aurora kinase A activity

4.1 Introduction

Processes involved in mitosis are targeted by two main treatment modalities that are currently under investigation in clinical trials in glioblastoma patients (discussed in the first section of the general introduction):

- the tumour treating fields (TTF), consisting in alternating electric fields, which cause cell death of the proliferating tumour population; although the mechanism underlying their cytotoxic effect is not fully clarified, proposed modes of action mainly involve cell division, with disruption of mitotic spindles during the metaphase to anaphase transition and aggregation of macromolecules and organelles during telophase[36];
- microtubule inhibitors, which cause cell death through stabilization of microtubules, disrupting intracellular transport during interphase and spindle assembly during mitosis[263].

Given that these therapeutic strategies have quite a broad mechanism of action and based on the increasing evidence associating specific mitotic kinases with GSC biology, I decided to adopt a focused approach, investigating mitotic phenotypes and characterizing cellular factors involved in asymmetric cell division, one of the key features of CSCs[141].

I will now give a brief introduction on general concepts related to mitosis, starting with a review of the literature on asymmetric cell division.

Most of the current knowledge on asymmetric cell division is based on studies using Drosophila melanogaster and Caenorhabditis elegans, i.e. fly and worm models. Four main steps are involved in asymmetric cell division: 1) symmetry is broken; 2) polarity is established; 3) fate determinants are segregated in specific regions; 4) mitotic spindle is positioned so that the fate determinants are correctly distributed in the two daughter cells[264]. A major role in these steps is played by the centrosome, the main microtubule organising centre in proliferating mammalian cells, which coordinates mitosis, cell polarity and motility[265]. Each centrosome is formed by two centrioles, composed of tubulin polymers and surrounded by a matrix of proteins, known as the pericentriolar material (PCM), comprising mainly pericentrin and γ-tubulin. During the cell cycle, centrosomes undergo the following changes: in G1, the pair of centrioles is surrounded by a relatively small amount of PCM; during S phase, centrioles duplicate; in G2, more abundant PCM accumulates around the centrioles, allowing them to organize the microtubules that form the mitotic spindle during M phase[266]. This process by which centrosomes form the two poles of the mitotic spindle in a dividing cell is regulated by several proteins, such as Plk1, Plk4, Aurora kinase A (AurA), Cyclin dependent kinase 1 (Cdk1)[267]. Given that the general principle and several genes encoding for symmetry regulators are conserved through species, findings from these studies have formed the bases of our

understanding of asymmetric cell division in normal stem cells. Though, whether and how these mechanisms apply to CSCs is still mostly unknown, suggesting the need for studies investigating mitotic phenotypes and characterizing structural and functional features of centrosomes and their regulatory proteins in GSCs and non-GSCs. These studies are also supported by data showing that: centrosome abnormalities are implicated in tumour initiation[268]; altered centrosomes are present in brain tumour patient specimens[269]; centrosome regulatory kinases, such as Plk1 and AurA, are overexpressed in glioblastomas and their expression levels are correlated to patient outcome[245, 270-274].

In this chapter, I report the results of my analysis of mitotic spindle and centrosome morphology in GSCs and non-GSCs. Based on the observation of a higher level of spindle abnormalities and a more pronounced maturation of centrosomes preceding cell division in GSCs, I explore whether these cells have an increased requirement for AurA activity, investigating the effects of the selective AurA inhibitor MLN8237 on the two subpopulations.

4.2 Glioblastoma stem cells have higher levels of mitotic spindle abnormalities

Cell division of GSCs remains poorly characterized. To my knowledge, the only publication analysing this process focused on examining the modes of cell division, i.e. symmetric or asymmetric, used to maintain a pool of GSCs[141]. Given the lack of data on GSC mitosis, I decided to start with analysing mitotic spindle phenotypes in GSCs and non-GSCs, using immunofluorescence and staining the two subpopulations for α-tubulin and γ-tubulin, as a method to visualize spindle microtubules and the PCM, respectively. I observed that there were significantly more abnormal mitotic spindles (monopolar and multipolar) in GSCs than in non-GSCs: in the G7 cell line, the percentages were 14% *vs* 4%, respectively (see figure 4.1.A). Figures 4.1.B-D show representative images of bipolar, monopolar and multipolar spindles. I then verified whether the difference in mitotic spindle abnormalities was a consequence of growth in suspension. I cultured non-GSCs as non-adherent aggregates by using tissue culture plastics that would not allow attachment. All randomly imaged mitotic cells had bipolar spindles, suggesting that growth conditions are not a confounding factor for the observed mitotic defects.

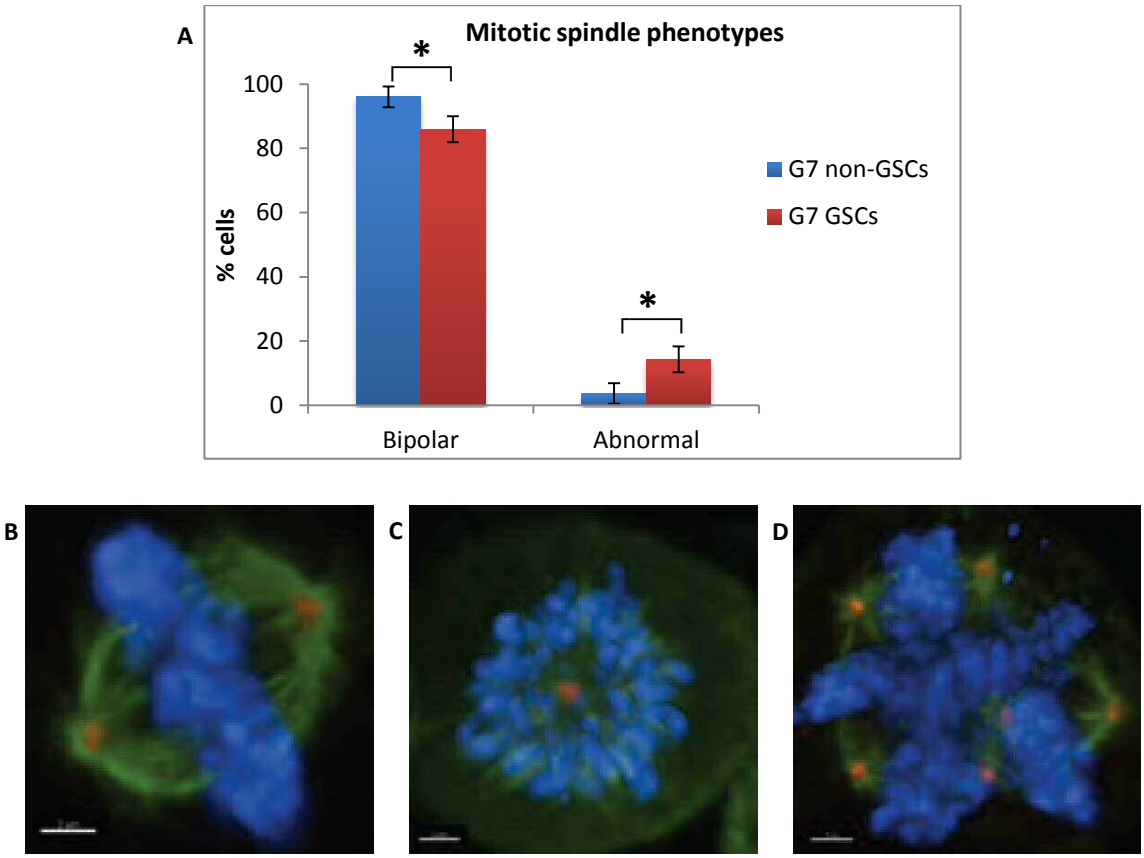

Figure 4.1 GSCs have a higher percentage of abnormal mitotic spindles than non-GSCs.

GSCs and non-GSCs were stained for α tubulin (green), γ tubulin (red) and DAPI (blue), to visualize mitotic spindle morphology. **A.** A graph displays the percentages of normal and abnormal spindles in G7 GSCs and non-GSCs. An average of 26 mitotic cells/condition/experiment were randomly imaged and scored. Results are representative of three independent experiments. Error bars indicate means ± SD (*p=0.0232, two tailed t-test). **B-D.** Representative images of mitotic phenotypes observed in G7 GSCs: bipolar (B), monopolar (C) and multipolar (D). Scale bar 2µm.

4.3 Glioblastoma stem cells have higher percentages of polyploid cells

In order to evaluate the consequences of the observed mitotic abnormalities in terms of aneuploidy, I analysed metaphase chromosome spreads. As seen in figure 4.2, examination of GSCs showed the presence of cells with large numbers of chromosomes. Given that cells in suspension tend to form aggregates and that, while evaluating mitotic spindles, I often noted, in the GSC subpopulation, two or more nuclei in close vicinity (see figure 4.3), I speculated that the difference in chromosome numbers between the two populations could be a consequence of cell clumping as well as a sign of polyploidy resulting from mitotic failure. In order to distinguish clumps from polyploid cells, I analysed both subpopulations following staining with phalloidin, a dye that allows visualization of the cell cortex. I found that, amongst GSCs, polyploid cells were much more frequent than in the non-GSC subpopulation: in the G7 cell line, the percentages were 25% *vs* 6%, respectively (see figure 4.4.A). Figures 4.4.B-C show representative images of GSCs and non-GSCs stained with phalloidin. These findings suggest that the higher percentage of mitotic spindle abnormalities results in higher levels of aneuploidy in GSCs.

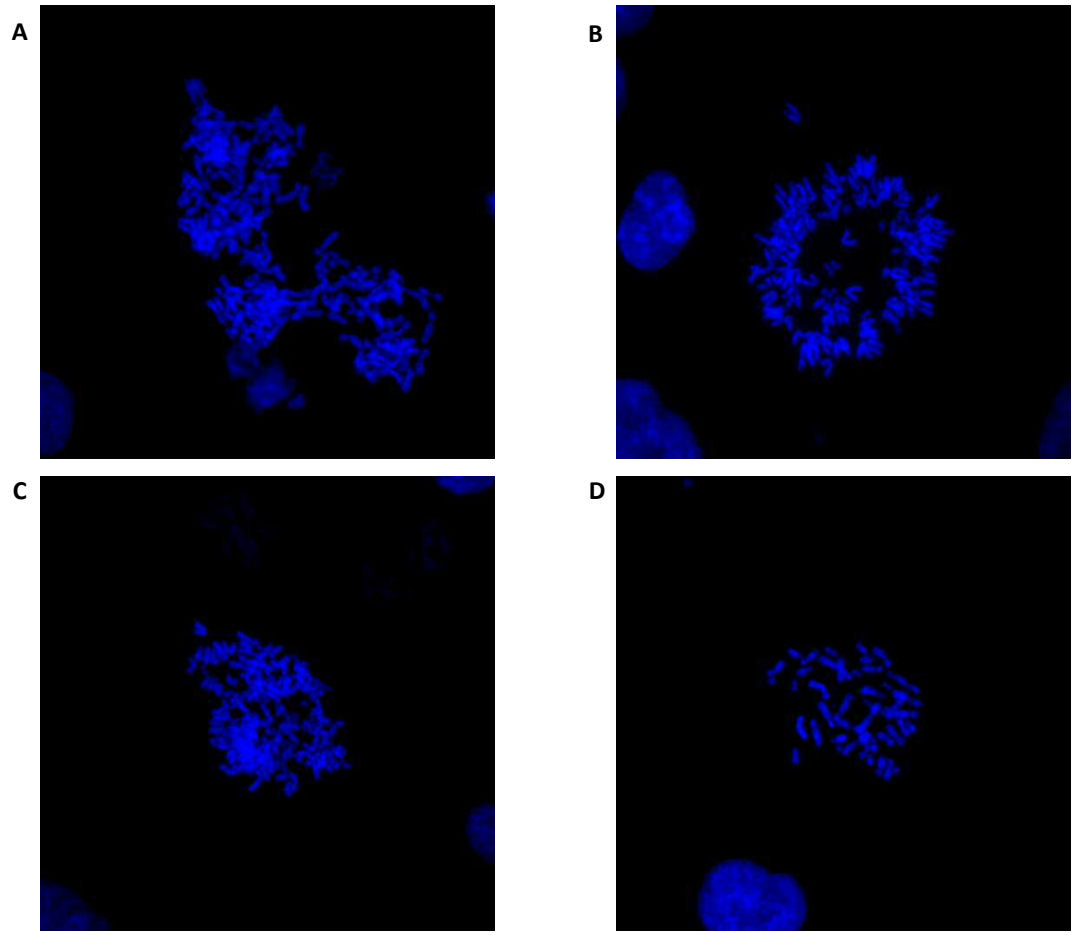

Figure 4.2 Chromosome spreads of GSCs show considerable numerical abnormalities.

Representative images of chromosome spreads of G7 GSCs (A-C) and non-GSCs (D).

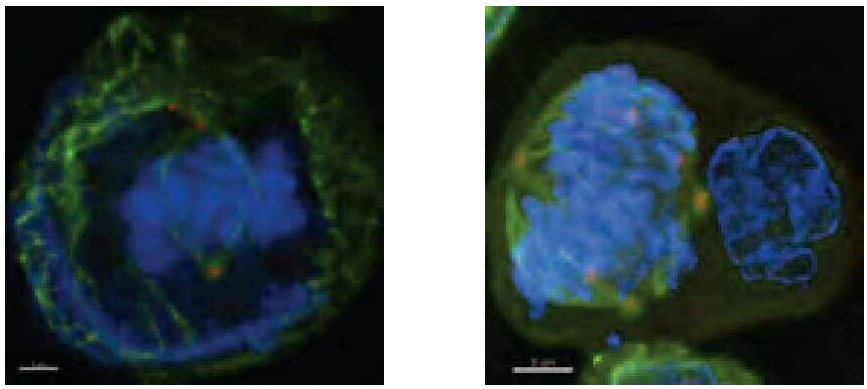

Figure 4.3 Observation of the GSC subpopulation shows several cellular images with two or more nuclei in close vicinity.

GSCs were stained for α tubulin (green), γ tubulin (red) and DAPI (blue). Representative images of G7 GSCs, with one nucleus undergoing mitosis and the other in interphase. Scale bar 2µm.

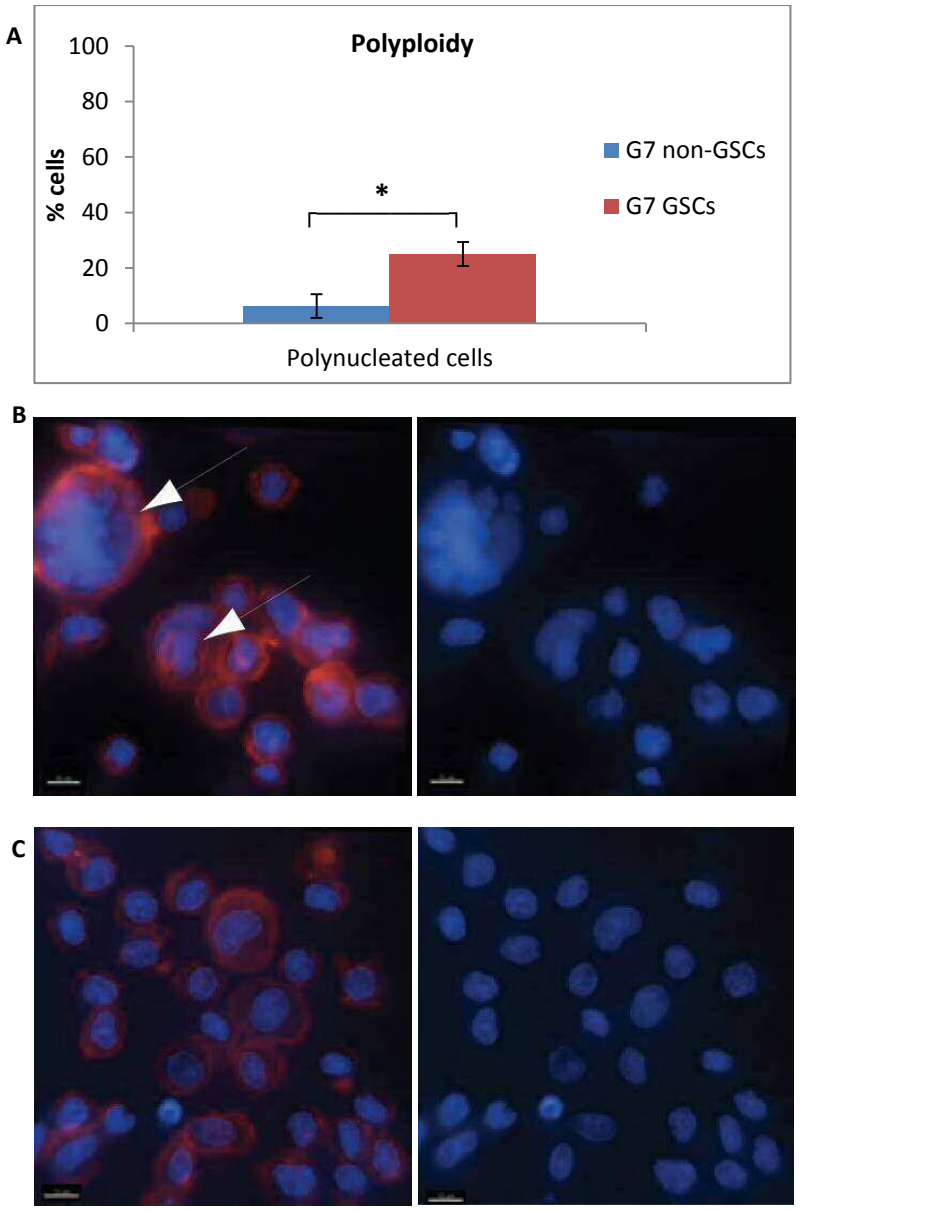

Figure 4.4 GSCs have a higher frequency of polyploid cells.

GSCs and non-GSCs were stained with phalloidin (red) and DAPI (blue) to visualize the cell cortex and nucleus. **A.** A graph shows the percentages of polynucleated cells in GSCs and non-GSCs. An average of 251 cells/condition/experiment were randomly imaged and scored. Results are representative of three independent experiments. Error bars indicate means ± SD (*p=0.000275, two tailed t-test). **B-C.** Representative images of GSCs (B) and non-GSCs (C). Arrows show polyploid cells. Scale bar 10µm.

4.4 Glioblastoma stem cells show a distinct centrosome cycle

Given that centrosomes have a pivotal role in mitotic spindle assembly, I investigated whether there were any distinctive features in the centrosome cycle of GSCs and non-GSCs. As a measure of centrosome maturation, i.e. the process by which PCM proteins accumulate around the centrioles in preparation for mitosis, I analysed distribution of γ-tubulin, one of the main PCM proteins, during the cell cycle. I quantified the size of centrosomal γ-tubulin staining, obtained with immunofluorescence, in interphase and mitotic cells from the two subpopulations. I then calculated the ratio between centrosomal γ-tubulin in mitotic and interphase cells to obtain a numerical estimate of accumulation of this protein at the centrosomes. GSCs exhibited a more pronounced accumulation of γ-tubulin at the centrosomes, with a ratio more than twofold higher than that of non-GSCs in the G7 cell line (see figure 4.5.A). Representative images from the two subpopulations are shown in figures 4.5.B-C.

In order to verify that the observed γ-tubulin staining was centrosomal, I tested whether it co-localized with centrin, a protein present in centrioles and PCM. As seen in figure 4.6, the centrosomal specificity of γ-tubulin staining was confirmed. Furthermore, a preliminary analysis of centrin distribution in interphase cells of the two subpopulations showed that amongst GSCs there were higher percentages of cells with increased centrosome staining compared to non-GSCs, suggesting more frequent centriole numerical abnormalities: 32% vs 17% in G7 GSCs and non-GSCs, respectively.

Taken together, these findings support the hypothesis that there are structural and/or functional differences between GSCs and non-GSCs with regards to centrosomes, suggesting the importance of investigating in detail regulatory proteins involved in the centrosome cycle, as a strategy to find specific therapeutic targets to kill GSCs. Amongst the various mitotic kinases, I decided to focus on AurA, a member of the Aurora kinase family that, differently to its paralogues B and C, mainly implicated in chromosome dynamics, is primarily involved in centrosome function and is one of the major regulators of its maturation.

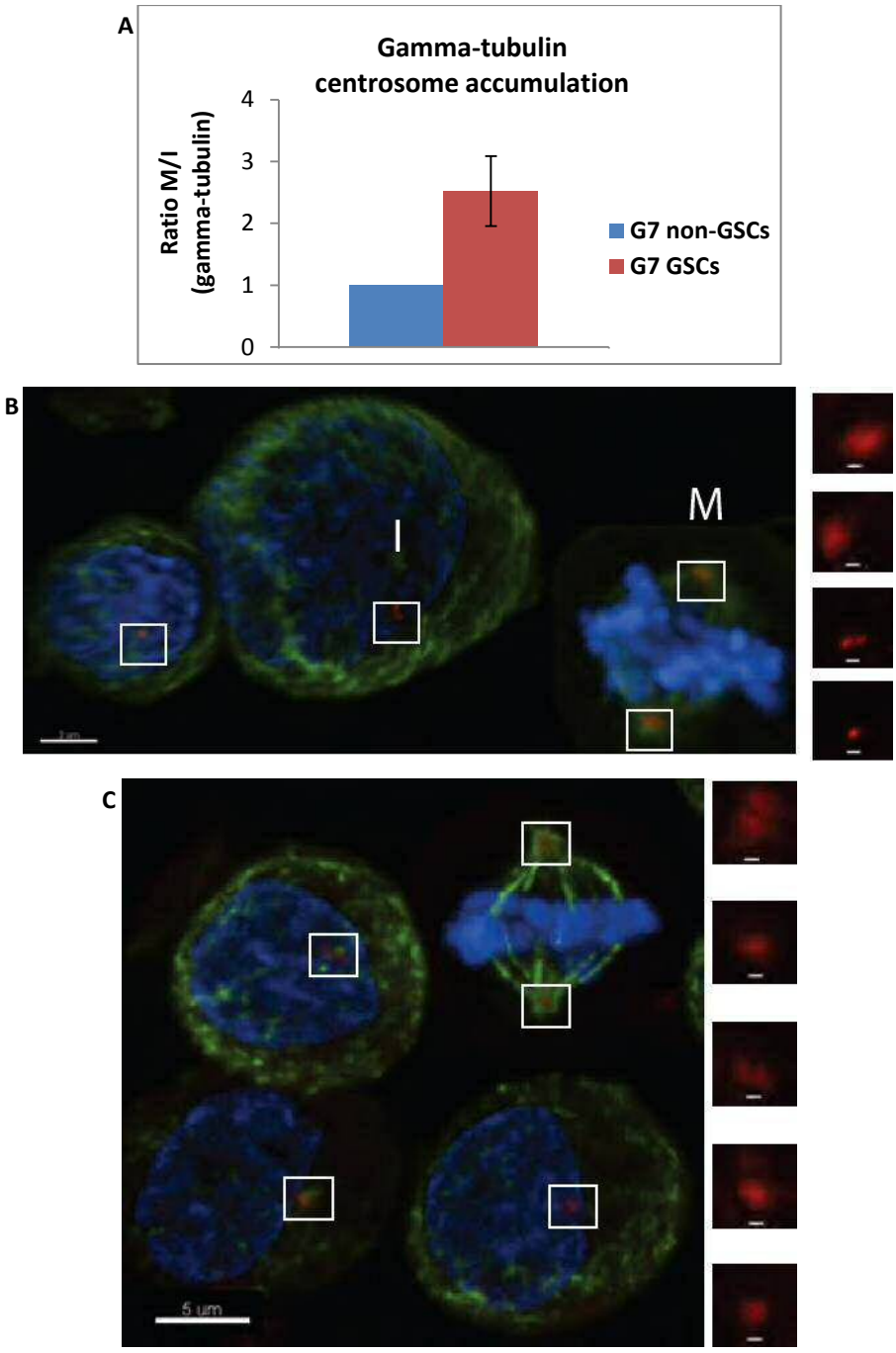

Figure 4.5 GSCs have a more pronounced centrosome maturation.

Cells were stained for α tubulin (green), γ tubulin (red) and DAPI (blue), to visualize the accumulation of γ tubulin as a measure of centrosome maturation. **A.** A graph shows the ratio between centrosomal γ-tubulin in mitotic and interphase cells in GSC and non-GSCs. An average of 144 cells/condition/experiment were randomly imaged and scored. Results are representative of three independent experiments. Error bars indicate means ± SD. **B-C.** Representative images of GSCs (B) and non-GSCs (C), with inserts showing γ tubulin staining in interphase (I) and mitotic (M) cells. Scale bar in main images 5µm and in inserts 500nm.

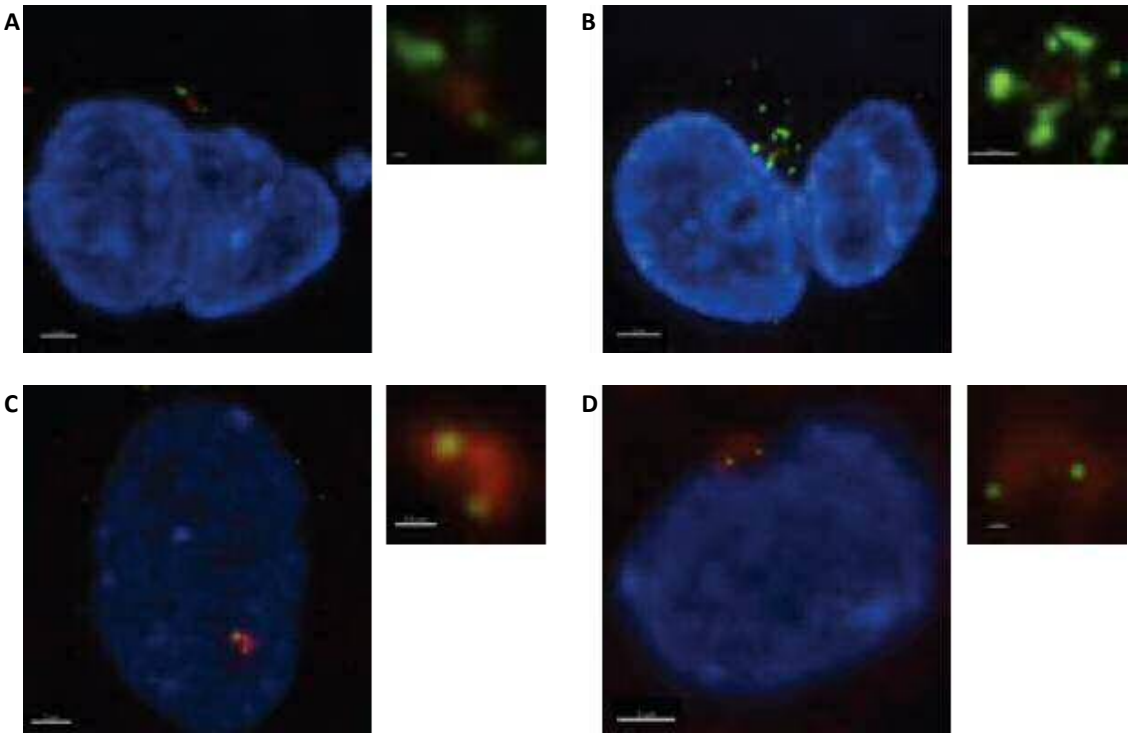

Figure 4.6 Gamma-tubulin and centrin-2 staining co-localize and show that GSCs have abnormal centrosomal patterns more frequently.

GSCs and non-GSCs were stained for centrin-2 (green), γ tubulin (red) and DAPI (blue), to confirm specific localization of γ tubulin staining at centrosomes. Representative images of GSCs (A-B) and non-GSCs (C-D) with inserts showing centrosomal area.

4.5 Distinctive centrosome features in glioblastoma stem cells are not a consequence of different levels of Aurora kinase A expression or activity

As a first step in investigating AurA, I quantified its expression in GSCs and non-GSCs. Western blot analysis of total AurA in the two subpopulations from three glioblastoma primary cell lines demonstrated no difference in its levels (see figure 4.7.A-B). Quantification with western blot of the phosphorylated fraction in the G7 cell line showed that GSCs and non-GSCs did not differ significantly in the active form either (see figure 4.7.C). In order to verify whether there was a distinct accumulation of phosphorylated AurA in mitotic GSCs, I evaluated its pattern of distribution with immunofluorescence in dividing cells from the two subpopulations: I observed a wide variation in the levels of this protein within each subpopulation and did not find a significant difference when comparing GSCs and non-GSCs (see figure 4.8). These findings suggest that the distinctive centrosome features detected in GSCs cannot be ascribed to dissimilarities in the levels of AurA activity in the two subpopulations.

The western blot quantification data is in contrast with results from a study evaluating the role of AurA in regulating self-renewal capacity of GSCs: the authors reported a reduction in total AurA expression levels following *in vitro* differentiation induced by exposure to serum[275]. The reasons for this discrepancy are difficult to identify, given that both studies, mine and theirs, performed the quantification using multiple primary cell lines and various techniques.

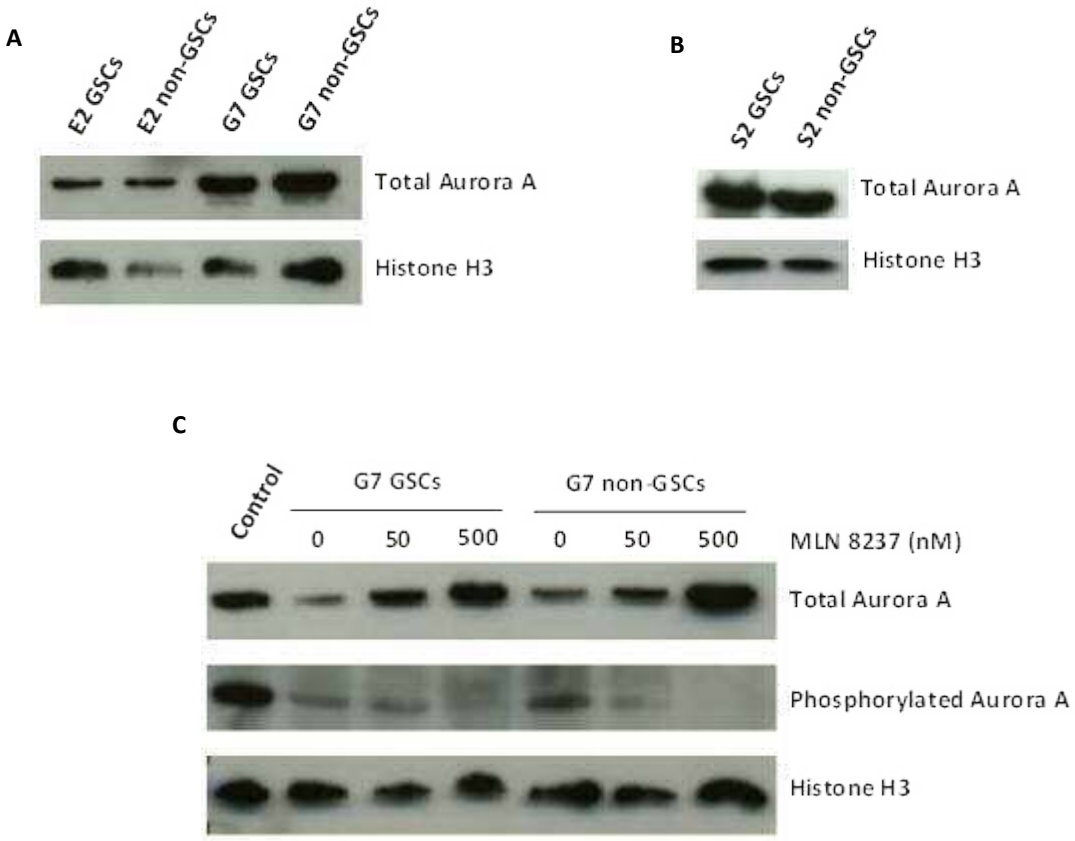

Figure 4.7 GSCs and non-GSCs do not differ in terms of total and phosphorylated Aurora A expression. **A-B**. Representative images of western blots showing total Aurora A expression in GSCs and non-GSCs of three different primary cell lines (E2, G7 and S2). **C.** Representative image of western blot showing total and phosphorylated Aurora A expression, baseline and after 24 hours of incubation with 0, 50 and 500 nM of MLN8237, in G7 GSCs and non-GSCs. "Control" is a sample of HeLa cells treated with 100 ng/uL nocodazole for 16-18 hours to obtain synchronization in M phase. Histone H3 was used as loading control in all experiments.

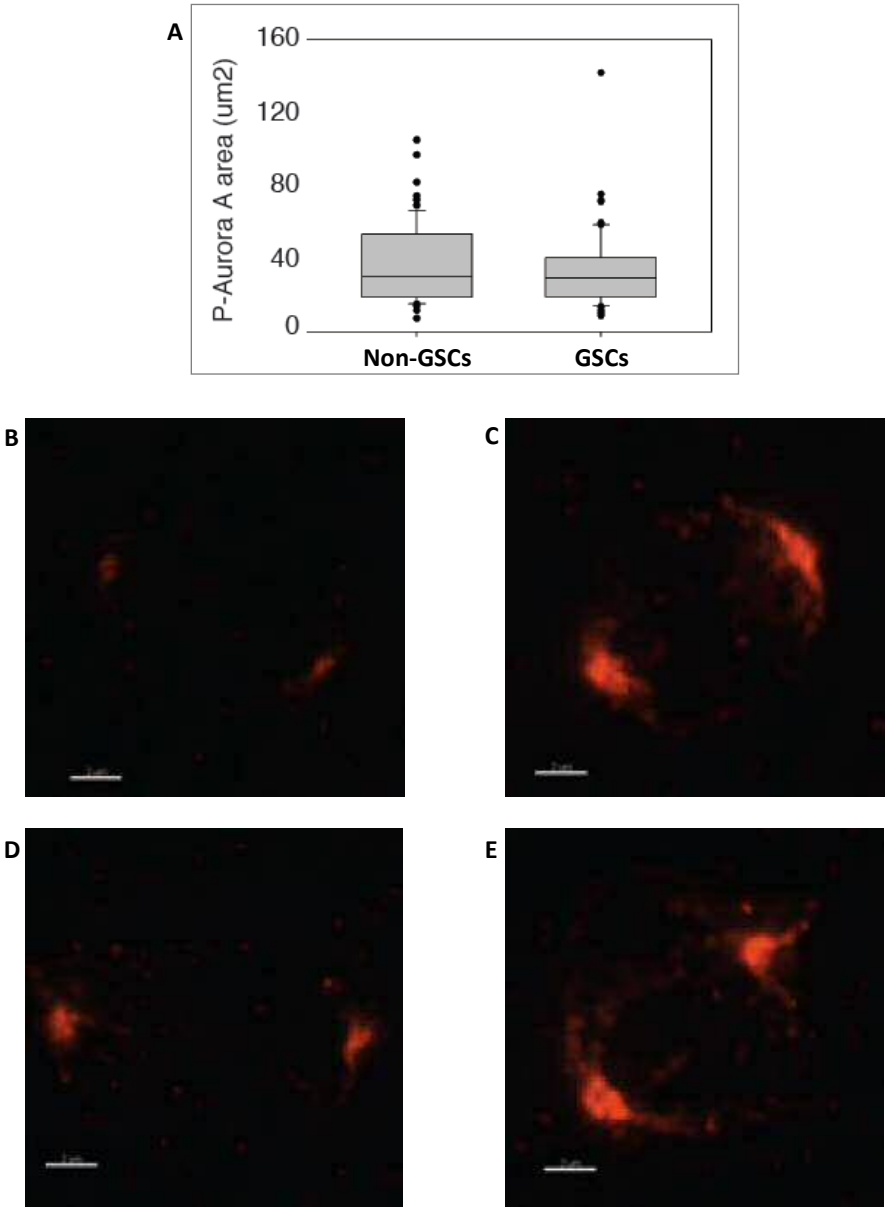

Figure 4.8 GSCs and non-GSCs do not differ in terms of distribution of phosphorylated Aurora A during mitosis.

GSCs and non-GSCs were stained for phosphorylated Aurora A (red) and its distribution was analysed in mitotic cells. **A.** A box plot shows the quantification of centrosomal phosphorylated Aurora A in mitotic GSCs and non-GSCs. An average of 22 mitotic cells/condition/experiment were randomly imaged and scored. **B-E.** Representative images of mitotic GSCs (B-C) and non-GSCs (D-E), showing considerable variability of phosphorylated Aurora A staining in both subpopulations. Scale bar 2µm.

4.6 Glioblastoma stem cells have more mitotic spindle abnormalities following inhibition of Aurora A activity

In order to test whether GSCs and non-GSCs differed in the requirement for AurA activity, I treated the two subpopulations with the selective AurA inhibitor MLN8237 and evaluated the effects on mitotic spindle phenotypes. I used low dose levels that had subtle effects on overall AurA kinase activity, based on the western blot quantification of phosphorylated AurA following MLN8237 treatment. This approach had the aim of addressing possible inhibitory effects on other mitotic kinases, particularly those on Aurora kinase B (AurB). Given that MLN8237 inhibits AurA with a selectivity of more than 200-fold over AurB[276], I considered as AurA-specific any observed effects. MLN8237 increased mitotic spindle abnormalities more frequently in GSCs than in non-GSCs, with the following percentages in the G7 cell line: 56% vs 14% at 25nM, 75% vs 29% at 50nM and 79% vs 47% at 100nM, respectively (see figure 4.9.A). The difference in response to MLN8237, despite the similar levels of AurA in the two subpopulations, is partially consistent with the results of a study reporting a correlation analysis between MLN8237 IC_{50} and AurA expression in established and primary glioblastoma cell lines: no association was found with levels of total AurA, while there was a week correlation with the phosphorylated fraction[277].

Analysis of specific types of mitotic spindle abnormalities showed that there was also a difference in the type of defect observed in the two subpopulations: non-GSCs displayed a moderate increase in both monopolar and multipolar spindles, while in GSCs there was a dramatic increase only in the monopolar phenotype, which is the most commonly reported spindle defect following AurA inhibition both *in vitro* and *in vivo*[276] (see figure 4.9.B-C). Figure 4.10 shows representative images of the most frequent mitotic spindle phenotype at each dose level of MLN8237 in the two subpopulations. As seen in these images, non-GSCs were able to maintain a bipolar phenotype, but displayed a reduction in the size of the mitotic spindle following AurA inhibition. This observation is in line with published data from the Hochegger team (with whom I worked from September 2010), reporting that AurA knockdown reduces spindle volume and width[278].

These findings suggest that the effects of subtle changes in AurA activity, induced by MLN8237 treatment, differ both quantitatively and qualitatively in GSCs and non-GSCs.

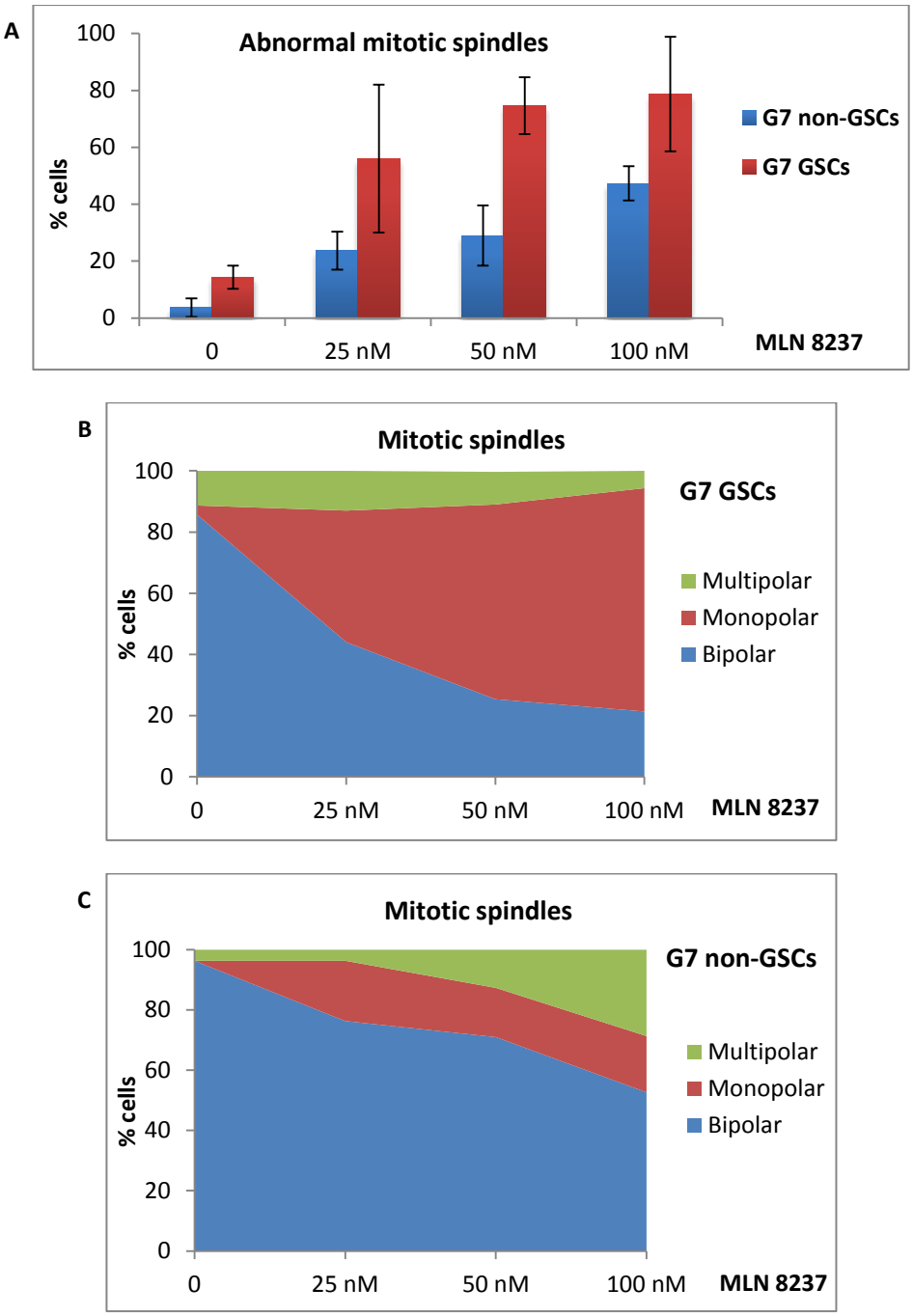

Figure 4.9 GSCs have more spindle abnormalities following treatment with MLN8237 than non-GSCs. GSCs and non-GSCs were treated with 0, 25, 50 and 100 nM of MLN 8237. Following 24 hours of incubation, they were fixed and stained for α tubulin, γ tubulin and DAPI, to visualize the morphology of mitotic spindles in the two subpopulations. **A.** A graph shows the percentages of abnormal mitotic spindles in GSCs and non-GSCs. An average of 26 mitotic cells/condition/experiment were randomly imaged and scored. Results are representative of three independent experiments. Error bars indicate means ± SD. **B-C.** Two diagrams display the distribution of different spindle phenotypes in GSCs and non-GSCs at the various MLN8237 dose levels.

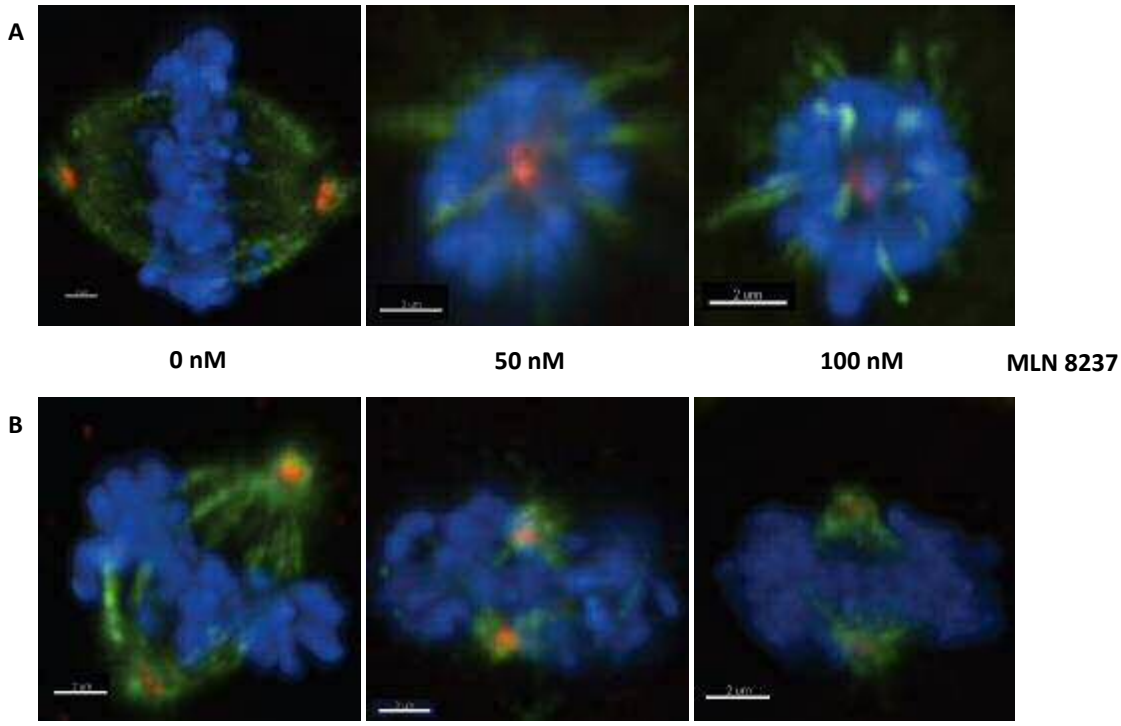

Figure 4.10 Aurora A inhibition disrupts the bipolarity of mitotic spindles more frequently in GSCs than in non-GSCs.

GSCs and non-GSCs were treated as described in figure 4.10 and stained for α tubulin (green), γ tubulin (red) and DAPI (blue) to visualize modifications in mitotic spindle morphology induced by MLN8237. Representative images of GSCs (A) and non-GSCs (B) treated with 0, 50 and 100 nM of MLN8237. Scale bar 2µm.

4.7 AuroraA inhibition does not induce a prolonged G2/M arrest in glioblastoma stem and non-stem cells

In order to characterize further the effects of AurA inhibition on GSCs and non-GSCs, I performed FACS analysis of the cell cycle distribution of the two subpopulations, baseline and following treatment with 25, 50 and 100 nM of MLN8237 (see figure 4.11). I observed a significant difference in the cell cycle profiles of untreated cells: GSCs displayed a higher percentage of cells with ≥4N DNA content than non-GSCs. Interestingly, FACS profiles of GSCs have a bifid appearance in the 4N area (see figures 4.11 and 4.14), which is consistent with the presence of populations with distinct degrees of aneuploidy, although the distribution into two discrete peaks is of uncertain interpretation, as one would expect a single broad peak as the result of cells with small and continuous variations in the number of chromosomes. Given that cells with a 4N FACS profile, simply obtained with propidium iodine staining, can be in G2, M or a tetraploid G1 phase, I identified and quantified the percentage of cells in G2 and M by immunofluorescence using antibodies against CENP-F and α-tubulin in conjunction with DAPI staining. As seen in figure 4.12, the two subpopulations had similar percentages of G2/M cells, confirming that the difference in the fraction of cells with 4N DNA content, observed in untreated samples, was due to a higher percentage of polyploid cells amongst GSCs.

With regards to the cell cycle distribution of treated samples from the two subpopulations, there was an increase in the ≥4N DNA content fraction in GSCs as well as non-GSCs. Immunofluorescence analysis, using antibodies against CENP-F and α-tubulin in conjunction with DAPI staining, demonstrated only slight increases in the G2/M fraction following treatment with 25, 50 and 100 nM of MLN8237. These data suggest that GSCs and non-GSCs do not differ significantly in their response to AurA inhibition in terms of variations in cell cycle distribution and that MLN8237 does not cause a considerable G2/M arrest in the two subpopulations.

These findings are in contrast with those from several studies reporting an increase in the G2/M fraction following inhibition of AurA, using small molecule inhibitors or RNAi[273, 276, 279-281]. The reasons for the difference in our results are difficult to interpret and might be: cell line dependent, as suggested by the wide variation in the magnitude of the G2/M arrest observed in various cell lines tested in one of these studies[281]; and dose-dependent, as indicated by the results of *in vitro* and *in vivo* experiments reported in two publications[276, 280].

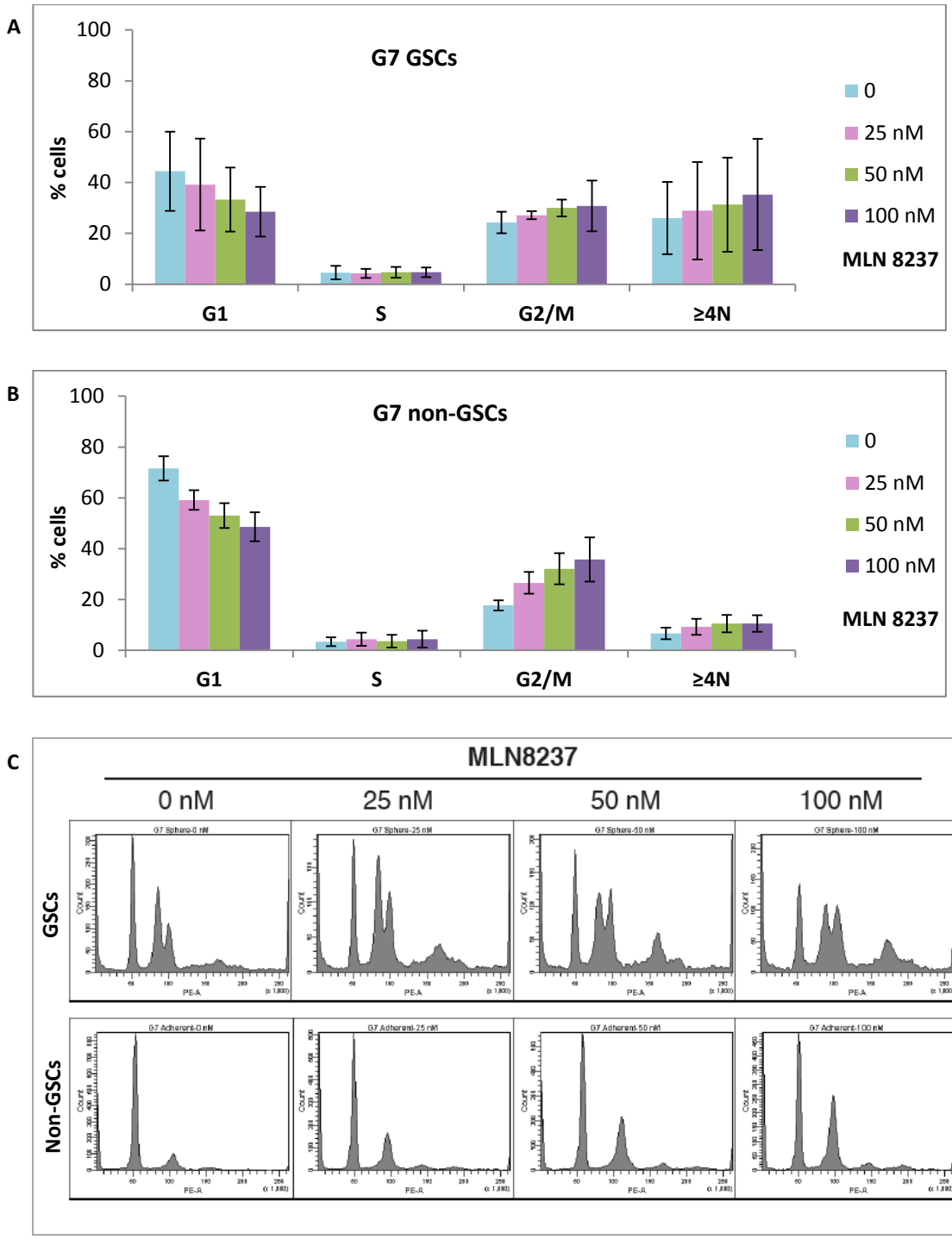

Figure 4.11 GSCs have a higher percentage of cells with ≥4N DNA content at baseline.

GSCs and non-GSCs were treated with 0, 25, 50 and 100 nM of MLN8237. Following 24 hours of incubation, they were fixed, stained with propidium iodide and analysed for DNA content, to evaluate cell cycle distribution of the two subpopulations. **A-B.** Two graphs show percentages of GSCs (A) and non-GSCs (B) in the various phases of the cell cycle, as quantified in the FACS analysis. Results are representative of three independent experiments. Error bars indicate means ± SD. **C.** Representative FACS diagrams of GSC and non-GSCs.

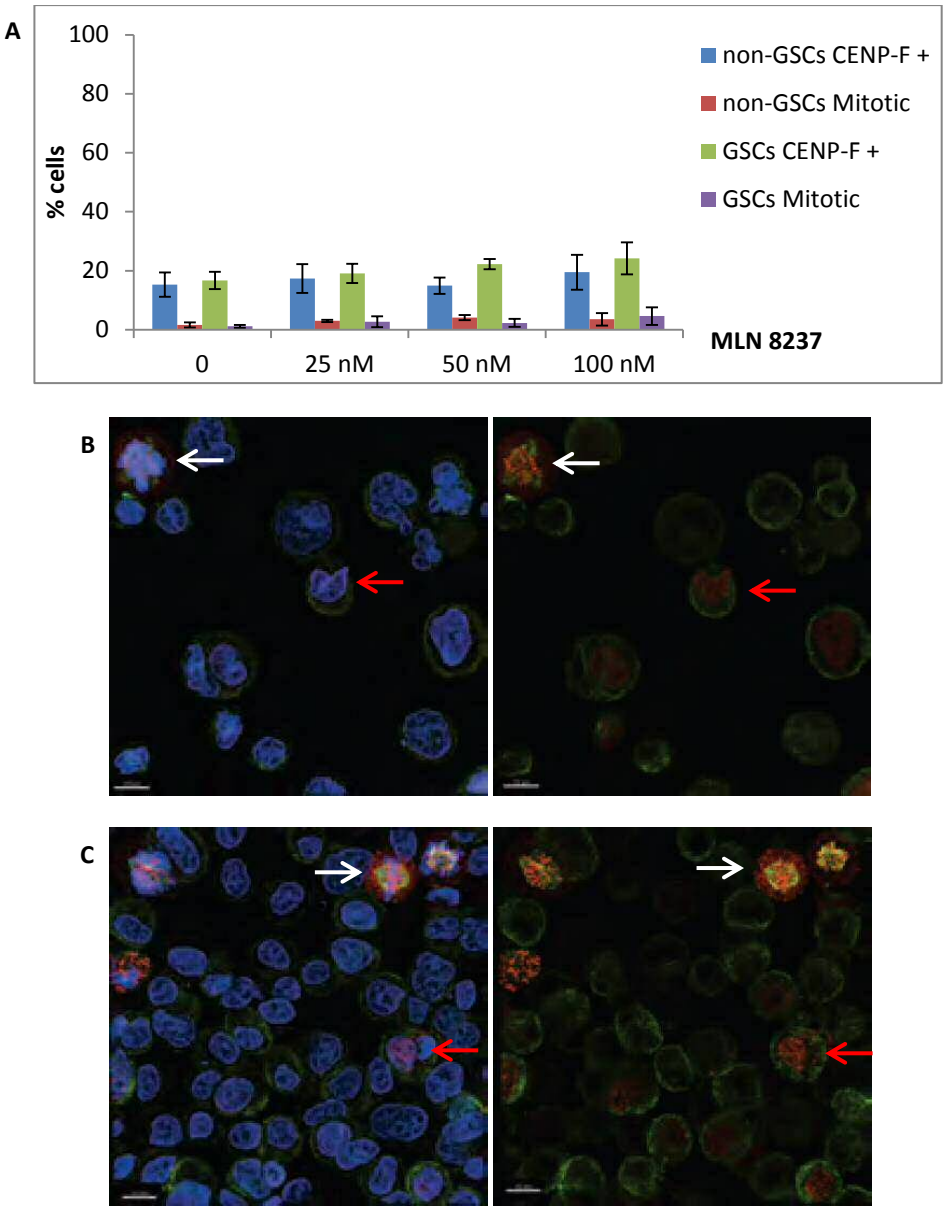

Figure 4.12 Aurora A inhibition does not cause a significant G2/M arrest in GSCs and non-GSCs.

GSCs and non-GSCs were treated with 0, 25, 50 and 100 nM of MLN8237. Following 24 hours of incubation, they were fixed and stained for α tubulin (green), CENP-F (red) and DAPI (blue), to visualize and quantify G2/M cells. **A.** A graph shows the percentages of cells in G2 and M phase in the two subpopulations at the various dose levels. An average of 309 cells/condition/experiment were randomly imaged and scored. Results are representative of three independent experiments. Error bars indicate means ± SD. **B-C.** Representative images of untreated GSCs (B) and non-GSCs (C). White arrows indicate mitotic cells, red arrows G2 cells. Scale bar 10 µm.

In order to further characterize the ability to undergo G2/M arrest of GSCs and non-GSCs, used in this project, I evaluated their response to nocodazole and paclitaxel, two compounds that induce increase in the G2/M fraction by disrupting microtubule dynamics and mitotic spindle assembly. Figures 4.13 and 4.14 display the results of an experiment testing the effect of these drugs on cell cycle distribution in GSCs and non-GSCs and in HeLa cells, used as a control population. In HeLa cells, MLN8237, nocodazole and paclitaxel (alone or in combination with MLN8237), all induced a significant increase in the fraction of cells with 4N DNA content positive for phosphorylated histone H3: from 2% to 26%, 35% and 33%, respectively, for the drugs used individually. While in GSCs and non-GSCs from the G7 cell line, there was only a slight increase, with percentages lower than 4% in both subpopulations following treatment. I further confirmed these findings, evaluating positivity for phosphorylated histone H3 with immunofluorescence in GSCs and non-GSCs treated with paclitaxel. As seen in the representative images shown in figure 4.15, paclitaxel treatment did not induce a considerable increase in the fraction of G2/M cells in both subpopulations.

Taken together, all the experiments analysing cell cycle distribution and induction of G2/M arrest suggest that the tested glioblastoma cells are prone to mitotic slippage, even in the presence of significant mitotic abnormalities observed in GSCs treated with MLN8237. Molecular mechanisms responsible for mitotic slippage are still partially unclear and their investigation in GSCs was beyond the scope of my project. This field will be investigated further by members of the Helfrid Hochegger laboratory.

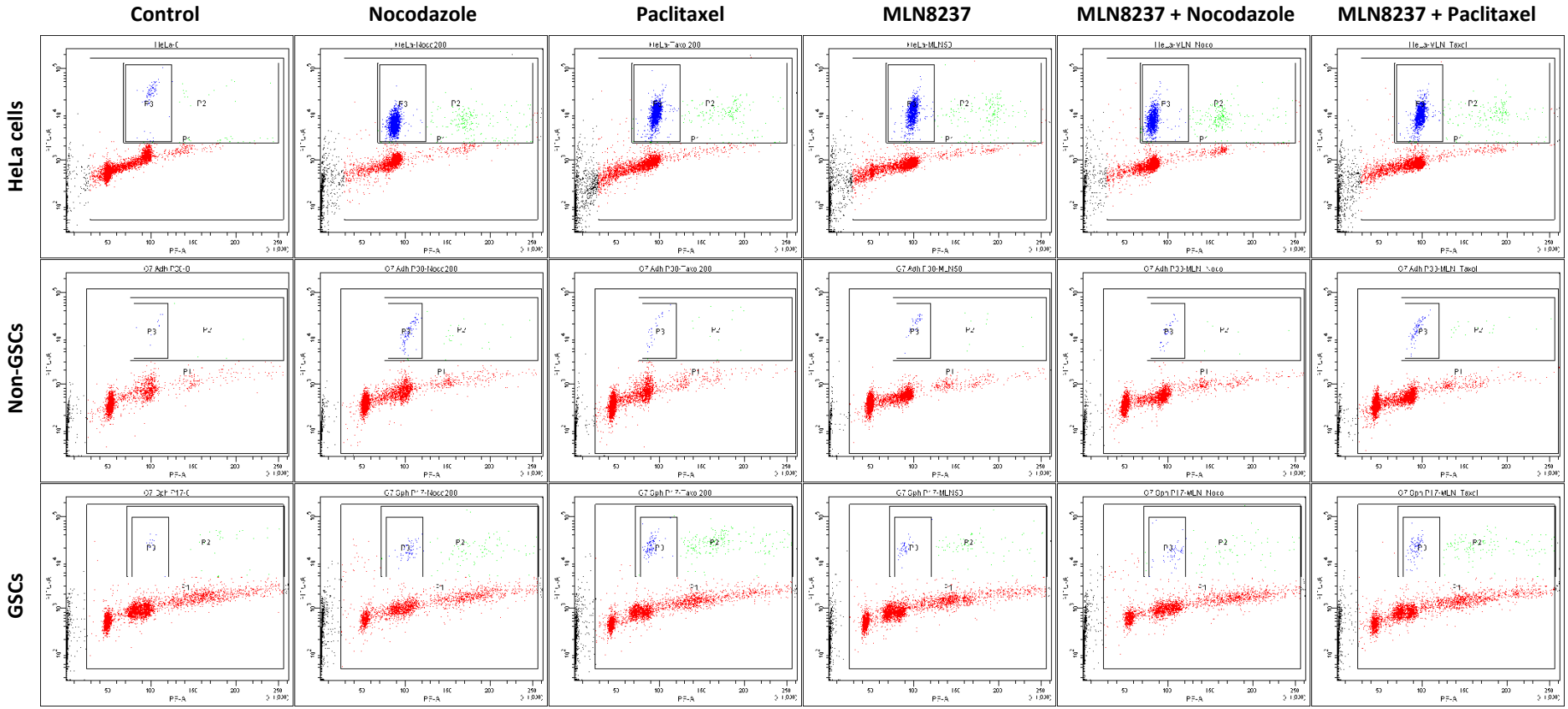

Figure 4.13 A small proportion of GSCs and non-GSCs undergoes G2/M arrest following treatment with nocodazole, paclitaxel and MLN8237.

HeLa cells, GSCs and non-GSCs were treated with nocodazole (200 nM), paclitaxel (200 nM), MLN8237 (50nM), nocodazole and MLN8237, paclitaxel and MLN8237, or left untreated. Following 16 hours of incubation, they were fixed and stained with anti-phosphorylated histone H3 antibody and propidium iodide, to evaluate the percentage of cells that underwent G2/M arrest. The dot plots show the results of one of the experiments. P1 (red) gate defines the population of interest, P2 (green) includes all cells that are positive for phosphorylated histone H3, P3 (blue) gates the positive cells with 4N DNA content that are likely to be arrested in G2/M phase.

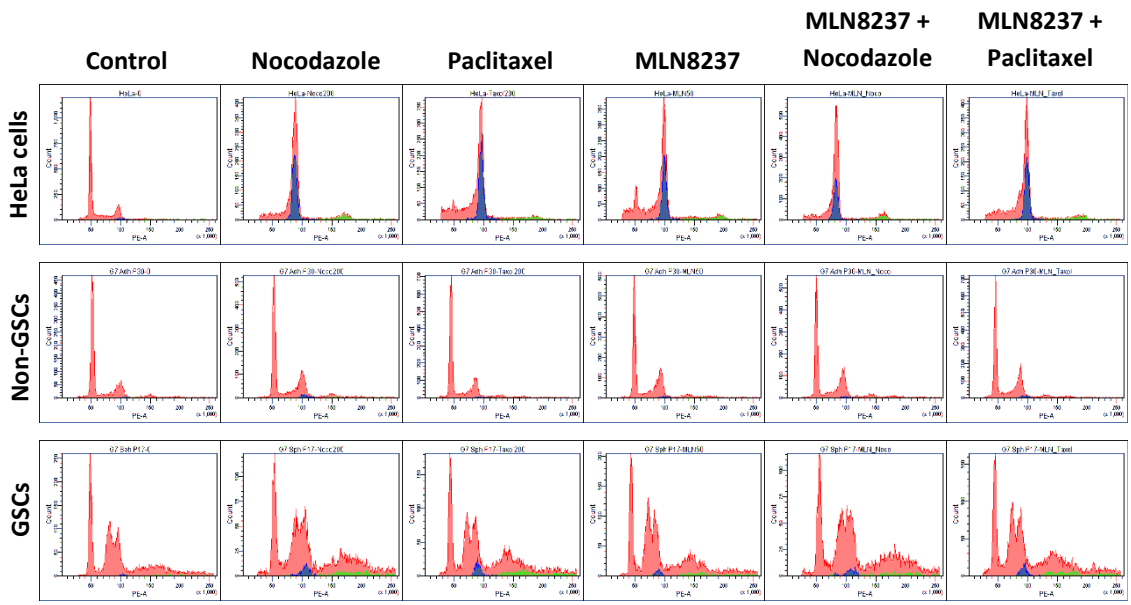

Treatment	HeLa cells		Non-GSCs		GSCs	
	P2	P3	P2	P3	P2	P3
Control	3.3	2.2	0.7	0.4	1.7	0.5
Nocodazole	41.2	34.7	4.0	3.0	8.2	3.6
Paclitaxel	38.5	33.3	1.4	0.9	10.9	3.9
MLN8237	31.7	26.4	1.8	1.4	4.7	1.6
MLN8237 + Nocodazole	31.6	25.6	1.6	1.2	5.8	2.6
MLN8237 + Paclitaxel	36.0	29.9	2.8	2.3	5.8	2.6

Figure 4.14 A small proportion of GSCs and non-GSCs undergoes G2/M arrest following treatment with nocodazole, paclitaxel and MLN8237.

HeLa cells, GSCs and non-GSCs were treated as described in figure 4.14. The histograms above and the table display the results from the experiment shown in figure 4.14, with the same colour coding.

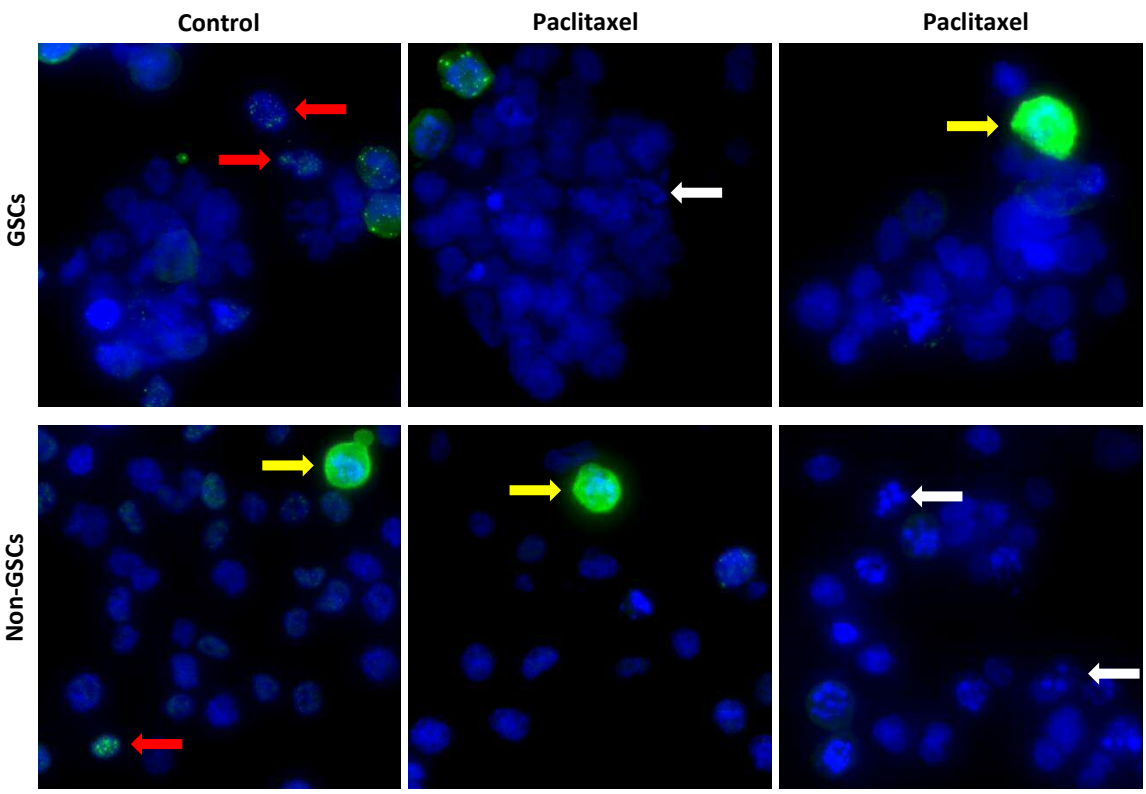

Figure 4.15 GSCs and non-GSCs do not display a significant G2/M arrest following paclitaxel treatment.

GSCs and non-GSCs were treated with 0 or 200 nM of paclitaxel, incubated for 16 hours, fixed and stained for phosphorylated histone H3 (green) and DAPI (blue), to visualize cells in G2 and M phase. Representative images show GSCs and non-GSCs, at baseline and after incubation with paclitaxel. Red arrows indicate examples of cells in G2, yellow arrows mitotic cells and white arrows dying cells.

4.8 Aurora A inhibition induces an increase in polyploid cells

In order to characterise the fraction of cells with ≥4N DNA content increased after AurA inhibition, I evaluated polyploidy using phalloidin and DAPI staining in the two subpopulations treated with MLN8237. I observed increasing percentages of giant polynucleated cells that were higher in GSCs: following treatment with 25, 50 and 100 nM of MLN8237, the scores were 37%, 47% and 54% in GSC samples, while they were 12%, 12% and 20% in non-GSCs (see figure 4.16.A). Representative images of treated cells from the two subpopulations are shown in figures 4.16.B-C.

The increase in polyploidy following MLN8237 treatment is consistent with results from other studies, though these reported this effect at higher dose levels or after longer incubation times[276, 280-282].

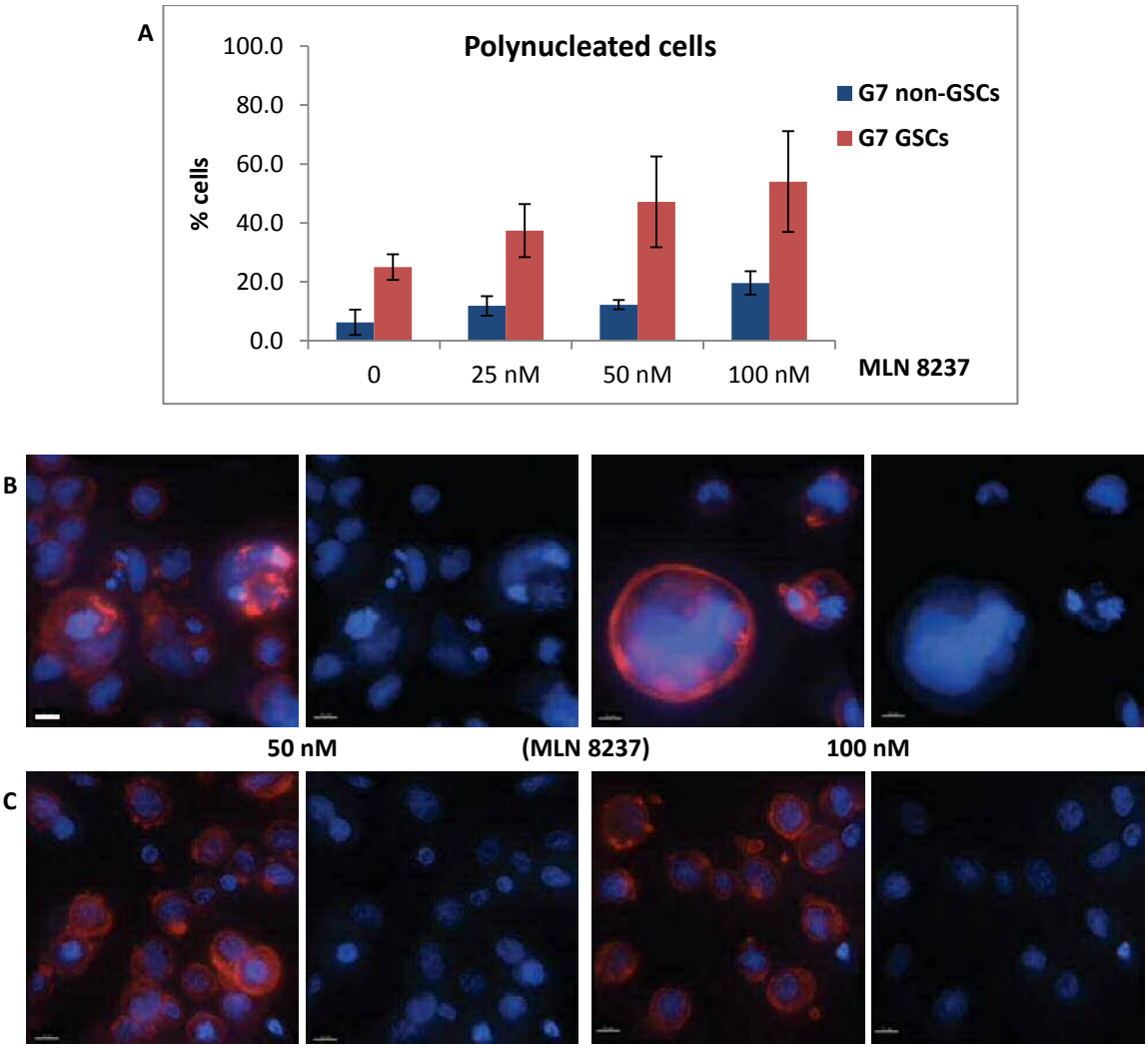

Figure 4.16 Aurora A inhibition induces an increase in polyploid cells that is more pronounced in GSCs. GSCs and non-GSCs were treated with 0, 25, 50 and 100 nM of MLN8237. Following 24 hours of incubation they were fixed, stained with phalloidin (red) and DAPI (blue), to evaluate polyploidy by visualizing the cell cortex and nucleus. **A.** A graph shows the percentages of polynucleated cells in the two subpopulations at the various dose levels. An average of 221 cells/condition/experiment were randomly imaged and scored. Results are representative of three independent experiments. Error bars indicate means ± SD. **B-C.** Representative images of GSCs (B) and non-GSCs (C) treated with 50 and 100 nM of MLN8237. Scale bar 10µm.

4.9 Glioblastoma stem cells form clumps when viewed with live cell imaging

In order to characterise the mechanism leading to polyploidy, I evaluated the feasibility of analysing cell fate of GSCs using live cell imaging. As seen in figure 4.17, single cell analysis was hampered by the formation of clumps during time-lapse microscopy. Based on the methodology used in the published study analysing cell division of GSCs, I tested whether coating the incubation chambers with laminin solved this issue by inducing attachment, but found no difference in cell clumping.

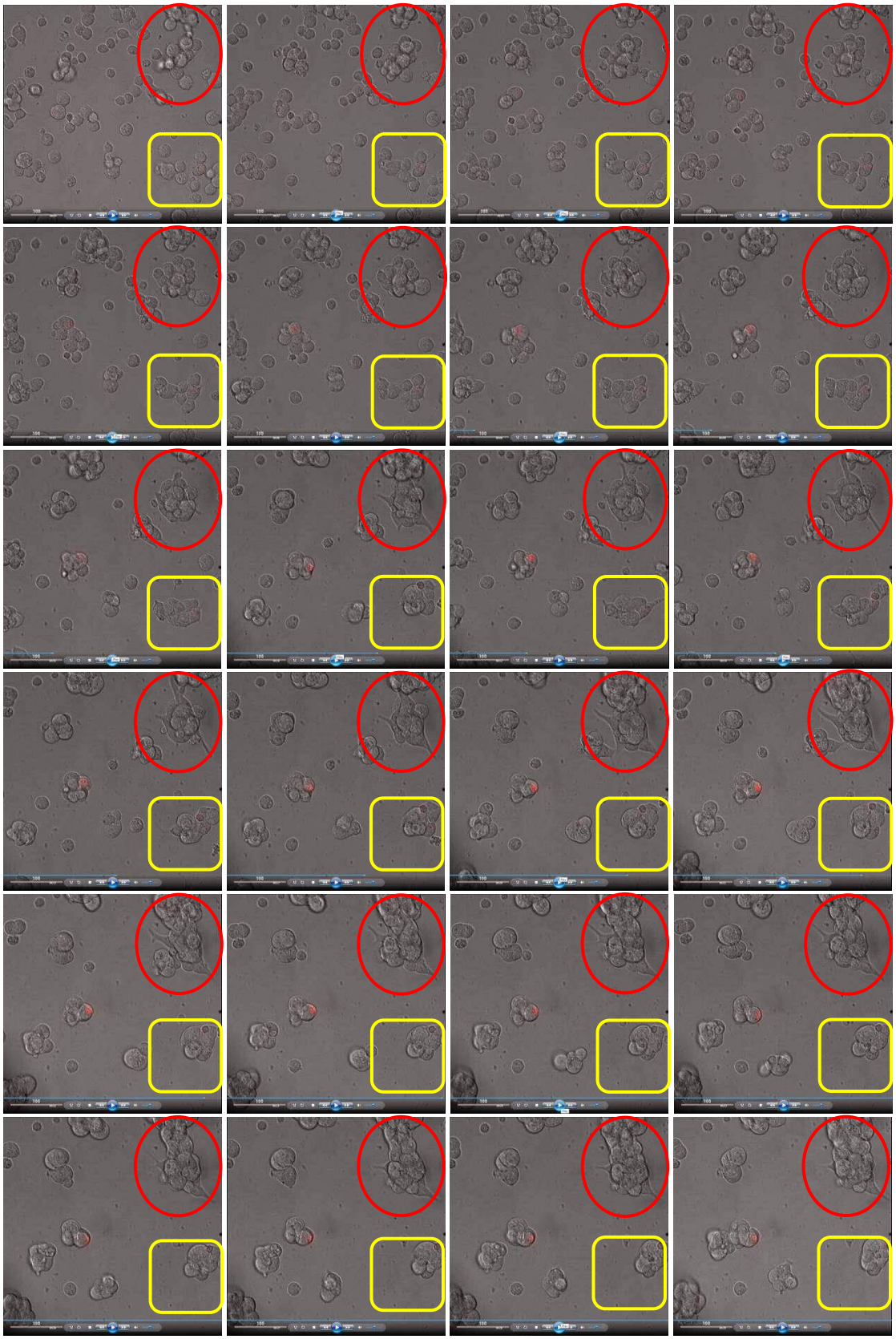

Figure 4.17 Live cell imaging shows that GSCs form clumps in the absence of treatment.

Representative images of a time-lapse sequence, showing behaviour of GSCs during a time interval of approximately 16 hours. The red and yellow shapes each identify and follow a group of cells in the whole time interval.

4.10 Polyploidy is not a result of cell fusion or entosis

Based on the observations of the live-cell imaging experiments, I considered processes other than aberrant mitosis that can be responsible for polyploidy in cancer cells, such as cell fusion and entosis, a form of cannibalism involving ingestion of live cells[283]. Considering that it is not possible to discriminate polyploid cells derived from cell fusion and mitotic defects simply based on their appearance, and that non-adherent growth conditions appear to facilitate entosis[284], I evaluated whether these processes contribute to the observed polyploidy amongst GSCs, baseline and following MLN8237 treatment. For this experiment, I marked cells separately with cell tracking dyes, mixed them and then treated them for 24 hours with 0 or 50 nM of MLN8237. The presence of polyploid cells containing both dyes was negligible in untreated and treated samples (see figure 4.18 for representative images), suggesting that cell fusion and entosis do not contribute significantly to polyploidy amongst GSCs and confirming that this is a result of the higher frequency of mitotic abnormalities.

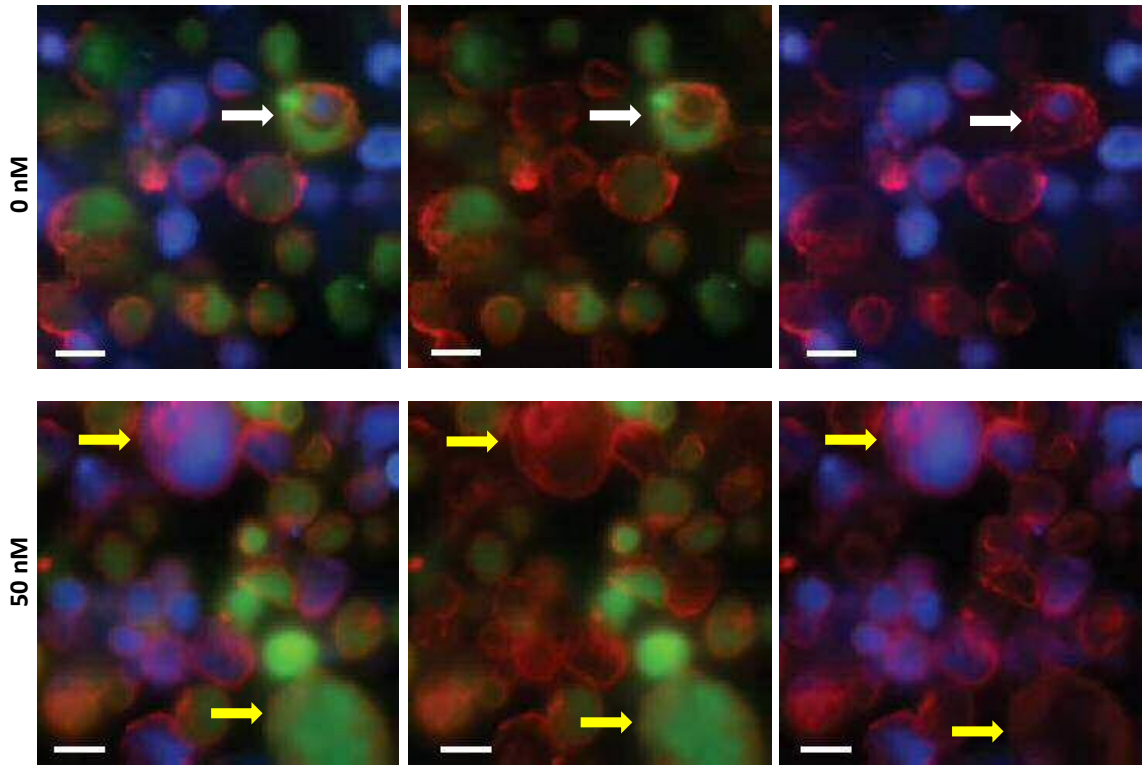

Figure 4.18 Cell fusion and entosis are responsible for a negligible percentage of polyploid cells amongst GSCs.

Two samples of GSCs were incubated separately with CellTracker Green and Blue, re-suspended in fresh medium and mixed prior to treatment with 0 or 50 nM MLN8237. Following 24 hours of incubation, they were fixed and stained with phalloidin, to visualize whether polyploid cells were due to fusion or entosis. Representative images of GSCs ± 50 nM of MLN 8237. White arrows indicate a polyploid cell resulting from cell fusion or entosis. Yellow arrows indicate polyploid cells resulting from mitotic defects. Scale bar 10µm.

4.11 Aurora A inhibition reduces clonogenicity of glioblastoma stem cells more efficiently

The data discussed above suggest that GSCs are prone to mitotic abnormalities, which do not induce a prolonged cell cycle arrest, as these cells are also prone to mitotic slippage. As a consequence, GSCs have higher percentages of polyploid cells, which increase rapidly following AurA inhibition. In order to test whether these features can be exploited therapeutically to improve outcome of glioblastoma patients, I evaluated sensitivity to MLN8237 of GSCs and non-GSCs from three primary cell lines (G7, E2 and G1). In two of these (G7 and E2), GSCs displayed a significantly more pronounced reduction in clonogenicity following AurA inhibition than non-GSCs, while in one cell line (G1) the survival curves did not indicate a clear superiority in the ability of MLN8237 to kill the GSC subpopulation (see figure 4.19). The reasons for the latter result are difficult to identify with the available data, but one contributing factor could be the high passage number (above 50) of the G1 cell line.

To my knowledge, this is the first comparative analysis of MLN8237 sensitivity of GSCs and non-GSCs. Another group evaluated response to MLN8237 in terms of clonogenic survival in different subpopulations of glioblastoma cells in two distinct studies. The first used a panel of ten cell lines, established and primary low-passage, grown in serum-containing medium as adherent cultures; these cells were treated with MLN8237 for 24 hours and colonies were quantified after 7 days[272]. The second used two primary cell lines, grown in serum-free medium as neurosphere cultures, and treated them with MLN8237 for the whole duration of the experiment, i.e. two weeks[277]. The authors reported IC_{50}'s between 60 and 225 nM for adherent cells, and 2.8 and 5.9 nM for the two GSC cell lines, suggesting that MLN8237 kills GSCs more effectively. Although the difference in IC_{50} is striking, the value of this comparison is hindered by the dissimilarities in the experimental design of the two studies.

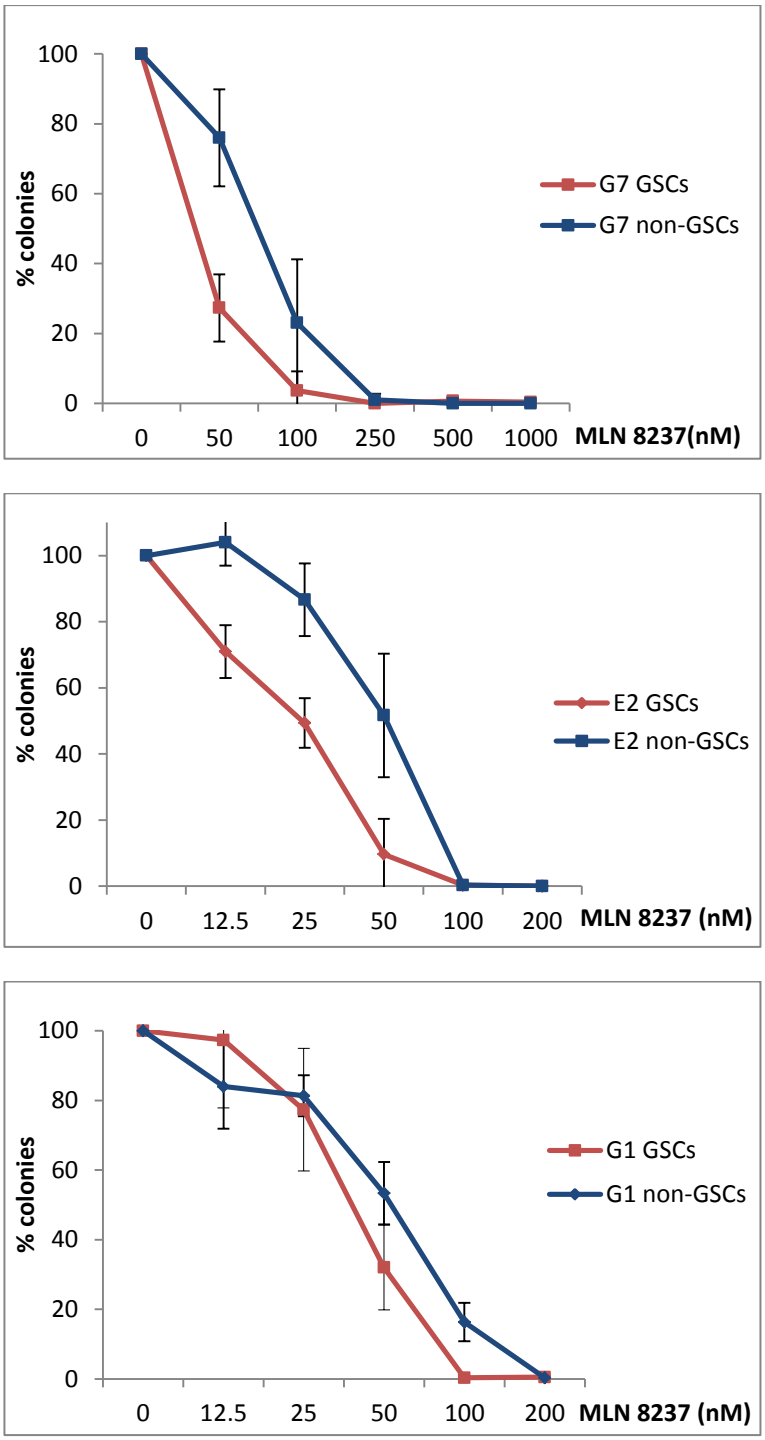

Figure 4.19 GSCs are more sensitive to Aurora A inhibition than non-GSCs.

Clonogenic survival assays comparing sensitivity of GSCs and non-GSCs from three primary glioblastoma cell lines (G7, E2 and G1) to MLN8237. Results are representative of three independent experiments. Error bars indicate means ± SD.

4.12 Apoptosis does not contribute significantly to MLN8237 cytotoxicity in GSCs and non-GSCs

Based on the results of the clonogenic survival assays, I investigated the possible mechanisms leading to cell death following MLN8237 treatment. First, I measured the contribution of apoptosis evaluating levels of cleaved caspase 3 in the two subpopulations in two experiments: in one, I performed western blot analysis after 24 hours of treatment with 0, 50 and 500 nM of MLN8237 (see figure 4.20.A); in the other, I used immunofluorescence to obtain a quantification at 24, 48 and 72 hours in samples treated with 50 nM of the AurA inhibitor (see figure 4.20.B). Western blot evaluation yielded no change in total caspase 3 and could not detect caspase 3 fragment at 24 hours in both subpopulations, even at the highest dose level. Quantification of one of the immunofluorescence experiments showed no change in non-GSCs and an increase in the percentage of cleaved caspase 3 positive cells, from 1% to 3%, at 24 hours in GSCs treated with MLN8237. These data suggest that apoptosis, at the most, is responsible for a small proportion of the cytotoxic effect of MLN8237 in GSCs.

The literature regarding apoptosis induction by AurA inhibitors is conflicting, with some studies showing negligible or modest levels of apoptosis following treatment and others reporting a considerable increase in this mode of cell death[276, 279, 281, 282, 285-289]. Several factors might be responsible for this inconsistency: analysis of various cell lines, as suggested by the difference in the results obtained in distinct cell lines within the same study[276, 282]; use of assays with different specificity for apoptosis detection (FACS analysis of Annexin V staining and sub-G1 fraction, western blot evaluation of cleaved caspases and PARP) and variation in experimental protocols (drugs, dose levels and treatment times). The importance of the methodology is demonstrated by the only publication, to my knowledge, reporting apoptosis evaluation in GSCs following MLN8237 treatment[285]. This study showed a considerable increase in Annexin V detection only after 9 days of incubation with 200 nmlo/L of MLN8237 in two neurosphere cell lines, while PARP cleavage increased from day 2 or 5.

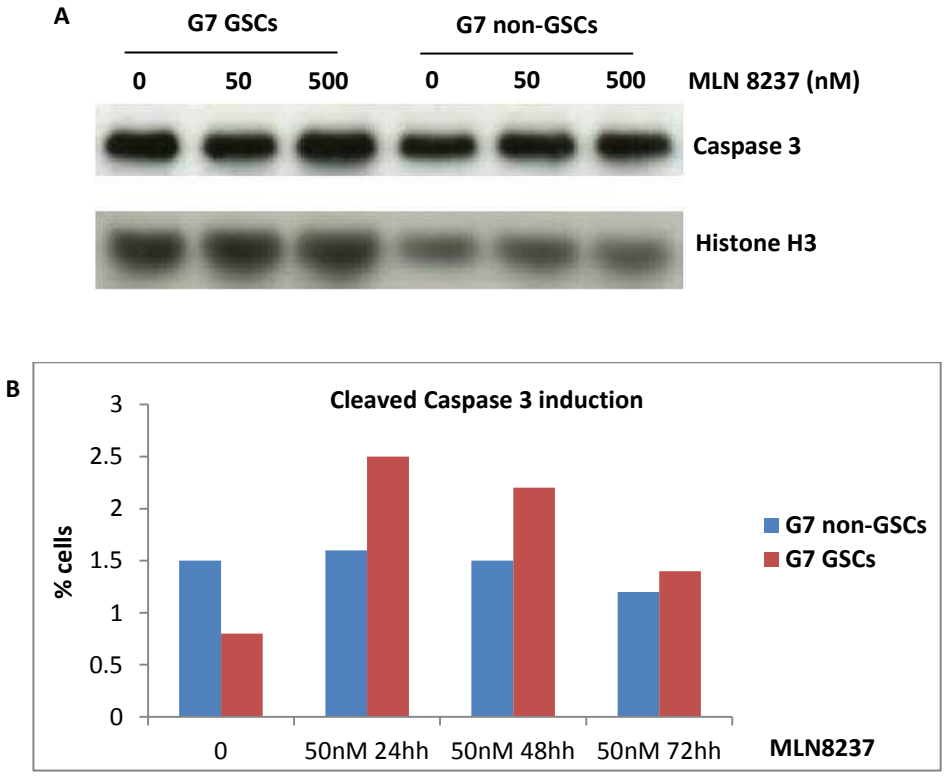

Figure 4.20 Aurora A inhibition does not induce a significant increase in Caspase 3 dependent death in GSCs and non-GSCs.

A. Representative image of western blot showing caspase 3 expression, baseline and after 24 hours of incubation with 0, 50 and 500 nM of MLN8237, in G7 GSCs and non-GSCs. Histone H3 was used as loading control. **B.** A diagram shows percentages of cleaved caspase 3 positive cells evaluated with immunofluorescence, at baseline and after 24, 48 and 72 hours of incubation with 50 nM of MLN8237, in G7 GSCs and non-GSCs. Results are from quantification of one out of two experiments performed.

4.13 Aurora A inhibition induces a dramatic increase in senescence in glioblastoma stem cells

Based on previous studies reporting the ability of MLN8237 to induce senescence[281, 287, 289], I evaluated levels of β-galactosidase in the two subpopulations, baseline and after 2 and 7 days of treatment with 50 nM of MLN8237 (see figure 4.21). I observed a significant increase in the percentage of senescent cells amongst GSCs, with 55% of these expressing the senescence marker at day 7, compared to 19% in non-GSCs. Consistently, the recent study, mentioned in the previous paragraph, also showed senescence induction in GSCs, but did not quantify it or perform a comparative analysis with non-GSCs[285]. In the light of these findings and given that senescent populations show an increase in Annexin V staining[290], it is likely that a proportion of Annexin V positive cells, observed in GSCs after 9 days of MLN8237 treatment in the latter study, were the result of senescence.

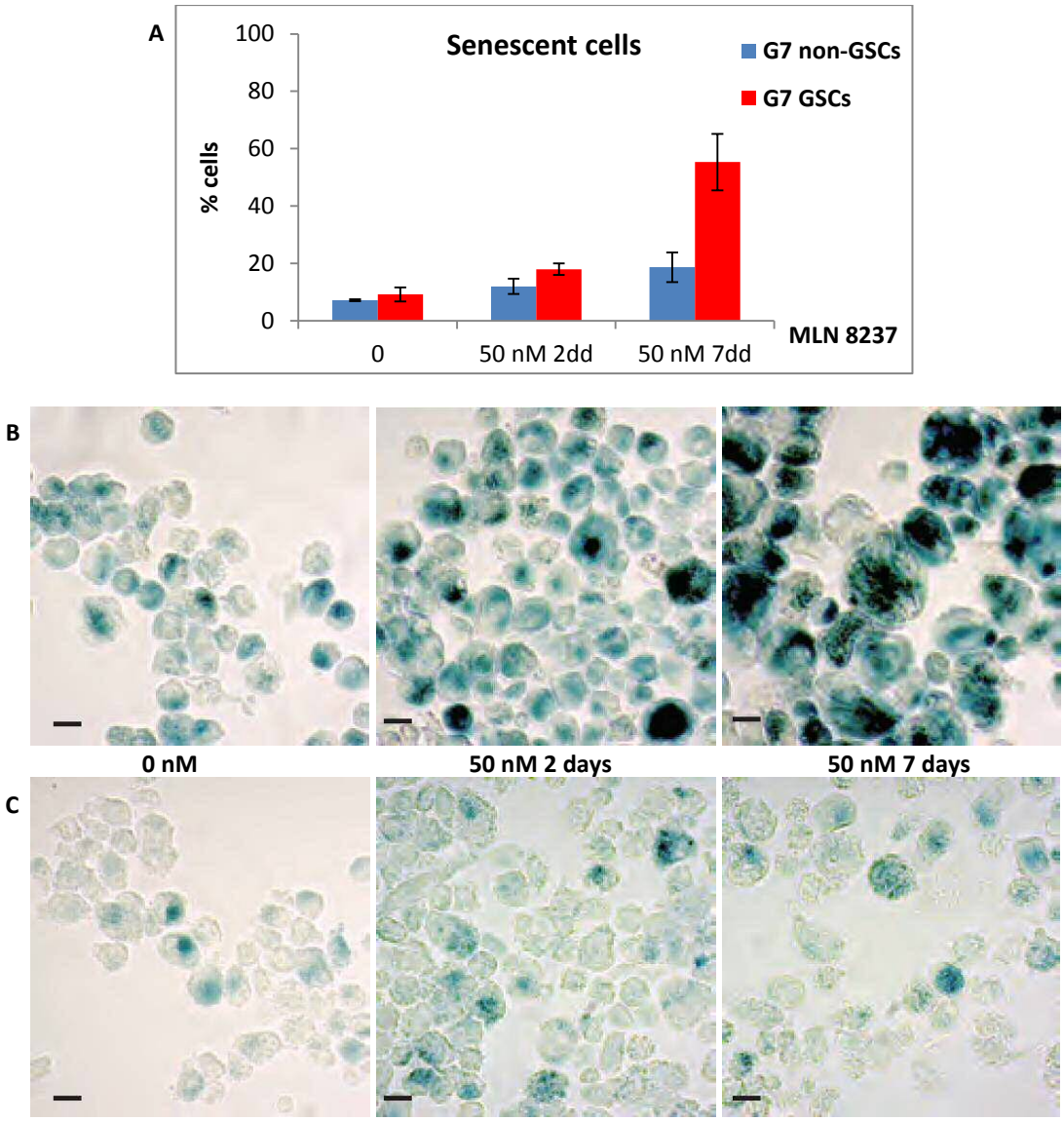

Figure 4.21 Aurora A inhibition induces senescence in glioblastoma cells that is markedly more pronounced in GSCs.

GSCs and non-GSCs were treated with 0 and 50 nM of MLN8237. Following 2 or 7 days of incubation, they were fixed and stained for β-galactosidase, to evaluate induction of senescence. **A.** A graph shows the percentages of senescent cells in the two subpopulations ± MLN8237. An average of 233 cells/condition/experiment were randomly imaged and scored. Results are representative of three independent experiments. Error bars indicate means ± SD. **B-C.** Representative images of GSCs (B) and non-GSCs (C), showing β-galactosidase staining (blue) at baseline and after 2 or 7 days of MLN8237 treatment. Scale bar 10μm.

4.14 Increased sensitivity of glioblastoma stem cells to Aurora A inhibition is not dependent on p53 status

Given the pivotal role of p53 in regulating fate of cancer cells following cytotoxic treatment, several studies analysed whether its status influences response to AurA inhibition, yielding conflicting results[286, 289]. Data produced by a member of Anthony Chalmers' group, Ross Carruthers, who performed DNA sequencing of p53 on GSCs and non-GSCs from G7 and E2 cell lines, demonstrating that they are all p53 wild type (data not shown), does not support a role of p53 status in determining the observed differential sensitivity of GSCs to AurA inhibition.

4.15 MLN8237 does not significantly radiosensitize GSCs and non-GSCs

Given that standard treatment against glioblastoma includes radiotherapy, I performed clonogenic survival assays with both subpopulations to test whether MLN8237 has a radiosensitizing effect and can be used in combination with ionizing radiation to improve patient outcome. While non-GSCs displayed no difference in the two treatment arms, in GSCs the addition of MLN8237 was slightly favourable, but this effect did not reach statistical significance at all dose levels (see figure 4.22). As I performed the experiment twice, a final repeat and a more detailed statistical analysis will help with the interpretation of these results. Two studies mentioned above analysed, in distinct experiments, the effect of combining MLN8237 with ionizing radiation on clonogenic survival of two GSC lines and four non-GSC lines[272, 277]. A comparison is not possible, given that the two sets of experiments had distinct protocols and used different doses, for each study as well as for each GSC line. The authors reported a potentiation of the effect of ionizing radiation by MLN8237, suggesting a synergistic effect. Another group testing the combination of another AurA inhibition with ionizing radiation in glioblastoma established and primary cell lines, found that depending on the radiation dose, the effect was synergistic, additive or antagonistic[273].

Based on the results of my preliminary clonogenic survival assays and on the findings of these studies, further characterization of the interaction between the two treatment modalities is needed to evaluate whether there is a rationale for a combined approach, especially if the absence of a significant G2/M arrest is confirmed, and, if so, which schedule (i.e. MLN8237 dose and timing) is the most advantageous.

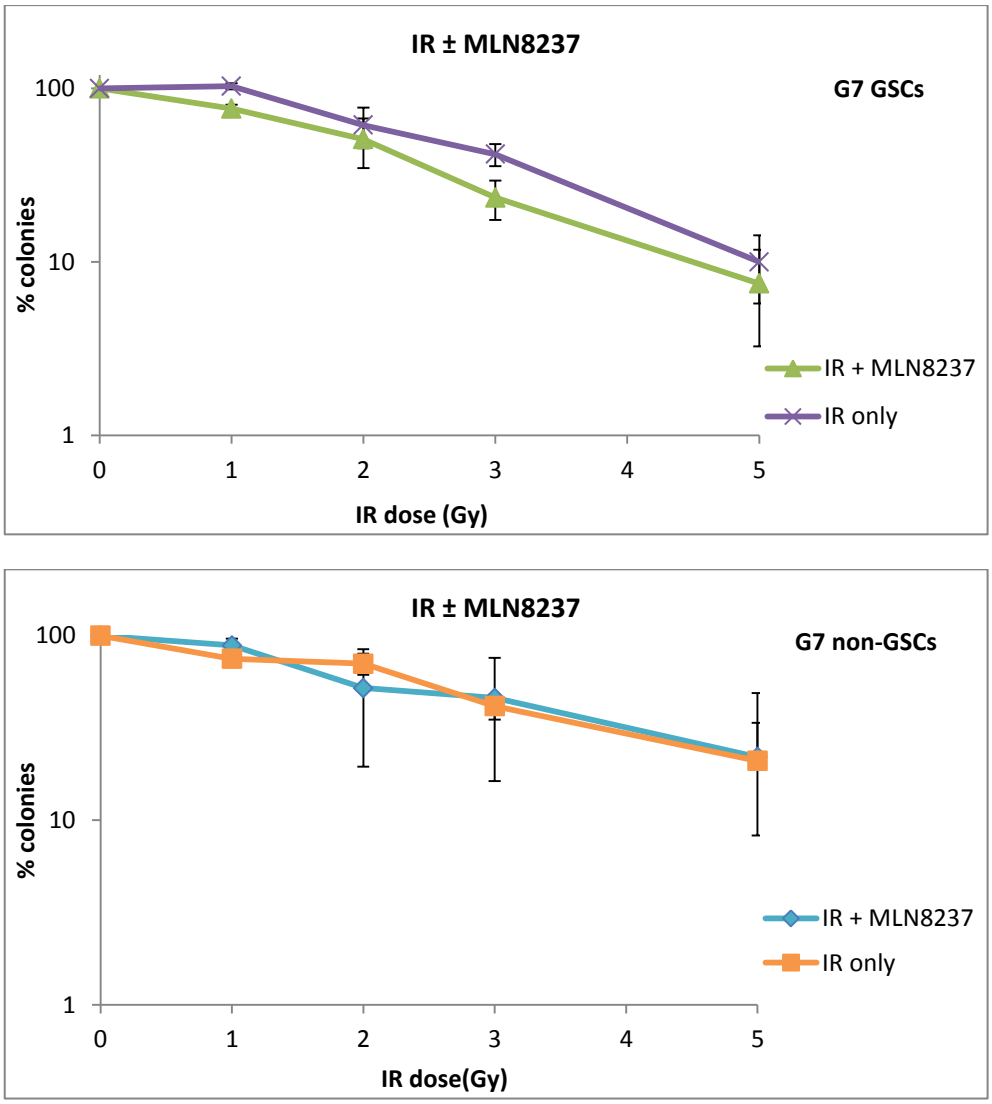

Figure 4.22 Aurora A inhibition does not have a significant radiosensitizing effect on GSCs or non-GSCs.

Clonogenic survival assays testing sensitivity of G7 GSCs and non-GSCs to ionizing radiation (IR) in combination with 25 nM of MLN8237. Results are representative of two independent experiments. Error bars indicate means ± SD.

4.16 Discussion

In this chapter I show that GSCs have distinctive features with regards to centrosome cycle and mitotic spindle phenotypes. I also demonstrate that GSCs are highly susceptible to subtle changes in AurA activity, which induce a rapid increase in polyploidy and subsequently in senescence, with a consistent reduction in clonogenicity. Given that these effects were more pronounced in GSCs than in non-GSCs, it is reasonable to propose that GSCs have distinctive features in processes preceding and regulating cell division which, on the one hand, enable them to display regenerative responses following cytotoxic treatment, while, on the other, they may constitute an Achilles' heel for GSCs, making them more susceptible to mitotic failure.

A particularly interesting outcome of my experiments is the correlation between levels of MLN8237-induced senescence and reduction in clonogenic survival in GSCs and non-GSCs. The value of this observation is confirmed by the findings of a recent *in vivo* study, testing the efficacy of MLN8237 against xenografts obtained through injection of GSC populations[285]. The authors reported prolonged survival in treated mice, which displayed tumours with morphological changes resembling abnormal arrested mitosis and senescence. The significance of these data is in the context of the proposed ability of CSCs to escape senescence and the reversible nature of drug-induced senescence used by a minority of cancer cells as a survival mechanism[291, 292]. My data, together with the results of the *in vivo* study, confute these theories and suggest that senescence induction is an effective mechanism to target GSCs effectively. Though, given that senescent cells acquire a secretory phenotype and release, amongst several factors, IL-6, which has been shown to have a positive effect on GSC survival and tumour growth[293-295], the possible role of senescence induction as an anti-GSC strategy needs to be confirmed in the clinical setting by pathology studies, aimed at verifying whether the *in vitro* and *in vivo* behaviour of GSCs applies to these cells in their natural tumoral niche.

In conclusion, the data shown in this chapter strengthens the rationale for the theory that links centrosome cycle, mitotic kinase inhibition and GSC targeting, supporting the approach undertaken in the second section of my project and highlighting the need for a more detailed characterization of centrosome biology and mitosis regulation in GSCs.

Chapter 5

Preliminary data on Polo-like kinase 1 inhibition and primary cilia in glioblastoma stem cells

5.1 Introduction

In this chapter I report unpublished results generated for two projects that were inspired by my findings on centrosome features and mitotic kinases in GSCs and non-GSCs: the first section investigates the effects of inhibiting Plk1 on GSCs and non-GSCs; the second analyses the presence of primary cilia in the two subpopulations, exploring the feasibility of studying these organelles in cells grown within the 3D culture system described in chapter three.

Given the role of Plk1 in centrosome cycle and mitosis progression, the main rationale for evaluating the outcome of its inhibition in GSCs and non-GSCs is that linking centrosome cycle, mitotic kinase inhibition and GSC targeting, as outlined at the end of the general introduction and at the beginning of chapter four.

The interest in primary cilia aroused in the context of centrosome cycle characterization in GSCs and non-GSCs and was emphasised by the known role of AurA in regulation of assembly and disassembly of this organelle[296, 297]. I will now give a brief introduction on primary cilia and the evidence supporting its investigation in GSCs. The primary cilium is a sensory organelle formed by: the basal body, which is derived from the mother centriole after its migration and anchorage to the plasma membrane during G1 phase; and the axoneme, which consists of 9 microtubule doublets that are in continuation with the basal body and protrude from the cell surface[267]. Despite important advances, our understanding is still limited with regards to the mechanisms underlying the switch between centriole and basal body and its correlation with cell cycle control, but increasing data suggests that disruption of these processes could contribute to the deregulated cancer growth[298]. The rationale for studying cilia in GSCs is mainly based on the implication of these organelles in several pathways, such as hedgehog, PDGF, Wnt and Notch signalling[299]. Although most of these pathways have been linked to GSC survival[300-302], the relevance of their ciliary component in GSCs is unknown. At the time of my experiments, no studies had been published on primary cilia in GSCs and there was only one publication regarding glioblastoma established cell lines[303]. Immunofluorescence analysis and electron microscopy observation showed no or immature cilia in four of five cell lines, suggesting that ciliogenesis was absent or incomplete; in one cell line, the authors identified less than 1% of cells with primary cilia in the latter stages of maturation. Recently, a study analysing primary cilia in GSCs *in vitro* was published and reported that in five primary cell lines 8 to 25% of cells presented cilia, with normal structure and trafficking ability[304]. This inconsistency is probably due to the differences in the cell lines used in the two studies. Analysis of glioblastoma patient specimens was performed by the same groups and also gave partially conflicting results: one reported the presence of primary cilia in all (twenty three)

biopsies, with a mixture of normal and aberrant forms[304]; the other found these organelles in all (seven) specimens, but these were defective in all but one[305]. These findings highlight the need for pathology studies on larger numbers of patient samples, with the aim of defining the relevance of ciliated cells in glioblastoma biology, as well as *in vitro* evaluation of the role of these organelles in survival responses of GSCs and non-GSCs, to identify possible therapeutic targets to improve patient outcomes.

5.2 Polo-like kinase 1 inhibition targets glioblastoma stem cells more effectively

In order to test whether GSCs and non-GSCs differ in their response to Plk1 targeting, I performed clonogenic survival assays testing the sensitivity of the two subpopulations to BI2536, a highly specific Plk1 inhibitor. In both cell lines (E2 and G7), GSCs showed significantly lower clonogenicity than non-GSCs, following treatment (see figure 5.1). To my knowledge, there are no other comparative analyses of sensitivity of GSCs and non-GSCs to Plk1 inhibition. Consistently with my findings, a study evaluating the effect of Plk1 inhibition on GSC features showed a drastic reduction in neurosphere ability following BI2536 treatment and, most importantly, also reported a prolonged survival of treated mice, suggesting the possible clnical relevance of this approach[245].

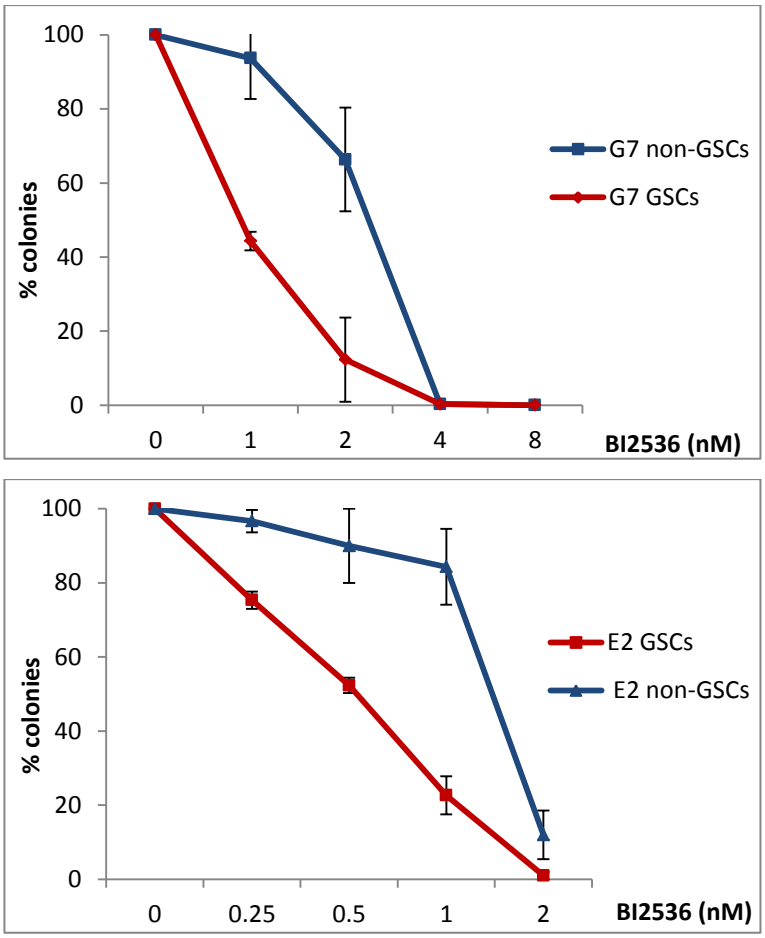

Figure 5.1 GSCs are more sensitive to BI2536 than non-GSCs.

Clonogenic survival assays comparing sensitivity of GSCs and non-GSCs from two primary glioblastoma cell lines (G7 and E2) to BI2536. Results are representative of three independent experiments. Error bars indicate means ± SD.

5.3 Higher sensitivity of glioblastoma stem cells to Plk1 inhibition is not correlated to induction of mitotic spindle abnormalities

Given the role of Plk1 in centrosome maturation and bipolar spindle formation, I tested whether GSCs and non-GSCs differed in their response to BI2536 in terms of mitotic spindle defects. As seen in figure 5.2, I observed no difference in the induction of spindle abnormalities between the two subpopulations and the higher dose level (4nM) caused an increase of aberrant mitosis only to about 30%, a much lower value than that seen with 100nM of MLN8237 (around 80%), which had a comparable cell killing effect (around 95% decrease in clonogenicity). These findings suggest that, at the dose levels used in my experiments, the reduced clonogenic survival following BI2536 treatment is only partially due to mitotic defects and that other mechanisms contribute to the cytotoxic effect of Plk1 inhibition and determine the higher sensitivity of GSCs.

This is the first comparative analysis of mitotic defects induced by a Plk1 inhibitor in matched GSCs and non-GSCs. The only published data on this topic comes from a study evaluating the effect of targeting Plk1 in GSCs[306]. The authors reported a much higher increase in spindle defects following treatment with BI2536, but did not state the dose used in the experiment. Given the lack of information and the much higher dose levels (10 to 100nM) used in other assays in the study, it is not possible to make a comparison with my findings.

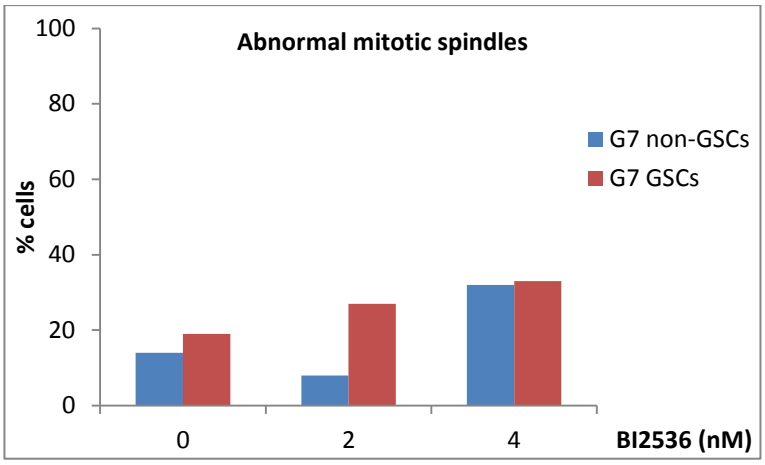

Figure 5.2 GSCs and non-GSCs do not differ in the frequency of spindle abnormalities following treatment with BI2536.

GSCs and non-GSCs were treated with 0, 2 and 4 nM of BI2536. Following 24 hours of incubation, they were fixed and stained for α tubulin, γ tubulin and DAPI, to visualize the morphology of mitotic spindles in the two subpopulations. The graph shows the percentages of abnormal mitotic spindles in GSCs and non-GSCs. An average of 29 mitotic cells/condition were randomly imaged and scored.

5.4 Cytotoxic doses of BI2536 do not induce a G2/M arrest in glioblastoma stem and non-stem cells

Given the role of Plk1 in regulation of mitotic entry and exit, I tested whether its inhibition caused a G2/M arrest in GSCs and non-GSCs. As seen in figure 5.3.A, the two subpopulations did not display a significant increase in the percentage of cells in G2 and M phases, following treatment with cytotoxic doses of BI2536. To my knowledge, the study mentioned in the previous paragraph is the only one published reporting a cell cycle analysis of primary GSCs following PLk1 inhibition[306]. The authors showed a considerable increase in the 4N DNA content fraction in the FACS profiles, following treatment with BI2536. Though, again it is not clear what dose they used in the specific experiment as they simply state that several doses, between 10 and 100 nM, were tested. The inconsistency in the findings could be due to two main factors: use of higher doses, given that the G2/M arrest might be dose-dependent, as suggested by the results of another study testing the effect of BI2536 on established glioblastoma cell lines[307]; different methodology, as FACS analysis of DNA content with PI staining does not distinguish between cells in G2/M and tetraploid cells in G1. A role of the latter factor is suggested by the presence of giant cells amongst GSCs, following treatment with BI2536, as seen in figures 5.3.B-C. Interestingly, these apparently polyploid cells were not visibly increased amongst non-GSCs despite the two subpopulations had similar percentages of mitotic spindle defects, suggesting that GSCs are more prone to rapid polyploidization. Further analysis of mitotic phenotypes and quantification of polyploid cells, using phalloidin staining, following BI2536, are needed to test this hypothesis and elucidate whether it represents one of the main determinants of the high sensitivity of GSCs to Plk1 inibition.

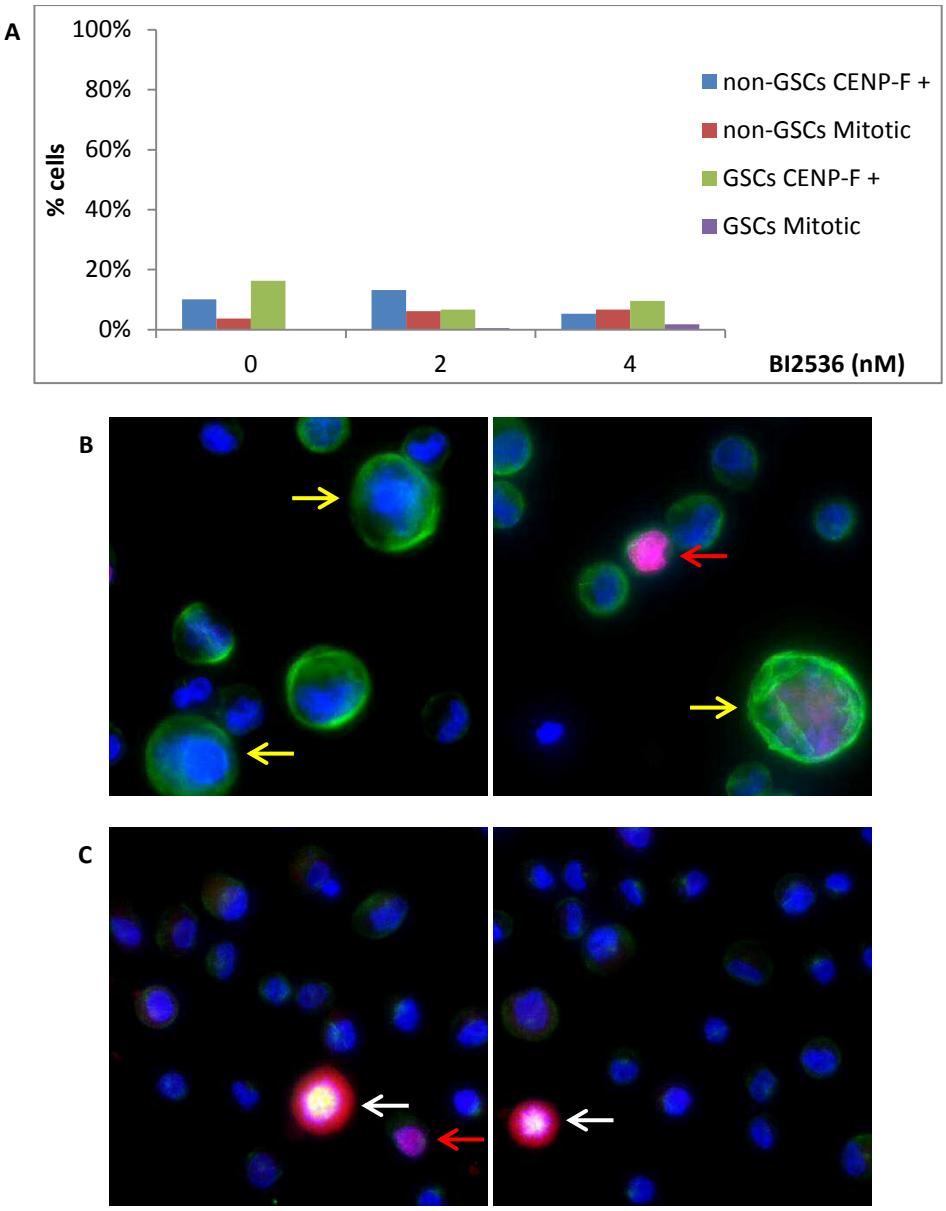

Figure 5.3 GSCs and non-GSCs do not undergo a considerable G2/M arrest following Plk1 inhibition. GSCs and non-GSCs were treated with 0, 2 and 4 nM of BI2536. Following 24 hours of incubation, they were fixed and stained for α tubulin (green), CENP-F (red) and DAPI (blue), to visualize and quantify G2/M cells. **A.** A graph shows the percentages of cells in G2 and M phase in the two subpopulations at the various dose levels. An average of 229 cells/condition were randomly imaged and scored. **B-C.** Representative images of GSCs (B) and non-GSCs (C) treated with 4nM of BI2536. White arrows indicate mitotic cells, red arrows G2 cells and yellow arrows giant cells.

5.5 Analysis of interphase functions of Plk1 is of potential interest in the context of the cytotoxic effect of BI2537 in glioblastoma cells

Several studies, using various established cancer cell lines, support a role of Plk1 in DNA replication and regulation of the checkpoint response during S phase, suggesting that it promotes DNA synthesis and progression through S phase[308-311]. These functions are of potential therapeutic interest and could be relevant to GSCs and their response to treatment, in the light of the results of a study showing that GSCs do not display inhibition of DNA synthesis post-radiation, with no or small reduction in new initiations, suggesting a lower activation of the intra-S-phase checkpoint[312]. The authors do not explore a mechanistic correlation between these observations and Plk1 activity, allowing speculation that this kinase might contribute to the distinctive response of GSCs in terms of DNA replication and regulation of the checkpoint response during S phase.

Based on these data, I started investigating the effect of Plk1 inhibition on the S phase fraction in the two subpopulations, by evaluating EdU staining with immunofluorescence. In the initial experiment, GSCs did not display a consistent change in the percentage of cells in S phase, while, amongst non-GSCs, there was a moderate increase (see figure 5.4). Representative images are shown in figure 5.5. Given that these preliminary observations are not sufficient to perform statistical analysis, their value is limited and they need to be substantiated by further experiments.

To my knowledge, there are no data in the literature regarding quantification of GSCs in S phase following Plk1 inhibition. The study mentioned in the previous paragraphs did not measure the fraction of GSCs in S phase in their FACS analysis[306]. Two other studies quantified the percentage of cells in the various phases of the cell cycle in glioblastoma established cell lines, with conflicting results: one reported a moderate increase in the S phase fraction, while the other showed no change or even a decrease, following treatment with BI2536[245, 307]. Given the preliminary nature of my data, other experiments are needed to confirm the small difference in S phase regulation observed between GSCs and non-GSCs, following BI2536 treatment, and, most importantly, investigate its relevance in terms of sensitivity of glioblastoma cells to Plk1 inhibition alone or in combination with DNA damaging agents, such as radiation and temozolomide.

In this context, based on findings of a study showing that Plk1 depletion induces DNA damage[313], I also tested the feasibility of combining foci analysis with Edu labelling. As seen in figure 5.5, I was able to obtain discrete 53BP1 foci in association with Edu staining, with an image quality suitable for quantification with the semi-automated method described in

chapter three. Furthermore, observation of the images from this preliminary experiment indicates that Plk1 inhibition might induce an increase in 53BP1 foci, particularly in GSCs (see figure 5.5), suggesting that DNA damage might be involved in determining the differential sensitivity of the two subpopulations to BI2536. More detailed analysis of BI2536-induced DNA damage and repair kinetics is necessary to confirm this hypothesis and give indications of possible strategies to exploit this effect therapeutically.

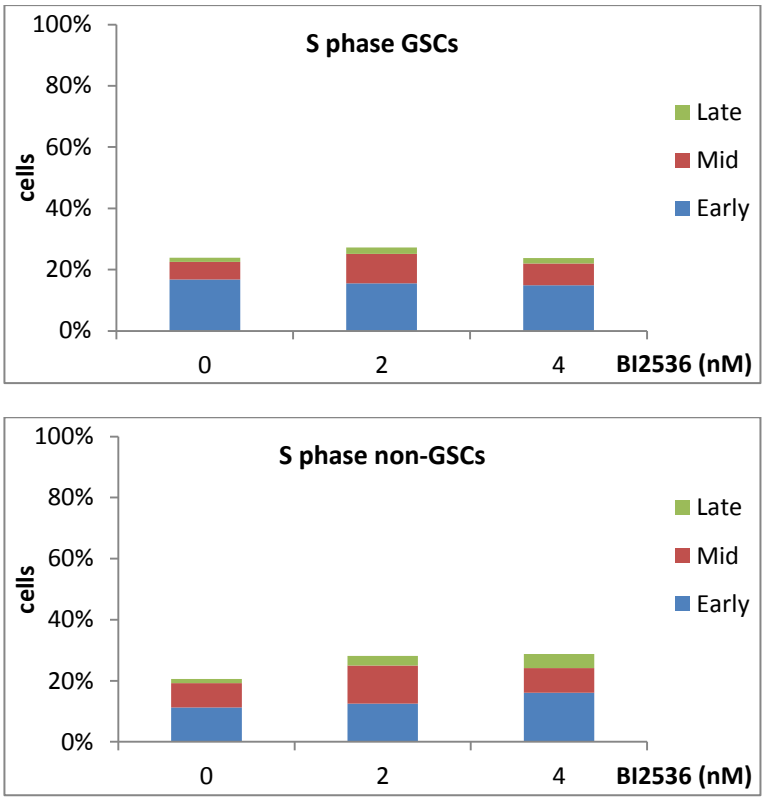

Figure 5.4 Quantification of S phase fraction in GSCs and non-GSCs with EdU labelling is feasible.

GSCs and non-GSCs were treated with 0, 2 and 4 nM of BI2536. Following 24 hours of incubation, they were labelled with Edu (red) with the Click-iT® kit (according to the manufacturer's protocol) and stained for 53BP1 (green) and DAPI (blue). The graphs show percentages of cells in S phase (specifying early, mid and late, based on the staining pattern, as seen in figure 5.6) in the two subpopulations at the various dose levels. An average of 141 cells/condition were randomly imaged and scored.

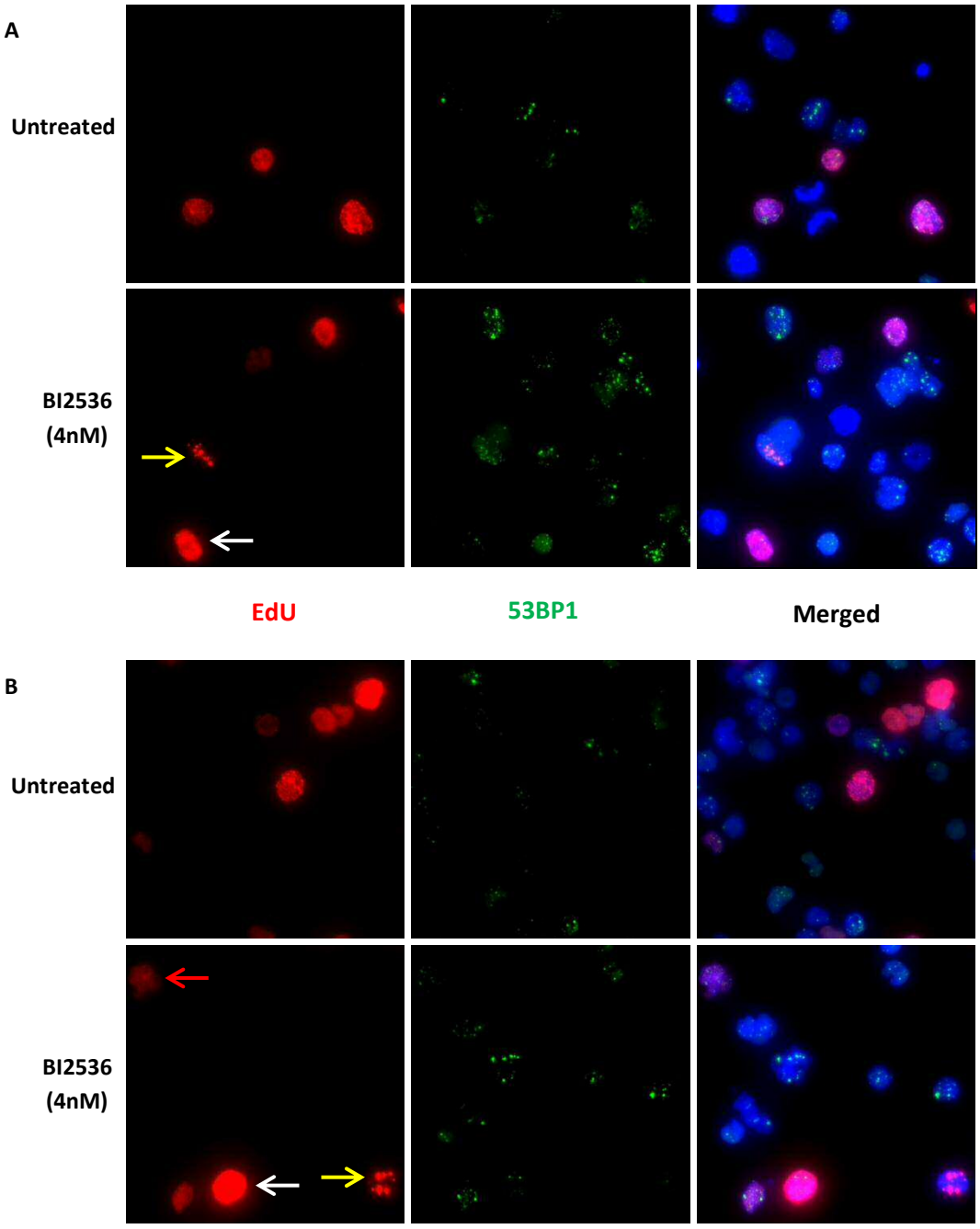

Figure 5.5 Simultaneous analysis of Edu labelling and 53BP1 foci in GSCs and non-GSCs is feasible.

GSCs and non-GSCs were treated as described in figure 5.5. Representative images of GSCs (A) and non-GSCs (B) treated with 0 or 4 nM of BI2536. White, red and yellow arrows indicate examples of cells in early, mid and late S phase, respectively.

5.6 Glioblastoma stem and non-stem cells display primary cilia *in vitro*

As a first step in analysing the presence of cilia in glioblastoma cells in vitro, I evaluated whether I could identify these organelles in cells processed with the standard immunofluorescence protocol, i.e. in cells retrieved from flasks and cytospun on coverslips. I was not able to identify cilia following staining for acetylated alpha-tubulin. Given that the study published at the time directly stained cells grown on poly-L-lysine coated coverslips, I speculated that retrieval or cytospinning might have an impact on visualization of cilia. To address this issue without changing culture conditions for GSCs, I tested whether I could visualize cilia in cells grown within Alvetex®. Use of an antibody against acetylated alpha-tubulin resulted in strong staining of microtubule structures throughout the cells in two GSC lines. As seen in figure 5.6, it was not possible to distinguish primary cilia amongst the other cellular structures bound by the antibody.

I then tested the use of an antibody against a protein more specifically localized in primary cilia, ADP-ribosylation factor-like protein 13B (Arl13B), involved in regulation of intraflagellar transport and ciliogenesis[314]. I found that a portion of GSCs and non-GSCs presented cilia (see figure 5.7). Although I did not quantify the percentage of cells with cilia in random images, observation of these suggests that a larger fraction of non-GSCs presents these organelles. Also, Arl13B staining was less strong in GSCs, as I obtained fainter images, even after increasing the acquisition settings, suggesting that there might be structural and functional differences between cilia in GSCs and non-GSCs. Quantitative and qualitative analysis of staining patterns of Arl13B and other ciliary components in GSCs and non-GSCs from several primary glioblastoma cell lines is needed to substantiate these observations. If the two subpopulations are confirmed to have distinctive ciliary features, future studies will investigate their correlation with processes regulating the transition from GSC to non-GSC phenotype, i.e. their link with differentiation, focusing at first on the role of molecules which have been involved both in ciliary function and stemness-maintenance, such as hedgehog and Notch.

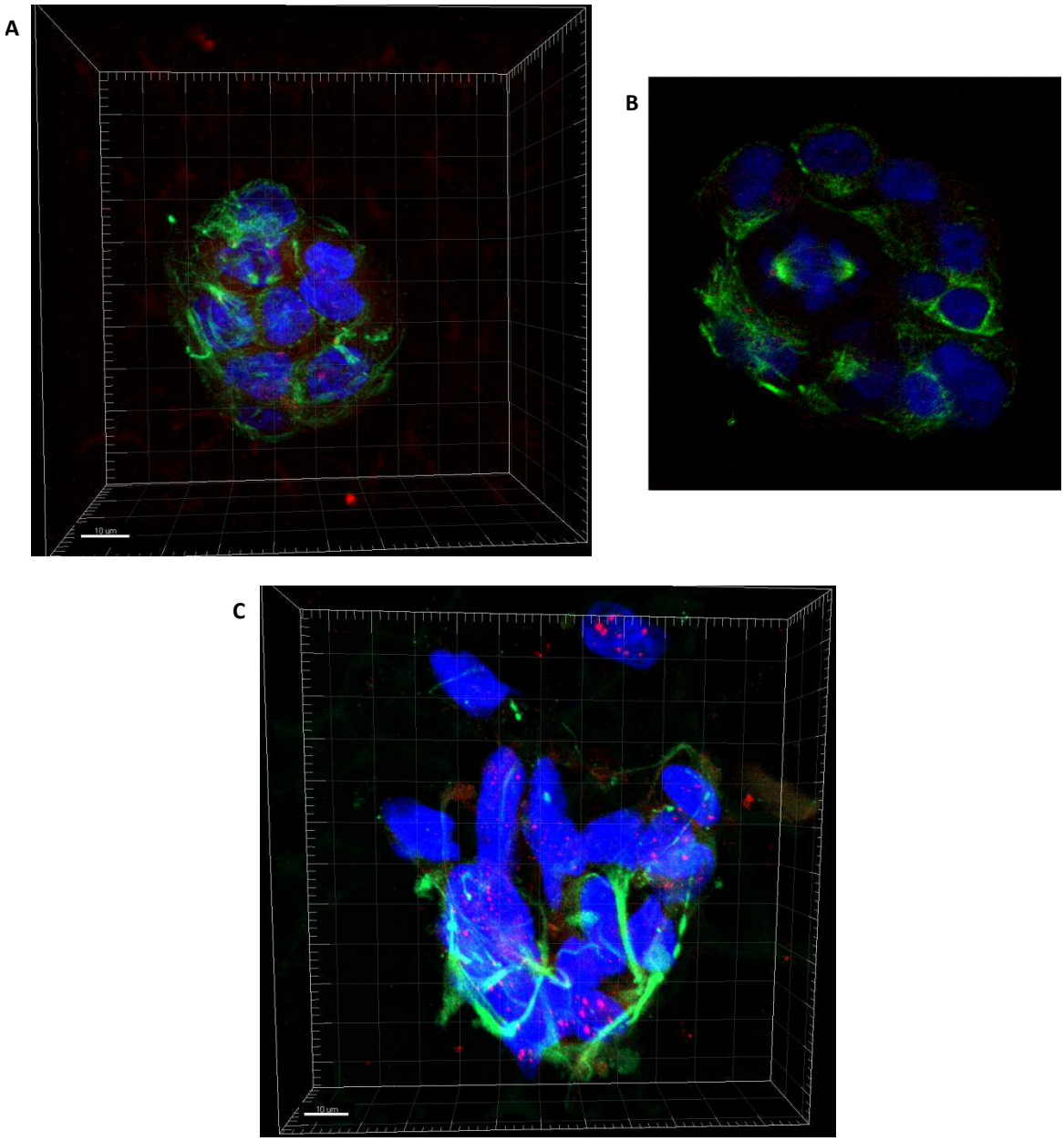

Figure 5.6 Staining for acetylated alpha-tubulin is very intense throughout the cells in GSCs grown within the scaffold.

Fluorescence confocal microscope images of G7 (A-B) and E2 (C) GSCs grown within the scaffold and stained for acetylated alpha-tubulin (green), gamma-tubulin (red) and DAPI (blue). Figure B is one of the images composing the Z-stack displayed in A, showing a cell undergoing mitosis in the heart of the sphere. Scale bar 10µm.

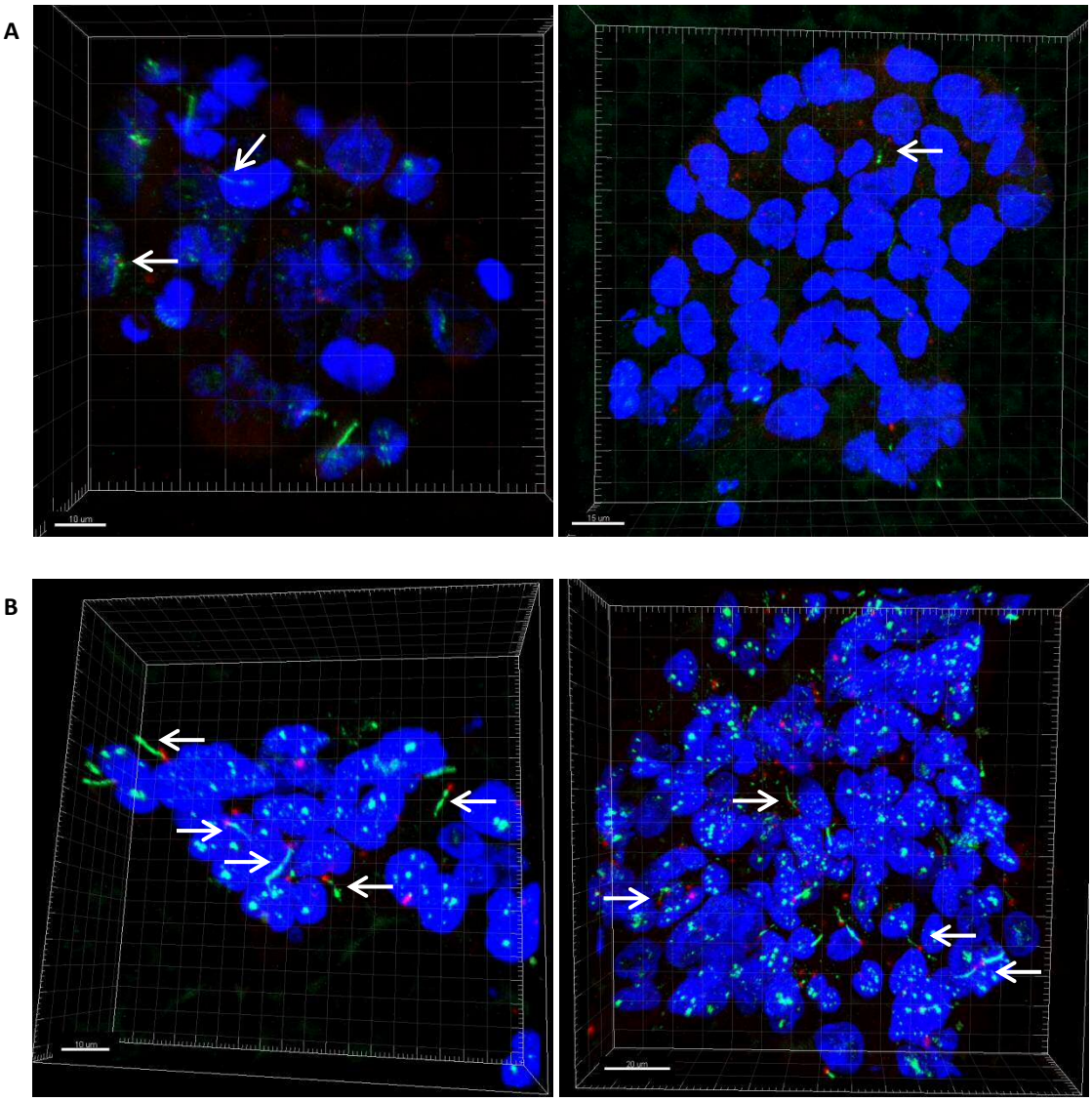

Figure 5.7 Staining for Arl13B shows presence of primary cilia in GSCs and non-GSCs grown within the scaffold.

Fluorescence confocal microscope images of G7 GSCs (A) and non-GSCs (B) grown within the scaffold and stained for Arl13B (green), gamma-tubulin (red) and DAPI (blue). White arrows indicate examples of primary cilia, with the basal body (identified with gamma-tubulin) shown in red and the axoneme (identified with Arl13B) in green.

5.7 Primary cilia are influenced by culture conditions

Given that serum withdrawal is one of the methods used to increase expression of cilia in normal cells, I tested whether changing culture conditions had an effect on Arl13B expression in the two subpopulations. Following 24 hours of incubation in non-GSC medium, GSCs displayed a staining pattern closer to that seen in non-GSCs, i.e. more cells presented cilia and Arl13B intensity was stronger (see figure 5.8.A). Consistently, after 24 hours of incubation in GSC medium, fewer non-GSCs had cilia and these appeared fainter (see figure 5.8.B). Given the preliminary nature of these observations, further experiments and quantitative analysis need to confirm these findings, investigating whether these variations are linked to changes in the differentiation status of these cells or to other mechanisms induced by modifications in the culture conditions.

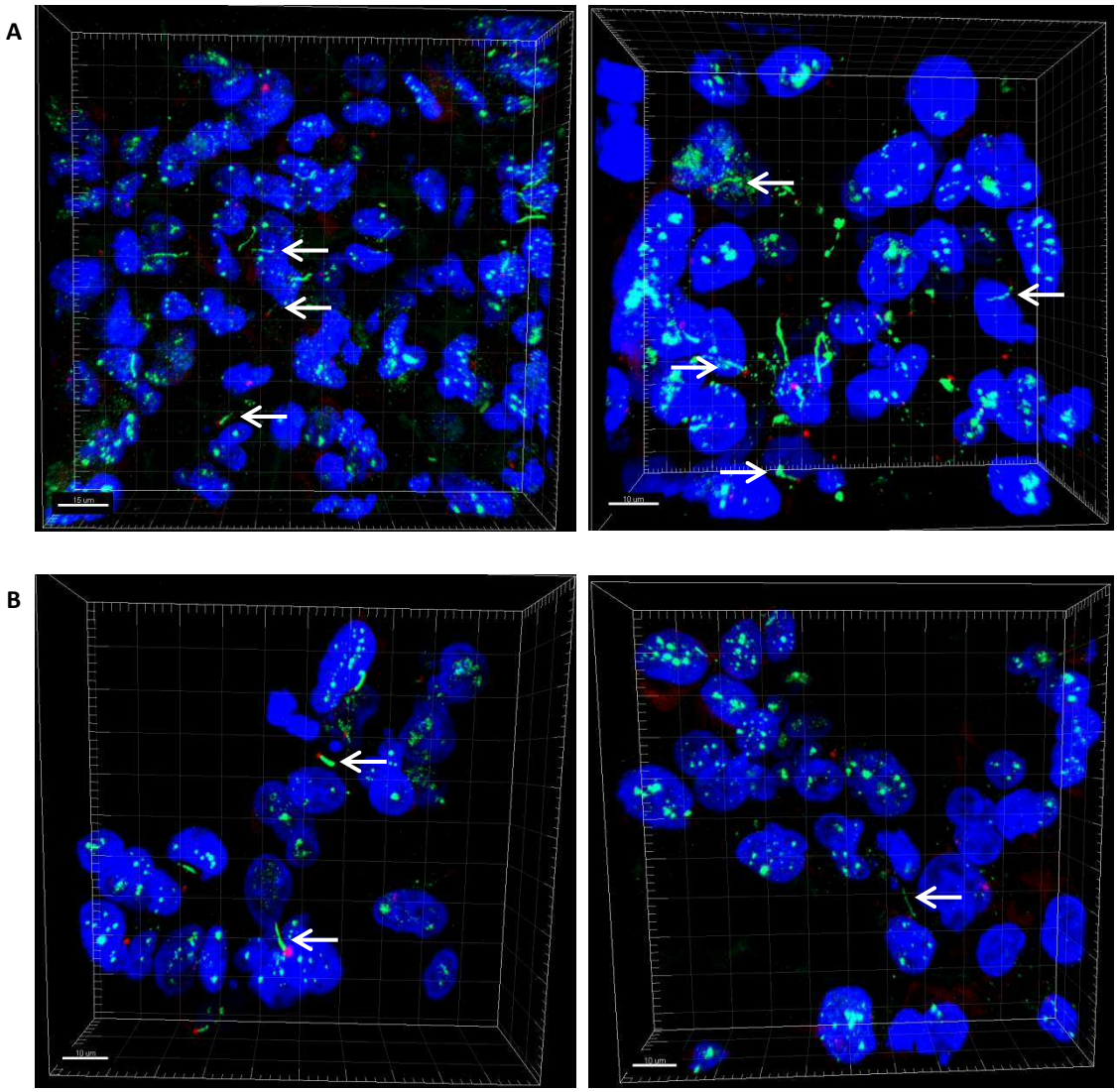

Figure 5.8 Swapping culture conditions affects Arl13B expression in GSCs and non-GSCs.

Fluorescence confocal microscope images of G7 GSCs (A) and non-GSCs (B) grown within the scaffold, incubated for 24 hours in non-GSC medium and GSC medium, respectively, and stained for Arl13B (green), gamma-tubulin (red) and DAPI (blue). White arrows indicate examples of primary cilia, with the basal body (identified with gamma-tubulin) shown in red and the axoneme (identified with Arl13B) in green.

5.8 Aurora A inhibition with MLN8237 affects ciliogenesis in GSCs and non-GSCs

Based on published data showing that inhibition of AurA with MLN8237 increases defects in primary cilia formation in cells from a mouse autosomal dominant polycystic kidney disease model[315], I evaluated whether similar effects were visible in GSCs and non-GSCs grown and treated within the scaffold. Following 24 hours of incubation with MLN8237, both subpopulations displayed changes in the appearance of cilia: amongst non-GSCs there was a clear increase in cilia malformations, with many organelles presenting two axonemes or bulges; while in GSCs the changes induced by the drug were more difficult to pinpoint based on simple observation, given that less cells presented cilia in untreated samples and that there was a variety of phenotypes amongst MLN8237-treated GSCs (see figure 5.9). Although consistent with published data, these findings need to be supported by further experiments, with a more detailed analysis of structural and functional modifications of cilia following AurA inhibition.

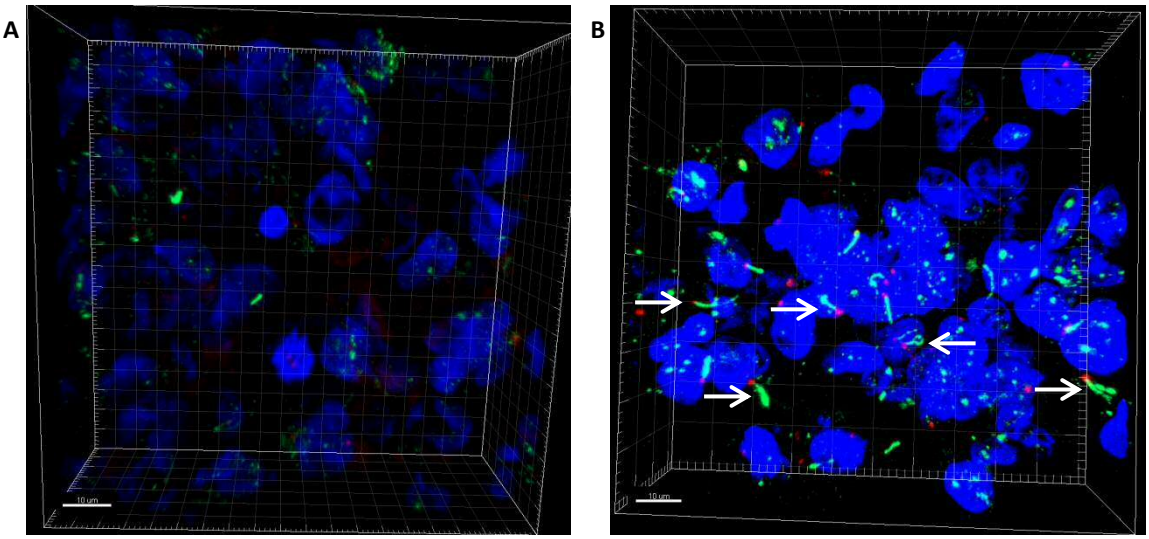

Figure 5.9 Ciliogenesis is altered in GSCs and non-GSCs following Aurora A inhibition.

Fluorescence confocal microscope images of G7 GSCs (A) and non-GSCs (B) grown within the scaffold, incubated for 24 hours with 50nM of MLN8237 and stained for Arl13B (green), gamma-tubulin (red) and DAPI (blue). White arrows indicate examples of aberrant primary cilia, with the basal body (identified with gamma-tubulin) shown in red and the axoneme (identified with Arl13B) in green. Scale bar 10µm.

5.9 Discussion

In this final chapter, I present preliminary data on the effects of Plk1 inhibition in glioblastoma primary cell lines, showing that GSCs are significantly more sensitive to BI2536 than non-GSCs. Unlike with AurA inhibition, the pronounced difference in terms of clonogenicity following Plk1 targeting cannot be correlated to induction of distinct levels of mitotic spindle defects in the two subpopulations, but the major consequence of both AurA and Plk1 inhibition in GSC appears to be polyploidization. It is likely that Plk1 inhibition causes a strong cytokinesis defect in the GSC that could only be scored appropriately using a live cell imaging assay. In my preliminary experiments, I started exploring the hypothesis that non-mitotic functions of Plk1 might play an important role in the cytotoxic effect observed following its inhibition. If confirmed by further tests and statistical analysis of quantitative data, this mechanism could address some of the doubts raised on the clinical relevance and utility of mitotic kinase inhibitors, based on the argument that these drugs target only dividing cells, which represent a negligible fraction (<1% to few percent) of tumoral cells in patients[263].

I also report preliminary observations on primary cilia in GSCs and non-GSCs, showing that these can be visualised and analysed in cells grown in a 3D culture system. The feasibility of studying cilia in an *in vitro* model, in which one can introduce several elements from the tumoral niche, is particularly intriguing given that these organelles function as antenna for cells, sensing chemical and mechanical signals from the microenvironment. In this context, given the increasing evidence supporting the importance of the interaction between primary cilia and ECM[316], the possibility of studying ciliary signalling in GSCs and non-GSCs grown within the scaffold coated with specific ECM components (shown in chapter three) is extremely exciting and might uncover mechanisms underlying how these cells sense and adapt to microenvironmental stimuli. Furthermore, if ciliary signalling plays a role in glioblastoma biology, another interesting line of research arising from my experiments is that regarding the role of disruption of cilia regulation by AurA in the anticancer effect of MLN8237. Given that Plk1 has also been involved in the pathway controlling cilia disassembly[317], this question should be extended to BI2536.

The data presented in this chapter are highly preliminary and do not allow any firm conclusions without further experimental data. However, an important point of these observations is that they strengthen the rationale for targeting mitotic kinases as an effective strategy against GSCs, but also suggest that the interphase functions of these proteins need to be investigated further, as their disruption is likely to be responsible for part of the cytotoxic effect of AurA and Plk1 inhibitors.

Chapter 6

Conclusions

This thesis presents the results of my research on patient-derived GSCs and non-GSCs, aimed at increasing our understanding of the biology of this aggressive brain tumour and, therefore, designing more efficacious anticancer treatments. For this scope, at first I optimized *in vitro* methods that allow analysis of sensitivity of GSCs and non-GSCs to ionizing radiation and chemotherapeutic drugs. Then, I focused on characterization of mitotic phenotypes and centrosome cycle in the two cellular subpopulations, with the aim of identifying targets for novel therapeutic approaches against glioblastomas. I tested sensitivity of GSCs and non-GSCs to these treatments employing the techniques I optimized in the first part of my project. In parallel, I developed the use of a 3D culture model for the two subpopulations and I showed how it can be applied to study centrosome cycle related features in GSCs and non-GSCs.

The optimization process of *in vitro* methods is described in chapter three, which includes two main sections: one reporting the experiments performed to develop a clonogenic survival assay that allows comparative analysis of sensitivity of GSCs and non-GSCs to ionizing radiation and cytotoxic agents, with each subpopulation cultured in its appropriate growth condition; the other showing how a 3D culture model can be used to investigate many features, including treatment responses, of GSCs and non-GSCs in the presence of various factors characteristic of their tumoral niche. The contribution of this work to cancer research is potentially significant, given that these techniques allow a more comprehensive approach, providing tools to analyse treatment responses related to intrinsic cellular characteristics as well as those induced by microenvironmental factors. Further development of such methodologies is likely to improve reliability and clinical significance of *in vitro* experiments, resulting in more accurate selection of therapeutic agents for *in vivo* pre-clinical studies.

The results of my analysis of cell division and centrosome morphology are described in chapter four, which also includes two parts: one showing that GSCs display a higher percentage of spindle abnormalities and more pronounced maturation of centrosomes preceding mitosis; the other demonstrating that inhibiting AurA, one of the main regulators of the centrosome cycle, is particularly effective in targeting GSCs, which, compared to non-GSCs, exhibit a higher increase in polyploidy and senescence, with a more pronounced reduction of clonogenicity. This section, therefore, addresses the central hypothesis of my project, demonstrating that it can be accepted as true, given that I show that centrosome cycle and cell division regulation of GSCs have distinctive features, which can be exploited to design therapeutic strategies that are both specific and effective against these cells.

Having recognised the need for further investigation of mitosis and centrosome biology in GSCs, I decided to build on these findings. So, I started analysing the effects of inhibiting Plk1

and characterizing primary cilia in glioblastoma cells. The preliminary data from these studies, presented in chapter five, on the one hand, strengthen the rationale for targeting mitotic kinases, on the other, they highlight the relevance of their interphase functions, suggesting that future research should also explore these in detail to enable the design of treatment combinations that exploit fully the potential benefits of inhibiting these proteins. Characterization experiments of primary cilia also have a methodological output, as they show the feasibility of analysing these organelles in GSCs and non-GSCs cultured in their appropriate growth condition within the 3D model described in chapter three.

My research on centrosome cycle and cell division is likely to give a meaningful contribution to our understanding of glioblastoma biology, as it demonstrates for the first time that *in vitro* GSCs differ from non-GSCs with regards to mitotic spindle phenotypes and centrosome maturation, providing a possible explanation for the high susceptibility of these cells to mitotic kinase inhibitors, observed in my experiments as well as in other studies.

Planned future studies arising from my work include the following:

- pathology analysis of xenografts and glioblastoma patient specimens, evaluating mitotic phenotypes and centrosome proteins in tissues co-stained with GSC markers. The aim of these studies is to test whether my *in vitro* findings truly reproduce behaviour of glioblastoma cells in their natural environment and, therefore, validate their clinical relevance.
- further pre-clinical evaluation of the anti-glioblastoma activity of AurA inhibitors:
  - analysis of fate of GSCs and non-GSCs, after AurA inhibition, using live-cell imaging;
  - evaluation of AurA inhibition as a targeted GSC treatment in xenografts, following establishment of biomarkers, such as aberrant spindle phenotypes and AurA phosphorylation;
  - more detailed *in vitro* analysis of potential synergistic effect of AurA inhibition and IR;
  - *in vivo* evaluation of activity of various treatment schedules (also with IR if *in vitro* experiments indicate advantageous interaction), measuring prevention of tumour formation and tumour regression.
- further pre-clinical evaluation of the anti-glioblastoma activity of Plk1 inhibitors:
  - analysis of fate of GSCs and non-GSCs, after Plk1 inhibition, using live-cell imaging;
  - evaluation of DNA damage induction following Plk1 inhibition and investigation of effect of combined treatment with IR.
- characterization of cilia in glioblastoma cells:

- quantitative and qualitative analysis of staining patterns of ciliary proteins in GSCs and non-GSCs grown within the 3D culture model, with or without specific ECM coating;
- investigation of the role of ciliary disruption in the anticancer effect of AurA and Plk1 inhibition, analysing treated cells grown on the 3D scaffold and xenografts.

Depending on their outcome, these studies might form the basis for designing future clinical trials testing the activity of mitotic kinase inhibitors in glioblastoma patients.

1. Dolecek, T.A., Propp, J.M., Stroup, N.E. & Kruchko, C. CBTRUS statistical report: primary brain and central nervous system tumors diagnosed in the United States in 2005-2009. *Neuro Oncol* **14 Suppl 5**, v1-49 (2012).
2. http://www.cancerresearchuk.org/cancer-info/cancerstats/types/brain/incidence/.
3. Maher EA, M.A. Neoplasms of the central nervous system. In Skarin AT [ed]: Dana-Farber Cancer Institute Atlas of Diagnostic Oncology, 3rd ed. St. Louis, Mosby, p 406. (2003).
4. Preusser, M. *et al.* Current concepts and management of glioblastoma. *Ann Neurol* **70**, 9-21 (2011).
5. Klein, M. *et al.* Neurobehavioral status and health-related quality of life in newly diagnosed high-grade glioma patients. *J Clin Oncol* **19**, 4037-4047 (2001).
6. Boele, F.W. *et al.* Health-related quality of life of significant others of patients with malignant CNS versus non-CNS tumors: a comparative study. *J Neurooncol* **115**, 87-94 (2013).
7. Crespo, I. *et al.* Molecular and Genomic Alterations in Glioblastoma Multiforme. *Am J Pathol* **185**, 1820-1833 (2015).
8. Mischel, P.S. *et al.* Identification of molecular subtypes of glioblastoma by gene expression profiling. *Oncogene* **22**, 2361-2373 (2003).
9. Shai, R. *et al.* Gene expression profiling identifies molecular subtypes of gliomas. *Oncogene* **22**, 4918-4923 (2003).
10. Tso, C.L. *et al.* Distinct transcription profiles of primary and secondary glioblastoma subgroups. *Cancer Res* **66**, 159-167 (2006).
11. Brennan, C. *et al.* Glioblastoma subclasses can be defined by activity among signal transduction pathways and associated genomic alterations. *PLoS One* **4**, e7752 (2009).
12. Verhaak, R.G. *et al.* Integrated genomic analysis identifies clinically relevant subtypes of glioblastoma characterized by abnormalities in PDGFRA, IDH1, EGFR, and NF1. *Cancer Cell* **17**, 98-110 (2010).
13. Kleihues, P. & Ohgaki, H. Primary and secondary glioblastomas: from concept to clinical diagnosis. *Neuro Oncol* **1**, 44-51 (1999).
14. Nutt, C.L. *et al.* Gene expression-based classification of malignant gliomas correlates better with survival than histological classification. *Cancer Res* **63**, 1602-1607 (2003).
15. Freije, W.A. *et al.* Gene expression profiling of gliomas strongly predicts survival. *Cancer Res* **64**, 6503-6510 (2004).
16. Liang, Y. *et al.* Gene expression profiling reveals molecularly and clinically distinct subtypes of glioblastoma multiforme. *Proc Natl Acad Sci U S A* **102**, 5814-5819 (2005).
17. Phillips, H.S. *et al.* Molecular subclasses of high-grade glioma predict prognosis, delineate a pattern of disease progression, and resemble stages in neurogenesis. *Cancer Cell* **9**, 157-173 (2006).
18. Holdhoff, M. *et al.* Use of personalized molecular biomarkers in the clinical care of adults with glioblastomas. *J Neurooncol* **110**, 279-285 (2012).
19. Weller, M., Stupp, R., Hegi, M. & Wick, W. Individualized targeted therapy for glioblastoma: fact or fiction? *Cancer J* **18**, 40-44 (2012).
20. Gorlia, T. *et al.* Nomograms for predicting survival of patients with newly diagnosed glioblastoma: prognostic factor analysis of EORTC and NCIC trial 26981-22981/CE.3. *Lancet Oncol* **9**, 29-38 (2008).
21. Laws, E.R. *et al.* Survival following surgery and prognostic factors for recently diagnosed malignant glioma: data from the Glioma Outcomes Project. *J Neurosurg* **99**, 467-473 (2003).
22. Stupp, R. *et al.* Effects of radiotherapy with concomitant and adjuvant temozolomide versus radiotherapy alone on survival in glioblastoma in a randomised phase III study: 5-year analysis of the EORTC-NCIC trial. *Lancet Oncol* **10**, 459-466 (2009).

23. Laperriere, N. *et al.* Optimal management of elderly patients with glioblastoma. *Cancer Treat Rev* **39**, 350-357 (2013).
24. Marina, O. *et al.* Treatment outcomes for patients with glioblastoma multiforme and a low Karnofsky Performance Scale score on presentation to a tertiary care institution. Clinical article. *J Neurosurg* **115**, 220-229 (2011).
25. Chaichana, K.L. *et al.* Factors associated with survival for patients with glioblastoma with poor pre-operative functional status. *J Clin Neurosci* **20**, 818-823 (2013).
26. http://www.nccn.org/professionals/physician_gls/f_guidelines.asp#site.
27. Brem, S., Cotran, R. & Folkman, J. Tumor angiogenesis: a quantitative method for histologic grading. *J Natl Cancer Inst* **48**, 347-356 (1972).
28. Plate, K.H., Breier, G., Weich, H.A., Mennel, H.D. & Risau, W. Vascular endothelial growth factor and glioma angiogenesis: coordinate induction of VEGF receptors, distribution of VEGF protein and possible in vivo regulatory mechanisms. *Int J Cancer* **59**, 520-529 (1994).
29. Calabrese, C. *et al.* A perivascular niche for brain tumor stem cells. *Cancer Cell* **11**, 69-82 (2007).
30. Friedman, H.S. *et al.* Bevacizumab alone and in combination with irinotecan in recurrent glioblastoma. *J Clin Oncol* **27**, 4733-4740 (2009).
31. Vredenburgh, J.J. *et al.* Bevacizumab plus irinotecan in recurrent glioblastoma multiforme. *J Clin Oncol* **25**, 4722-4729 (2007).
32. http://www.ema.europa.eu/docs/en_GB/document_library/EPAR_-_Assessment_Report_-_Variation/human/000582/WC500075000.pdf.
33. http://ecancer.org/news/4119-asco-2013--no-survival-benefit-to-adding-bevacizumab-to-standard-first-line-chemoradiation-for-glioblastoma.php.
34. Chamberlain, M.C. Bevacizumab for the treatment of recurrent glioblastoma. *Clin Med Insights Oncol* **5**, 117-129 (2011).
35. Fonkem, E. & Wong, E.T. NovoTTF-100A: a new treatment modality for recurrent glioblastoma. *Expert Rev Neurother* **12**, 895-899 (2012).
36. Kirson, E.D. *et al.* Disruption of cancer cell replication by alternating electric fields. *Cancer Res* **64**, 3288-3295 (2004).
37. Kirson, E.D. *et al.* Alternating electric fields arrest cell proliferation in animal tumor models and human brain tumors. *Proc Natl Acad Sci U S A* **104**, 10152-10157 (2007).
38. Stupp, R. *et al.* NovoTTF-100A versus physician's choice chemotherapy in recurrent glioblastoma: a randomised phase III trial of a novel treatment modality. *Eur J Cancer* **48**, 2192-2202 (2012).
39. http://clinicaltrials.gov/ct2/show/NCT00916409?term=NCT%2300916409&rank=1.
40. Loges, S., Schmidt, T. & Carmeliet, P. Mechanisms of resistance to anti-angiogenic therapy and development of third-generation anti-angiogenic drug candidates. *Genes Cancer* **1**, 12-25 (2010).
41. Hamerlik, P. *et al.* Autocrine VEGF-VEGFR2-Neuropilin-1 signaling promotes glioma stem-like cell viability and tumor growth. *J Exp Med* **209**, 507-520 (2012).
42. Kim, Y. *et al.* Platelet-derived growth factor receptors differentially inform intertumoral and intratumoral heterogeneity. *Genes Dev* **26**, 1247-1262 (2012).
43. Sunayama, J. *et al.* Crosstalk between the PI3K/mTOR and MEK/ERK pathways involved in the maintenance of self-renewal and tumorigenicity of glioblastoma stem-like cells. *Stem Cells* **28**, 1930-1939 (2010).
44. Nassiri, F. *et al.* Endoglin (CD105): a review of its role in angiogenesis and tumor diagnosis, progression and therapy. *Anticancer Res* **31**, 2283-2290 (2011).
45. Bockhorn, M. *et al.* Differential vascular and transcriptional responses to anti-vascular endothelial growth factor antibody in orthotopic human pancreatic cancer xenografts. *Clin Cancer Res* **9**, 4221-4226 (2003).

46. Sanchez-Elsner, T., Botella, L.M., Velasco, B., Langa, C. & Bernabeu, C. Endoglin expression is regulated by transcriptional cooperation between the hypoxia and transforming growth factor-beta pathways. *J Biol Chem* **277**, 43799-43808 (2002).
47. Ricci-Vitiani, L. *et al.* Tumour vascularization via endothelial differentiation of glioblastoma stem-like cells. *Nature* **468**, 824-828 (2010).
48. Wang, R. *et al.* Glioblastoma stem-like cells give rise to tumour endothelium. *Nature* **468**, 829-833 (2010).
49. Soda, Y. *et al.* Transdifferentiation of glioblastoma cells into vascular endothelial cells. *Proc Natl Acad Sci U S A* **108**, 4274-4280 (2011).
50. Smith, S.J. *et al.* CD105 (Endoglin) exerts prognostic effects via its role in the microvascular niche of paediatric high grade glioma. *Acta Neuropathol* **124**, 99-110 (2012).
51. Liu, D. *et al.* Tie2/TEK modulates the interaction of glioma and brain tumor stem cells with endothelial cells and promotes an invasive phenotype. *Oncotarget* **1**, 700-709 (2010).
52. Martin, V. *et al.* Tie2-mediated multidrug resistance in malignant gliomas is associated with upregulation of ABC transporters. *Oncogene* **28**, 2358-2363 (2009).
53. Graff, J.R. *et al.* The protein kinase Cbeta-selective inhibitor, Enzastaurin (LY317615.HCl), suppresses signaling through the AKT pathway, induces apoptosis, and suppresses growth of human colon cancer and glioblastoma xenografts. *Cancer Res* **65**, 7462-7469 (2005).
54. Desgrosellier, J.S. & Cheresh, D.A. Integrins in cancer: biological implications and therapeutic opportunities. *Nat Rev Cancer* **10**, 9-22 (2010).
55. Mittelbronn, M., Warth, A., Meyermann, R., Goodman, S. & Weller, M. Expression of integrins alphavbeta3 and alphavbeta5 and their ligands in primary and secondary central nervous system neoplasms. *Histol Histopathol* **28**, 749-758 (2013).
56. Janouskova, H. *et al.* Integrin alpha5beta1 plays a critical role in resistance to temozolomide by interfering with the p53 pathway in high-grade glioma. *Cancer Res* **72**, 3463-3470 (2012).
57. Wernicke, A.G. *et al.* Prostate-specific membrane antigen as a potential novel vascular target for treatment of glioblastoma multiforme. *Arch Pathol Lab Med* **135**, 1486-1489 (2011).
58. Network, T.C.G.A.R. Comprehensive genomic characterization defines human glioblastoma genes and core pathways. *Nature* **455**, 1061-1068 (2008).
59. Aldape, K.D. *et al.* Immunohistochemical detection of EGFRvIII in high malignancy grade astrocytomas and evaluation of prognostic significance. *J Neuropathol Exp Neurol* **63**, 700-707 (2004).
60. Lund-Johansen, M. *et al.* Effect of epidermal growth factor on glioma cell growth, migration, and invasion in vitro. *Cancer Res* **50**, 6039-6044 (1990).
61. Jansen, M., Yip, S. & Louis, D.N. Molecular pathology in adult gliomas: diagnostic, prognostic, and predictive markers. *Lancet Neurol* **9**, 717-726 (2010).
62. Babu, R. & Adamson, D.C. Rindopepimut: an evidence-based review of its therapeutic potential in the treatment of EGFRvIII-positive glioblastoma. *Core Evid* **7**, 93-103 (2012).
63. Morgan, R.A. *et al.* Recognition of glioma stem cells by genetically modified T cells targeting EGFRvIII and development of adoptive cell therapy for glioma. *Hum Gene Ther* **23**, 1043-1053 (2012).
64. Clark, P.A. *et al.* Activation of multiple ERBB family receptors mediates glioblastoma cancer stem-like cell resistance to EGFR-targeted inhibition. *Neoplasia* **14**, 420-428 (2012).
65. Du, J. *et al.* Bead-based profiling of tyrosine kinase phosphorylation identifies SRC as a potential target for glioblastoma therapy. *Nat Biotechnol* **27**, 77-83 (2009).

66. Stettner, M.R. *et al.* Lyn kinase activity is the predominant cellular SRC kinase activity in glioblastoma tumor cells. *Cancer Res* **65**, 5535-5543 (2005).
67. Lu, K.V. *et al.* Fyn and SRC are effectors of oncogenic epidermal growth factor receptor signaling in glioblastoma patients. *Cancer Res* **69**, 6889-6898 (2009).
68. Lennartsson, J. & Ronnstrand, L. Stem cell factor receptor/c-Kit: from basic science to clinical implications. *Physiol Rev* **92**, 1619-1649 (2012).
69. Nobusawa, S., Stawski, R., Kim, Y.H., Nakazato, Y. & Ohgaki, H. Amplification of the PDGFRA, KIT and KDR genes in glioblastoma: a population-based study. *Neuropathology* **31**, 583-588 (2011).
70. Puputti, M. *et al.* Amplification of KIT, PDGFRA, VEGFR2, and EGFR in gliomas. *Mol Cancer Res* **4**, 927-934 (2006).
71. Joensuu, H., Puputti, M., Sihto, H., Tynninen, O. & Nupponen, N.N. Amplification of genes encoding KIT, PDGFRalpha and VEGFR2 receptor tyrosine kinases is frequent in glioblastoma multiforme. *J Pathol* **207**, 224-231 (2005).
72. Sun, L. *et al.* Neuronal and glioma-derived stem cell factor induces angiogenesis within the brain. *Cancer Cell* **9**, 287-300 (2006).
73. Nakada, M., Hayashi, Y. & Hamada, J. Role of Eph/ephrin tyrosine kinase in malignant glioma. *Neuro Oncol* **13**, 1163-1170 (2011).
74. Binda, E. *et al.* The EphA2 receptor drives self-renewal and tumorigenicity in stem-like tumor-propagating cells from human glioblastomas. *Cancer Cell* **22**, 765-780 (2012).
75. Miao, H. *et al.* EphA2 promotes infiltrative invasion of glioma stem cells in vivo through cross-talk with Akt and regulates stem cell properties. *Oncogene* (2014).
76. Bleau, A.M. *et al.* PTEN/PI3K/Akt pathway regulates the side population phenotype and ABCG2 activity in glioma tumor stem-like cells. *Cell Stem Cell* **4**, 226-235 (2009).
77. Sunayama, J. *et al.* Dual blocking of mTor and PI3K elicits a prodifferentiation effect on glioblastoma stem-like cells. *Neuro Oncol* **12**, 1205-1219 (2010).
78. Soeda, A. *et al.* Hypoxia promotes expansion of the CD133-positive glioma stem cells through activation of HIF-1alpha. *Oncogene* **28**, 3949-3959 (2009).
79. Wei, Y. *et al.* Activation of PI3K/Akt pathway by CD133-p85 interaction promotes tumorigenic capacity of glioma stem cells. *Proc Natl Acad Sci U S A* **110**, 6829-6834 (2013).
80. Firat, E., Weyerbrock, A., Gaedicke, S., Grosu, A.L. & Niedermann, G. Chloroquine or chloroquine-PI3K/Akt pathway inhibitor combinations strongly promote gamma-irradiation-induced cell death in primary stem-like glioma cells. *PLoS One* **7**, e47357 (2012).
81. Wang, W.J. *et al.* NVP-BEZ235, a novel dual PI3K/mTOR inhibitor, enhances the radiosensitivity of human glioma stem cells in vitro. *Acta Pharmacol Sin* **34**, 681-690 (2013).
82. Wen, P.Y., Lee, E.Q., Reardon, D.A., Ligon, K.L. & Alfred Yung, W.K. Current clinical development of PI3K pathway inhibitors in glioblastoma. *Neuro Oncol* **14**, 819-829 (2012).
83. Kong, D.S. *et al.* Prognostic significance of c-Met expression in glioblastomas. *Cancer* **115**, 140-148 (2009).
84. Liu, W. *et al.* c-Met expression is associated with time to recurrence in patients with glioblastoma multiforme. *J Clin Neurosci* **18**, 119-121 (2011).
85. Olmez, O.F. *et al.* The immunohistochemical expression of c-Met is an independent predictor of survival in patients with glioblastoma multiforme. *Clin Transl Oncol* **16**, 173-177 (2014).
86. Trusolino, L., Bertotti, A. & Comoglio, P.M. MET signalling: principles and functions in development, organ regeneration and cancer. *Nat Rev Mol Cell Biol* **11**, 834-848 (2010).

87. Jun, H.J. *et al.* Acquired MET expression confers resistance to EGFR inhibition in a mouse model of glioblastoma multiforme. *Oncogene* **31**, 3039-3050 (2012).
88. Lu, K.V. *et al.* VEGF inhibits tumor cell invasion and mesenchymal transition through a MET/VEGFR2 complex. *Cancer Cell* **22**, 21-35 (2012).
89. Jahangiri, A. *et al.* Gene expression profile identifies tyrosine kinase c-Met as a targetable mediator of antiangiogenic therapy resistance. *Clin Cancer Res* **19**, 1773-1783 (2013).
90. Lal, B., Xia, S., Abounader, R. & Laterra, J. Targeting the c-Met pathway potentiates glioblastoma responses to gamma-radiation. *Clin Cancer Res* **11**, 4479-4486 (2005).
91. Buchanan, I.M. *et al.* Radiosensitization of glioma cells by modulation of Met signalling with the hepatocyte growth factor neutralizing antibody, AMG102. *J Cell Mol Med* **15**, 1999-2006 (2011).
92. Welsh, J.W. *et al.* The c-Met receptor tyrosine kinase inhibitor MP470 radiosensitizes glioblastoma cells. *Radiat Oncol* **4**, 69 (2009).
93. Li, Y. *et al.* c-Met signaling induces a reprogramming network and supports the glioblastoma stem-like phenotype. *Proc Natl Acad Sci U S A* **108**, 9951-9956 (2011).
94. Joo, K.M. *et al.* MET signaling regulates glioblastoma stem cells. *Cancer Res* **72**, 3828-3838 (2012).
95. Rath, P. *et al.* In Vivo c-Met Pathway Inhibition Depletes Human Glioma Xenografts of Tumor-Propagating Stem-Like Cells. *Transl Oncol* **6**, 104-111 (2013).
96. Jun, H.J., Bronson, R.T. & Charest, A. Inhibition of EGFR induces a c-MET-driven stem cell population in glioblastoma. *Stem Cells* **32**, 338-348 (2014).
97. Marks, P.A. & Xu, W.S. Histone deacetylase inhibitors: Potential in cancer therapy. *J Cell Biochem* **107**, 600-608 (2009).
98. Adamopoulou, E. & Naumann, U. HDAC inhibitors and their potential applications to glioblastoma therapy. *Oncoimmunology* **2**, e25219 (2013).
99. Galanis, E. *et al.* Phase II trial of vorinostat in recurrent glioblastoma multiforme: a north central cancer treatment group study. *J Clin Oncol* **27**, 2052-2058 (2009).
100. Weller, M. *et al.* Prolonged survival with valproic acid use in the EORTC/NCIC temozolomide trial for glioblastoma. *Neurology* **77**, 1156-1164 (2011).
101. Kerkhof, M. *et al.* Effect of valproic acid on seizure control and on survival in patients with glioblastoma multiforme. *Neuro Oncol* **15**, 961-967 (2013).
102. Barker, C.A., Bishop, A.J., Chang, M., Beal, K. & Chan, T.A. Valproic acid use during radiation therapy for glioblastoma associated with improved survival. *Int J Radiat Oncol Biol Phys* **86**, 504-509 (2013).
103. Chinnaiyan, P. *et al.* Postradiation sensitization of the histone deacetylase inhibitor valproic acid. *Clin Cancer Res* **14**, 5410-5415 (2008).
104. Shabason, J.E., Tofilon, P.J. & Camphausen, K. Grand rounds at the National Institutes of Health: HDAC inhibitors as radiation modifiers, from bench to clinic. *J Cell Mol Med* **15**, 2735-2744 (2011).
105. Sun, P. *et al.* DNER, an epigenetically modulated gene, regulates glioblastoma-derived neurosphere cell differentiation and tumor propagation. *Stem Cells* **27**, 1473-1486 (2009).
106. Orzan, F. *et al.* Enhancer of Zeste 2 (EZH2) is up-regulated in malignant gliomas and in glioma stem-like cells. *Neuropathol Appl Neurobiol* **37**, 381-394 (2011).
107. Chalmers, A.J. Overcoming resistance of glioblastoma to conventional cytotoxic therapies by the addition of PARP inhibitors. *Anticancer Agents Med Chem* **10**, 520-533 (2010).
108. Tentori, L. *et al.* Poly(ADP-ribose) polymerase inhibitor increases growth inhibition and reduces G(2)/M cell accumulation induced by temozolomide in malignant glioma cells. *Glia* **40**, 44-54 (2002).

109. Tentori, L. *et al.* Systemic administration of GPI 15427, a novel poly(ADP-ribose) polymerase-1 inhibitor, increases the antitumor activity of temozolomide against intracranial melanoma, glioma, lymphoma. *Clin Cancer Res* **9**, 5370-5379 (2003).
110. Dungey, F.A., Loser, D.A. & Chalmers, A.J. Replication-dependent radiosensitization of human glioma cells by inhibition of poly(ADP-Ribose) polymerase: mechanisms and therapeutic potential. *Int J Radiat Oncol Biol Phys* **72**, 1188-1197 (2008).
111. Russo, A.L. *et al.* In vitro and in vivo radiosensitization of glioblastoma cells by the poly (ADP-ribose) polymerase inhibitor E7016. *Clin Cancer Res* **15**, 607-612 (2009).
112. Venere, M. *et al.* Therapeutic targeting of constitutive PARP activation compromises stem cell phenotype and survival of glioblastoma-initiating cells. *Cell Death Differ* **21**, 258-269 (2014).
113. Postma, T.J. *et al.* A phase II study of paclitaxel in chemonaive patients with recurrent high-grade glioma. *Ann Oncol* **11**, 409-413 (2000).
114. Fountzilas, G. *et al.* Radiation and concomitant weekly administration of paclitaxel in patients with glioblastoma multiforme. A phase II study. *J Neurooncol* **45**, 159-165 (1999).
115. Langer, C.J. *et al.* Phase II radiation therapy oncology group trial of weekly paclitaxel and conventional external beam radiation therapy for supratentorial glioblastoma multiforme. *Int J Radiat Oncol Biol Phys* **51**, 113-119 (2001).
116. Fellner, S. *et al.* Transport of paclitaxel (Taxol) across the blood-brain barrier in vitro and in vivo. *J Clin Invest* **110**, 1309-1318 (2002).
117. Fitzgerald, D.P. *et al.* TPI-287, a new taxane family member, reduces the brain metastatic colonization of breast cancer cells. *Mol Cancer Ther* **11**, 1959-1967 (2012).
118. Oehler, C. *et al.* Patupilone (epothilone B) for recurrent glioblastoma: clinical outcome and translational analysis of a single-institution phase I/II trial. *Oncology* **83**, 1-9 (2012).
119. Jeyapalan, S. *et al.* Paclitaxel Poliglumex, Temozolomide, and Radiation for Newly Diagnosed High-grade Glioma: A Brown University Oncology Group Study. *Am J Clin Oncol* (2013).
120. Semiond, D., Sidhu, S.S., Bissery, M.C. & Vrignaud, P. Can taxanes provide benefit in patients with CNS tumors and in pediatric patients with tumors? An update on the preclinical development of cabazitaxel. *Cancer Chemother Pharmacol* **72**, 515-528 (2013).
121. Beppu, T. *et al.* Change of oxygen pressure in glioblastoma tissue under various conditions. *J Neurooncol* **58**, 47-52 (2002).
122. Ogawa, K. *et al.* Phase II trial of radiotherapy after hyperbaric oxygenation with multiagent chemotherapy (procarbazine, nimustine, and vincristine) for high-grade gliomas: long-term results. *Int J Radiat Oncol Biol Phys* **82**, 732-738 (2012).
123. Clavo, B. *et al.* Modification of loco-regional microenvironment in brain tumors by spinal cord stimulation. Implications for radio-chemotherapy. *J Neurooncol* **106**, 177-184 (2012).
124. Frankland-Searby, S. & Bhaumik, S.R. The 26S proteasome complex: an attractive target for cancer therapy. *Biochim Biophys Acta* **1825**, 64-76 (2012).
125. Yin, D. *et al.* Proteasome inhibitor PS-341 causes cell growth arrest and apoptosis in human glioblastoma multiforme (GBM). *Oncogene* **24**, 344-354 (2005).
126. Liu, P. *et al.* Cytotoxic effect of disulfiram/copper on human glioblastoma cell lines and ALDH-positive cancer-stem-like cells. *Br J Cancer* **107**, 1488-1497 (2012).
127. Paranjpe, A., Zhang, R., Ali-Osman, F., Bobustuc, G.C. & Srivenugopal, K.S. Disulfiram is a direct and potent inhibitor of human O6-methylguanine-DNA methyltransferase (MGMT) in brain tumor cells and mouse brain and markedly increases the alkylating DNA damage. *Carcinogenesis* **35**, 692-702 (2014).

128. Vlachostergios, P.J., Hatzidaki, E., Stathakis, N.E., Koukoulis, G.K. & Papandreou, C.N. Bortezomib downregulates MGMT expression in T98G glioblastoma cells. *Cell Mol Neurobiol* **33**, 313-318 (2013).
129. Kubicek, G.J. *et al.* Phase I trial using proteasome inhibitor bortezomib and concurrent temozolomide and radiotherapy for central nervous system malignancies. *Int J Radiat Oncol Biol Phys* **74**, 433-439 (2009).
130. Vlashi, E. *et al.* In vivo imaging, tracking, and targeting of cancer stem cells. *J Natl Cancer Inst* **101**, 350-359 (2009).
131. Vlashi, E. *et al.* Metabolic state of glioma stem cells and nontumorigenic cells. *Proc Natl Acad Sci U S A* **108**, 16062-16067 (2011).
132. Zhang, F., Paterson, A.J., Huang, P., Wang, K. & Kudlow, J.E. Metabolic control of proteasome function. *Physiology (Bethesda)* **22**, 373-379 (2007).
133. Lagadec, C. *et al.* The RNA-binding protein Musashi-1 regulates proteasome subunit expression in breast cancer- and glioma-initiating cells. *Stem Cells* **32**, 135-144 (2014).
134. Gong, X., Schwartz, P.H., Linskey, M.E. & Bota, D.A. Neural stem/progenitors and glioma stem-like cells have differential sensitivity to chemotherapy. *Neurology* **76**, 1126-1134 (2011).
135. Ye, F. *et al.* Protective properties of radio-chemoresistant glioblastoma stem cell clones are associated with metabolic adaptation to reduced glucose dependence. *PLoS One* **8**, e80397 (2013).
136. Triscott, J. *et al.* Disulfiram, a drug widely used to control alcoholism, suppresses the self-renewal of glioblastoma and over-rides resistance to temozolomide. *Oncotarget* **3**, 1112-1123 (2012).
137. Westhoff, M.A. *et al.* Inhibition of NF-kappaB signaling ablates the invasive phenotype of glioblastoma. *Mol Cancer Res* **11**, 1611-1623 (2013).
138. Hothi, P. *et al.* High-throughput chemical screens identify disulfiram as an inhibitor of human glioblastoma stem cells. *Oncotarget* **3**, 1124-1136 (2012).
139. Clarke, M.F. *et al.* Cancer stem cells--perspectives on current status and future directions: AACR Workshop on cancer stem cells. *Cancer Res* **66**, 9339-9344 (2006).
140. He, S., Nakada, D. & Morrison, S.J. Mechanisms of stem cell self-renewal. *Annu Rev Cell Dev Biol* **25**, 377-406 (2009).
141. Lathia, J.D. *et al.* Distribution of CD133 reveals glioma stem cells self-renew through symmetric and asymmetric cell divisions. *Cell Death Dis* **2**, e200 (2011).
142. Butowski, N. *et al.* A phase II study of concurrent temozolomide and cis-retinoic acid with radiation for adult patients with newly diagnosed supratentorial glioblastoma. *Int J Radiat Oncol Biol Phys* **61**, 1454-1459 (2005).
143. Piccirillo, S.G. *et al.* Bone morphogenetic proteins inhibit the tumorigenic potential of human brain tumour-initiating cells. *Nature* **444**, 761-765 (2006).
144. Tate, C.M. *et al.* A BMP7 variant inhibits the tumorigenic potential of glioblastoma stem-like cells. *Cell Death Differ* **19**, 1644-1654 (2012).
145. Lee, J. *et al.* Epigenetic-mediated dysfunction of the bone morphogenetic protein pathway inhibits differentiation of glioblastoma-initiating cells. *Cancer Cell* **13**, 69-80 (2008).
146. Yan, K. *et al.* Glioma cancer stem cells secrete Gremlin1 to promote their maintenance within the tumor hierarchy. *Genes Dev* **28**, 1085-1100 (2014).
147. Ignatova, T.N. *et al.* Human cortical glial tumors contain neural stem-like cells expressing astroglial and neuronal markers in vitro. *Glia* **39**, 193-206 (2002).
148. Singh, S.K. *et al.* Identification of a cancer stem cell in human brain tumors. *Cancer Res* **63**, 5821-5828 (2003).
149. Singh, S.K. *et al.* Identification of human brain tumour initiating cells. *Nature* **432**, 396-401 (2004).

150. Mannino, M. & Chalmers, A.J. Radioresistance of glioma stem cells: intrinsic characteristic or property of the 'microenvironment-stem cell unit'? *Mol Oncol* **5**, 374-386 (2011).
151. Bao, S. *et al.* Stem cell-like glioma cells promote tumor angiogenesis through vascular endothelial growth factor. *Cancer Res* **66**, 7843-7848 (2006).
152. Bao, S. *et al.* Glioma stem cells promote radioresistance by preferential activation of the DNA damage response. *Nature* **444**, 756-760 (2006).
153. Beier, D. *et al.* CD133(+) and CD133(-) glioblastoma-derived cancer stem cells show differential growth characteristics and molecular profiles. *Cancer Res* **67**, 4010-4015 (2007).
154. Wang, J. *et al.* CD133 negative glioma cells form tumors in nude rats and give rise to CD133 positive cells. *Int J Cancer* **122**, 761-768 (2008).
155. Ogden, A.T. *et al.* Identification of A2B5+CD133- tumor-initiating cells in adult human gliomas. *Neurosurgery* **62**, 505-514; discussion 514-505 (2008).
156. Chang, C.J. *et al.* Enhanced radiosensitivity and radiation-induced apoptosis in glioma CD133-positive cells by knockdown of SirT1 expression. *Biochem Biophys Res Commun* **380**, 236-242 (2009).
157. Son, M.J., Woolard, K., Nam, D.H., Lee, J. & Fine, H.A. SSEA-1 is an enrichment marker for tumor-initiating cells in human glioblastoma. *Cell Stem Cell* **4**, 440-452 (2009).
158. Liu, Q. *et al.* Molecular properties of CD133+ glioblastoma stem cells derived from treatment-refractory recurrent brain tumors. *J Neurooncol* **94**, 1-19 (2009).
159. Lathia, J.D. *et al.* Integrin alpha 6 regulates glioblastoma stem cells. *Cell Stem Cell* **6**, 421-432 (2010).
160. Hemmati, H.D. *et al.* Cancerous stem cells can arise from pediatric brain tumors. *Proc Natl Acad Sci U S A* **100**, 15178-15183 (2003).
161. Galli, R. *et al.* Isolation and characterization of tumorigenic, stem-like neural precursors from human glioblastoma. *Cancer Res* **64**, 7011-7021 (2004).
162. Yuan, X. *et al.* Isolation of cancer stem cells from adult glioblastoma multiforme. *Oncogene* **23**, 9392-9400 (2004).
163. Gunther, H.S. *et al.* Glioblastoma-derived stem cell-enriched cultures form distinct subgroups according to molecular and phenotypic criteria. *Oncogene* **27**, 2897-2909 (2008).
164. Fael Al-Mayhani, T.M. *et al.* An efficient method for derivation and propagation of glioblastoma cell lines that conserves the molecular profile of their original tumours. *J Neurosci Methods* **176**, 192-199 (2009).
165. Pollard, S.M. *et al.* Glioma stem cell lines expanded in adherent culture have tumor-specific phenotypes and are suitable for chemical and genetic screens. *Cell Stem Cell* **4**, 568-580 (2009).
166. Brescia, P., Richichi, C. & Pelicci, G. Current strategies for identification of glioma stem cells: adequate or unsatisfactory? *J Oncol* **2012**, 376894 (2012).
167. Barrantes-Freer, A. *et al.* CD133 Expression Is Not Synonymous to Immunoreactivity for AC133 and Fluctuates throughout the Cell Cycle in Glioma Stem-Like Cells. *PLoS One* **10**, e0130519 (2015).
168. Sun, Y. *et al.* CD133 (Prominin) negative human neural stem cells are clonogenic and tripotent. *PLoS One* **4**, e5498 (2009).
169. Jaksch, M., Munera, J., Bajpai, R., Terskikh, A. & Oshima, R.G. Cell cycle-dependent variation of a CD133 epitope in human embryonic stem cell, colon cancer, and melanoma cell lines. *Cancer Res* **68**, 7882-7886 (2008).
170. Mak, A.B. *et al.* CD133 protein N-glycosylation processing contributes to cell surface recognition of the primitive cell marker AC133 epitope. *J Biol Chem* **286**, 41046-41056 (2011).

171. Chaichana, K., Zamora-Berridi, G., Camara-Quintana, J. & Quinones-Hinojosa, A. Neurosphere assays: growth factors and hormone differences in tumor and nontumor studies. *Stem Cells* **24**, 2851-2857 (2006).
172. Valent, P. *et al.* Cancer stem cell definitions and terminology: the devil is in the details. *Nat Rev Cancer* **12**, 767-775 (2012).
173. Sampetrean, O. & Saya, H. Characteristics of glioma stem cells. *Brain Tumor Pathol* **30**, 209-214 (2013).
174. Pallini, R. *et al.* Expression of the stem cell marker CD133 in recurrent glioblastoma and its value for prognosis. *Cancer* **117**, 162-174 (2011).
175. Strojnik, T., Rosland, G.V., Sakariassen, P.O., Kavalar, R. & Lah, T. Neural stem cell markers, nestin and musashi proteins, in the progression of human glioma: correlation of nestin with prognosis of patient survival. *Surg Neurol* **68**, 133-143; discussion 143-134 (2007).
176. Mangiola, A. *et al.* Stem cell marker nestin and c-Jun NH2-terminal kinases in tumor and peritumor areas of glioblastoma multiforme: possible prognostic implications. *Clin Cancer Res* **13**, 6970-6977 (2007).
177. Zhang, M. *et al.* Nestin and CD133: valuable stem cell-specific markers for determining clinical outcome of glioma patients. *J Exp Clin Cancer Res* **27**, 85 (2008).
178. Pallini, R. *et al.* Cancer stem cell analysis and clinical outcome in patients with glioblastoma multiforme. *Clin Cancer Res* **14**, 8205-8212 (2008).
179. Zeppernick, F. *et al.* Stem cell marker CD133 affects clinical outcome in glioma patients. *Clin Cancer Res* **14**, 123-129 (2008).
180. Murat, A. *et al.* Stem cell-related "self-renewal" signature and high epidermal growth factor receptor expression associated with resistance to concomitant chemoradiotherapy in glioblastoma. *J Clin Oncol* **26**, 3015-3024 (2008).
181. Chinnaiyan, P. *et al.* The prognostic value of nestin expression in newly diagnosed glioblastoma: report from the Radiation Therapy Oncology Group. *Radiat Oncol* **3**, 32 (2008).
182. Laks, D.R. *et al.* Neurosphere formation is an independent predictor of clinical outcome in malignant glioma. *Stem Cells* **27**, 980-987 (2009).
183. Sihto, H. *et al.* Tumour microvessel endothelial cell KIT and stem cell factor expression in human solid tumours. *Histopathology* **55**, 544-553 (2009).
184. Colman, H. *et al.* A multigene predictor of outcome in glioblastoma. *Neuro Oncol* **12**, 49-57 (2010).
185. Rossi, M. *et al.* beta-catenin and Gli1 are prognostic markers in glioblastoma. *Cancer Biol Ther* **11**, 753-761 (2011).
186. Metellus, P. *et al.* Prognostic impact of CD133 mRNA expression in 48 glioblastoma patients treated with concomitant radiochemotherapy: a prospective patient cohort at a single institution. *Ann Surg Oncol* **18**, 2937-2945 (2011).
187. Kim, K.J. *et al.* The presence of stem cell marker-expressing cells is not prognostically significant in glioblastomas. *Neuropathology* **31**, 494-502 (2011).
188. He, J. *et al.* Expression of glioma stem cell marker CD133 and O6-methylguanine-DNA methyltransferase is associated with resistance to radiotherapy in gliomas. *Oncol Rep* **26**, 1305-1313 (2011).
189. Adam, S.A. *et al.* ALDH1A1 is a marker of astrocytic differentiation during brain development and correlates with better survival in glioblastoma patients. *Brain Pathol* **22**, 788-797 (2012).
190. Nakata, S. *et al.* LGR5 is a marker of poor prognosis in glioblastoma and is required for survival of brain cancer stem-like cells. *Brain Pathol* **23**, 60-72 (2013).
191. Sandberg, C.J. *et al.* Comparison of glioma stem cells to neural stem cells from the adult human brain identifies dysregulated Wnt- signaling and a fingerprint associated with clinical outcome. *Exp Cell Res* **319**, 2230-2243 (2013).

192. Shibahara, I. *et al.* The expression status of CD133 is associated with the pattern and timing of primary glioblastoma recurrence. *Neuro Oncol* **15**, 1151-1159 (2013).
193. Kase, M. *et al.* Impact of CD133 positive stem cell proportion on survival in patients with glioblastoma multiforme. *Radiol Oncol* **47**, 405-410 (2013).
194. Binder, Z.A. *et al.* Podocalyxin-like protein is expressed in glioblastoma multiforme stem-like cells and is associated with poor outcome. *PLoS One* **8**, e75945 (2013).
195. Shin, J.H., Lee, Y.S., Hong, Y.K. & Kang, C.S. Correlation between the prognostic value and the expression of the stem cell marker CD133 and isocitrate dehydrogenase1 in glioblastomas. *J Neurooncol* **115**, 333-341 (2013).
196. Dahlrot, R.H. *et al.* Prognostic value of Musashi-1 in gliomas. *J Neurooncol* **115**, 453-461 (2013).
197. Lathia, J.D. *et al.* High-throughput flow cytometry screening reveals a role for junctional adhesion molecule a as a cancer stem cell maintenance factor. *Cell Rep* **6**, 117-129 (2014).
198. Hale, J.S. *et al.* Cancer stem cell-specific scavenger receptor 36 drives glioblastoma progression. *Stem Cells* **32**, 1746-1758 (2014).
199. Lathia, J.D. *et al.* Direct in vivo evidence for tumor propagation by glioblastoma cancer stem cells. *PLoS One* **6**, e24807 (2011).
200. Chen, J. *et al.* A restricted cell population propagates glioblastoma growth after chemotherapy. *Nature* **488**, 522-526 (2012).
201. Gilbertson, R.J. & Graham, T.A. Cancer: Resolving the stem-cell debate. *Nature* **488**, 462-463 (2012).
202. McCarthy, N. Cancer stem cells: Tracing clones. *Nat Rev Cancer* **12**, 579 (2012).
203. Christensen, K., Schroder, H.D. & Kristensen, B.W. CD133 identifies perivascular niches in grade II-IV astrocytomas. *J Neurooncol* **90**, 157-170 (2008).
204. Li, Z. *et al.* Hypoxia-inducible factors regulate tumorigenic capacity of glioma stem cells. *Cancer Cell* **15**, 501-513 (2009).
205. Hovinga, K.E. *et al.* Inhibition of notch signaling in glioblastoma targets cancer stem cells via an endothelial cell intermediate. *Stem Cells* **28**, 1019-1029 (2010).
206. Charles, N. *et al.* Perivascular nitric oxide activates notch signaling and promotes stem-like character in PDGF-induced glioma cells. *Cell Stem Cell* **6**, 141-152 (2010).
207. Zhu, T.S. *et al.* Endothelial cells create a stem cell niche in glioblastoma by providing NOTCH ligands that nurture self-renewal of cancer stem-like cells. *Cancer Res* **71**, 6061-6072 (2011).
208. Galan-Moya, E.M. *et al.* Secreted factors from brain endothelial cells maintain glioblastoma stem-like cell expansion through the mTOR pathway. *EMBO Rep* **12**, 470-476 (2011).
209. Infanger, D.W. *et al.* Glioblastoma stem cells are regulated by interleukin-8 signaling in a tumoral perivascular niche. *Cancer Res* **73**, 7079-7089 (2013).
210. Lathia, J.D. *et al.* Laminin alpha 2 enables glioblastoma stem cell growth. *Ann Neurol* **72**, 766-778 (2012).
211. Nakada, M. *et al.* Integrin alpha3 is overexpressed in glioma stem-like cells and promotes invasion. *Br J Cancer* **108**, 2516-2524 (2013).
212. Seidel, S. *et al.* A hypoxic niche regulates glioblastoma stem cells through hypoxia inducible factor 2 alpha. *Brain* **133**, 983-995 (2010).
213. Heddleston, J.M., Li, Z., McLendon, R.E., Hjelmeland, A.B. & Rich, J.N. The hypoxic microenvironment maintains glioblastoma stem cells and promotes reprogramming towards a cancer stem cell phenotype. *Cell Cycle* **8**, 3274-3284 (2009).
214. Warburg, O. On respiratory impairment in cancer cells. *Science* **124**, 269-270 (1956).
215. Hsu, P.P. & Sabatini, D.M. Cancer cell metabolism: Warburg and beyond. *Cell* **134**, 703-707 (2008).

216. Pistollato, F. *et al.* Hypoxia and succinate antagonize 2-deoxyglucose effects on glioblastoma. *Biochem Pharmacol* **80**, 1517-1527 (2010).
217. Wei, J. *et al.* Hypoxia potentiates glioma-mediated immunosuppression. *PLoS One* **6**, e16195 (2011).
218. Badie, B. & Schartner, J.M. Flow cytometric characterization of tumor-associated macrophages in experimental gliomas. *Neurosurgery* **46**, 957-961; discussion 961-952 (2000).
219. Parney, I.F., Waldron, J.S. & Parsa, A.T. Flow cytometry and in vitro analysis of human glioma-associated macrophages. Laboratory investigation. *J Neurosurg* **110**, 572-582 (2009).
220. da Fonseca, A.C. & Badie, B. Microglia and macrophages in malignant gliomas: recent discoveries and implications for promising therapies. *Clin Dev Immunol* **2013**, 264124 (2013).
221. Yi, L. *et al.* Glioma-initiating cells: a predominant role in microglia/macrophages tropism to glioma. *J Neuroimmunol* **232**, 75-82 (2011).
222. Ye, X.Z. *et al.* Tumor-associated microglia/macrophages enhance the invasion of glioma stem-like cells via TGF-beta1 signaling pathway. *J Immunol* **189**, 444-453 (2012).
223. Zhang, J., Stevens, M.F. & Bradshaw, T.D. Temozolomide: mechanisms of action, repair and resistance. *Curr Mol Pharmacol* **5**, 102-114 (2012).
224. Hegi, M.E. *et al.* Correlation of O6-methylguanine methyltransferase (MGMT) promoter methylation with clinical outcomes in glioblastoma and clinical strategies to modulate MGMT activity. *J Clin Oncol* **26**, 4189-4199 (2008).
225. Blough, M.D. *et al.* Sensitivity to temozolomide in brain tumor initiating cells. *Neuro Oncol* **12**, 756-760 (2010).
226. Beier, D. *et al.* Temozolomide preferentially depletes cancer stem cells in glioblastoma. *Cancer Res* **68**, 5706-5715 (2008).
227. Liu, G. *et al.* Analysis of gene expression and chemoresistance of CD133+ cancer stem cells in glioblastoma. *Mol Cancer* **5**, 67 (2006).
228. Fouse, S.D., Nakamura, J.L., James, C.D., Chang, S. & Costello, J.F. Response of primary glioblastoma cells to therapy is patient specific and independent of cancer stem cell phenotype. *Neuro Oncol* **16**, 361-371 (2014).
229. Persano, L. *et al.* BMP2 sensitizes glioblastoma stem-like cells to Temozolomide by affecting HIF-1alpha stability and MGMT expression. *Cell Death Dis* **3**, e412 (2012).
230. Villalva, C. *et al.* O6-Methylguanine-Methyltransferase (MGMT) Promoter Methylation Status in Glioma Stem-Like Cells is Correlated to Temozolomide Sensitivity Under Differentiation-Promoting Conditions. *Int J Mol Sci* **13**, 6983-6994 (2012).
231. Batchelor, T.T. *et al.* Improved tumor oxygenation and survival in glioblastoma patients who show increased blood perfusion after cediranib and chemoradiation. *Proc Natl Acad Sci U S A* **110**, 19059-19064 (2013).
232. Pascal, J. *et al.* Mechanistic patient-specific predictive correlation of tumor drug response with microenvironment and perfusion measurements. *Proc Natl Acad Sci U S A* **110**, 14266-14271 (2013).
233. Pistollato, F. *et al.* Intratumoral hypoxic gradient drives stem cells distribution and MGMT expression in glioblastoma. *Stem Cells* **28**, 851-862 (2010).
234. Tamura, K. *et al.* Accumulation of CD133-positive glioma cells after high-dose irradiation by Gamma Knife surgery plus external beam radiation. *J Neurosurg* **113**, 310-318 (2010).
235. Cheng, L. *et al.* L1CAM regulates DNA damage checkpoint response of glioblastoma stem cells through NBS1. *EMBO J* **30**, 800-813 (2011).
236. McCord, A.M., Jamal, M., Williams, E.S., Camphausen, K. & Tofilon, P.J. CD133+ glioblastoma stem-like cells are radiosensitive with a defective DNA damage response compared with established cell lines. *Clin Cancer Res* **15**, 5145-5153 (2009).

237. Yang, Y.P. *et al.* Resveratrol suppresses tumorigenicity and enhances radiosensitivity in primary glioblastoma tumor initiating cells by inhibiting the STAT3 axis. *J Cell Physiol* **227**, 976-993 (2012).
238. Carruthers, R. *et al.* Abrogation of radioresistance in glioblastoma stem-like cells by inhibition of ATM kinase. *Mol Oncol* **9**, 192-203 (2015).
239. Vecchio, D. *et al.* Predictability, efficacy and safety of radiosensitization of glioblastoma-initiating cells by the ATM inhibitor KU-60019. *Int J Cancer* **135**, 479-491 (2014).
240. Lim, Y.C. *et al.* Increased sensitivity to ionizing radiation by targeting the homologous recombination pathway in glioma initiating cells. *Mol Oncol* **8**, 1603-1615 (2014).
241. Ropolo, M. *et al.* Comparative analysis of DNA repair in stem and nonstem glioma cell cultures. *Mol Cancer Res* **7**, 383-392 (2009).
242. Jamal, M., Rath, B.H., Tsang, P.S., Camphausen, K. & Tofilon, P.J. The brain microenvironment preferentially enhances the radioresistance of CD133(+) glioblastoma stem-like cells. *Neoplasia* **14**, 150-158 (2012).
243. Ding, Y. *et al.* Cancer-Specific requirement for BUB1B/BUBR1 in human brain tumor isolates and genetically transformed cells. *Cancer Discov* **3**, 198-211 (2013).
244. Joshi, K. *et al.* MELK-dependent FOXM1 phosphorylation is essential for proliferation of glioma stem cells. *Stem Cells* **31**, 1051-1063 (2013).
245. Lee, C. *et al.* Polo-like kinase 1 inhibition kills glioblastoma multiforme brain tumor cells in part through loss of SOX2 and delays tumor progression in mice. *Stem Cells* **30**, 1064-1075 (2012).
246. Beier, D. *et al.* Efficacy of clinically relevant temozolomide dosing schemes in glioblastoma cancer stem cell lines. *J Neurooncol* **109**, 45-52 (2012).
247. Lee, J. *et al.* Tumor stem cells derived from glioblastomas cultured in bFGF and EGF more closely mirror the phenotype and genotype of primary tumors than do serum-cultured cell lines. *Cancer Cell* **9**, 391-403 (2006).
248. De Witt Hamer, P.C. *et al.* The genomic profile of human malignant glioma is altered early in primary cell culture and preserved in spheroids. *Oncogene* **27**, 2091-2096 (2008).
249. Ernst, A. *et al.* Genomic and expression profiling of glioblastoma stem cell-like spheroid cultures identifies novel tumor-relevant genes associated with survival. *Clin Cancer Res* **15**, 6541-6550 (2009).
250. Collet, B. *et al.* Proteomic analysis underlines the usefulness of both primary adherent and stem-like cell lines for studying proteins involved in human glioblastoma. *J Proteomics* **110**, 7-19 (2014).
251. Mollet, M., Godoy-Silva, R., Berdugo, C. & Chalmers, J.J. Acute hydrodynamic forces and apoptosis: a complex question. *Biotechnol Bioeng* **98**, 772-788 (2007).
252. Bokhari, M., Carnachan, R.J., Cameron, N.R. & Przyborski, S.A. Culture of HepG2 liver cells on three dimensional polystyrene scaffolds enhances cell structure and function during toxicological challenge. *J Anat* **211**, 567-576 (2007).
253. http://reinnervate.com/publications-testimonials/publications/.
254. Bellail, A.C., Hunter, S.B., Brat, D.J., Tan, C. & Van Meir, E.G. Microregional extracellular matrix heterogeneity in brain modulates glioma cell invasion. *Int J Biochem Cell Biol* **36**, 1046-1069 (2004).
255. Niibori-Nambu, A. *et al.* Glioma initiating cells form a differentiation niche via the induction of extracellular matrices and integrin alphaV. *PLoS One* **8**, e59558 (2013).
256. Lobrich, M. *et al.* gammaH2AX foci analysis for monitoring DNA double-strand break repair: strengths, limitations and optimization. *Cell Cycle* **9**, 662-669 (2010).
257. Ivashkevich, A., Redon, C.E., Nakamura, A.J., Martin, R.F. & Martin, O.A. Use of the gamma-H2AX assay to monitor DNA damage and repair in translational cancer research. *Cancer Lett* **327**, 123-133 (2012).

258. Markova, E., Schultz, N. & Belyaev, I.Y. Kinetics and dose-response of residual 53BP1/gamma-H2AX foci: co-localization, relationship with DSB repair and clonogenic survival. *Int J Radiat Biol* **83**, 319-329 (2007).
259. West, C.M., Davidson, S.E., Roberts, S.A. & Hunter, R.D. The independence of intrinsic radiosensitivity as a prognostic factor for patient response to radiotherapy of carcinoma of the cervix. *Br J Cancer* **76**, 1184-1190 (1997).
260. Bjork-Eriksson, T. *et al.* The in vitro radiosensitivity of human head and neck cancers. *Br J Cancer* **77**, 2371-2375 (1998).
261. Yang, M.Y. *et al.* An innovative three-dimensional gelatin foam culture system for improved study of glioblastoma stem cell behavior. *J Biomed Mater Res B Appl Biomater* (2014).
262. Florczyk, S.J. *et al.* Porous chitosan-hyaluronic acid scaffolds as a mimic of glioblastoma microenvironment ECM. *Biomaterials* **34**, 10143-10150 (2013).
263. Komlodi-Pasztor, E., Sackett, D.L. & Fojo, A.T. Inhibitors targeting mitosis: tales of how great drugs against a promising target were brought down by a flawed rationale. *Clin Cancer Res* **18**, 51-63 (2012).
264. Gonczy, P. Mechanisms of asymmetric cell division: flies and worms pave the way. *Nat Rev Mol Cell Biol* **9**, 355-366 (2008).
265. Yamashita, Y.M., Mahowald, A.P., Perlin, J.R. & Fuller, M.T. Asymmetric inheritance of mother versus daughter centrosome in stem cell division. *Science* **315**, 518-521 (2007).
266. Nigg, E.A. & Raff, J.W. Centrioles, centrosomes, and cilia in health and disease. *Cell* **139**, 663-678 (2009).
267. Bettencourt-Dias, M., Hildebrandt, F., Pellman, D., Woods, G. & Godinho, S.A. Centrosomes and cilia in human disease. *Trends Genet* **27**, 307-315 (2011).
268. Basto, R. *et al.* Centrosome amplification can initiate tumorigenesis in flies. *Cell* **133**, 1032-1042 (2008).
269. Pihan, G.A. *et al.* Centrosome defects and genetic instability in malignant tumors. *Cancer Res* **58**, 3974-3985 (1998).
270. Klein, A. *et al.* Overexpression and amplification of STK15 in human gliomas. *Int J Oncol* **25**, 1789-1794 (2004).
271. Loh, J.K. *et al.* Differential expression of centrosomal proteins at different stages of human glioma. *BMC Cancer* **10**, 268 (2010).
272. Lehman, N.L. *et al.* Aurora A is differentially expressed in gliomas, is associated with patient survival in glioblastoma and is a potential chemotherapeutic target in gliomas. *Cell Cycle* **11**, 489-502 (2012).
273. Barton, V.N. *et al.* Aurora kinase A as a rational target for therapy in glioblastoma. *J Neurosurg Pediatr* **6**, 98-105 (2010).
274. Samaras, V. *et al.* Comparative immunohistochemical analysis of aurora-A and aurora-B expression in human glioblastomas. Associations with proliferative activity and clinicopathological features. *Pathol Res Pract* **205**, 765-773 (2009).
275. Xia, Z. *et al.* AURKA governs self-renewal capacity in glioma-initiating cells via stabilization/activation of beta-catenin/Wnt signaling. *Mol Cancer Res* **11**, 1101-1111 (2013).
276. Manfredi, M.G. *et al.* Characterization of Alisertib (MLN8237), an investigational small-molecule inhibitor of aurora A kinase using novel in vivo pharmacodynamic assays. *Clin Cancer Res* **17**, 7614-7624 (2011).
277. Hong, X. *et al.* The selective Aurora-A kinase inhibitor MLN8237 (alisertib) potently inhibits proliferation of glioblastoma neurosphere tumor stem-like cells and potentiates the effects of temozolomide and ionizing radiation. *Cancer Chemother Pharmacol* **73**, 983-990 (2014).
278. Hegarat, N. *et al.* Aurora A and Aurora B jointly coordinate chromosome segregation and anaphase microtubule dynamics. *J Cell Biol* **195**, 1103-1113 (2011).

279. El-Sheikh, A. *et al.* Inhibition of Aurora Kinase A enhances chemosensitivity of medulloblastoma cell lines. *Pediatr Blood Cancer* **55**, 35-41 (2010).
280. Moretti, L. *et al.* MLN8054, a small molecule inhibitor of aurora kinase a, sensitizes androgen-resistant prostate cancer to radiation. *Int J Radiat Oncol Biol Phys* **80**, 1189-1197 (2011).
281. Gorgun, G. *et al.* A novel Aurora-A kinase inhibitor MLN8237 induces cytotoxicity and cell-cycle arrest in multiple myeloma. *Blood* **115**, 5202-5213 (2010).
282. Tomita, M. & Mori, N. Aurora A selective inhibitor MLN8237 suppresses the growth and survival of HTLV-1-infected T-cells in vitro. *Cancer Sci* **101**, 1204-1211 (2010).
283. Krajcovic, M. & Overholtzer, M. Mechanisms of ploidy increase in human cancers: a new role for cell cannibalism. *Cancer Res* **72**, 1596-1601 (2012).
284. Overholtzer, M. *et al.* A nonapoptotic cell death process, entosis, that occurs by cell-in-cell invasion. *Cell* **131**, 966-979 (2007).
285. Van Brocklyn, J.R. *et al.* Aurora-A inhibition offers a novel therapy effective against intracranial glioblastoma. *Cancer Res* **74**, 5364-5370 (2014).
286. Nair, J.S., Ho, A.L. & Schwartz, G.K. The induction of polyploidy or apoptosis by the Aurora A kinase inhibitor MK8745 is p53-dependent. *Cell Cycle* **11**, 807-817 (2012).
287. Huck, J.J. *et al.* MLN8054, an inhibitor of Aurora A kinase, induces senescence in human tumor cells both in vitro and in vivo. *Mol Cancer Res* **8**, 373-384 (2010).
288. Wan, X.B. *et al.* Inhibition of Aurora-A results in increased cell death in 3-dimensional culture microenvironment, reduced migration and is associated with enhanced radiosensitivity in human nasopharyngeal carcinoma. *Cancer Biol Ther* **8**, 1500-1506 (2009).
289. Liu, Y. *et al.* Targeting aurora kinases limits tumour growth through DNA damage-mediated senescence and blockade of NF-kappaB impairs this drug-induced senescence. *EMBO Mol Med* **5**, 149-166 (2013).
290. Wagner, M. *et al.* Replicative senescence of human endothelial cells in vitro involves G1 arrest, polyploidization and senescence-associated apoptosis. *Exp Gerontol* **36**, 1327-1347 (2001).
291. La Porta, C.A., Zapperi, S. & Sethna, J.P. Senescent cells in growing tumors: population dynamics and cancer stem cells. *PLoS Comput Biol* **8**, e1002316 (2012).
292. Wang, Q. *et al.* Polyploidy road to therapy-induced cellular senescence and escape. *Int J Cancer* **132**, 1505-1515 (2013).
293. Rodier, F. & Campisi, J. Four faces of cellular senescence. *J Cell Biol* **192**, 547-556 (2011).
294. Coppe, J.P. *et al.* Senescence-associated secretory phenotypes reveal cell-nonautonomous functions of oncogenic RAS and the p53 tumor suppressor. *PLoS Biol* **6**, 2853-2868 (2008).
295. Wang, H. *et al.* Targeting interleukin 6 signaling suppresses glioma stem cell survival and tumor growth. *Stem Cells* **27**, 2393-2404 (2009).
296. Inoko, A. *et al.* Trichoplein and Aurora A block aberrant primary cilia assembly in proliferating cells. *J Cell Biol* **197**, 391-405 (2012).
297. Pugacheva, E.N., Jablonski, S.A., Hartman, T.R., Henske, E.P. & Golemis, E.A. HEF1-dependent Aurora A activation induces disassembly of the primary cilium. *Cell* **129**, 1351-1363 (2007).
298. Kobayashi, T. & Dynlacht, B.D. Regulating the transition from centriole to basal body. *J Cell Biol* **193**, 435-444 (2011).
299. Han, Y.G. & Alvarez-Buylla, A. Role of primary cilia in brain development and cancer. *Curr Opin Neurobiol* **20**, 58-67 (2010).
300. Clement, V., Sanchez, P., de Tribolet, N., Radovanovic, I. & Ruiz i Altaba, A. HEDGEHOG-GLI1 signaling regulates human glioma growth, cancer stem cell self-renewal, and tumorigenicity. *Curr Biol* **17**, 165-172 (2007).

301. Cenciarelli, C. *et al.* PDGF receptor alpha inhibition induces apoptosis in glioblastoma cancer stem cells refractory to anti-Notch and anti-EGFR treatment. *Mol Cancer* **13**, 247 (2014).
302. Fan, X. *et al.* NOTCH pathway blockade depletes CD133-positive glioblastoma cells and inhibits growth of tumor neurospheres and xenografts. *Stem Cells* **28**, 5-16 (2010).
303. Moser, J.J., Fritzler, M.J. & Rattner, J.B. Primary ciliogenesis defects are associated with human astrocytoma/glioblastoma cells. *BMC Cancer* **9**, 448 (2009).
304. Sarkisian, M.R. *et al.* Detection of primary cilia in human glioblastoma. *J Neurooncol* **117**, 15-24 (2014).
305. Moser, J.J., Fritzler, M.J. & Rattner, J.B. Ultrastructural characterization of primary cilia in pathologically characterized human glioblastoma multiforme (GBM) tumors. *BMC Clin Pathol* **14**, 40 (2014).
306. Danovi, D. *et al.* A high-content small molecule screen identifies sensitivity of glioblastoma stem cells to inhibition of polo-like kinase 1. *PLoS One* **8**, e77053 (2013).
307. Pezuk, J.A. *et al.* Polo-like kinase 1 inhibition causes decreased proliferation by cell cycle arrest, leading to cell death in glioblastoma. *Cancer Gene Ther* **20**, 499-506 (2013).
308. Song, B., Liu, X.S., Davis, K. & Liu, X. Plk1 phosphorylation of Orc2 promotes DNA replication under conditions of stress. *Mol Cell Biol* **31**, 4844-4856 (2011).
309. Wu, Z.Q. & Liu, X. Role for Plk1 phosphorylation of Hbo1 in regulation of replication licensing. *Proc Natl Acad Sci U S A* **105**, 1919-1924 (2008).
310. Giraldez, S. *et al.* SCF(FBXW7alpha) modulates the intra-S-phase DNA-damage checkpoint by regulating Polo like kinase-1 stability. *Oncotarget* **5**, 4370-4383 (2014).
311. Yata, K. *et al.* Plk1 and CK2 act in concert to regulate Rad51 during DNA double strand break repair. *Mol Cell* **45**, 371-383 (2012).
312. Lim, Y.C. *et al.* A role for homologous recombination and abnormal cell-cycle progression in radioresistance of glioma-initiating cells. *Mol Cancer Ther* **11**, 1863-1872 (2012).
313. Yim, H. & Erikson, R.L. Polo-like kinase 1 depletion induces DNA damage in early S prior to caspase activation. *Mol Cell Biol* **29**, 2609-2621 (2009).
314. Li, Y., Wei, Q., Zhang, Y., Ling, K. & Hu, J. The small GTPases ARL-13 and ARL-3 coordinate intraflagellar transport and ciliogenesis. *J Cell Biol* **189**, 1039-1051 (2010).
315. Nikonova, A.S. *et al.* Nedd9 restrains renal cystogenesis in Pkd1-/- mice. *Proc Natl Acad Sci U S A* **111**, 12859-12864 (2014).
316. Seeger-Nukpezah, T. & Golemis, E.A. The extracellular matrix and ciliary signaling. *Curr Opin Cell Biol* **24**, 652-661 (2012).
317. Lee, K.H. *et al.* Identification of a novel Wnt5a-CK1varepsilon-Dvl2-Plk1-mediated primary cilia disassembly pathway. *EMBO J* **31**, 3104-3117 (2012).

Appendix

MOLECULAR ONCOLOGY 5 (2011) 374–386

available at www.sciencedirect.com

www.elsevier.com/locate/molonc

Review

Radioresistance of glioma stem cells: Intrinsic characteristic or property of the 'microenvironment-stem cell unit'?

Mariella Mannino[a], *Anthony J. Chalmers*[b,*]

[a]*Genome Damage and Stability Centre, University of Sussex, Brighton BN1 9RQ, UK*
[b]*Beatson Institute for Cancer Research, University of Glasgow, Glasgow G61 1BD, UK*

ARTICLE INFO

Article history:
Received 22 December 2010
Received in revised form
10 May 2011
Accepted 11 May 2011
Available online 20 May 2011

Keywords:
Glioblastoma
Radioresistance
Microenvironment
Glioma stem cell
Radiation

ABSTRACT

There is increasing evidence that glioblastoma possess 'stem-like' cells, low concentrations of which can initiate a tumour. It has been proposed that these cells are radioresistant, and that this property contributes to the poor treatment outcomes of these tumours. In this paper we propose that radioresistance is not simply an intrinsic characteristic of glioma stem cells but a result of interactions between these cells and microenvironmental factors, i.e. the 'microenvironment – stem cell unit'. The critical role of the microenvironment, along with glioma stem cells, is supported directly or indirectly by the following observations: glioma stem cells have been shown to reside preferentially in specific niches, the characteristics of which are known to influence cellular responses to radiation; radiation modifies environmental factors; and, contrarily to the consistency of clinical data, *in vitro* experiments have reported a wide variety in the radiation response of these cells.

The paper, therefore, focuses on the interaction between tumour stem cells and the microenvironment, analyzing how its various elements (endothelial cells, extracellular matrix, cytokines, nitric oxide, oxygen levels) are affected by radiation and how these might influence the response of tumour stem cells to radiation.

Finally, we summarize the ongoing debate on the optimal culture conditions for glioma stem cells and the difficulties in designing assays that reliably characterize their radiation response.

1. Introduction

There is increasing evidence that human glioblastoma possess 'stem-like' cells, small numbers of which are capable of initiating a tumour that closely resembles the original cancer. It has been proposed that these tumour initiating cells are resistant to radiation therapy, and that this property contributes to the poor treatment outcomes associated with these tumours. After analyzing the conflicting data published on this subject over the past seven years, this article proposes that radioresistance is not simply an intrinsic characteristic of glioma stem cells but a result of the interaction between these cells and microenvironmental factors, i.e. a property of the 'microenvironment-stem cell unit'. The latter term is used to

* *Corresponding author*. Tel.: +44 141 301 7097; fax: +44 141 301 7095.
E-mail address: anthony.chalmers@glasgow.ac.uk (A.J. Chalmers).
1574-7891/$ – see front matter © 2011 Federation of European Biochemical Societies. Published by Elsevier B.V. All rights reserved.
doi:10.1016/j.molonc.2011.05.001

define a functional entity which includes both tumour stem cells and microenvironmental factors. The critical role of interactions between the microenvironment and glioma stem cells is supported directly or indirectly by the following observations: (1) glioma stem cells have been shown to reside preferentially in specific niches, the characteristics of which are known to influence cellular responses to radiation; (2) radiation modifies environmental factors; and (3) contrarily to the relative consistency of clinical data, *in vitro* experiments have reported a wide variation in the radiation responses of glioma stem cells.

The paper, therefore, focuses on the interaction between tumour stem cells and the microenvironment, analyzing how its various elements (endothelial cells, extracellular matrix, cytokines, nitric oxide, oxygen levels) are affected by radiation and how these factors might influence the response of tumour stem cells to radiation.

Finally, we will summarize the ongoing debate on how best to culture glioma stem cells to facilitate their study *in vitro*, and consider the difficulties encountered when designing assays to characterize their radiation responses.

2. Glioma stem cells: how strong is the evidence for their intrinsic radioresistance?

2.1. 'Stem-like' cells in glioblastoma

The first experimental evidence for the existence of "stem-like" cells in glial brain tumours was reported in 2002, when these malignancies were shown to contain cells that were capable of clone-formation under culture conditions used in the study of 'normal' neural stem cells, and could also be induced to undergo differentiation along astrocytic and neural lineages (Ignatova et al., 2002). Two years later, a study using an intracranial xenograft model provided evidence for the ability of a subpopulation of cells isolated from glioblastoma specimens to induce tumours *in vivo* at a very high frequency. Injection of as few as 100 selected cells into the brains of NOD-SCID (non-obese diabetic, severe combined immunodeficient) mice was sufficient for the formation of human brain tumours, which phenotypically resembled the patient's original specimen and could be serially transplanted. In contrast, injection of up to 10^5 negatively-selected cells did not generate tumours (Singh et al., 2004). Thereafter, several studies have analysed the behaviour of primary glioblastoma cell lines sorted by expression of candidate stem cell markers (CD133, A2B5, SEEA-1) or by growth pattern (sphere or adherent) in serum free medium (SFM) supplemented with growth factors. These cells were characterised in terms of self-renewal (tested with the neurosphere formation assay, NFA), differentiation potential and *in vivo* tumorigenicity (tested in intracranial xenograft models). On one hand, the reported data strongly support the existence of a subpopulation of highly tumorigenic cells, as indicated by the tumour induction rates observed for putative stem cells in individual studies (see Table 1). On the other hand, the inconsistencies between the various studies highlight the limitations of present cell sorting methods and the need for standardisation of assays that test for 'stemness' (Singh et al., 2004; Hemmati et al., 2003; Galli et al., 2004; Yuan et al., 2004; Bao et al., 2006a,; Beier et al., 2007; Wang et al., 2008; Gunther et al., 2008; Ogden et al., 2008; Son et al., 2009; Liu et al., 2009; Kondo et al., 2004; Chang et al., 2009; Clement et al., 2010). A detailed analysis of the validity of individual markers or techniques is beyond the scope of this paper but an excellent overview of the topic is provided in a recent review (Campos and Herold-Mende, 2011).

2.2. Radiation responses of glioma stem cells

The accumulating evidence that only a small subpopulation of cells is capable of giving rise to a tumour has led to the theory that the almost inevitable recurrence of glioblastoma is due to persistence of these cells despite multimodality treatment. Several clinical studies have investigated the prognostic value of putative stem cell markers and related cellular features in tumour specimens. Although these studies have generally involved relatively small numbers of patients and have tended to focus on only one or two markers, the results have consistently supported the implication of glioma stem cells in treatment resistance. In a retrospective study of 95 glioma specimens of different grades (47 glioblastomas), multivariate analysis including histological grade, patient age and extent of resection showed significant associations of CD133 expression ($>1\%$ *vs* $\leq 1\%$ positive cells) and organization of these cells in clusters (cluster *vs* single cells) with shorter overall survival (Zeppernick et al., 2008). Similarly, a prospective multivariate analysis of specimens from 44 patients with glioblastoma indicated that CD133 expression ($>2\%$ *vs* $\leq 2\%$ positive cells) and *in vitro* neurosphere formation ability (present *vs* absent) were prognostic factors for a higher risk of death. This association was independent of symptom duration, extent of surgical resection, patient age, MGMT status and p53 status (Pallini et al., 2008). Consistent with these results are two additional retrospective analyses of glioma specimens. One reported significantly lower survival in patients with gliomas co-expressing CD133 and nestin (Zhang et al., 2008), the other showed a correlation between decreasing overall survival and increasing levels of nestin expression in tumour cells (Strojnik et al., 2007).

The greatest limitation of these data is the retrospective design of three out of the four studies. Also, although the results of the latter two studies were generated by multivariate analysis, their value is lessened because adjustments were made only for tumour grade in the former study and for patient age and sex in the latter, without incorporating the other established prognostic factors. Despite these weaknesses, the consistency of the association between prognosis and expression of the putative stem cell marker CD133 in all four studies is striking.

Evidence for a role of glioma stem cells in determining treatment resistance also comes from a recent publication that analysed expression of CD133 in glioma specimens from ten patients that had undergone surgical resection before and after high-dose irradiation delivered by stereotactic radiosurgery (Gamma Knife) followed by external beam radiation (Tamura et al., 2010). The percentage of CD133+ cells was significantly higher in the post-treatment tumour material than in the original specimens. Although these data do not

Table 1 – Studies characterizing glioma cells in terms of self-renewal (tested with the neurosphere formation assay) and *in vivo* tumorigenicity (tested in xenograft models).

Study	Number of glioma cell lines	Cell sorting method	Neurosphere formation assay			*In vivo* tumorigenicity assay	
			Plating method	Analysis	Results	Method	Results
Hemmati et al., 2003	10 (2 glioblastoma)	Culture condition (SFM)	Serial dilution of cells from dissociated neurospheres (1000 cells/ml)	Presence of neurospheres (within 2–4 wks)	"In all cases neurospheres were visible"	IC injection of 5×10^4 cells (glioblastoma) into neonatal rats (# NS)	Observed migration, differentiation and proliferation of cells (after 4 wks)
Kondo et al., 2004	1 rat glioma cell line (C6)	Ability to extrude actively Hoechst 33342	FACS sorting (1 cell/well)	% of cells forming neurospheres	SP: 70% Non-SP: 0	Intraperitoneal injection of 10^5 cells (6 mice per cell type)	Presence of tumour: SP: 100% Non-SP: ~30%
Galli et al., 2004	6 glioblastoma (5 primary and 1 secondary glioblastoma)	Culture condition (SFM)	"Cells derived from the dissociation of clonal single neurospheres were seeded in 48-well plates"	Number of neurospheres per dissociated clone after 8–10 days	Primary glioblastoma cell lines: 28–85 Secondary glioblastoma cell line: 26 U87 cell line: 90	Injection of: • 2×10^5 cells into the striatum (IC) of Scid/bg mice (# NS) • 3×10^6 cells into the flank (SC) of Scid/bg mice (# NS)	Take efficiency: • 100% IC model (7 wks) • 50% SC model (6 wks)
Singh et al., 2004	4 glioblastoma	Magnetic sorting for CD133 expression	Serial dilution (range: 200 to 1 cell/well)	% of wells without neurospheres after 7 days	CD133+ cells: • >90% with < 10 cells/well • 0 with ~60 cells/well CD133− cells: 100%	IC injection of: • 100 (4 mice) or 1000 (5 mice) CD133+ cells • 1×10^5 (12 mice) CD133− cells	Presence of tumour: • CD133+ cells: 100% (6–13 wks) • CD133− cells: 0 (12–13 wks)
Yuan et al., 2004	6 glioblastoma	Culture condition (SFM)	Serial dilution (1–2 cells/well)	Number of positive wells after 14 days	Sphere culture cells: 3–5% Monolayer culture cells: 0	IC injection of: • 5000 (6 mice) or 5×10^4 (6 mice) sphere culture cells • 5×10^4 (6 mice) or 2.5×10^5 (6 mice) monolayer culture cells	Presence of tumour (after 6 wks): • sphere culture cells: 100% • monolayer culture cells: 0
Bao et al., 2006a,b	3 glioblastoma (+3 xenografts)	Magnetic or FACS sorting for CD133 expression	NS	% of cells forming neurospheres	CD133+ cells: 76–83% CD133- cells: 0 Total cells: 2.4–3.4%	IC injection of various numbers of cells	Minimum number of cells for tumor initiation (after 8 wks): • 500–1000 for CD133+ cells • No detected tumour with 2×10^6 CD133− cells • $2–4 \times 10^4$ unsorted cells Presence of tumour:

Beier et al., 2007	22 glioblastoma (15 primary and 7 secondary glioblastoma)	Magnetic sorting for CD133 expression	Serial dilution (1 cell/well)	% of neurospheres per plated cells (after 42 days)	CD133+ cells: 2–5% CD133− cells[a]: 0 CD133− cells[b]: 0.5–2%	IC injection of 10^5 or 10^6 cells in T-lymphocyte-deficient NMRI$^{(nu/nu)}$ mice (6 mice per cell population)	• CD133+ cells: 100% • CD133− cells[a]: 0 • CD133− cells[b]: 100% (within 50 days)
Wang et al., 2008	11 glioblastoma	Culture condition (SFM) or FACS sorting for CD133 expression	–	–	–	IC injection into nude immunodeficient rats of: • 10 spheroids • CD133- cells (# NS)	Take rate: • Spheroids: NS (tumour present) • CD133− cells: 19/28 rats
Gunther et al., 2008	9 glioblastoma	Culture condition (SFM)	Serial dilution (1 cell/well)	% cells forming neurospheres after 14 days	Sphere or semi-adherent growing cells: 16.9–53.8% Adherent growing cells: 0	IC injection of 1.5×10^5 or 1000 cells into NMRI$^{(nu/nu)}$ mice	Presence of tumour: • Sphere or semi-adherent growing cells: ○16/18 for 1.5×10^5 cells ○37/46 for 1000 cells • Adherent growing cells: ○1/6 for 1.5×10^5 cells ○0/6 for 1000 cells
Ogden et al., 2008	25 (16 glioblastoma)	FACS sorting for A2B5 ± CD133 expression	–	–	–	IC injection of: • 4000 to 1×10^5 A2B5+ CD133+ cells (4 mice) • 1×10^4 to 2.2×10^5 A2B5+ CD133− cells (14 mice) • 1×10^5 to 1.2×10^5 A2B5− CD133− cells (10 mice)	Presence of tumour: • A2B5+ CD133+ cells 100% • A2B5+ CD133− cells 92% • A2B5− CD133− cells 10%
Chang et al., 2009	7 glioblastoma	Magnetic sorting for CD133 expression	NS	Number of neurospheres	CD133+ cells: ~250 CD133− cells: ~20	IC injection of 5000 or 1×10^4 cells (28 SCID mice per group)	Presence of tumour: • CD133+ cells: 100% • CD133− cells: 0.
Son et al., 2009	12 glioblastoma (+12 established cell lines)	Magnetically or FACS sorting for SEEA-1 ± CD133 expression	Limiting dilution (5–50 cells/well)	% of wells without neurospheres after 2–3 weeks	SSEA-1+ cells[c]: • 20–80% with <5 cells/well • 10–60% with ~10 cells/well • 0 with >10 cells/well SSEA-1- cells[c]: • 70–95% with <5 cells/well • 50–85% with ~10 cells/well • 40% with 25–50 cells/well	IC injection of 1000, 10^4 or 3×10^5 cells in NOD/SCID mice	Presence of tumour: • SSEA-1+ cells: 21/21 • SSEA-1- cells: ○0/13 for 1000 and 10^4 cells ○2/9 for 3×10^5 cells • unsorted cells: ○2/5 for 1000 cells ○5/6 for 10^4 cells ○6/6 for 3×10^5 cells

(continued on next page)

Table 1 (*continued*)

Study	Number of glioma cell lines	Cell sorting method	Neurosphere formation assay			*In vivo* tumorigenicity assay	
			Plating method	Analysis	Results	Method	Results
Liu et al., 2009	2 glioblastoma	FACS sorting for CD133 expression	–	–	–	IC injection of: • 5–10 × 10^3 CD133+ cells (12 SCID mice) • 5 × 10^5 CD133− cells (20 SCID mice)	Presence of tumour: • CD133+ cells: 11/12 • CD133− cells: 0/20
Clement et al., 2010	5 glioblastoma (4 primary, 1 secondary glioblastoma)	Intrinsic autofluorescence and morphology	NS (1 cell/well)	Number of spheres per plated wells after two or five *in vitro* passages	Second sphere[d]: • $FL1^+$: 3/192 to 18/192 (1.6–9.4%) • $FL1^0$: 1/192 to 6/192 (0.5–3.1%) Fifth sphere: • $FL1^+$: 1/192 to 12/315 (0.5–3.8%) • $FL1^0$: 0 to 1/192 (0–0.5%)	IC injection of: • 10^3 to 10^5 $FL1^+$ cells (24 nude mice) • 10^4 to 10^5 $FL1^0$ cells (23 nude mice)	Presence of tumour: • $FL1^+$: 100% • $FL1^0$: 13%

FACS, fluorescence activated cell sorting. IC, intracranial. NS: not specified. SC, subcutaneous. SFM, serum-free medium. SP, side population. SSEA-1, stage-specific embryonic antigen 1. wks, weeks. #, number.

a These cells were derived from CD133 + sphere cultures.

b These cells were from adherently growing CD133- sphere cultures.

c These percentages are derived from graphs included in the publication.

d $FL1^+$ cells were defined as those displaying autofluorescence emission around 520 nm (in the FL1 channel) upon laser excitation at 488 nm.

establish a causative relationship, they are consistent with the hypothesis that glioma stem cells are capable of surviving high doses of radiation.

Because radiation therapy is the primary treatment modality for patients with glioblastoma, the proposed radioresistance of glioma stem cells is a corollary of the theory that holds tumour stem cells responsible for the very low cure rates observed. However, laboratory studies comparing radiation responses of glioma stem cells with those of differentiated or 'non-stem' glioma cells have until now produced conflicting data. To our knowledge there are only two studies (Bao et al., 2006a; McCord et al., 2009) that have performed a comparative analysis of clonogenic survival assays in the two cellular subpopulations. Clonogenic survival is traditionally recognized as the 'gold standard' endpoint for testing intrinsic radiosensitivity in a clinically relevant manner. In the first published paper (Bao et al., 2006a,), colony formation assays were performed using CD133+ and CD133− cells derived either from a biopsy specimen or from glioma xenografts. Cells were either irradiated (5 Gray (Gy)) or left untreated. Colony formation rates were not quantified, but representative images of surviving colonies were presented to support a relative radioresistance of CD133+ cells. As a measure of post-irradiation clonogenicity, the study also reported tumour formation rates of CD133+ and CD133− cells derived from tumour specimens or glioma xenografts. The authors demonstrated that *in vitro* irradiation with 2 Gy did not significantly affect tumourigenicity of CD133+ cells, while a higher dose of 5 Gy resulted in a 5–10 fold increase in the minimum number of cells required for tumour initiation compared to unirradiated cells (evaluated after 8 weeks). As CD133− cells did not generate tumours, comparison of radiation response curves, and therefore radiosensitivity, of CD133+ and CD133− cells by this method was not feasible. In the more recent study (McCord et al., 2009) reporting clonogenic analysis of primary cell lines obtained from glioblastoma specimens, the surviving clonogenic fraction of CD133+ cells was significantly higher than that of the CD133− population in one of the two cell lines tested. Interestingly, when clonogenic assays were performed on a panel of CD133+ primary cell lines and three established glioma cell lines, substantial variability was observed in their survival curves, with all six CD133+ cell lines being more radiosensitive than the established cell lines. These findings highlight the heterogeneity of *in vitro* radiosensitivity that exists amongst primary cell lines, despite prospective selection for putative stem cell markers, and illustrate the inherent problems associated with comparing radiosensitivity parameters across cell lines of different origins.

To further investigate the intrinsic radiosensitivity of glioma stem cells relative to non-stem cells, the authors of the landmark Bao study (Bao et al., 2006a) analysed additional radiation responses of the two subpopulations *in vitro* and *in vivo*. An *in vitro* cell mixing and repopulation experiment, in which CD133+ and CD133− cells from a tumour specimen were differentially labelled, mixed in definite ratios and left untreated or irradiated (5 Gy), showed that, after 8 days of culture, the percentage of CD133+ cells increased from 5% to ~80% in the irradiated population and to ~25% in the untreated one. In the corresponding *in vivo* study, in which CD133+ and CD133− cells were labelled, mixed and implanted into the brains of athymic nude mice that were subsequently irradiated (5 Gy) or left untreated, the ratio of CD133+:CD133− cells increased from 0.2 to more than 4 in the irradiated mice and to ~2 in the control group. These data are consistent with enhanced survival of glioma stem cells after radiation but also indicate that, under these conditions, a component of the survival advantage of CD133+ cells over CD133− cells is independent of radiation.

To identify possible mechanisms underlying an intrinsic radioresistance of CD133+ cells, proteins involved in apoptosis and early DNA damage checkpoint responses were analysed in cells derived from tumour specimens and xenografts (Bao et al., 2006a). Western blot for cleaved caspase-3 (before and 24 h after 2 or 5 Gy) and immunofluorescence staining for Annexin-V-FITC (before and 20 h after 3 Gy) both showed lower rates of apoptosis in CD133+ cells compared to CD133− cells. Furthermore, analysis of phosphorylated ATM, Rad17, Chk1 and Chk2 (before and 1 h after 3 Gy) demonstrated higher activation of these cell cycle checkpoint proteins in CD133+ cells than in CD133− cells. Alkaline comet assays and quantification of cells staining positively for phosphorylated histone 2AX performed before and after irradiation (3 Gy) were consistent with a potential mechanism involving faster resolution of both single and double strand breaks in CD133+ cells than in CD133− cells.

A more recent study also compared CD133+ and CD133− populations from primary glioma cell lines with regard to early DNA damage checkpoint responses and DNA repair capacity. While increased activation of Chk 1 and Chk2 was confirmed in both irradiated (1 h post 3 Gy) and unirradiated CD133+ cells, no significant difference in DNA damage induction or repair was observed between the two cellular subpopulations, as measured by comet assay and phosphorylated histone 2AX positivity (Ropolo et al., 2009).

Two further studies have analysed *in vitro* viability of glioma stem and non-stem cells (defined by expression of CD133) after irradiation and demonstrated a higher percentage of surviving cells in the former population (Chang et al., 2009; Lomonaco et al., 2009). These observations are of limited value, however, as viability at early time points is not a measure of clonogenicity and may not correlate with a clinically relevant response to radiation.

Finally, four studies have shown that radiosensitivity of glioma stem cells can be increased by inhibiting specific proteins (SirT1 (Chang et al., 2009), Notch (Wang et al., 2010b), Chk1/Chk2 (Bao et al., 2006a), autophagy-related proteins Beclin and ATG5 (Lomonaco et al., 2009)), two of which (Chang et al., 2009; Wang et al., 2010b) have been associated with stemness or tumorigenicity. Although these findings suggest that there are intrinsic cellular features of glioma stem cells that can be targeted to modify radiation responses, the specificity of these mechanisms to this cellular subpopulation needs to be investigated further.

More detailed discussion of relevant aspects of the DNA damage response in carcinogenesis and cancer treatment, including glioblastoma, is provided in three articles that are also published in this edition of Molecular Oncology. These reviews cover chromosomal instability (Krämer et al.) and therapeutic approaches targeting defects in DNA repair (Evers and Helleday) and replication stress (Toledo et al.).

In summary, although a number of findings indicate that there are differences between the radiation responses of glioma stem cells and their differentiated counterparts, it is difficult to evaluate their significance in terms of radiosensitivity for the following reasons: 1) the importance of apoptosis in determining clonogenicity after radiation has not been established and probably varies between cell types (Steel, 2001); 2) the apoptosis data refer to single time points whereas the time-course of apoptosis after radiation varies considerably between cell lines; 3) DNA damage responses need to be interpreted in the light of clonogenic survival data as their validity in terms of predicting for radiosensitivity is still under debate (Lobrich et al., 2010). Also, the inconsistency of the DNA repair data suggest that some mechanisms may be cell line specific. Considering the extensive heterogeneity of glioblastoma, the conclusion that intrinsic radioresistance of CD133+ cells is responsible for treatment resistance should probably be applied with caution at this stage.

The variability and scarcity of existing data regarding radiosensitivity of glioma stem cells and non-stem cells can, on one hand, be viewed as a reflection of the inherent difficulties in designing clonogenic survival assays for cellular populations that present distinct growth patterns and require different culture conditions. On the other hand, since existing experimental models testing radiation responses do not take into account factors present in the tumour microenvironment, they can also be considered as an indication of the need for more representative assays for determining cellular radiosensitivity. This consideration together with the observation that glioma stem cells reside preferentially in specific niches (Zeppernick et al., 2008; Calabrese et al., 2007; Li et al., 2009; Christensen et al., 2008) leads to our proposal that radioresistance is more likely to be a property of the 'microenvironment-stem cell unit', a functional entity within which glioma stem cells are able to maintain or enhance intrinsic cellular features that contribute to radiation resistance.

Indirect evidence for the relevance of the 'microenvironment-stem cell unit' in determining radiosensitivity comes from a recent study comparing induction and repair of radiation-induced DNA damage in CD133+ cells grown *in vitro* and as intracranial xenografts. Levels of phosphorylated histone 2AX foci decreased more rapidly in the *in vivo* setting, suggesting a more efficient DNA repair ability of these cells in the presence of microenvironmental factors (Jamal et al., 2010). Also consistent with the proposed theory are the results of a study that used a 3-dimensional organotypic 'explant' system of surgical glioblastoma specimens to test the effect of radiation and/or Notch inhibition on glioma stem cells (Hovinga et al., 2010). Radiation alone (10 Gy) had a dramatically lower impact on self-renewal capacity of tumour cells in the explants than in neurosphere cultures. The effect of Notch inhibition also varied between the two models, causing a further decrease in neurosphere formation rate only when tumour cells were treated in the explant setting. The importance of the 'microenvironment-stem cell unit' is also indicated by a study that used mouse models of medulloblastoma to investigate mechanisms responsible for regional differences in radiation responses (Hambardzumyan et al., 2008). After demonstrating that Akt signalling exerts different effects in nestin-expressing cells residing in the perivascular niche compared with cells forming the tumour bulk, the authors conclude that in order to detect cell-type-specific responses it is critical to use models that recapitulate the various cell types within an appropriate environment.

Despite the limitations of these studies (for example, the uncertain validity of radiation-induced foci and apoptosis levels as predictive indices of cellular radiosensitivity and the possibility that neurosphere culture conditions select for specific subpopulations), they all highlight the importance of interrogating the 'microenvironment-stem cell unit' when investigating the biology of therapeutic radiation responses.

3. 'Microenvironment-stem cell unit': is this the true radioresistant entity in glioblastomas?

In order to understand how the tumour microenvironment influences radiation responses of glioma stem cells, it is essential to characterize the niche in which they are thought to reside. Studies investigating whether glioma stem cells exist in specific niches have analyzed the distribution in tumour specimens of cells positive for CD133 or other markers associated with a stem cell phenotype. The first published series (Calabrese et al., 2007) evaluated the distance of nestin+ and nestin− cells from the nearest CD34+ endothelial cell in frozen sections from ten glioblastoma specimens. Nestin+ cells, three quarters of which co-expressed CD133, were significantly closer to capillaries than were nestin− cells. Also, 3D reconstruction of serial images from four glioma specimens, using multiphoton laser-scanning microscopy, showed that nestin+ tumour cells were often in direct contact with tumour capillaries. A close relationship between CD133+ cells and vascular structures was also found in a study (Christensen et al., 2008) analyzing paraffin sections from seventy-two glioblastoma specimens: 54% of tumours exhibited CD133+ niches, which were defined as "a limited entity of cells corresponding to a minimum of 5–10 cells identifiable at low magnification". Many of these entities were perivascular or associated with necrotic regions. The latter association was indirectly confirmed by immunofluorescence studies on frozen tumour samples, which demonstrated co-expression of CD133 and hypoxia inducible factor 2α (HIF2α). Finally, a study that was mentioned in the previous section reported that CD133+ cells were found in clusters in 41 of 47 glioblastoma specimens (Zeppernick et al., 2008).

The interaction of glioma stem cells with blood vessels, and more specifically with endothelial cells and vascular endothelial growth factor (VEGF), is one of the main areas of interest in this field (Knizetova et al., 2008). New insights were recently offered by two studies, which demonstrated that CD133+ cells are capable of undergoing differentiation along the endothelial lineage and that a subpopulation of endothelial cells within glioblastomas are directly derived from tumour cells (Ricci-Vitiani et al., 2010; Wang et al., 2010a). Regardless of the function and/or fate of glioma stem cells in the perivascular area, their presence in this niche prompts the question of whether there are specific elements in such regions that contribute to radiation resistance. Apart from the obvious interaction with endothelial cells, glioma stem cells residing in perivascular regions are in contact with extracellular matrix

(ECM) components that are preferentially expressed within and around blood vessels. The vascular basement membrane is composed of collagen, fibronectin, laminin, heparan sulphate, entactin and vitronectin, while the tumour ECM surrounding blood vessels is rich in tenascin C, secreted protein acidic and rich in cystein (SPARC) and thrombospondin. Interestingly, all components but vitronectin are scarcely present in the remaining tumour ECM. A clear and schematic representation of the heterogeneous distribution of ECM proteins in glioblastoma is provided in a review discussing their role in modulating glioma cell invasion (Bellail et al., 2004). An additional component of the perivascular niche is nitric oxide (NO), synthesized by endothelial nitric oxide synthase (eNOS) which is known to be highly expressed in vessels within glioblastomas (Iwata et al., 1999).

Expanding on these observations, the following paragraphs will analyze evidence relating to the theory that elements of the perivascular niche (endothelial cells, ECM proteins, NO and relevant cytokines) and hypoxic areas modulate cellular responses to radiation. This discussion will include data derived from studies of glioblastoma along with information from other cancers. A schematic representation of these interactions is given in Figure 1.

3.1. *Endothelial cells*

Several studies analyzing the association between endothelial cells and glioma stem cells support the hypothesis that interactions between these two cellular populations are reciprocal. On the one hand, glioma stem cells have been shown to exert a pro-angiogenic effect that is mediated by stimulation of endothelial cells through production of VEGF (Bao et al., 2006a; Folkins et al., 2009; Salmaggi et al., 2006). A recent study investigating the interaction between glioma and endothelial cells in both a 3D co-culture system and an *in vivo* model demonstrated that glioblastoma cells became incorporated into the tumour vasculature (Shaifer et al., 2010). Interestingly, vascular networks formed in co-culture remained stable for weeks, unlike those arising from endothelial cells alone, which regressed soon after formation. On the other hand, endothelial cells have been proven to play a role in glioma stem cell maintenance. The evidence for this comes from the previously mentioned study by Hovinga (Hovinga et al., 2010) and colleagues that used a 3-dimensional organotypic 'explant' system of surgical glioblastoma specimens. Selective elimination of endothelial cells from the model casued a >50% reduction in the neurosphere formation capacity of single cells obtained by dissociation of the explants. Data from other central nervous system tumour types are consistent with these results. A study comparing the ability of endothelial and other cells (CD133− tumour cells, fibroblasts or astrocytes) to maintain the viability of CD133+/nestin+ tumour cells derived from medulloblastoma and ependymoma demonstrated that a larger percentage of tumour spheres survived if they were co-cultured with endothelial cells for 5 days. After 2 weeks, these spheres were up to five times larger than those grown

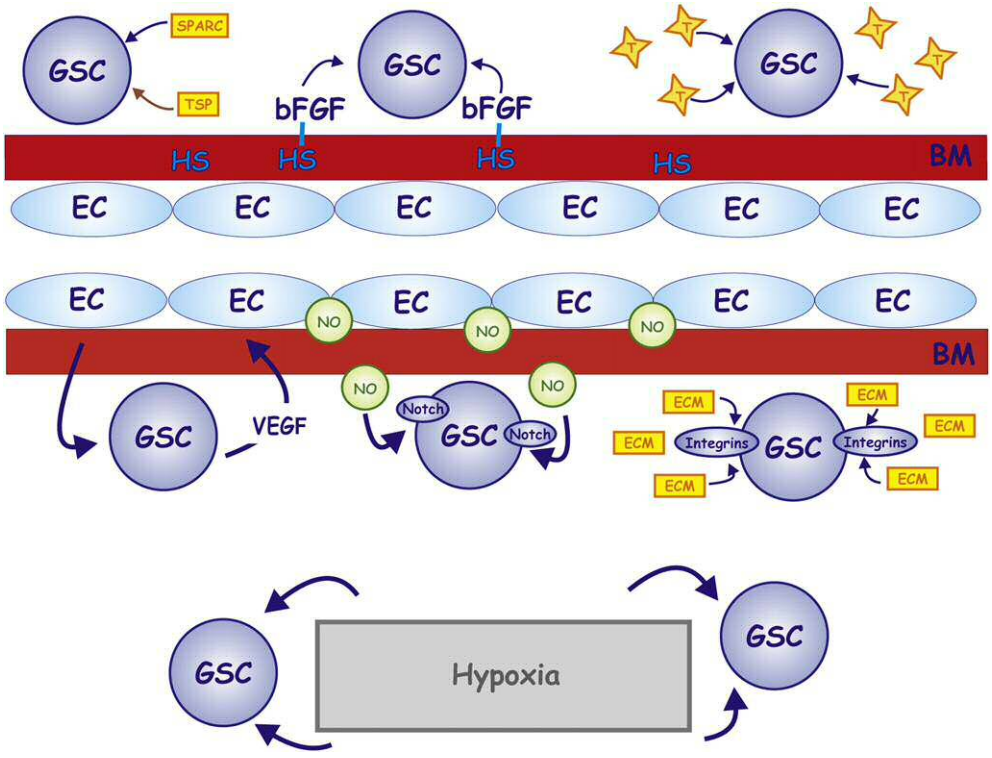

Figure 1 – Schematic representation of interactions (proven or suggested by data on other cell types) between glioma stem cells and components of the microenvironment. Blue arrows indicate a positive regulation, the brown arrow a negative one, in terms of proliferation and/or radioresistance. bFGF, basic fibroblast growth factor. BM, basement membrane. EC, endothelial cell. ECM, extracellular matrix. GSC, glioma stem cell. HS, heparin sulphate. NO, nitric oxide. SPARC, secreted protein acidic and rich in cystein. T, tenascin C. TSP, thrombospondin.

with control cells (Calabrese et al., 2007). Co-culture with endothelial cells was also more likely to maintain self-renewal of CD133+/nestin+ brain tumour cells, demonstrated by the ability of these cells to generate spheres after two weeks of co-culture with the various cell types (Calabrese et al., 2007).

Evidence for reciprocal regulation of radiation responses between endothelial and tumour cells is accumulating. The above mentioned study investigating the interaction between glioma and endothelial cells in a 3-dimensional co-culture system demonstrated a survival advantage after irradiation (6 Gy) for mosaic vasculature compared to blood vessels formed by endothelial cells alone. Similarly, a study comparing radiation-induced apoptosis in endothelial cells either in mono-culture or in co-culture with glioma cells showed that after 3 Gy there were significantly higher levels of apoptosis in the mono-cultured cells (Brown et al., 2004). Consistent with these findings are the results of a study analyzing the effect of endothelial susceptibility to apoptosis on radiation-induced apoptosis in fibrosarcoma and melanoma *in vivo* models. After a large single dose of 15 Gy, tumour cell apoptosis increased in tumours with an apoptosis-sensitive endothelium (grown in *asmase*$^{+/+}$ or Bax$^{+/+}$ mice), but not in those with apoptosis resistant endothelial cells derived from *asmase*$^{-/-}$ or Bax$^{-/-}$ mice (Garcia-Barros et al., 2003).

Although suggestive of a radioprotective effect of glioma cells on endothelial cells, the correlation between radiosensitivity of gliomas and the endpoints used in these *in vitro* studies (regression of blood vessels and apoptosis of endothelial cells) is not known. Furthermore, the use of large single doses of radiation in these experiments limits extrapolation of the findings to the clinical setting. Further evidence including clonogenic survival data is required to confirm the existence of an enhancing feedback loop between endothelial and glioma stem cells that might modulate radiation responses and thence survival. In the light of the two recent studies reporting the existence within glioblastomas of a subpopulation of endothelial cells derived directly from glioma stem cells (Ricci-Vitiani et al., 2010; Wang et al., 2010a), the underlying mechanisms of such a relationship are likely to be complex and multifaceted and their elucidation will require detailed analysis in robust model systems.

3.2. *ECM components*

The spatial association of glioma stem cells with specific ECM components expressed within and around blood vessels is particularly intriguing given that evidence is accumulating across cancer types for the importance of cell-ECM interactions in influencing the response of tumour cells to radiation. Review of the relevant literature identifies three main mechanisms that might influence glioma stem cell survival and radiosensitivity. ECM components have been proposed to 1) serve as a deposit for proteins which modulate radiation responses, 2) operate as a substratum for the activation of pro-survival integrin-mediated signalling cascades in tumour cells following radiation, and 3) create a more favourable niche for proliferation of cells that survive irradiation.

The first property is suggested by the ability of heparan sulphate, a component of the basement membrane, to bind basic Fibroblast Growth Factor (bFGF) (Folkman et al., 1988), which has been shown to stimulate growth (Loilome et al., 2009) and inhibit radiation-induced apoptosis (Bao et al., 2006a) of glioma stem cells *in vitro*. More evidence for a modulatory role of this growth factor in radiation responses comes from studies on other cell types. bFGF has been found to increase radioresistance of endothelial cells both in clonogenic survival assays and an *in vivo* model where it protected against development of lethal radiation pneumonitis (Fuks et al., 1994). A protective effect was also demonstrated in HeLa cells, using clonogenic survival assays (CohenJonathan et al., 1997). Studies analysing the effect of bFGF on clonogenicity of glioma stem cells post-irradiation are needed to test more rigorously the potential radioprotective role of bFGF in these cells. Heparan sulphate acts as a binding site for many additional proteins (Lindahl and Li, 2009); these should also be interrogated with regards to their effect on glioma stem cell survival.

The second mechanism finds its basis in the literature correlating increased radioresistance of glioma cell cultures with expression and activation of integrins β1 (Cordes et al., 2006), αvβ3 and αvβ5 (Monferran et al., 2008). The role of integrins in modulating radiation responses has been demonstrated in various cancer types (Sandfort et al., 2007). A study comparing clonogenic survival of glioma cells irradiated 24 h after plating on fibronectin, Matrigel, bovine serum albumin (BSA) or polystyrene showed that the first two substrata significantly increased survival, but only in one of the four cell lines tested (Cordes et al., 2003). However, substratum-dependent survival has also been demonstrated in a lung carcinoma cell line and a lung fibroblast stem cell line (Cordes and van Beuningeni, 2003). Characterization of the effects of glioma stem cell attachment to the various ECM components present in the tumour is essential in order to clarify whether any of these factors play a role in determining the fate of glioma stem cells after irradiation.

The third mechanism is supported by three observations related to tenascin C. This molecule stimulates tumour cell proliferation (Midwood and Orend, 2009); its expression in glioma specimens correlates inversely with the degree of cell differentiation (Higuchi et al., 1993); and a study analysing radiation-induced connective tissue changes in women who had undergone radiation therapy for breast cancer demonstrated an increased expression of tenascin C in irradiated areas(Riekki et al., 2001). Taken together, these data suggest that a post-irradiation increase in tenascin C, which is already overexpressed in the perivascular niche where glioma stem cells preferentially reside, might have a protective role. The likely mechanism involves tenascin C stimulating proliferation of surviving cells thus counterbalancing radiation cell killing. The role of this molecule in treatment resistance is also suggested by an immunohistochemical study, in which a significant reduction in survival was observed in glioblastoma patients whose tumours strongly expressed tenascin C (87 patients), compared to those with reduced expression (12 patients) (Leins et al., 2003). Preliminary but encouraging evidence supporting tenascin C as a therapeutic target in glioblastoma has been reported in radioimmunotherapy studies (Reardon et al., 2002; Reardon et al., 2008) and a clinical study in which tenascin C was downregulated by RNA interference (Rolle et al., 2010).

Modulation of glioma stem cell radiation responses by other ECM components such as SPARC and thrombospondin

is less well supported, although data from other cancer sites suggest they might exert a radiosensitizing effect (Tai et al., 2005; Maxhimer et al., 2009). These factors merit further investigation in the context of glioblastoma, especially with regards to SPARC, expression of which has been reported to correlate inversely with survival in astrocytic tumours (Rich et al., 2005; Capper et al., 2010).

Taken together these data highlight the importance of studies analysing the complex interactions between various ECM components and tumour cells, in order to clarify how the vicinity of glioma stem cells to specific elements influences their survival post-irradiation. As mentioned previously, however, the heterogeneity observed amongst glioblastomas indicates that the individual mechanisms outlined above are likely to exert different levels of influence on treatment responses in different patients.

3.3. *Nitric oxide*

A role for NO in promoting radioresistance of glioma stem cells is suggested by two recent publications. One, using a genetically engineered mouse model of platelet derived growth factor (PDGF)-induced glioma, demonstrated that endothelial nitric oxide synthase (eNOS) co-localized with endothelial cells that were surrounded by tumour cells which co-expressed nestin, Notch and the NO receptor soluble guanylyl cyclase. Furthermore, NO activated Notch signaling and promoted stemness in primary cultured mouse glioma cells (Charles et al., 2010). The other study showed that inhibition of the Notch pathway with γ-secretase inhibitors (GSI) increased radiosensitivity of glioma stem cells (defined as CD133+ cells). Expression of the constitutively active intracellular domains of Notch1 or Notch2, which function downstream of γ-secretase, rendered glioma stem cells more resistant to radiation than control cells, regardless of treatment with GSI (Wang et al., 2010b). Given this evidence, it is plausible to speculate that, in the perivascular niche, NO synthesized by highly expressed eNOS activates the Notch pathway in adjacent glioma stem cells and increases their radioresistance.

3.4. *Hypoxia*

The role of hypoxia in radioresistance of tumours was first observed more than a century ago and is now well established (Overgaard, 2007). In general, the reduced cellular radiosensitivity observed in a hypoxic environment is thought to be due to the different fate of free radicals produced in the cell by radiation. The reaction of these radicals with oxygen changes and stabilizes their chemical composition so that DNA damage is more likely to occur. This is often described as chemical 'fixation'. In the absence of oxygen, free radicals are more likely to react with H^+ ions, returning to their original form and reducing the level of DNA damage (Horsman and Overgaard, 2002). Tumour cells that survive hypoxic stress generate a range of pro-survival responses that are induced by transcription of various genes in response to the hypoxia inducible factor (HIF) family of transcription factors. Evidence for a differential response of glioma stem cells to hypoxia was found in a study that reported higher levels of HIF2α and various HIF-regulated genes in these cells compared to non-stem cells (Li et al., 2009). Furthermore, knockdown of HIFs in glioma stem cells resulted in reduced stemness *in vitro* and *in vivo*. A recent study conducted in orthotopic glioblastoma xenografts showed that increasing intratumoral oxygenation through normalization of the vasculature by treatment with interferon-beta or bevacizumab enhanced radiosensitivity of these tumours (McGee et al., 2010).

The hypoxia-stem cell interaction may therefore be viewed as a typical example of the role of the 'microenvironment-stem cell unit', in the sense that hypoxic conditions maintain and enhance intrinsic cellular features of glioma stem cells rendering them more resistant to treatment.

4. Future directions for pre-clinical studies

Ever since the isolation of glioma stem cells, using cell culture techniques developed for the study of neural stem cells, characterization of the radiation responses of this cellular subpopulation has proved to be very challenging. If, on one hand, culturing glioma stem cells as non-adherent spheres in serum-free medium supplemented with growth factors has the advantage of exploiting a recognized feature of these cells and has been shown to preserve tumour genotype and phenotype (Lee et al., 2006; Hamer et al., 2008), on the other it introduces several uncertainties.

Fundamentally, comparisons of radiation sensitivity in stem and non-stem cell populations are limited by the requirement for different culture conditions to maintain their respective phenotypic features. Furthermore, conventional clonogenic survival assays require some degree of cellular adhesion to the substratrum on which the cells are cultured. Three main strategies have been adopted to try to circumvent these issues: 1) exposure of both populations to serum-free medium without growth factors for 24 h post-irradiation followed by transfer to serum-containing medium (Bao et al., 2006a); 2) plating of both populations on poly-L-lysine coated wells in serum-free medium (McCord et al., 2009); 3) maintaining each cellular population in the appropriate medium, and quantifying clonogenicity of differentiated cells by colony formation and stem cell clonogenicity by neurosphere formation (Wang et al., 2010b). The first two approaches have the advantage of exposing the two populations to the same conditions during the experiment and of comparing the same type of colony, but it is very likely that the pro-attachment methods (growth factor withdrawal, serum-containing medium or poly-L-lysine coating) induce some degree of differentiation among the stem cells. Also, it is not possible to control for a potential differential effect of these changes on cellular responses to radiation damage. The third approach has the advantage of studying the radiosensitivity of the two cellular populations without compromising their culture conditions, but it requires comparison of two distinct types of colonies, formation rates of which might be influenced in different and unpredictable ways by the different methodologies.

In order to address some of these problems, and other issues related to characterization of cells growing as non-adherent sphere cultures, alternative techniques for culturing glioma stem cells are being investigated. To date two studies have been published proposing protocols for adherent cultures of glioma stem cells in serum-free medium, using

ECM (Al-Mayhani et al., 2009) or laminin (Pollard et al., 2009b) as attachment factors. Both studies claim that 2D (adherent monolayer) cultures are superior to 3D (non-adherent sphere) cultures because they provide uniformity of exposure to growth factors, oxygen and nutrients, which would result in a more homogeneous cellular population. Further evidence is needed in order to evaluate whether these techniques offer a more efficient method for culturing glioma stem cells and whether they can be implemented in clonogenic survival assays to improve the reliability of radiosensitivity studies (Reynolds and Vescovi, 2009; Pollard et al., 2009a).

As well as exploring such innovations, it is essential that researchers in this field consider, and control for wherever possible, biases related to stem cell culture conditions. These include potential effects of growth factors on cell cycle progression, DNA repair pathways and apoptosis. There is increasing evidence that epidermal growth factor (EGF) and fibroblast growth factor (FGF) interact with processes involved in the radiation response. Studies analyzing the effect of these growth factors in maintenance of glioma and neural stem cells suggest that EGF and FGF activate pathways that modulate proteins involved in cell cycle progression and apoptosis (Loilome et al., 2009; Sato et al., 2010). An impact of EGF and FGF on apoptosis (measured as percentage of Annexin-V positive cells) has been clearly shown in both CD133+ and CD133− glioblastoma cells exposed to serum-free medium, with or without irradiation (Bao et al., 2006a). Evidence for a possible link between DNA repair pathways and EGF and FGF is derived from investigations on other cancer cell lines. A study in bronchial carcinoma cells analyzed the relationship between EGFR localization and DNA repair after irradiation and showed that nuclear translocation of the receptor resulted in increased activity of DNA-dependent protein kinase (DNA-PK, a key component of the non-homologous end-joining pathway) (Dittmann et al., 2005). Although the study found a correlation of nuclear import of EGFR with irradiation but not with exposure to EGF, an effect of long-term stimulation with EGF cannot be excluded as the cells were treated with the growth factor at a single concentration and were analyzed after a maximum of 20 min. The possible relevance of these factors is supported by data from a model of wound repair, which showed that long-term exposure to EGF was required in order to observe its stimulatory effect (Buckley et al., 1985). Evidence for a link between FGF and DNA-PK activity comes from a study on HeLa cells, in which up-regulation of the DNA repair enzyme correlated with the radioprotective effect of the growth factor (Ader et al., 2002). Given the cell specific nature of many of the biological effects of growth factors, the relevance of these interactions to glioma stem cells should be investigated before any conclusions are drawn.

It is hoped that the design of future radiation response studies will take into consideration these factors, both to increase the accuracy of comparative studies and to enhance our understanding of the role of these proteins in regulating radiosensitivity.

If radioresistance is a property of the 'microenvironment-stem cell unit', as this paper proposes, it is essential that experimental models are developed that allow investigation of radiation responses of glioma stem cells in conditions that resemble as closely as possible their tumoral niche. Exciting advances in 3D tissue culture systems have been accomplished and to date have been applied predominantly to embryonic or adult stem cells used in studies of developmental biology and regenerative medicine. Available models vary greatly in composition and complexity, ranging from simple 3D scaffolds consisting of synthetic self-assembling peptide hydrogels (Thonhoff et al., 2008), biodegradable polymers (Levenberg et al., 2003) or polystyrene (Bokhari et al., 2007), to *in vitro* systems that couple 3D matrices with microfluidic devices that enable multi-parameter manipulation(Vickerman et al., 2008). Studies comparing the phenotypes of a variety of cell types grown in 2D and 3D models have clearly demonstrated the functional superiority of the latter. These systems have the capacity to allow exploration of the interactions that occur between the various elements discussed in this paper. A promising approach in this context is also the three-dimensional explant system used in the above mentioned Hovinga study (Hovinga et al., 2010). It is hoped that these models will prove to be efficient tools to accurately identify targets for the modulation of radiation response and enable the development of new therapeutic agents to improve outcomes for patients with glioblastoma.

5. Conclusions

While data demonstrating the existence of glioma stem cells continue to accumulate, the published evidence supporting the hypothesis that radioresistance of glioblastoma is caused simply by an intrinsic property of glioma stem cells is less convincing. Data from gliomas and other cancer models strongly support a complementary theory that radiation responses are determined by the 'microenvironment-stem cell unit'. Based on published data, a variety of mechanisms that might contribute to the radioresistance of this functional unit have been proposed. In order to identify therapeutically relevant targets, it is critical that future studies are conducted in model systems that enable these mechanisms to be investigated further.

REFERENCES

Ader, I., et al., 2002. The radioprotective effect of the 24 kDa FGF-2 isoform in HeLa cells is related to an increased expression and activity of the DNA dependent protein kinase (DNA-PK) catalytic subunit. Oncogene 21 (42), 6471–6479.

Al-Mayhani, T.M.F., et al., 2009. An efficient method for derivation and propagation of glioblastoma cell lines that conserves the molecular profile of their original tumours. Journal of Neuroscience Methods 176 (2), 192–199.

Bao, S.D., et al., 2006a. Glioma stem cells promote radioresistance by preferential activation of the DNA damage response. Nature 444 (7120), 756–760.

Bao, S.D., et al., 2006b. Stem cell-like glioma cells promote tumour angiogenesis through vascular endothelial growth factor. Cancer Research 66 (16), 7843–7848.

Beier, D., et al., 2007. CD133(+) and CD133(−) glioblastoma-derived cancer stem cells show differential growth characteristics and molecular profiles. Cancer Research 67 (9), 4010–4015.

Bellail, A.C., et al., 2004. Microregional extracellular matrix heterogeneity in brain modulates glioma cell invasion. International Journal of Biochemistry & Cell Biology 36 (6), 1046–1069.

Bokhari, M., et al., 2007. Novel cell culture device enabling three-dimensional cell growth and improved cell function. Biochemical and Biophysical Research Communications 354 (4), 1095–1100.
Brown, C.K., et al., 2004. Glioblastoma cells block radiation-induced programmed cell death of endothelial cells. Febs Letters 565 (1–3), 167–170.
Buckley, A., et al., 1985. Sustained release of epidermal growth factor accelerates wound repair. Proceedings of the National Academy of Sciences of the United States of America 82 (21), 7340–7344.
Calabrese, C., et al., 2007. A perivascular niche for brain tumor stem cells. Cancer Cell 11 (1), 69–82.
Campos, B., Herold-Mende, C.C., 2011. Insight into the complex regulation of CD133 in glioma. International Journal of Cancer 128 (3), 501–510. Feb 1.
Capper, D., et al., 2010. Secreted protein, acidic and rich in cysteine (SPARC) expression in astrocytic tumour cells negatively correlates with proliferation, while vascular SPARC expression is associated with patient survival. Neuropathology and Applied Neurobiology 36 (3), 183–197.
Chang, C.J., et al., 2009. Enhanced radiosensitivity and radiation-induced apoptosis in glioma CD133-positive cells by knockdown of SirT1 expression. Biochemical and Biophysical Research Communications 380 (2), 236–242.
Charles, N., et al., 2010. Perivascular nitric oxide activates Notch signaling and promotes stem-like character in PDGF-Induced glioma cells. Cell Stem Cell 6 (2), 141–152.
Christensen, K., Schroder, H.D., Kristensen, B.W., 2008. CD133 identifies perivascular niches in grade II-IV astrocytomas. Journal of Neuro-Oncology 90 (2), 157–170.
Clement, V., et al., 2010. Marker-independent identification of glioma-initiating cells. Nature Methods 7 (3), 224–228.
CohenJonathan, E., et al., 1997. Radioresistance induced by the high molecular forms of the basic fibroblast growth factor is associated with an increased G(2) delay and a hyperphosphorylation of p34(CDC2) in HeLa cells. Cancer Research 57 (7), 1364–1370.
Cordes, N., et al., 2003. Irradiation differentially affects substratum-dependent survival, adhesion, and invasion of glioblastoma cell lines. British Journal of Cancer 89 (11), 2122–2132.
Cordes, N., et al., 2006. Beta 1-integrin-mediated signaling essentially contributes to cell survival after radiation-induced genotoxic injury. Oncogene 25 (9), 1378–1390.
Cordes, N., van Beuningeni, D., 2003. Cell adhesion to the extracellular matrix protein fibronectin modulates radiation-dependent G2 phase arrest involving integrin-linked kinase (ILK) and glycogen synthase kinase-3 beta (GSK-3 beta) in vitro. British Journal of Cancer 88 (9), 1470–1479.
Dittmann, K., et al., 2005. Radiation-induced epidermal growth factor receptor nuclear import is linked to activation of DNA-dependent protein kinase. Journal of Biological Chemistry 280 (35), 31182–31189.
Folkins, C., et al., 2009. Glioma tumor stem-like cells promote tumor angiogenesis and Vasculogenesis via vascular endothelial growth factor and Stromal-derived factor 1. Cancer Research 69 (20), 8216 (vol 69, pg 7243, 2009).
Folkman, J., et al., 1988. A heparin-binding angiogenic protein – basic fibroblast growth factor – is stored within basement membrane. American Journal of Pathology 130 (2), 393–400.
Fuks, Z., et al., 1994. Basic fibroblast growth factor protects endothelial cells against radiation-induced programmed cell death in vitro and in vivo. Cancer Research 54 (10), 2582–2590.
Galli, R., et al., 2004. Isolation and characterization of tumorigenic, stem-like neural precursors from human glioblastoma. Cancer Research 64 (19), 7011–7021.
Garcia-Barros, M., et al., 2003. Tumor response to radiotherapy regulated by endothelial cell apoptosis. Science 300 (5622), 1155–1159.
Gunther, H.S., et al., 2008. Glioblastoma-derived stem cell-enriched cultures form distinct subgroups according to molecular and phenotypic criteria. Oncogene 27 (20), 2897–2909.
Hambardzumyan, D., et al., 2008. PI3K pathway regulates survival of cancer stem cells residing in the perivascular niche following radiation in medulloblastoma in vivo. Genes & Development 22 (4), 436–448.
Hamer, P., et al., 2008. The genomic profile of human malignant glioma is altered early in primary cell culture and preserved in spheroids. Oncogene 27 (14), 2091–2096.
Hemmati, H.D., et al., 2003. Cancerous stem cells can arise from pediatric brain tumors. Proceedings of the National Academy of Sciences of the United States of America 100 (25), 15178–15183.
Higuchi, M., et al., 1993. Expression of Tenascin in human gliomas – its relation to histological malignancy, tumor dedifferentiation and angiogenesis. Acta Neuropathologica 85 (5), 481–487.
Horsman, M.R., Overgaard, J., 2002. The oxygen effect and tumour microenvironment. In: Steel, G. (Ed.), Basic Clinical Radiobiology. Arnold, pp. 158–168.
Hovinga, K.E., et al., 2010. Inhibition of Notch signaling in glioblastoma targets cancer stem cells via an endothelial cell Intermediate. Stem Cells 28 (6), 1019–1029.
Ignatova, T.N., et al., 2002. Human cortical glial tumors contain neural stem-like cells expressing astroglial and neuronal markers in vitro. Glia 39 (3), 193–206.
Iwata, S., et al., 1999. Endothelial nitric oxide synthase expression in tumor vasculature is correlated with malignancy in human supratentorial astrocytic tumors. Neurosurgery 45 (1), 24–28.
Jamal, M., et al., 2010. Microenvironmental regulation of glioblastoma radioresponse. Clinical Cancer Research 16 (24), 6049–6059.
Knizetova, P., Darling, J.L., Bartek, J., 2008. Vascular endothelial growth factor in astroglioma stem cell biology and response to therapy. Journal of Cellular and Molecular Medicine 12 (1), 111–125.
Kondo, T., Setoguchi, T., Taga, T., 2004. Persistence of a small subpopulation of cancer stem-like cells in the C6 glioma cell line. Proceedings of the National Academy of Sciences of the United States of America 101 (3), 781–786.
Lee, J., et al., 2006. Tumor stem cells derived from glioblastomas cultured in bFGF and EGF more closely mirror the phenotype and genotype of primary tumors than do serum-cultured cell lines. Cancer Cell 9 (5), 391–403.
Leins, A., et al., 2003. Expression of tenascin-C in various human brain tumors and its relevance for survival in patients with astrocytoma. Cancer 98 (11), 2430–2439.
Levenberg, S., et al., 2003. Differentiation of human embryonic stem cells on three-dimensional polymer scaffolds. Proceedings of the National Academy of Sciences of the United States of America 100 (22), 12741–12746.
Li, Z., et al., 2009. Hypoxia-Inducible factors Regulate tumorigenic Capacity of glioma stem cells. Cancer Cell 15 (6), 501–513.
Lindahl, U., Li, J.P., 2009. Interactions between heparan sulfate and proteins – design and functional implications. In: International Review of Cell and Molecular Biology, Vol. 276. Elsevier Academic Press Inc, San Diego, pp. 105–159.
Liu, Q.H., et al., 2009. Molecular properties of CD133+ glioblastoma stem cells derived from treatment-refractory recurrent brain tumors. Journal of Neuro-Oncology 94 (1), 1–19.
Lobrich, M., et al., 2010. Gamma H2AX foci analysis for monitoring DNA double-strand break repair Strengths, limitations and optimization. Cell Cycle 9 (4), 662–669.

Loilome, W., et al., 2009. Glioblastoma cell growth is suppressed by disruption of fibroblast growth factor pathway signaling. Journal of Neuro-Oncology 94 (3), 359–366.
Lomonaco, S.L., et al., 2009. The induction of autophagy by gamma-radiation contributes to the radioresistance of glioma stem cells. International Journal of Cancer 125 (3), 717–722.
Maxhimer, J.B., et al., 2009. Radioprotection in normal tissue and Delayed tumor growth by Blockade of CD47 signaling. Science Translational Medicine 1 (3).
McCord, A.M., et al., 2009. CD133(+) glioblastoma stem-like cells are radiosensitive with a defective DNA damage response compared with established cell lines. Clinical Cancer Research 15 (16), 5145–5153.
McGee, M.C., et al., 2010. Improved intratumoral oxygenation through vascular normalization increases glioma sensitivity to ionizing radiation. International Journal of Radiation Oncology • Biology • Physics 76 (5), 1537–1545.
Midwood, K.S., Orend, G., 2009. The role of tenascin-C in tissue injury and tumorigenesis. Journal of cell communication and signaling 3, 287–310.
Monferran, S., et al., 2008. Alpha v beta 3 and alpha v beta 5 integrins control glioma cell response to ionising radiation through ILK and RhoB. International Journal of Cancer 123 (2), 357–364.
Ogden, A.T., et al., 2008. Identification of A2B5(+)CD133-tumor-initiating cells in adult human gliomas. Neurosurgery 62 (2), 505–514.
Overgaard, J., 2007. Hypoxic radiosensitization: adored and ignored. Journal of Clinical Oncology 25 (26), 4066–4074.
Pallini, R., et al., 2008. Cancer stem cell analysis and clinical outcome in patients with glioblastoma multiforme. Clinical Cancer Research 14 (24), 8205–8212.
Pollard, S., et al., 2009a. Brain cancer stem cells: a level playing field. Cell Stem Cell 5 (5), 468–469.
Pollard, S.M., et al., 2009b. Glioma stem cell lines expanded in adherent culture have tumor-specific phenotypes and are suitable for chemical and genetic screens. Cell Stem Cell 4 (6), 568–580.
Reardon, D.A., et al., 2002. Phase II trial of murine I-131-labeled antitenascin monoclonal antibody 81C6 administered into surgically created resection cavities of patients with newly diagnosed malignant gliomas. Journal of Clinical Oncology 20 (5), 1389–1397.
Reardon, D.A., et al., 2008. A pilot study: I-131-Antitenascin monoclonal antibody 81c6 to deliver a 44-Gy resection cavity boost. Neuro-Oncology 10 (2), 182–189.
Reynolds, B.A., Vescovi, A.L., 2009. Brain cancer stem cells: think twice before going flat. Cell Stem Cell 5 (5), 466–467.
Ricci-Vitiani, L., et al., 2010. Tumour vascularization via endothelial differentiation of glioblastoma stem-like cells. Nature 468 (7325), 824–828 (vol 468, pg 824, 2010).
Rich, J.N., et al., 2005. Gene expression profiling and genetic markers in glioblastoma survival. Cancer Research 65 (10), 4051–4058.
Riekki, R., et al., 2001. Radiation therapy induces tenascin expression and angiogenesis in human skin. Acta Dermato-Venereologica 81 (5), 329–333.
Rolle, K., et al., 2010. Promising human brain tumors therapy with interference RNA intervention (iRNAi). Cancer Biology & Therapy 9 (5), 396–406.
Ropolo, M., et al., 2009. Comparative analysis of DNA repair in stem and Nonstem glioma cell cultures. Molecular Cancer Research 7 (3), 383–392.
Salmaggi, A., et al., 2006. Glioblastoma-derived tumorospheres identify a population of tumor stem-like cells with angiogenic potential and enhanced multidrug resistance phenotype. Glia 54 (8), 850–860.
Sandfort, V., Koch, U., Cordes, N., 2007. Cell adhesion-mediated radioresistance revisited. International Journal of Radiation Biology 83 (11–12), 727–732.
Sato, A., et al., 2010. Regulation of neural stem/progenitor cell maintenance by PI3K and mTOR. Neuroscience Letters 470 (2), 115–120.
Shaifer, C.A., Huang, J.H., Lin, P.C., 2010. Glioblastoma cells incorporate into tumor vasculature and contribute to vascular radioresistance. International Journal of Cancer 127 (9), 2063–2075.
Singh, S.K., et al., 2004. Identification of human brain tumour initiating cells. Nature 432 (7015), 396–401.
Son, M.J., et al., 2009. SSEA-1 Is an Enrichment Marker for tumor-initiating Cells in human glioblastoma. Cell Stem Cell 4 (5), 440–452.
Steel, G.G., 2001. The case against apoptosis. Acta Oncologica 40 (8), 968–975.
Strojnik, T., et al., 2007. Neural stem cell markers, nestin and musashi proteins, in the progression of human glioma: correlation of nestin with prognosis of patient survival. Surgical Neurology 68 (2), 133–144.
Tai, I.T., et al., 2005. Genome-wide expression analysis of therapy-resistant tumors reveals SPARC as a novel target for cancer therapy. Journal of Clinical Investigation 115 (6), 1492–1502.
Tamura, K., et al., 2010. Accumulation of CD 133-positive glioma cells after high-dose irradiation by gamma knife surgery plus external beam radiation clinical article. Journal of Neurosurgery 113 (2), 310–318.
Thonhoff, J.R., et al., 2008. Compatibility of human fetal neural stem cells with hydrogel biomaterials in vitro. Brain Research 1187, 42–51.
Vickerman, V., et al., 2008. Design, fabrication and implementation of a novel multi-parameter control microfluidic platform for three-dimensional cell culture and real-time imaging. Lab on a Chip 8 (9), 1468–1477.
Wang, J., et al., 2008. CD133 negative glioma cells form tumors in nude rats and give rise to CD133 positive cells. International Journal of Cancer 122 (4), 761–768.
Wang, R., et al., 2010. Glioblastoma stem-like cells give rise to tumour endothelium. Nature 468 (7325), 829–833.
Wang, J.L., et al., 2010b. Notch promotes radioresistance of glioma stem cells. Stem Cells 28 (1), 17–28.
Yuan, X.P., et al., 2004. Isolation of cancer stem cells from adult glioblastoma multiforme. Oncogene 23 (58), 9392–9400.
Zeppernick, F., et al., 2008. Stem cell marker CD133 affects clinical outcome in glioma patients. Clinical Cancer Research 14 (1), 123–129.
Zhang, M.Y., et al., 2008. Nestin and CD133: valuable stem cell-specific markers for determining clinical outcome of glioma patients. Journal of Experimental & Clinical Cancer Research 27, 7.

Stem Cell Research (2014) 13, 135–143

Available online at www.sciencedirect.com

ScienceDirect

www.elsevier.com/locate/scr

SHORT REPORT

Differential sensitivity of Glioma stem cells to Aurora kinase A inhibitors: Implications for stem cell mitosis and centrosome dynamics

Mariella Mannino [a], Natividad Gomez-Roman [b], Helfrid Hochegger [a,*], Anthony J. Chalmers [b,*]

[a] Genome Damage and Stability Centre, University of Sussex, Brighton BN19RQ, UK
[b] Institute of Cancer Sciences, University of Glasgow, Glasgow G12 8QQ, UK

Received 20 November 2013; received in revised form 1 April 2014; accepted 2 May 2014
Available online 11 May 2014

Abstract Glioma stem-cell-like cells are considered to be responsible for treatment resistance and tumour recurrence following chemo-radiation in glioblastoma patients, but specific targets by which to kill the cancer stem cell population remain elusive. A characteristic feature of stem cells is their ability to undergo both symmetric and asymmetric cell divisions. In this study we have analysed specific features of glioma stem cell mitosis. We found that glioma stem cells appear to be highly prone to undergo aberrant cell division and polyploidization. Moreover, we discovered a pronounced change in the dynamic of mitotic centrosome maturation in these cells. Accordingly, glioma stem cell survival appeared to be strongly dependent on Aurora A activity. Unlike differentiated cells, glioma stem cells responded to moderate Aurora A inhibition with spindle defects, polyploidization and a dramatic increase in cellular senescence, and were selectively sensitive to Aurora A and Plk1 inhibitor treatment. Our study proposes inhibition of centrosomal kinases as a novel strategy to selectively target glioma stem cells.

Introduction

In the past decade, stem-cell-like cancer cells have been identified in several tumours and implicated in treatment resistance. Glioblastoma is one of the most extensively studied cancer types in relation to treatment resistance and the cancer stem cell (CSC) model. This is probably due to the poor outcome of patients treated for this disease (median overall survival of 14.6 months) (Stupp et al., 2009) and to the almost inevitable recurrence following chemo-radiation, which renders glioblastomas a valuable model for study of cancer cell resistance to radiation and chemotherapy. Several clinical series have found a correlation between glioma stem cell (GSC) features in patient specimens (expression of putative GSC markers, neurosphere formation ability *in vitro*) and tumour recurrence and poorer prognosis (Strojnik et al., 2007; Zhang et al., 2008; Zeppernick et al., 2008; Pallini et al., 2008). Furthermore, a recent study using a genetically engineered mouse model of glioma identified a relatively quiescent subpopulation of cells

* Corresponding authors.
E-mail addresses: h.hochegger@sussex.ac.uk (H. Hochegger), anthony.chalmers@glasgow.ac.uk (A.J. Chalmers).

http://dx.doi.org/10.1016/j.scr.2014.05.001
1873-5061/

that was responsible for post-chemotherapy tumour growth, through its capacity to produce transient subsets of highly proliferating cells (Chen et al., 2012). These findings reinforced the rationale for the GSC theory and highlighted the importance of processes regulating cellular growth, such as DNA replication and mitosis, in the context of treatment resistance.

Current standard therapy for glioblastoma consists of debulking surgery followed by radiation with concomitant and adjuvant administration of the alkylating agent temozolomide (Stupp et al., 2009). Most studies investigating intrinsic GSC resistance have focused on the role of DNA damage responses and repair. However, experimental data from these studies are conflicting and response mechanisms of GSCs to radiation and chemotherapy remain controversial (Beier et al., 2011). Other stem cell features, such as those involved in regulating cell division, are only poorly understood in GSCs, but could provide clinically relevant targets to improve treatment outcomes. A paramount feature of stem cell mitosis is the ability to divide both symmetrically and asymmetrically, giving rise to differentiating daughter cells as well as maintaining a pool of self-renewing stem cells (Lathia et al., 2011). Studies in fruit fly neuronal stem cells have demonstrated a critical role for the centrosome in establishing asymmetry during mitosis (Yamashita et al., 2007). Centrosomes are the microtubule organising centres in animal cells that form the poles of the mitotic spindle. They are regulated by several mitotic kinases including Aurora kinase A (AurA), Polo-like kinase 1 (Plk1) and Cyclin dependent kinase 1 (Cdk1) (Nigg and Stearns, 2011). Inhibitors of these kinases have long been implicated as potential cancer therapies (Harrison et al., 2009). A recent study has highlighted Plk1 inhibition as a strategy to selectively kill GSC enriched populations (Lee et al., 2012). Moreover, AurA is overexpressed in glioblastomas (Loh et al., 2010; Lehman et al., 2012); its expression levels have been correlated with patient outcome (Barton et al., 2010); and data from other tumour sites suggest a role for AurA in CSC behaviour (Cammareri et al., 2010; Chefetz et al., 2011). However, a link between centrosome biology, mitotic kinase inhibition and GSC targeting has not been established.

In this study we analysed centrosome and mitotic spindle morphology in glioblastoma stem cell enriched and differentiated populations. We report a higher frequency of abnormal spindles and a more pronounced maturation of centrosomes preceding mitosis in GSC enriched populations. This prompted us to investigate whether differences in mitotic spindle dynamics could provide a novel therapeutic strategy by which GSC populations could be specifically targeted. We show that AurA and Plk1, both involved in centrosome maturation and bipolar spindle assembly can be targeted to kill GSCs more effectively, and propose that this strategy might improve outcomes for patients with glioblastoma.

Results

Neurosphere cultures of primary glioblastoma cells generate invasive intracranial xenografts in immunodeficient mice

Consistent with previously published data (Fael Al-Mayhani et al., 2009), primary glioblastoma cells cultured as non-adherent neurospheres in serum-free medium expressed high levels of stem cell markers including CD133, nestin and Sox2 (Fig. 1A, supplementary Fig. S1A,B), low levels of astrocytic differentiation markers including GFAP (supplementary Fig. S1B) and generated invasive intracranial xenografts in CD1 nude mice. Intracranial injection of 10^5 E2 cells cultured as neurospheres ('E2 GSC') generates tumours in 100% of mice and these tumours were highly invasive. In addition to a mass at the injection site (Fig. 1B), tumour cells identified by human specific HLA-1ABC and Ki67 staining were detected throughout both hemispheres (Supplementary Fig. S1C). Quantitative analysis of Ki67 positive cells in whole brain slices harvested at various timepoints demonstrated increasing tumour cell burden up to 20 weeks after injection (Fig. 1B, supplementary Fig. S1C). In contrast, injection of 10^5 E2 cells cultured as monolayers in serum-containing medium ('E2 diff') failed to generate tumour masses and tumour cells did not infiltrate the brain. Very low numbers of HLA-1ABC or Ki67 positive cells were detected (Fig. 1B). Injection of 10^5 G7 cells cultured as neurospheres ('G7 GSC') generated tumours in 100% of mice; all tumours were highly invasive at the tumour margins (Fig. 1B). Injection of 10^5 G7 cells cultured as monolayers in serum-containing medium ('G7 diff') also generated tumours but these had well defined edges and did not exhibit the invasive pattern observed in G7 GSC derived tumours (Fig. 1B).

Glioblastoma stem cells are prone to mitotic failure and show a distinct pattern of centrosome maturation

Cell division of GSCs remains scarcely characterised, despite its role in maintaining stemness and generating cellular diversity (Lathia et al., 2011). To understand whether mitosis in these cells presents specific features that can be targeted therapeutically, we analysed their mitotic spindles by immunofluorescence. GSC enriched populations had a significantly higher frequency of abnormal mitotic spindles (monopolar or multipolar) compared to more differentiated populations: 14% *vs.* 4%, respectively (Fig. 1C). While scoring mitosis in the GSC enriched populations we frequently observed cells with two or more nuclei (Fig. 1C). To clarify whether these were cell aggregates or truly polyploid cells, we stained both cell populations with phalloidin to visualise the cell cortex. This allowed us to differentiate between single cells with two or more nuclei and closely attached cells with two single nuclei. Consistent with the mitotic spindle data, this analysis revealed that GSC enriched populations had a much higher percentage of polyploid cells compared to more differentiated populations: 25% *vs.* 6%, respectively (Fig. 1D). In order to test whether the increase in abnormal spindles was due to growth in suspension, we analysed spindle phenotypes in differentiated cells cultured as non-adherent aggregates and found that all imaged cells had bipolar spindles (data not shown), suggesting that the neurosphere growth is not a confounding factor for the observed mitotic phenotypes. To our knowledge, this is the first study reporting a higher frequency of abnormal mitotic spindles and polyploidy in GSC enriched populations *in vitro*.

While analysing spindle morphology we noted a distinct pattern in the distribution of γ-tubulin at the centrosomes in the GSC populations that was characterised by a marked

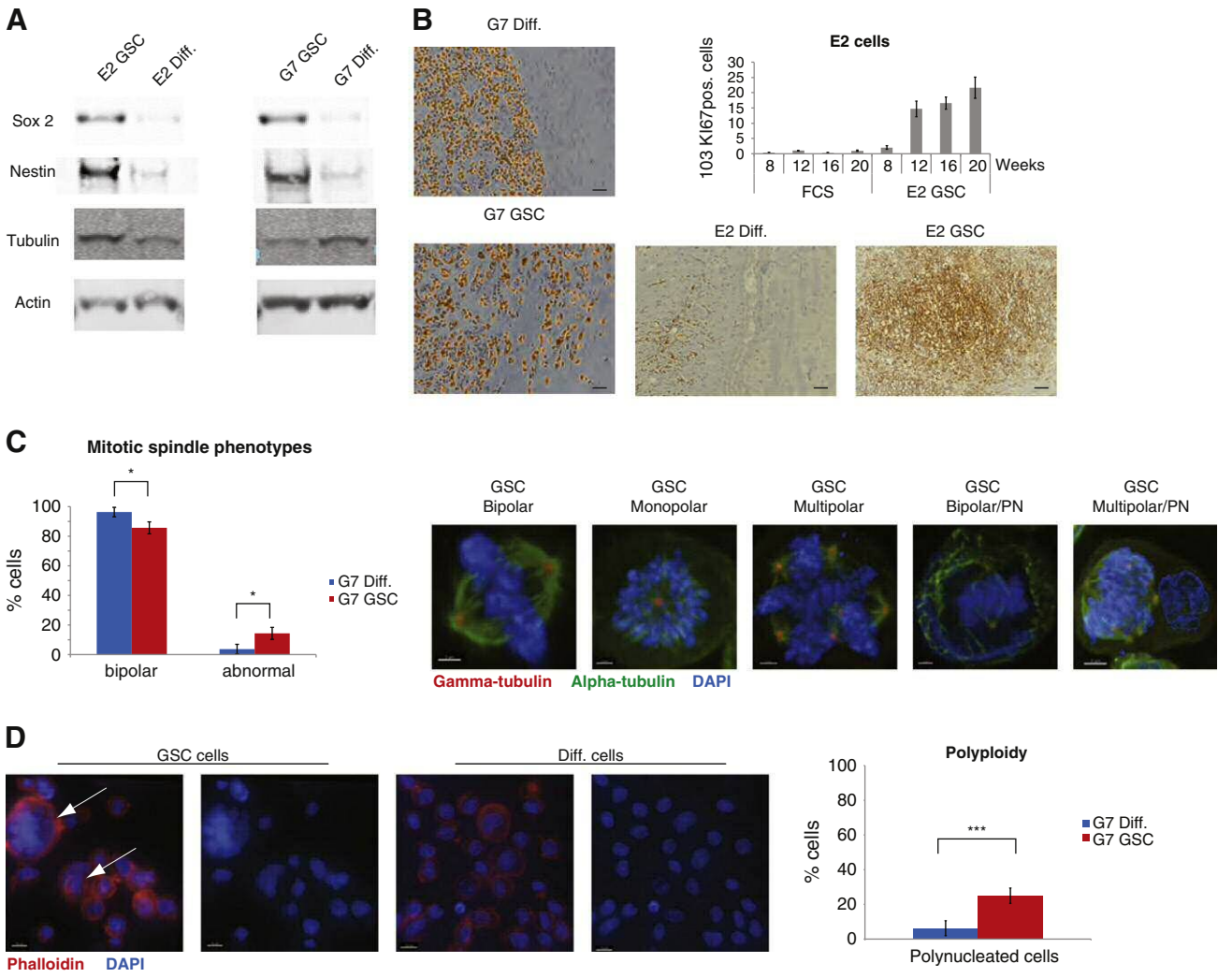

Figure 1 Primary glioblastoma cells cultured as neurospheres in serum-free conditions express high levels of stem cell markers, form invasive intracranial xenografts in immunodeficient mice and have a higher frequency of abnormal mitotic spindles and a distinct pattern of centrosome maturation. (A) Immunoblot analysis of lysates of E2 and G7 primary glioblastoma cell cultures was performed, probing for the stem cell markers Sox2 and nestin, with tubulin and actin as loading controls (GSCs—glioma stem cells cultured as neurospheres in serum-free medium, diff.—differentiated, adherent cells cultured in serum-containing medium) (B) Immunohistochemistry was performed on sections of brains of CD1 nude mice that had been injected with 10^5 E2 or G7 glioblastoma cells that had been cultured to enrich for GSC or to promote differentiation. Sections were stained for Ki67 (G7 images on left) to interrogate local brain invasion and for HLA-1ABC to identify tumour cells of human origin (E2 images below histogram). To measure tumour cell burden in highly infiltrative E2 derived xenografts, quantitative analysis of Ki67 positive cells in whole brain sections was performed using ZenBlue software. Number of Ki67 positive cells per section was plotted against time after injection of E2 GSC and differentiated cells (Scale bar at 50 μm). (C) Cells were stained for α tubulin (green), γ tubulin (red) and DAPI (blue), to visualise the mitotic spindle morphology: on the left, a diagram shows the percentages of normal and abnormal spindles in glioma stem cells and differentiated cells. On the right are representative images of mitotic phenotypes (Scale bar 2 μm). PN: polynucleated cells. An average of 26 mitotic cells/condition/experiment were identified randomly and scored (*p = 0.0232, two tailed *t*-test). (D) Cells were stained with phalloidin (red) and DAPI (blue) to visualise the cell cortex and nucleus: on the left are representative images of GSC and diff. cells (scale bar 10 μm); on the right, a diagram shows the percentages of polynucleated cells in the two populations. An average of 251 cells/condition/experiment were identified randomly and scored (***p = 0.000275, two tailed *t*-test).

increase in γ-tubulin at the mitotic centrosomes compared to differentiated cells. Given the role of centrosomes in bipolar spindle assembly, we further analysed the distribution of γ-tubulin in the two glioblastoma cell populations. For this purpose we measured the size of the γ-tubulin area in both interphase and mitotic cells (Fig. 2A). The specificity of the centrosomal γ-tubulin staining was confirmed by co-localization with centrin (supplementary Fig. S2A). This quantitative analysis revealed a more pronounced centrosomal accumulation of γ-tubulin at mitosis in GSCs, compared to

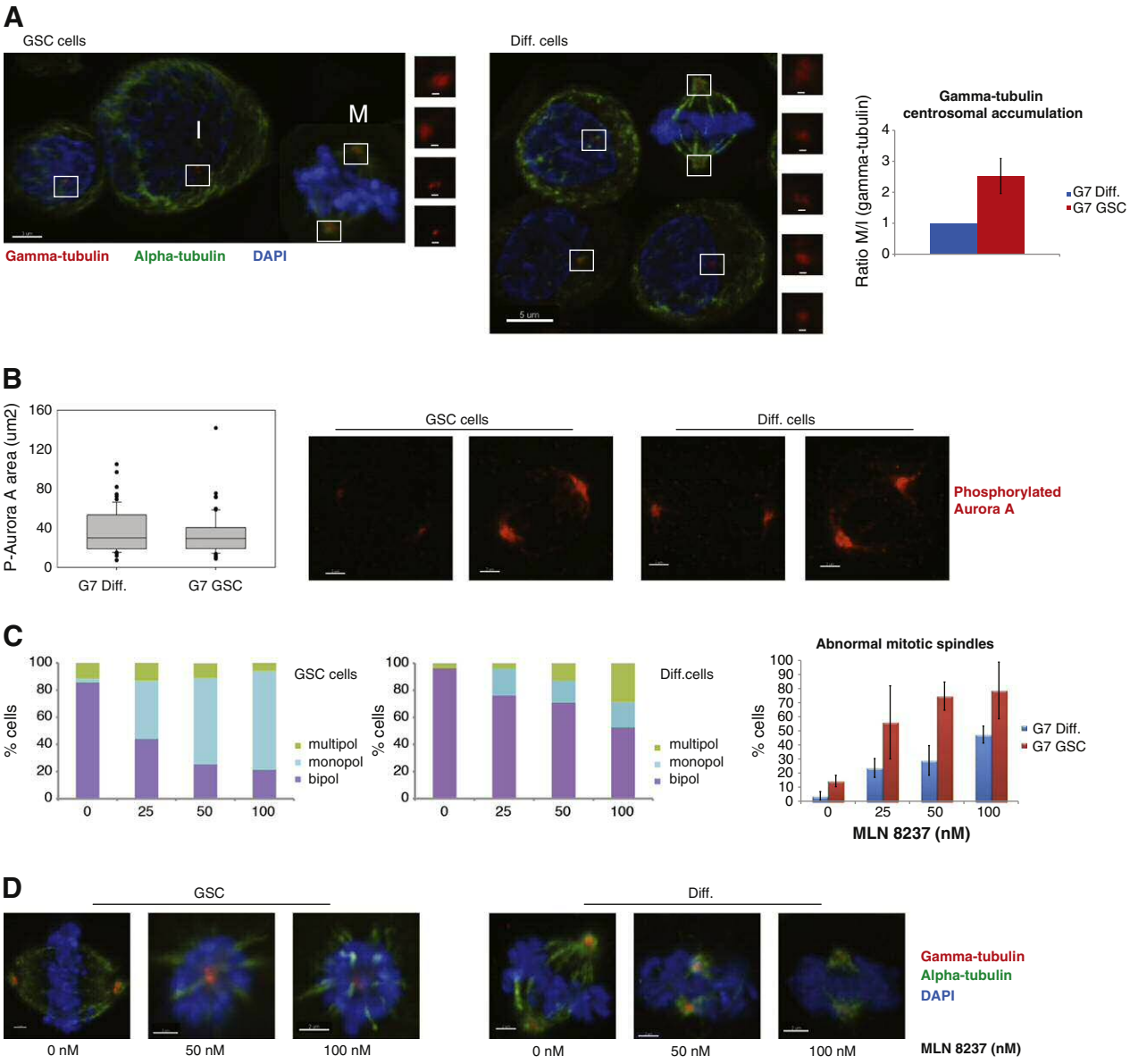

Figure 2 Glioblastoma stem cells have more abnormal spindles following treatment with Aurora A inhibitors. (A) Cells were stained for α tubulin (green), γ tubulin (red) and DAPI (blue), to visualise the accumulation of γ tubulin during centrosome maturation: at the top are representative images of GSC and diff. cells (scale bar 5 μm), with inserts showing γ tubulin staining in interphase (I) and mitotic (M) cells (scale bar 500 nm); at the bottom, a diagram shows the ratio between centrosomal γ-tubulin in mitotic and interphase cells, as a measure of centrosome maturation, in GSC and diff. populations. An average of 144 cells/condition/experiment were identified randomly and scored. All results are representative of three independent experiments. Error bars indicate means ± SD. (B) Cells were stained for P-AurA (red) and mitotic cells were analysed: on the left, a box plot shows the quantification of P-AurA in mitotic centrosomes in diff. and GSC cells; on the right are representative images of mitotic cells in the two populations (scale bar 2 μm). An average of 22 mitotic cells/condition/experiment were identified randomly and scored. (C–D) Cells were treated with MLN8237 (0, 25, 50 and 100 nM) and after 24 h they were fixed and stained for α tubulin (green), γ tubulin (red) and DAPI (blue), to visualise the mitotic spindle morphology. (B) On the left, two diagrams show the distribution of different spindle phenotypes in GSC and diff. cells; on the right a diagram shows the percentages of abnormal mitotic spindles in the two populations. (C) Representative images of GSC and diff. cells ± MLN8237 (scale bar 2 μm). An average of 26 mitotic cells/condition/experiment were identified randomly and scored. All results are representative of three independent experiments. Error bars indicate means ± SD.

differentiated cells (Fig. 2A). Thus, centrosome maturation, measured as the ratio between centrosomal γ-tubulin in mitotic and interphase cells, was increased more than twofold in GSCs. This finding, together with the difference in mitotic phenotypes, highlights the importance of investigating in detail GSC division and the processes leading to it, in order to find effective and specific ways of targeting this population.

Glioblastoma stem cell enriched populations have more abnormal spindles following treatment with Aurora A inhibitors

Since GSCs display a more pronounced accumulation of γ-tubulin at the centrosome during mitotic entry, we reasoned that this could be an interesting point of attack for a targeted therapeutic approach. For this purpose we focused on AurA, which is a major regulator of mitotic centrosome maturation. The differences in centrosome dynamics could not be attributed to different levels of activity of AurA in the two cell populations (supplementary Fig. S2B–C and Fig. 2B). To analyse the requirement for AurA activity in the two populations, we treated stem and differentiated glioma cells with the AurA inhibitor MLN8237, using low dose levels that only had subtle effects on overall AurA kinase activity (supplementary Fig. S2C). Given that MLN8237 has a selectivity of more than 200-fold for AurA over Aurora kinase B (Manfredi et al., 2011), we can assume that any observed effects are AurA specific. Interestingly, treatment with the inhibitor induced more abnormal spindles in GSC enriched populations at all dose levels compared to more differentiated cells: 56% *vs.* 14% at 25 nM, 75% *vs.* 29% at 50 nM and 79% *vs.* 47% at 100 nM, respectively (Fig. 2C). The two populations of cells also exhibited a different response to AurA inhibition in terms of the type of spindle defect. GSC enriched populations showed a dramatic increase only in monopolar spindles, while their more differentiated counterparts showed a moderate increase in both monopolar and multipolar spindles (Fig. 2C). Fig. 2D shows representative images of treated cells. These data suggest that GSCs are highly susceptible to subtle changes in AurA activity.

Aurora A inhibition induces an increase in polyploidy

To further understand the consequences of AurA inhibitor treatment on GSCs we analysed parameters of cell cycle distribution in the two cell populations. Several studies have reported a G2/M arrest following inhibition of AurA, either by small molecule inhibitors or by RNAi (Gorgun et al., 2010). In our study the baseline cell cycle profiles of the two populations differed significantly: GSC enriched populations had a higher percentage of cells with 4 N and >4 N DNA content (Fig. 3A). Cells with a 4 N FACS profile can be in G2, M or a quatroploid G1 phase. To distinguish between these cell cycle states, we scored the percentage of cells in G2 and M by immunofluorescence using CENP-F, α-tubulin and DAPI staining (for a representative example, see Fig. 3B). The G2/M fraction was similar in the two populations, confirming that the difference in cells with 4 N DNA content was due to polyploidy. Cell cycle profiles of the two populations 24 h after treatment with MLN8237 showed an increase in the 4 N and >4 N DNA content fraction in both populations. Immunofluorescence analysis showed only subtle increases in the percentage of G2 and M phase cells after treatment, suggesting that AurA inhibition does not induce a prolonged G2/M arrest in these cells, despite a significant increase of mitotic aberrations following MLN8237 treatment (Fig. 2).

To confirm and characterise the moderate increase in the ≥4 N fraction, we stained with phalloidin cells after AurA

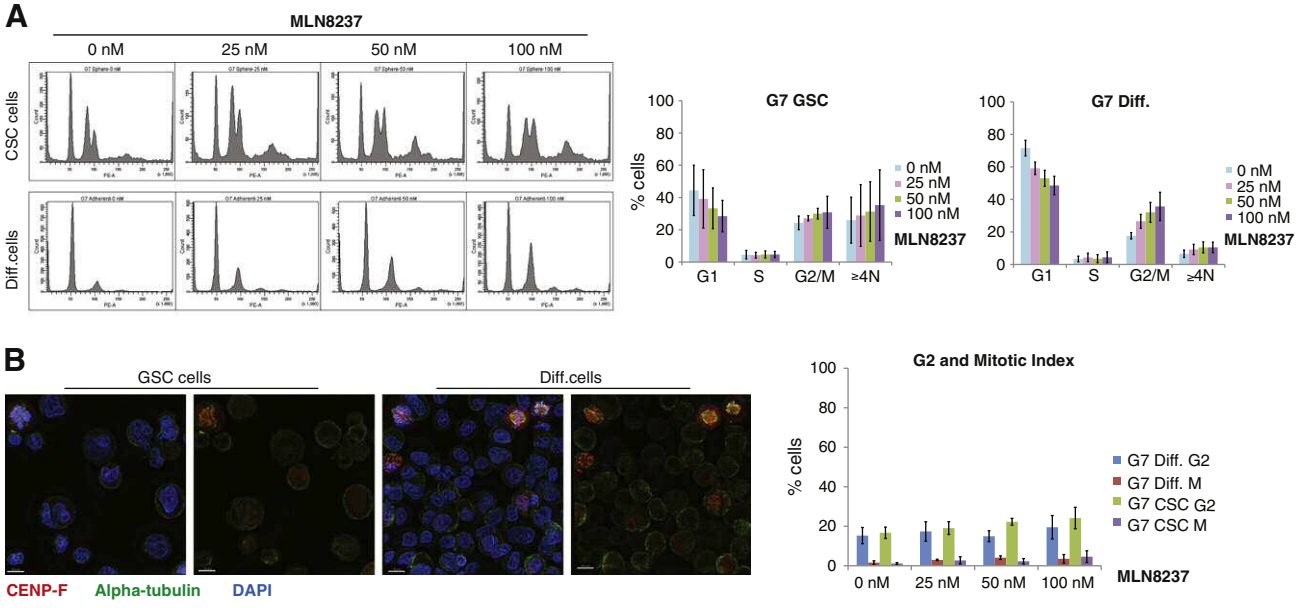

Figure 3 Aurora A inhibition does not cause a significant G2/M arrest in glioblastoma cells. (A) Cells were treated with MLN8237 (0, 25, 50 and 100 nM) and after 24 h they were fixed, stained with propidium iodide (PI) and analysed for DNA content: on the left are representative FACS diagrams of GSC and diff. cells; on the right, two diagrams show percentages of cells in the various phases of the cell cycle, quantified in the FACS analysis. (B) Cells were treated with MLN8237 (0, 25, 50 and 100 nM) and after 24 h they were fixed and stained for α tubulin (green), CENP-F (red) and DAPI (blue), to visualise G2/M cells: on the left are representative images of GSC and diff. cells; on the right, a diagram shows the percentages of cells in G2 and M in the two populations ± MLN8237. An average of 309 cells/condition/experiment were identified randomly and scored. All results are representative of three independent experiments. Error bars indicate means ± SD.

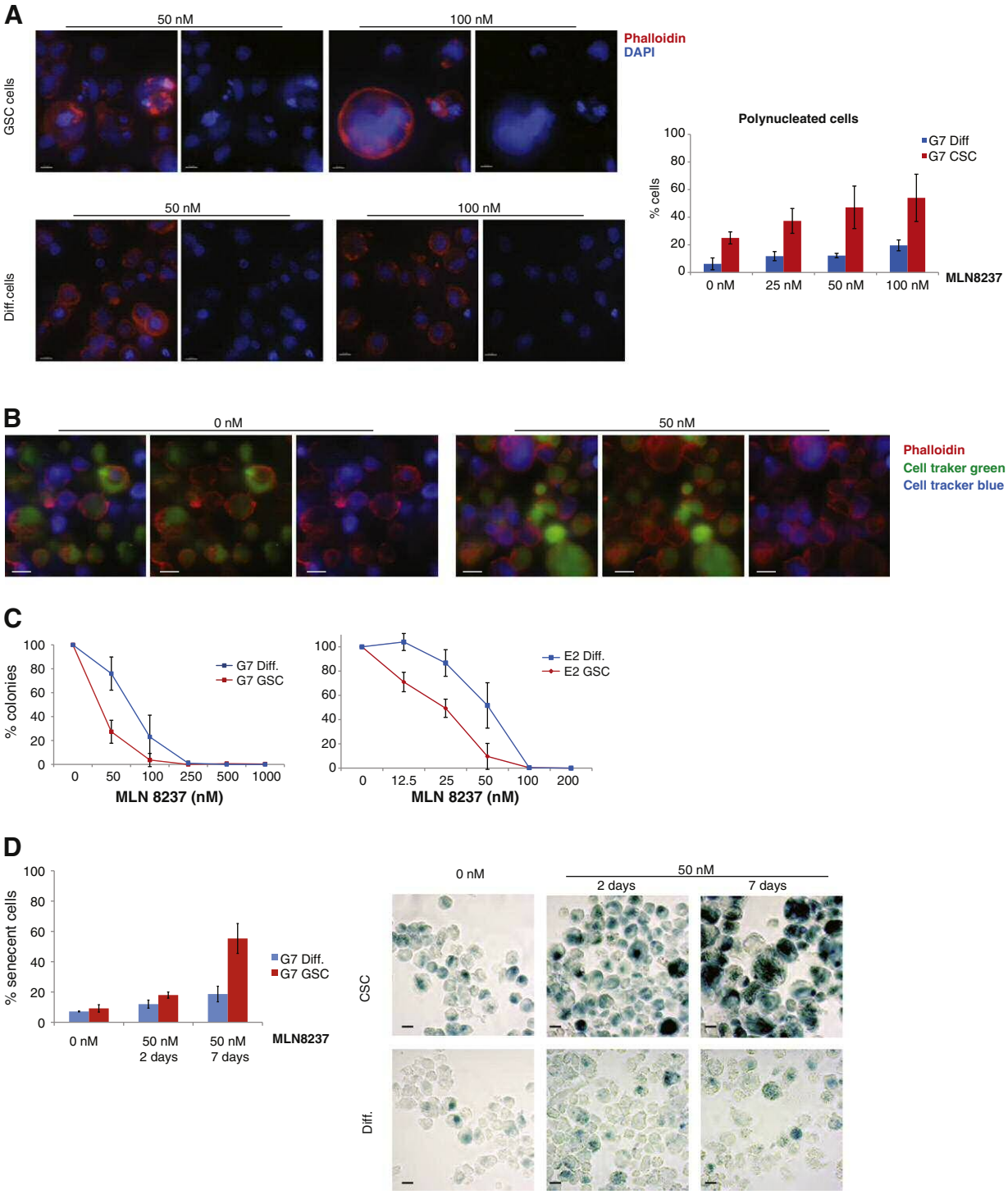

Figure 4 Glioblastoma stem cells are killed more efficiently by MLN8237. (A) Cells were treated with MLN8237 (0, 25, 50 and 100 nM) and after 24 h they were fixed, stained with phalloidin (red) and DAPI (blue), to visualise the cell cortex and nucleus: on the left are representative images of GSC and diff. cells (scale bar 10 μm); on the right, a diagram shows the percentages of polynucleated cells in the two populations ± MLN8237. An average of 221 cells/condition/experiment were identified randomly and scored. (B) Cells were incubated separately with CellTracker Green and Blue, re-suspended in fresh medium, incubated for 24 h ± 50 nM MLN8237 and then fixed and stained with phalloidin: representative images of sphere cells ± MLN8237 (scale bar 10 μm). (C) Clonogenic assays showing survival of sphere and adherent cells ± MLN8237. (D) Cells were treated with MLN8237 (0 and 50 nM) and after 2 or 7 days they were fixed and stained for β-galactosidase: on the left, a diagram shows the percentages of senescent cells in the two populations ± MLN8237; on the right are representative images of sphere and adherent cells ± MLN8237. (scale bar 10 μm). An average of 233 cells/condition/experiment were identified randomly and scored. All results are representative of three independent experiments. Error bars indicate means ± SD.

inhibition. This analysis detected an increasing number of giant polynucleated cells that was more pronounced in the GSC population: 37%, 47% and 54% of these cells were polyploid after 25, 50 and 100 nM treatments, compared with 12%, 12% and 20% in the more differentiated populations (Fig. 4A). That these percentages were higher than indicated by the FACS data is probably explained by the large size of some polyploid cells causing them to evade FACS analysis.

Polyploidy can be caused by several mechanisms: abnormal mitosis, endoreduplication, cell fusion and entosis (Krajcovic and Overholtzer, 2012). Given that cell appearance does not distinguish between the products of cell fusion and mitotic failure, and that entosis has been observed mainly under non-adherent growth conditions (Overholtzer et al., 2007), we tested the extent to which these different processes were responsible for baseline and post-treatment levels of polyploidy amongst GSCs. Cells were marked separately with cell tracking dyes, mixed then incubated for 24 h with or without MLN8237 (Fig. 4B). In both treated and untreated samples the vast majority of polyploid cells originated from the same mother cell, suggesting that in GSCs polyploidy is not a result of cell fusion or entosis, but rather a consequence of mitotic defects.

Increase in polyploidy correlates with increased sensitivity to Aurora A inhibition and induction of senescence

Our analysis suggests that GSCs are prone to undergoing mitotic failure and are highly susceptible to subtle changes in AurA activity levels. The observed increase in monopolar spindles does not cause a prolonged mitotic arrest suggesting that these cells are prone to mitotic slippage. This is also reflected in the rapid polyploidization observed after MLN8237 treatment. Taken together these observations indicate that chemical inhibitors of mitosis might be useful therapeutic agents that specifically target the GSC population. We tested this hypothesis by measuring the sensitivity of glioblastoma stem cell enriched and more differentiated populations to MLN8237 and found that two independent GSC lines were indeed killed more efficiently by the AurA inhibitor (Fig. 4C). We further tested our hypothesis by analysing the effect on clonogenicity of inhibiting another centrosome kinase, Plk1, with BI2536: again, two independent GSC lines had a lower survival than their differentiated counterparts (supplementary Fig. 3).

In order to understand the cause of death in glioblastoma stem cell enriched and more differentiated populations following AurA inhibition, we measured levels of apoptosis and senescence. While MLN8237 did not increase apoptosis as judged by cleaved Caspase 3 levels in either population (supplementary Fig. 4A), a significant increase in the number of senescent cells was observed. Seven days after AurA inhibition, 55% of GSCs expressed a marker of senescence, compared with only 19% of differentiated cells (Fig. 4D). The negligible level of apoptosis is consistent with some published studies (Huck et al., 2010; Liu et al., 2013) but not with others (Gorgun et al., 2010). Recent literature is also conflicting with regard to the correlation between cell fate following AurA inhibition and p53 status (Liu et al., 2013; Nair et al., 2012; Liu et al., 2013). To test whether the different response to MLN8237 was due to p53 status, we analysed levels of p53 expression in glioblastoma stem cell enriched and more differentiated populations in three primary cell lines: there was no common pattern of p53 levels in the various cell lines when comparing the two subpopulations (supplementary Fig. 4B–D). This suggests that the increased sensitivity of GSCs to AurA inhibition is not dependent on p53 status.

Several studies in a variety of cancer models have shown that cellular senescence is induced *in vivo* by chemotherapy and radiotherapy (Roninson, 2003). Although a large body of evidence links senescence to tumour suppression, recent data suggests that, in a minority of cancer cells, senescence associated polyploidy can be reversible and might constitute a survival mechanism. A clinicopathological analysis of specimens from patients with non-small cell lung cancer undergoing surgery after neo-adjuvant chemotherapy showed that β-galactosidase staining was correlated with decreased overall survival (Wang et al., 2013). Moreover, one of the features of senescent cells is the acquisition of a secretory phenotype, which creates a niche that can affect adjacent cells (Rodier and Campisi, 2011). Amongst the released factors is IL-6 (Coppe et al., 2008), which has been reported to promote GSC survival and tumour growth (Wang et al., 2009). These findings suggest a possible link between chemotherapy-induced senescence, GSCs and treatment resistance. Our survival data clearly indicate that senescence following MLN8237-induced mitotic failure causes a reduction of neurosphere formation in GSCs and generally decreases the clonogenic potential of glioma cells. Hence we propose that induction of senescence by polyploidy could be a promising anticancer strategy that targets GSCs, rather than a survival mechanism. Given the limitations of a single cell survival assay in this context, our findings highlight the need for *in vivo* studies and pathological analysis to clarify the role of senescence associated polyploidy in GSC biology and treatment outcomes.

Another significant outcome of our study is the difference in centrosome maturation and mitotic spindle phenotypes between GSC enriched and differentiated populations. To our knowledge there are no previous reports on this aspect of GSC biology. The high susceptibility of GSCs to subtle changes in levels of kinases involved in the centrosome cycle is particularly interesting if we consider the literature on the role of symmetric and asymmetric divisions in cancer. Defects in regulation of switch between asymmetric and symmetric divisions have been speculated to be involved in carcinogenesis (Morrison and Kimble, 2006), and therefore might be strongly linked to generation of GSCs. GSCs *in vitro* divide mainly by symmetric division, but are able to increase the asymmetric mode following growth factor withdrawal, *i.e.* a differentiation stimulus (Lathia et al., 2011). Normal adult stem cells seem to switch from asymmetrical to symmetrical division following injury (Morrison and Kimble, 2006). The study mentioned previously (Chen et al., 2012), which used a genetically engineered mouse model of glioma, reported data on transient subsets of highly proliferating tumour cells post-chemotherapy. In this study the growth patterns were consistent with an initial prevalence of symmetric divisions followed by a switch to asymmetrical mode. Based on this data and on our findings, we speculate that GSC mitosis confers more plasticity and

increased regenerative ability to these cells, but also renders them more susceptible to mitotic failure.

Mechanisms regulating mitosis, as well as senescence, in GSCs, are still poorly understood and need to be investigated further, especially with pathology studies that would be able to confirm whether our *in vitro* findings apply to GSCs in their natural microenvironment.

Materials and methods

Cell lines and cell culture

E2 and G7 primary glioblastoma cell lines were derived from freshly resected GBM specimens as previously described (Fael Al-Mayhani et al., 2009) and generously provided by Colin Watts (Cambridge). Tissue collection protocols were compliant with the UK Human Tissue Act 2004 (HTA Licence ref 12315) and approved by the local regional Ethics Committee (LREC ref 04/Q0108/60). Informed consent was obtained from each patient before surgery. Briefly, anonymised patient resection specimens were homogenised and seeded in serum free (SF) media to form spheroid aggregates which were then collected and plated onto extracellular matrix coated flasks. (ECM 1:10 dilution, Sigma). Cells were allowed to form a primary monolayer then passaged in SF medium. Each cell line was subsequently cultured as paired cancer stem cell enriched (GSC) and differentiated (diff) cell lines by passaging in either SF media or differentiating media (DM). GSC enriched populations were cultured as neurospheres in Neurobasal-A medium (Invitrogen) supplemented with B-27 (Invitrogen), epidermal growth factor (20 ng/ml, Invitrogen PHG0313), fibroblast growth factor (20 ng/ml, Invitrogen PHG0263), glutamine and penicillin/streptomycin (referred to as 'sphere cells' or 'GSC' in figures). Differentiated populations were derived from these cells by culturing them as adherent cells in MEM supplemented with HyClone (Thermo Scientific HyClone, 12822966), NEAA, glutamine and penicillin/streptomycin (referred to as 'adherent' or 'diff' cells in figures).

Reagents

In all experiments with AurA inhibition we incubated cells with MLN8237 (Millenium) for 24 h. For clonogenic survival assays we added the reagents to the plates and left them for the whole duration of the experiment.

Immunostaining

For centrosome maturation, mitotic spindle and cell cycle analysis, cells were collected from flasks, spun down, re-suspended, pipetted on Concanavalin A (Sigma) coated coverslips and fixed with 70% methanol for 5 min. For P-AurA analysis, cells were cytospun on Concanavalin A coated coverslips and fixed with 4% paraformaldehyde and 70% methanol, sequentially for 5 min each. Cells were permeabilized in PBS 0.3% Triton for 5 min, blocked in 3% BSA for 30 min and probed with primary antibodies for 60 min. Slides were rinsed and probed with Alexa Fluor secondary antibodies (Invitrogen) for 60 min. Coverslips were mounted using ProLong Gold mounting solution containing DAPI (Molecular Probes). The following primary antibodies were used: HLA Class 1ABC (EMR8-5, Abcam ab70328), Ki67, CD133, nestin, Sox2, GFAP, α tubulin (Abcam ab7291, ab18251), γ tubulin (Abcam ab11316), centrin-2 (gift from Elmar Schiebel), CENP-F (Abcam ab5), and P-AurA (Cell Signalling 3079).

Images were acquired on a microscope (DeltaVision) equipped with a UPLS Apochromat NA 1.40, 60× or 100× oil immersion objective (Olympus), standard filter sets (excitation 360/40, 490/20, and 555/28; emission 457/50, 528/38, and 617/40), and a camera (CoolSNAP HQ2; Photometrics). Z series of 0.3 μm stacks were acquired using softWoRx software (version 4.0.0; Applied Precision) and deconvolution was performed using SVI Huygens Professional Deconvolution Software (Version 3.5). For quantitative data on γ tubulin and P-AurA centrosomal localization, DeltaVision files were imported into Imaris software (version 6.3.0; Bitplane) for 3D rendering measurements using the surface rendering algorithm for γ tubulin and P-AurA signals. Measurements were then exported to Excel (Microsoft) and plotted. The data was further analysed using Mann–Whitney *U* test.

For ploidy analysis, cells were collected from flasks, spun down, re-suspended, pipetted on Concanavalin A coated coverslips and fixed with 4% paraformaldehyde for 10 min. Cells were permeabilized, blocked and probed with phalloidin (Invitrogen) for 30 min. Coverslips were mounted as above.

FACS analysis

It was performed as previously described (Hegarat et al., 2011).

Cell tracking

Cells were incubated separately with 1 μM CellTracker Green CMFDA (5-Chloromethylfluorescein Diacetate) and 1 μM CellTracker Blue CMAC (7-Amino-4-Chloromethylcoumarin) (both from Molecular Probes) for 45 min, spun down, re-suspended in fresh medium and incubated for 24 h ±50 nM MLN8237. Cells were then fixed and stained with phalloidin as in the ploidy analysis. Coverslips were mounted using Fluoromount (Sigma).

Clonogenic survival assay

Clonogenics were performed plating the cell suspension in 96 well plates, at an ideal concentration of 1 cell/well (200 μl). Each subpopulation of cells was plated in the appropriate medium. EGF and FGF are added to the GSC plates on days 5, 10 and 15. Neurospheres and adherent colonies were counted on day 21 using the Gel Count (Oxford Optronix) and methylene blue staining, respectively.

β-galactosidase staining

Cells were treated with MLN8237 and after 2 and 7 days they were fixed and stained for β-galactosidase according to the manufacture's protocol (Abcam). Images were acquired on a microscope Axio Lb A1 (Zeiss) equipped with an AxioCam ERc 5 s and a 40× objective.

Acknowledgments

We would like to thank the members of the Hochegger and Chalmers labs for their support. AC was funded by an MRC senior clinical fellowship G0802755, HH was funded by a CRUK senior research fellowship grant number C28206/A14499.

Appendix A. Supplementary data

Supplementary data to this article can be found online at http://dx.doi.org/10.1016/j.scr.2014.05.001.

References

Barton, V.N., et al., 2010. Aurora kinase A as a rational target for therapy in glioblastoma. J. Neurosurg. Pediatr. 6, 98–105.

Beier, D., Schulz, J.B., Beier, C.P., 2011. Chemoresistance of glioblastoma cancer stem cells—much more complex than expected. Mol. Cancer 10, 128.

Cammareri, P., et al., 2010. Aurora-a is essential for the tumorigenic capacity and chemoresistance of colorectal cancer stem cells. Cancer Res. 70, 4655–4665.

Chefetz, I., Holmberg, J.C., Alvero, A.B., Visintin, I., Mor, G., 2011. Inhibition of Aurora-A kinase induces cell cycle arrest in epithelial ovarian cancer stem cells by affecting NFkB pathway. Cell Cycle 10, 2206–2214.

Chen, J., et al., 2012. A restricted cell population propagates glioblastoma growth after chemotherapy. Nature 488, 522–526.

Coppe, J.P., et al., 2008. Senescence-associated secretory phenotypes reveal cell-nonautonomous functions of oncogenic RAS and the p53 tumor suppressor. PLoS Biol. 6, 2853–2868.

Fael Al-Mayhani, T.M., et al., 2009. An efficient method for derivation and propagation of glioblastoma cell lines that conserves the molecular profile of their original tumours. J. Neurosci. Methods 176, 192–199.

Gorgun, G., et al., 2010. A novel Aurora-A kinase inhibitor MLN8237 induces cytotoxicity and cell-cycle arrest in multiple myeloma. Blood 115, 5202–5213.

Harrison, M.R., Holen, K.D., Liu, G., 2009. Beyond taxanes: a review of novel agents that target mitotic tubulin and microtubules, kinases, and kinesins. Clin. Adv. Hematol. Oncol. 7, 54–64.

Hegarat, N., et al., 2011. Aurora A and Aurora B jointly coordinate chromosome segregation and anaphase microtubule dynamics. J. Cell Biol. 195, 1103–1113.

Huck, J.J., et al., 2010. MLN8054, an inhibitor of Aurora A kinase, induces senescence in human tumor cells both in vitro and in vivo. Mol. Cancer Res. 8, 373–384.

Krajcovic, M., Overholtzer, M., 2012. Mechanisms of ploidy increase in human cancers: a new role for cell cannibalism. Cancer Res. 72, 1596–1601.

Lathia, J.D., et al., 2011. Distribution of CD133 reveals glioma stem cells self-renew through symmetric and asymmetric cell divisions. Cell Death Dis. 2, e200.

Lee, C., et al., 2012. Polo-like kinase 1 inhibition kills glioblastoma multiforme brain tumor cells in part through loss of SOX2 and delays tumor progression in mice. Stem Cells 30, 1064–1075.

Lehman, N.L., et al., 2012. Aurora A is differentially expressed in gliomas, is associated with patient survival in glioblastoma and is a potential chemotherapeutic target in gliomas. Cell Cycle 11, 489–502.

Liu, Y., et al., 2013. Targeting aurora kinases limits tumour growth through DNA damage-mediated senescence and blockade of NF-kappaB impairs this drug-induced senescence. EMBO Mol. Med. 5, 149–166.

Loh, J.K., et al., 2010. Differential expression of centrosomal proteins at different stages of human glioma. BMC Cancer 10, 268.

Manfredi, M.G., et al., 2011. Characterization of Alisertib (MLN8237), an investigational small-molecule inhibitor of aurora A kinase using novel in vivo pharmacodynamic assays. Clin. Cancer Res. 17, 7614–7624.

Morrison, S.J., Kimble, J., 2006. Asymmetric and symmetric stem-cell divisions in development and cancer. Nature 441, 1068–1074.

Nair, J.S., Ho, A.L., Schwartz, G.K., 2012. The induction of polyploidy or apoptosis by the Aurora A kinase inhibitor MK8745 is p53-dependent. Cell Cycle 11, 807–817.

Nigg, E.A., Stearns, T., 2011. The centrosome cycle: centriole biogenesis, duplication and inherent asymmetries. Nat. Cell Biol. 13, 1154–1160.

Overholtzer, M., et al., 2007. A nonapoptotic cell death process, entosis, that occurs by cell-in-cell invasion. Cell 131, 966–979.

Pallini, R., et al., 2008. Cancer stem cell analysis and clinical outcome in patients with glioblastoma multiforme. Clin. Cancer Res. 14, 8205–8212.

Rodier, F., Campisi, J., 2011. Four faces of cellular senescence. J. Cell Biol. 192, 547–556.

Roninson, I.B., 2003. Tumor cell senescence in cancer treatment. Cancer Res. 63, 2705–2715.

Strojnik, T., Rosland, G.V., Sakariassen, P.O., Kavalar, R., Lah, T., 2007. Neural stem cell markers, nestin and musashi proteins, in the progression of human glioma: correlation of nestin with prognosis of patient survival. Surg. Neurol. 68, 133–143 (discussion 143–4).

Stupp, R., et al., 2009. Effects of radiotherapy with concomitant and adjuvant temozolomide versus radiotherapy alone on survival in glioblastoma in a randomised phase III study: 5-year analysis of the EORTC–NCIC trial. Lancet Oncol. 10, 459–466.

Wang, H., et al., 2009. Targeting interleukin 6 signaling suppresses glioma stem cell survival and tumor growth. Stem Cells 27, 2393–2404.

Wang, Q., et al., 2013. Polyploidy road to therapy-induced cellular senescence and escape. Int. J. Cancer 132, 1505–1515.

Yamashita, Y.M., Mahowald, A.P., Perlin, J.R., Fuller, M.T., 2007. Asymmetric inheritance of mother versus daughter centrosome in stem cell division. Science 315, 518–521.

Zeppernick, F., et al., 2008. Stem cell marker CD133 affects clinical outcome in glioma patients. Clin. Cancer Res. 14, 123–129.

Zhang, M., et al., 2008. Nestin and CD133: valuable stem cell-specific markers for determining clinical outcome of glioma patients. J. Exp. Clin. Cancer Res. 27, 85.